

MULTI-OMICS APPROACH TO INVESTIGATE THE ROLES OF XYLOGLUCAN  
ENDOTRANSGLYCOSYLASE/HYDROLASES (XTHs) IN AGRICULTURALLY  
IMPORTANT PLANTS



by  
Burcu Gür

Submitted to Graduate School of Natural and Applied Sciences  
in Partial Fulfillment of the Requirements  
for the Degree of Doctor of Philosophy in  
Biotechnology

Yeditepe University  
2018

MULTI-OMICS APPROACH TO INVESTIGATE THE ROLES OF XYLOGLUCAN  
ENDOTRANSGLYCOSYLASE/HYDROLASES (XTHs) IN AGRICULTURALLY  
IMPORTANT PLANTS (XTHs)

APPROVED BY:

Assist. Prof. Dr. Andrew John Harvey  
(Thesis Supervisor)

  
.....

Prof. Dr. Berna Sarıyar Akbulut

  
.....

Prof. Dr. Işıl Aksan Kurnaz

  
.....

Assoc. Prof. Dr. Ali Özhan Aytekin

  
.....

Assist. Prof. Dr. Bahar Soğutalmaz Özdemir

  
.....

DATE OF APPROVAL: ...../...../2018

## ACKNOWLEDGEMENTS

First of all, I would like to express my sincere gratitude to my advisor Assist. Prof. Dr. Andrew John Harvey for his tutelage and guidance in my journey to become a research scientist. I was fortunate enough to pursue my thesis under a supervisor who believed in me. I further want to thank my lab partner Dr. Merve Seven for being a wonderful colleague and a dear friend. I am grateful for her collaboration and endless help during this process.

While pursuing my PhD I have come across many amazing people. Among those whom I wish to thank are, Ezgi Türksever for her positive influence on the work environment and her invaluable contribution to the team; Ümit Cem Derman for being a good listener; Dr. Hülya Pınar Akdemir Koç for her assistance with data computation and her valued friendship; Arman Akşit for sharing my misery and letting me know that reconnection with an old friend is always possible; Brian Starmach for supporting me spiritually throughout writing this thesis; my jury members, Assist. Prof. Dr. Bahar Soğutmaz Özdemir, Prof. Dr. Işıl Aksan Kurnaz, Assoc. Prof. Dr. Ali Özhan Aytekin and Assist. Prof. Dr. Sanem Argın for their instruction and advice throughout my thesis course; Assist. Prof. Dr. Emrah Nikerel for his expertise and advice; Prof. Dr. Ece Genç and Prof. Dr. İnci Özden for sharing their lab and HPLC instrument; distinguished head of the Genetics and Bioengineering Department Prof. Dr. Fikrettin Şahin; Yüksel Tohumculuk Company and Menemen National Gene Bank for the generous gift of capsicum seeds; and TÜBİTAK for funding the projects 110T956 and 113Z816 we worked on during the research process.

Finally, I wish to pay a special token of gratitude to my family for their eternal love and understanding; my father Tacettin Gür for being my rock, my mother Birsen Gür for her nurturance, and my brother Murat Gür who has been my biggest supporter even from a great distance.

## ABSTRACT

### MULTI-OMICS APPROACH TO INVESTIGATE THE ROLES OF XYLOGLUCAN ENDOTRANSGLYCOSYLASE/HYDROLASES (XTHs) IN AGRICULTURALLY IMPORTANT PLANTS

Modification of the carbohydrate molecules in the cell walls of plants is essential for growth, including maturation and response to external factors, a task fulfilled by enzymes like xyloglucan endotransglycosylase/hydrolases (XTHs). Many experiments have demonstrated that certain *XTH* genes are up-regulated during a variety of abiotic stresses. Recent work has further shown that when a capsicum *XTH* gene was over-expressed in both *Arabidopsis* and tomato plants, it conferred greatly increased levels of resistance to drought and salt stresses. In this project, rice, tomato and capsicum XTH enzymes were examined at genomic, transcriptomic, and protein levels to give a better understanding of their functions within the plants. Detailed analyses of protein substrate specificities and kinetics of the XTH enzymes revealed active enzymes that showed a distinct preference for an unsubstituted basal form of xyloglucan. Using tamarind xyloglucan TXG as a donor and XXXG (X7) oligosaccharide as an acceptor, demonstrated the highest activity for each enzyme. That preference was stronger with capsicum XTH enzymes which agrees well with what is known about Solanaceae family, and in particular capsicum, forms of xyloglucan which only have the XXXG structure with little to no galactosylation. Rice, tomato and capsicum XTH enzymes were able to show activity with hydroxyethyl cellulose (HEC) as the donor substrate and a variety of acceptor substrates such as, XT, CT, BB etc. However, the ratio between activities on xyloglucan molecules and other carbohydrate molecules was higher with capsicum XTH enzymes than it was with tomato and rice XTH enzymes. Phenotypic observation of different pepper varieties under abiotic stress conditions revealed tolerant and susceptible varieties. Transcriptomic analyses of *CaXTH2* & *3* demonstrated that these genes were upregulated under abiotic stress conditions. Varieties that were considered to be phenotypically tolerant generally seemed to upregulate capsicum *XTH* gene expression earlier and stronger compared to less tolerant varieties under stress conditions. However, there was no direct evidence that upregulation of these genes improved stress tolerance.

## ÖZET

### TARIMSAL AÇIDAN ÖNEMLİ BİTKİLERDE KSİLOGLUKAN ENDOTRANSGLİKOZİLAZ/HİDROLAZ ENZİMLERİNİN ROLLERİNİN ARAŞTIRILMASI İÇİN MULTI-OMİKS YAKLAŞIMI

Bitki hücre duvarında bulunan karbonhidrat moleküllerinin modifikasyonu, bitki büyümesi, olgunlaşması ve bitkinin dış faktörlere cevabı açısından büyük önem taşımaktadır. Bu görev, ksiloglukan endotransglikozilaz/hidrolaz (XTH) enzimleri tarafından yerine getirilmektedir. Birçok deney belli *XTH* genlerinin çeşitli abiyotik streslerde anlamlarının indüklendiğini göstermiştir. Son çalışmalar, acı biber (*Capsicum annuum*) *XTH* genlerinin, Arabidopsis ve domates bitkilerinde fazladan anlatırıldıkları zaman, büyük ölçekte artan susuzluk ve tuz stresine direnç sağladıklarını göstermiştir. Bu projede, pirinç, domates ve biber XTH enzimleri, bitkideki fonksiyonlarının daha iyi anlaşılabilmesi için genom, transkriptom ve protein seviyelerinde incelenmiştir.

XTH enzimlerinin, detaylı protein substrat özgüllüğü ve kinetik analizi, süstitüe edilmemiş temel yapıya sahip ksiloglukan molekülüne kesin tercihe sahip aktif enzimleri göstermiştir. Çalışma dahilindeki her XTH enzimi, en fazla aktiviteyi TXG donör ve X7 akseptör substratları ile göstermiştir. Substrat tercihinin, biber XTH enzimleri açısından daha güçlü olduğu gözlenmiştir. Bu durum, Solanaceae ailesi ile ilgili bilinenlerle ve sadece XXXG yapısı olan ve galaktozilasyon olmayan ksiloglukan formları içeren biber bitkisi ile örtüşmektedir. Pirinç, domates ve biber XTH enzimleri, HEC donor substratı ve farklı akseptör substratları (XT, CT, BB) üzerinde de etki göstermiştir. Ancak ksiloglukan molekülleri ve diğer karbonhidrat molekülleri üzerindeki aktivite değerleri arasındaki fark, biber enzimlerinde, pirinç ve domates enzimlerinde olduğundan daha fazla bulunmuştur.

Farklı varyeteden biber bitkilerinin abiyotik stres altındaki fenotipik incelemeleri toleranslı ve duyarlı varyetelerin açığa çıkmasına sebep olmuştur. CaXTH2&3 genlerinin transkriptomik analizleri bu genlerin abiyotik stres koşullarında anlatımlarının indüklendiğini göstermiştir. Toleranslı olduğu düşünülen varyetelerde gen anlatımının toleranslı olmayan varyetelere göre genelde daha erken ve daha güçlü indüklendiği görülse de biber *XTH* genlerinin abiyotik strese toleransı arttırdığına dair kesin bir kanıt bulunamamıştır.

## TABLE OF CONTENTS

ACKNOWLEDGEMENTS.....	ii
ABSTRACT.....	iv
ÖZET .....	v
LIST OF FIGURES .....	ix
LIST OF TABLES.....	xvii
LIST OF SYMBOLS/ABBREVIATIONS.....	xx
1. INTRODUCTION.....	1
1.1. AIM OF THE THESIS.....	1
1.2. CAPSICUM ANNUUM .....	2
1.3. ABIOTIC STRESS .....	3
1.4. PLANT CELL WALLS .....	5
1.5. TYPES OF PLANT CELL WALL.....	6
1.6. PLANT CELL WALL STRUCTURE.....	7
1.6.1. Cellulose .....	9
1.6.2. Pectins.....	14
1.6.3. $\beta$ -Glucan.....	14
1.6.4. Arabinoxylans .....	16
1.6.5. Mannans.....	17
1.6.6. Xyloglucans .....	19
1.7. XYLOGLUCAN ENDOTRANSGLYCOSYLASE/HYDROLASE ENZYMES	25
1.7.1. XTH Phylogeny .....	26
1.7.2. Activity .....	28
1.7.2.1. Xyloglucan Endotransglycosylase Activity .....	28
1.7.2.2. Xyloglucan Endohydrolase Activity .....	30
1.7.2.3. Substrate Specificity .....	30
1.7.3. Mechanisms .....	31
1.8. HETEROLOGOUS PROTEIN PRODUCTION AND PICHIA PASTORIS .....	34
1.8.1. AOX1 Promoter Used in Pichia pastoris .....	35
2. MATERIALS AND METHODS .....	36

2.1. TARGET/HOST SELECTION AND CODON OPTIMIZATION FOR HETEROLOGOUS PROTEIN PRODUCTION .....	36
2.2. HEAT SHOCK TRANSFORMATION AND OBTAINING PLASMIDS .....	36
2.3. TRANSFORMATION INTO YEAST .....	37
2.4. SELECTION OF THE ACTIVE ENZYME PRODUCING COLONIES.....	37
2.4.1. Selection of OsXTH1 and SIXTH4 Producing Colonies.....	37
2.4.2. Selection of CaXTH1,CaXTH2 and CaXTH3 Producing Colonies.....	38
2.4.3. TCA-Acetone Precipitation, SDS-PAGE, Western Blotting.....	38
2.5. PREPARATION OF DONOR AND ACCEPTOR SUBSTRATES .....	39
2.6. HPLC ANALYSIS .....	40
2.7. LARGE SCALE PROTEIN PRODUCTION AND PURIFICATION.....	40
2.8. PH OPTIMIZATION .....	42
2.9. ACTIVITY ANALYSES .....	42
2.10. CAPSICUM PLANT GROWTH.....	43
2.11. SALT STRESS APPLICATIONS .....	45
2.12. COLD STRESS APPLICATIONS .....	46
2.13. DROUGHT STRESS APPLICATIONS.....	47
2.14. PRIMER DESIGN FOR QPCR STUDIES.....	48
2.15. RNA ISOLATION, CDNA SYNTHESIS, NEXT GENERATION SEQUENCING (NGS) AND QPCR .....	49
3. RESULTS.....	53
3.1. PROTEIN PRODUCTION AND ENZYME CHARACTERIZATION .....	53
3.1.1. Target/Host Selection and Codon Optimization.....	53
3.1.2. Active Enzyme Producing Colonies .....	54
3.1.2.1. OsXTH1 and SIXTH4 Enzymes .....	54
3.1.2.2. CaXTH1, CaXTH2 and CaXTH3 Enzymes.....	55
3.1.3. Large Scale Production .....	58
3.1.3.1. OsXTH1 and SIXTH4 Enzymes .....	58
3.1.3.2. CaXTH1, CaXTH2 and CaXTH3 Enzymes.....	62
3.1.4. pH Optimization .....	68
3.1.4.1. OsXTH1 and SIXTH4 Enzymes .....	68
3.1.4.2. CaXTH1, CaXTH2 and CaXTH3 Enzymes.....	68

3.1.5.	Substrate Specificity .....	69
3.1.5.1.	OsXTH1 Enzyme .....	69
3.1.5.2.	SIXTH4 Enzyme .....	70
3.1.5.3.	CaXTH1 Enzyme .....	70
3.1.5.4.	CaXTH2 Enzyme .....	71
3.1.5.5.	CaXTH3 Enzyme .....	71
3.1.6.	Enzyme Characterization .....	72
3.1.6.1.	OsXTH1 Enzyme .....	72
3.1.6.2.	SIXTH4 Enzyme .....	77
3.1.6.3.	CaXTH1 Enzyme .....	80
3.1.6.4.	CaXTH2 Enzyme .....	86
3.1.6.5.	CaXTH3 Enzyme .....	90
3.1.7.	Enzyme Kinetics .....	95
3.1.7.1.	CaXTH1 Enzyme .....	96
3.1.7.2.	CaXTH2 Enzyme .....	97
3.1.7.3.	CaXTH3 Enzyme .....	98
3.2.	CAPSICUM PLANT GROWTH TRIALS .....	99
3.3.	SALT STRESS.....	102
3.4.	COLD STRESS.....	114
3.5.	DROUGHT STRESS .....	118
3.6.	RNA ISOLATION AND cDNA SYNTHESIS .....	121
3.7.	GENE EXPRESSION STUDIES .....	122
3.7.1.	Salt Stress Expression Levels for CaXTH2 and CaXTH3 Genes .....	126
3.7.2.	Cold Stress Expression Levels for CaXTH2 and CaXTH3 .....	132
3.7.3.	Drought Stress Expression Levels for CaXTH2 and CaXTH3 .....	134
3.8.	NEXT GENERATION SEQUENCING (NGS) .....	136
4.	DISCUSSION.....	145
5.	CONCLUSION .....	163
	REFERENCES .....	166
	APPENDIX A.....	182

## LIST OF FIGURES

Figure 1.1. Structure of primary plant cell wall.....	8
Figure 1.2. Structural formula of cellulose $\beta$ -(1 $\rightarrow$ 4) glucan polymer chain. In brackets cellobiose is indicated.....	10
Figure 1.3. Electron micrograph of lamellae from the side wall of <i>Chaetomorpha melagonium</i> from outside the cell.....	11
Figure 1.4. The cellulose synthase (CESA) complex in a cellular context. Trans-Golgi network (TGN), microtubules (blue; MT).....	12
Figure 1.5. Cellulose synthase and cellulose synthase like genes in a phylogenetic tree in higher plants.....	13
Figure 1.6. General structure of $\beta$ -glucan and its debranching with lichenase. Dotted arrows show the lichenase hydrolysis sites.....	15
Figure 1.7. Model structures of xylans from different sources.....	16
Figure 1.8. Representative structures of mannans in different forms and the enzymes required for hydrolysis.....	18
Figure 1.9. Glucopyranose ring, D stereoisomer in the chair like formation .....	23
Figure 1.10. Xyloglucan side chain structures and nomenclature defined so far .....	24
Figure 1.11. Phylogenetic tree of various GH16 plant enzymes showing the standard Groups I/II, IIIA and IIIB that contain XET-acting enzymes.....	27

Figure 1.12. . Figurative explanation of product formation from endotransglycosylase activity .....	29
Figure 1.13. Figurative explanation of product formation from hydrolase activity .....	30
Figure 1.14. Enzyme binds to the donor substrate and cleaves it later on transglycosylation or hydrolysis activity is carried out.....	31
Figure 1.15. Structures of XTH enzymes and a closely related GH16 $\beta$ -(1 $\rightarrow$ 3);(1 $\rightarrow$ 4) glucanase.....	33
Figure 1.16. A schematic demonstration of XET and XEH mechanism. Xyloglucan (glucosyl units of xyloglucan in blue and xylosyl units in orange) binds to the enzyme....	33
Figure 3.1. PCR results of <i>SIXTH4</i> and <i>OsXTH1</i> genes on 1 per cent agarose gel .....	54
Figure 3.2. SDS-PAGE of TCA-acetone precipitated CaXTH1 and CaXTH2 proteins from small scale cultures of different colonies on 12 per cent polyacrylamide gel .....	56
Figure 3.3. Western results of TCA-acetone precipitated CaXTH1 and CaXTH2 proteins from small scale cultures of different colonies .....	56
Figure 3.4. HPLC chromatogram of CaXTH1 enzyme from different colonies on TXG-XGO substrate couple .....	57
Figure 3.5. HPLC chromatogram of CaXTH2 enzyme from different colonies on TXG-XGO substrate couple .....	57
Figure 3.6. SDS-PAGE results for the active enzyme producing colonies on a Coomassie dyes 12 per cent polyacrylamide gel.....	58
Figure 3.7. Western blotting results for the active enzyme producing colonies after treatment with Anti-6XHis antibody on a nitrocellulose membrane .....	59

Figure 3.8. Silver staining results for OsXTH1 after Superdex 75 16/100 column chromatography, on 12,5 per cent SDS-PAGE gel .....	60
Figure 3.9. Western results for OsXTH1 after Superdex 75 16/100 column chromatography, on nitrocellulose membrane.....	61
Figure 3.10. Silver staining results for the first two fractions collected from previous polishing procedure of OsXTH1 after Superdex 75 16/100 column chromatography, on 12,5 per cent SDS-PAGE gel.....	61
Figure 3.11. CaXTH3 fractions 1-15 that were obtained and concentrated after polishing procedure on a 12 per cent polyacrylamide gel after Silver Staining .....	63
Figure 3.12. CaXTH3 fractions 1-15 that were obtained and concentrated after polishing procedure on a nitrocellulose membrane after treatment with Anti-6X His antibody.....	63
Figure 3.13. CaXTH1 fractions 1 to 18 that were obtained and concentrated after polishing procedure on 12 per cent polyacrylamide gel after Silver Staining.....	64
Figure 3.14. CaXTH1 fractions 1 to 18 that were obtained and concentrated after polishing procedure on nitrocellulose membrane after treatment with Anti-6X His antibody .....	65
Figure 3.15. CaXTH2 fractions 1 to 9 that were obtained and concentrated after polishing procedure on 12 per cent polyacrylamide gel after Silver Staining.....	66
Figure 3.16. CaXTH2 fractions 1 to 9 that were obtained and concentrated after polishing procedure on nitrocellulose membrane after treatment with Anti-6X His antibody .....	66
Figure 3.17. Purified and concentrated CaXTH1, CaXTH2 and CaXTH3 enzymes on 12 per cent polyacrylamide gel after coomassie blue staining .....	67
Figure 3.18. pH optimization of OsXTH1 and SIXTH4 enzyme using McIlvaine buffer between pH range 4 and 6,5.....	68

Figure 3.19. pH optimization of CaXTH1, CaXTH2 and CaXTH3 enzyme using McIlvaine buffer between pH range 4 and 7.....	69
Figure 3.20. OsXTH1 enzyme activity in relation to time of incubation based on HPLC analysis, with each graph showing a different substrate couple .....	76
Figure 3.21. SIXTH4 enzyme activity in relation to time of incubation, with each graph showing a different substrate couple .....	79
Figure 3.22. CaXTH1 enzyme activity in relation to time of incubation, with each graph showing a different substrate couple .....	84
Figure 3.23. CaXTH2 enzyme activity in relation to time of incubation based on HPLC analysis, with each graph showing a different substrate couple .....	89
Figure 3.24. CaXTH3 enzyme activity in relation to time of incubation based on HPLC analysis, with each graph showing a different substrate couple .....	94
Figure 3.25. Michaelis-Menten (reaction rate ( $\mu\text{M}$ product/min) vs final X7 concentration ( $\mu\text{M}$ )) graph of CaXTH1 enzyme .....	97
Figure 3.26. Lineweaver-Burke (1/reaction rate (min/ $\mu\text{M}$ product) vs 1/X7 concentration (1/ $\mu\text{M}$ )) graph of CaXTH1 .....	97
Figure 3.27. Michaelis-Menten (reaction rate ( $\mu\text{M}$ product/min) vs final X7 concentration ( $\mu\text{M}$ )) graph of CaXTH2 enzyme .....	98
Figure 3.28. Lineweaver-Burke (1/reaction rate (min/ $\mu\text{M}$ product) vs 1/X7 concentration (1/ $\mu\text{M}$ )) graph of CaXTH2 .....	98
Figure 3.29. Michaelis-Menten (reaction rate ( $\mu\text{M}$ product/min) vs final X7 concentration ( $\mu\text{M}$ )) graph of CaXTH3 enzyme .....	99

Figure 3.30. Lineweaver-Burke (1/reaction rate (min/ $\mu$ M product) vs 1/X7 concentration (1/ $\mu$ M)) graph of CaXTH3 .....	99
Figure 3.31. Root-shoot length comparison of the 11-day-old MS agar grown Erzurum seedlings that were incubated in 70 per cent EtOH for 1,5 min, and 5 per cent NaOCl for 10 min, 15 per cent NaOCl for 20 min 25 per cent NaOCl for 10 min .....	101
Figure 3.32. Phenotypic examination of 11-day-old Erzurum seedlings grown on 0,5 per cent agar media with 0 mM, 50 mM, 100 mM NaCl.....	102
Figure 3.33. Phenotypic examination of 11-day-old Erzurum seedlings grown on 0,5 per cent agar media with 0 mM, 5 mM NaCl, 10 mM, 20 mM, 30 mM, 40 mM NaCl .....	104
Figure 3.34. Phenotypic examination of 11-day-old Erzurum seedlings grown on MS agar media with 0 mM NaCl, MS agar media with 25 mM NaCl, MS agar media with 50 mM NaCl.....	105
Figure 3.35. Phenotypic examination of 11-day-old Cila seedlings grown on MS agar media with 0 mM NaCl, MS agar media with 25 mM NaCl, MS agar media with 50 mM NaCl.....	109
Figure 3.36. Phenotypic examination of 11-day-old Aktör seedlings grown on MS agar media with 0 mM NaCl, MS agar media with 25 mM NaCl, MS agar media with 50 mM NaCl.....	110
Figure 3.37. Phenotypic examination of 11-day-old Samuray seedlings grown on MS agar media with 0 mM NaCl, MS agar media with 25 mM NaCl, MS agar media with 50 mM NaCl.....	111
Figure 3.38. Phenotypic examination of 3-week-old Çanakkale seedlings whose roots were soaked into 200 mM NaCl solution for 0 min, 10 min, 30 min, 120 min.....	112

Figure 3.39. Phenotypic examination of 3-week-old Kahramanmaraş seedlings whose roots were soaked into 200 mM NaCl solution for 0 min, 10 min, 30 min, 120 min.....	113
Figure 3.40. Phenotypic examination of 4-week-old Mert seedlings that were exposed to cold stress for 0 hour, 2 hour, 4 hour, 8 hour, 12 hour, 24 hour .....	115
Figure 3.41 Phenotypic observation of 3-week-old Mert seedlings after 4, 8 and 12 hour cold stress treatments across the experimental and control groups .....	116
Figure 3.42. Phenotypic observation of 3-week-old Kahramanmaraş seedlings after 4, 8 and 12 hour cold stress treatments across the experimental and control groups .....	117
Figure 3.43. Phenotypic observation of 4-week-old Mert seedlings in response to different levels of drought stress .....	119
Figure 3.44. Phenotypic observation of 4-week-old Cila seedlings in response to different levels of drought stress .....	120
Figure 3.45. Agarose (1 per cent) gel results of the RNAs obtained from 3 different varieties of capsicum varieties .....	121
Figure 3.46. Agarose (1 per cent) gel results of the RNAs obtained from the leaf samples of drought stress treated capsicum varieties and leaf-root samples of salt stress treated capsicum varieties.....	122
Figure 3.47. HPLC trace of the separation of Reference gene <i>CaActin</i> at 260 nm .....	123
Figure 3.48. HPLC chromatogram trace of the separated fragments of pUC19 after digestion with HpaII enzyme .....	123
Figure 3.49. Amplification curve of <i>CaActin</i> standards from $10^7$ to $10^2$ copies/ $\mu$ l after performing QPCR with gene specific primers.....	124

Figure 3.50. Melt curve analysis of <i>Caa-Tubulin</i> standards from $10^7$ to $10^2$ copies/ $\mu$ l after QPCR with gene specific primers.....	124
Figure 3.51. cq value vs copy number graphs of <i>CaXTH2</i> and <i>CaXTH3</i> that were generated following QPCR with gene specific primers and gene standards ( $10^2$ - $10^9$ copies/ $\mu$ l) .....	125
Figure 3.52. Copy numbers of <i>CaXTH2</i> and <i>CaXTH3</i> genes from root tissues of 5-day-old 0 mM, 25 mM and 50 mM NaCl containing agar grown Aktör and Seki varieties .....	126
Figure 3.53. Copy numbers of <i>CaXTH2</i> and <i>CaXTH3</i> genes from root tissues of 5-day-old 0 mM, 25 mM and 50 mM NaCl containing agar grown Cila and Samuray varieties .....	128
Figure 3.54. Copy numbers of <i>CaXTH2</i> and <i>CaXTH3</i> genes from leaf and root tissues of Çanakkale seedlings whose roots were soaked into 200 mM NaCl solution for 0 min-10 min-30 min-120 min .....	130
Figure 3.55. Copy numbers of <i>CaXTH2</i> and <i>CaXTH3</i> genes from leaf and root tissues of Kahramanmaraş seedlings whose roots were soaked into 200 mM NaCl solution for 0 min-10 min-30 min-120 min .....	132
Figure 3.56. Copy numbers of <i>CaXTH2</i> and <i>CaXTH3</i> genes from leaf tissues of 3-week-old Mert and Kahramanmaraş seedlings after 4, 8 and 12 hour cold stress treatments across the experimental and control groups.....	133
Figure 3.57. Copy numbers of <i>CaXTH2</i> and <i>CaXTH3</i> genes from leaf tissues of 4-week-old Mert and Cila seedlings after they reached 5 per cent -10 per cent -20 per cent loss in their fresh weight in comparison to control group plants .....	135
Figure 3.58. RNA Integrity analysis of Total RNA from leaf tissue of <i>Capsicum annum</i> cv. Karamanmaraş after 8 hours of cold-stress treatment .....	137

Figure 3.59. RNA size-fractionation analysis of mRNA from leaf tissue of <i>Capsicum annum</i> cv. Karamanmaraş after 8 hours of cold-stress treatment.....	138
Figure 3.60. Genome position and gen expression depth graphics of <i>CaXTH1</i> gene of Mert variety obtained by NGS analyses after RNA sequencing for MC0, MC8 and MS8 samples paired with Zunla database .....	139
Figure 3.61. Genome position and gen expression depth graphics of <i>CaXTH1</i> gene of Mert varieties Mert and Kahramanmaraş, obtained by NGS analyses after RNA sequencing for MC8, KC8, KS8 an MS8 samples paired with Zunla database .....	140
Figure 3.62. Genome position and gen expression depth graphics of <i>CaXTH2</i> gene of Mert varieties Mert and Kahramanmaraş, obtained by NGS analyses after RNA sequencing for MC0, KC0, MC8, KC8, KS8 an MS8 samples paired with Zunla database .....	141
Figure 3.63. Genome position and gen expression depth graphics of <i>CaXTH3</i> gene of Mert varieties Mert and Kahramanmaraş, obtained by NGS analyses after RNA sequencing for MC0, KC0, MC8, KC8, KS8 an MS8 samples paired with Zunla database .....	143

## LIST OF TABLES

Table 2.1. Forward and reverse primer sequences for <i>CaXTH1</i> , <i>CaXTH2</i> and <i>CaXTH3</i> genes for QPCR studies .....	48
Table 3.1. Selected plant genes for heterologous production .....	53
Table 3.2. Activity showing donor and acceptor substrates for OsXTH1 enzyme .....	70
Table 3.3. Activity showing donor and acceptor substrates for SIXTH4 enzyme.....	70
Table 3.4. Activity showing donor and acceptor substrates for CaXTH1 enzyme .....	71
Table 3.5. Activity showing donor and acceptor substrates for CaXTH2 enzyme .....	71
Table 3.6. Activity showing donor and acceptor substrates for CaXTH3enzyme .....	72
Table 3.7. The activity levels of the OsXTH1 enzyme on different substrate couples in picokatal/mg value and as percentages in relation to TXG-XGO substrate couple which was set to 100 per cent.....	76
Table 3.8. The activity levels of the SIXTH4 enzyme on different substrate couples in picokatal/mg value and as percentages in relation to TXG-XGO substrate couple which was set to 100 per cent.....	80
Table 3.9. The activity levels of the CaXTH1 enzyme on different substrate couples in picokatal/mg value and as percentages in relation to TXG-XGO substrate couple which was set to 100 per cent.....	85
Table 3.10. The activity levels of the CaXTH2 enzyme on different substrate couples in picokatal/mg value and as percentages in relation to TXG-XGO substrate couple which was set to 100 per cent.....	90

Table 3.11. The activity levels of the CaXTH3 enzyme on different substrate couples in picokatal/mg value and as percentages in relation to TXG-XGO substrate couple which was set to 100 per cent.....	94
Table 3.12. Post Hoc analysis and comparison of root-shoot lengths, root numbers and germination rates of 11-day-old MS agar grown Erzurum seedlings that were treated with different concentrated NaOCl solutions for different time periods following incubation in 70 per cent EtOH for 1,5 min .....	101
Table 3.13. Post Hoc analysis and comparison of root-shoot lengths and root numbers of 11-day-old Erzurum seedlings grown on 0,5 per cent agar medias including 0 mM NaCl, 5 mM NaCl, 10 mM NaCl, 20 mM NaCl, 30 mM NaCl and 40 mM NaCl .....	103
Table 3.14. Post Hoc analysis and comparison of root-shoot lengths and root numbers of 11-day-old Erzurum seedlings grown on MS agar medias including 0 mM NaCl, 25 mM NaCl, 50 mM NaCl.....	105
Table 3.15. Average length of primary roots, shoots and germination rates of 11-day-old Cila seedlings across 3 different concentrations of NaCl .....	107
Table 3.16. Average length of primary roots, shoots and germination rates of 11-day-old Samuray seedlings across 3 different concentrations of NaCl .....	107
Table 3.17. Average length of primary roots, shoots and germination rates of 11-day-old Aktör seedlings across 3 different concentrations of NaCl .....	107
Table 3.18. Average length of primary roots, shoots and germination rates of 11-day-old Seki seedlings across 3 different concentrations of NaCl.....	108
Table 3.19. Copy numbers of <i>CaXTH2</i> and <i>CaXTH3</i> genes from root tissues of Aktör and Seki seedlings that were grown on MS agar containin 0 mM-25 mM-50 mM NaCl.....	127

Table 3.20. Copy numbers of <i>CaXTH2</i> and <i>CaXTH3</i> genes from root tissues of Cila and Samuray seedlings that were grown on MS agar containing 0 mM-25 mM-50 mM NaCl .....	129
Table 3.21. Copy numbers of <i>CaXTH2</i> and <i>CaXTH3</i> genes from leaf and root tissues of Çanakkale seedlings whose roots were soaked into 200 mM NaCl solution for 0 min-10 min-30 min-120 min .....	130
Table 3.22. Copy numbers of <i>CaXTH2</i> and <i>CaXTH3</i> genes from leaf and root tissues of Kahramanmaraş seedlings whose roots were soaked into 200 mM NaCl solution for 0 min-10 min-30 min-120 min .....	131
Table 3.23. Copy numbers of <i>CaXTH2</i> and <i>CaXTH3</i> genes from leaf tissues of 3-week-old Mert seedlings after 4, 8 and 12 hour cold stress treatments across the experimental and control groups .....	134
Table 3.24. Copy numbers of <i>CaXTH2</i> and <i>CaXTH3</i> genes from leaf tissues of 3-week-old Kahramanmaraş seedlings after 4, 8 and 12 hour cold stress treatments across the experimental and control groups.....	134
Table 3.25. Copy numbers of <i>CaXTH2</i> and <i>CaXTH3</i> genes from leaf tissues of 4-week-old Mert and Cila seedlings after they reached 5 per cent -10 per cent -20 per cent loss in their fresh weight in comparison to control group plants .....	136
Table 4.1. Kinetic parameters of CaXTH1, CaXTH2 and CaXTH3 enzymes.....	152
Table 4.2. XTH enzymes as paired with substrates showing the highest activity .....	155

**LIST OF SYMBOLS/ABBREVIATIONS**

AGA	Apiogalacturonan
AgNO <sub>3</sub>	Silver nitrate
AOX	Alcohol oxidase
Asp	Aspartate
At	<i>Arabidopsis thaliana</i>
a. u.	Arbitrary unit
BA	Glucotetraose A
BB	Glucotetraose B
BBG	Barley β-glucan
BC	Glucotetraose C
BMGY	Buffered glycerol-complex medium
BMMY	Buffered methanol-complex medium
bp	Base pair
BSA	Bovine serum albumin
Ca	<i>Capsicum annuum</i>
CAZy	Carbohydrate-active enzymes
cDNA	Complementary DNA
CESA	Cellulose synthase
CFP	Cyan fluorescent protein
CM	Carob galactomannan
COR/LAE	Cold regulated/late embryogenesis-abundant
Cq	Quantification cycle
Csl	Cellulose synthase-like
CT	Cellotetraose
Cys	Cysteine
DGM	Di-galactosyl mannopentaose
DNA	Deoxyribonucleic acid
ds	Double stranded
<i>E. coli</i>	<i>Escherichia coli</i>
EtOH	Ethanol

FPLC	Fast protein liquid chromatography
Fucp	Fucopyranose
Gal	Galactose
Galp	Galactopyranosyl
GalpA	Galatopyranosyluronic acid
GH16	Glycoside hydrolase family 16
Glc	Glucose
GlcP	Glucopyranose
Gln	Glutamine
Glu	Glutamate
GM	Guar galactomannan
GM3	Galactosyl mannotriose
HCl	Hydrochloric acid
HEC	Hydroxyethyl cellulose
HG	Homogalacturonan
HPAEC	High pH anion exchange chromatography
HPLC	High pressure liquid chromatography
HSPs	Heat-shock proteins
Hv	<i>Hordeum vulgare</i>
K <sub>2</sub> CO <sub>3</sub>	Potassium carbonate
kDa	Kilo Dalton
KGM	Konjac glucomannan
LB	Luria-Bertani
LG	Lupin galactan
LT	Laminaritetraose
MALDI-TOF-MS	Matrix assisted laser desorption ionization-time of flight mass spectrometry
MES	2-(N-morpholino) ethanesulfonic acid
<i>Mr</i>	Relative molecular mass
MS	Murashige and Skoog
MT	Mannotetraose
MT	Microtubules
NaCl	Sodium chloride

NaOCl	Sodium hypochlorite
NF	Normalization factor
nm	Nanometer
NMR	Nuclear magnetic resonance
OD	Optic density
OLIMP	Oligosaccharide mass profiling
ORF	Open reading frame
Os	<i>Oryza sativa</i>
PCR	Polymerase chain reaction
Ptt	<i>Populus tremula</i> x <i>Populus tremuloides</i> hybrid
QPCR	Quantitative polymerase chain reaction
RG	Rhamnogalacturonan
RNA	Ribonucleic acid
rpm	Revolutions per minute
rRNA	Ribosomal RNA
SDS-PAGE	Sodium dodecyl sulfate polyacrylamide gel electrophoresis
Sl	<i>Solanum lycopersicum</i>
SR	Sulforhodamine
TBL	Trichome Birefringence-Like
TBST	Tris buffered saline with Tween
T-DNA	Transfer DNA
TGN	Trans-Golgi network
T <sub>m</sub>	Melting temperature
Tm	<i>Tropaeolum majus</i>
TXG	Tamarind seed xyloglucan
v/v	volume/volume
WAX	Wheat arabinoxylan
w/v	weight/volume
w/w	weight/weight
X7	Xyloglucan heptasaccharides
XEH	Xyloglucan hydrolase
XET	Xyloglucan endotransglycosylase
XGA	Xylogalacturonan

XGO	Xyloglucan oligosaccharide
XT	Xylotetraose
XTH	Xyloglucan endotransglycosylase/Hydrolase
Xyl	Xylose
Xylp	Xylopyranose
YFP	Yellow fluorescent protein
YPDS	Yeast extract peptone dextrose medium with sorbitol
6X-His	Polyhistidine-tag



# 1. INTRODUCTION

## 1.1. AIM OF THE THESIS

Plant cell walls, where the XTH enzymes are active, are perhaps the most important aspect of the plant in protecting itself from, and interacting with, its environment. An understanding of the structure, function, and interaction of the carbohydrates and proteins present in the cell wall is critical if we are to be able to manipulate the properties of plant cell walls in order to increase yield and protect the plant from external stresses. XTH enzymes modify the plant cell wall during a variety of processes by cleavage and re-ligation and/or the irreversible hydrolysis of the major cell wall polysaccharide, xyloglucan. XTH enzymes have been demonstrated to be capable of transglycosylation of xyloglucan chains. The possibility of these XTH enzymes to work on a number of different cellulosic and non-cellulosic polysaccharides besides xyloglucan in the cell wall, increases the potential of this class of enzyme to be involved in many important cell wall processes. Characterization of the enzymatic properties and roles of individual gene products is highly desirable due to the potential roles of these genes in processes like growth, development, signalling, strengthening or loosening of the wall and response to external factors.

The goal of this study was to fully characterize the genes and the gene products of rice (OsXTH1) and tomato (SlXTH4) which are monocot and dicot plants, respectively, and their enzymes fall into Group I in the phylogenetic tree, as well as three pepper XTHs (CaXTH1-2-3) that were shown to be upregulated under stress conditions in previous studies and fall into Group II. While it has been known for some time that many XTH genes are up or down-regulated during both biotic and abiotic plant stresses, the reasons for these changes and the mechanisms that they employ are not well understood. Analyses of transcript data, and enzyme substrate specificity information is intended to give as complete a picture as possible of the likely role/s of these genes/enzymes in the plant.

## 1.2. CAPSICUM ANNUUM

Pepper (*Capsicum annuum* L.) has been produced and used in a wide range of places around the world. Different cuisines and food industries use capsicum because the plant itself is very nutritious containing high amounts of vitamin C in its structure along with vitamin A and the vitamin B complexes. The fruits of this plant are consumed in various ways including in salads, hot dishes and are even dried, in the case of paprika, as well as are used in spice mixes, such as curry powder. The estimated consumption amount was determined as 0,5 g /person per day in Europe. Capsicum was domesticated in North and South America however today, it is mostly cultivated in Asia, Africa and various Mediterranean countries. China leads the world's countries in the cultivation of fresh peppers with a total dedicated area of 652510 hectares, followed by Indonesia and Nigeria, respectively. Turkey comes the fourth place with 88000 hectares of land dedicated to pepper cultivation [1-3].

The berry like fruits of this plant can be in various shapes, colours and taste. Bell pepper, cayenne, jalapenos, christmas peppers (ornamental) are included in the capsicum species. The carotenoids and the alkaloids in the structure render the plant suitable for ready-made and take-away foods, as they act as natural flavouring and colouring agents making the food more appetizing for the consumers [4]. In addition to being nutritious, beta-carotenoids and vitamin C and A also function as antioxidants and scavenge free radicals protecting biological systems from oxidative damage [3, 5]. The fruits of capsicum have pungent properties due to the alkaloids in its content. Capsaicin (trans-8-methyl-N-vanillyl-6-Noneamide) is the leading alkaloid which causes mucosal irritation; it also determines the hotness level of the pepper. Besides flavouring, capsaicin may also be used for medical purposes like treating rheumatoid arthritis, diabetic neuropathy and cluster headache, along with anti-cancer, anti-obesity and neuro-protective properties [6, 7].

There are 25-30 defined species of capsicum and of these five species have been domesticated including *C. annuum*-L, *C. frutescens*-Mill., *C. baccatum*-L., *C. chinense*, and *C. pubescens*, with *Capsicum annuum* being the most broadly grown species [5]. The capsicum genus comes from the Solanaceae family. There are 102 genera and nearly 2500 species which are included in the Solanaceae family. Some of the important species are deadly nightshade (*Solanum nigrum*), potato (*Solanum tuberosum*), eggplant which is also

known as brinjal and aubergine (*S. melongena*), capsicum, (*Capsicum annuum* and *C. frutescens*), tobacco (*Nicotiana tabacum*), and tomato (*Solanum lycopersicum*) (<http://www.britannica.com>). A study done using tomato cDNAs revealed that pepper and tomato genomic content was similar to each other, the capsicum sequences were complementary to tomato cDNAs [8]. Phylogenetically they are included in the same group (II). Choi and co-workers over expressed an abiotic stress inducible capsicum gene, *CaXTH3* (*Capsicum annuum* endotransglycosylase 3) in tomato (*Solanum lycopersicum*) and found that transgenic tomato plants had improved tolerance against salt and drought stresses without showing phenotypic affects which may support the genome similarity between capsicum and tomato [9].

### 1.3. ABIOTIC STRESS

Abiotic stress is defined as the negative influence of non-living elements on living organisms. In the case of abiotic stress conditions a specific environment must be affected and altered from its normal state which creates a negative impact on the physiology of living population. Environmental changes, such as extreme temperatures (cold, frost, high temperatures), drought, increased salinity, waterlogging, increased concentration of heavy metals, are usually considered as abiotic stress factors [10].

Unlike animals, plants tend to get affected by environmental changes more easily and profoundly since they live in a soil-plant-atmosphere continuum environment [11]. Among the abiotic stress factors that affect plants, one of the most common is cold stress. Cold causes alterations in the plant energy metabolism decreasing the number of reactions catalyzed by enzymes which results in a metabolic imbalance; this may result from the increased risk of protein misfolding. Cold also attenuates the water uptake, therefore in the presence of cold stress, deposition of cold-regulated/late embryogenesis-abundant (COR/LEA) proteins are often increased since they can function as high-molecular weight osmoprotectants. In a study with the grass *Festuca pratensis*, cold stress was shown to affect the rate of photosynthesis. Other studies also represent the differences in carbohydrate metabolism (up-regulation of catabolic pathways and down-regulation of anabolic pathways) in plants exposed to cold. Heat stress also affects plant metabolism creating a noticeable risk for protein misfolding and denaturation of intracellular proteins

and complexes. Therefore, the concentration of heat-shock proteins (HSPs) is increased during heat stress as they have chaperone functions. Reduced water availability induces drought stress, leading to cellular dehydration. Upon drought stress, cell elongation is inhibited in the shoot due to reduced water uptake; however roots continue to grow in order to reach water-rich zones. A number of abiotic stresses often occur simultaneously with drought stress, such as high temperatures. In addition, the reduction in water levels increases the concentration of salts, leading to salinity, and other toxic compounds [10, 12, 13].

Plants respond to environmental changes and develop adaptive mechanisms. The response-adaptation process can be divided into different stages. When the plant is first exposed to the stress factor, it creates a shock and plants show greater susceptibility to the stress conditions. Following the first stress shock, acclimation begins. At this phase, plant tolerance increases and a new homeostasis starts. The new homeostasis is maintained under stress conditions until the exhaustion phase which happens if the plant is exposed to the stress for too long and cannot sustain stress-induced homeostasis. Recovery phase comes after the stress condition is over and a cellular homeostasis, adaptive to non-stress conditions, starts. Proteome composition differs according to each stage [10]. In order to adapt to environmental changes and gain tolerance, plants activate related gene expression. Stress inducible genes are divided into two groups depending on their protein products. The first group of these genes are immediately translated into their products as an adaptive mechanism when treated with stress; osmotic regulatory proteins, anti-freezing proteins, and LEA protein are among the examples. The second group of genes' translation products are incorporated in regulation of gene expression and signalling pathways. Transcriptional elements, such as *APETALA2/EREBP*, *bZIP*, *WRKY*, and *MYB*, are considered to be in the second group of genes [11].

During stress, plant cells go through a number of structural changes for acclimation including shoot growth during waterlogging or shading. The active process requires cell expansion and elongation which is made possible by cell wall modification. The cell wall is an important factor in plant stress resistance. Cells may use their wall as a barrier against pathogen attack or ice crystal formation. Cell wall proteins are important in the plants response since they take part in modifying the cell wall [13]. Park and co-workers described *CaDI* genes in *Capsicum annuum* treated with drought stress. *CaDI2* and *CaDI3*

were shown to code proteins homologs of the xyloglucan endotransglycosylase (*XET*) family in tomato; *CaDI4* on the other hand was similar to the *LEA* like gene family [14]. *Oryza sativa* L. gene expression levels were studied under cold, drought and heat stress. *OsXTH9* gene was shown to be up-regulated upon stress conditions [15]. Xyloglucan enzyme activity was shown to relieve stress by controlling the growing and wall strengthening processes. Transglycosylase activity of this enzyme provides new xyloglucan chains which are transported to the cell wall and strengthen it [13].

Xyloglucan endotransglycosylase/hydrolase enzymes are responsible for the re-modelling of cell wall. Because of their functions they play physiologically important roles in plant stress response. Under various abiotic stress conditions, such as drought, high salinity, cold, and the stress hormone ethylene, the level of isolated cDNA clones, *pCaXTH1*, *pCaXTH2*, and *pCaXTH3* was increased in capsicum plants [16]. Based on these results, *35S-CaXTH3* transgenic Arabidopsis plants were created. Although there was increased tolerance to drought stress and high salinity, the transgenic Arabidopsis plants' leaves displayed abnormal morphology. Activity of *35S-CaXTH3* gene was shown to increase small-sized cells in layers leading to disorganized and high number of mesophyll cells with reduce amounts of starch. The functional *CaXTH3* in Arabidopsis changes cell wall construction as a response to abiotic stress [16]. *35S-CaXTH3* construct was also used for obtaining transgenic tomato (*Solanum lycopersicum*) plants via transformation with *Agrobacterium tumefaciens* [9]. Transgenic plants showed enhanced tolerance to drought and salt stresses. In the meantime there were no phenotypic effects on the plant, chlorophyll existence was maintained in the leaves, and normal root growth was observed. They were also still green and unwithered, no morphological changes were reported even after 2 weeks of drought treatment. Reconstruction of the cell wall results in closures of stomatas therefore decreasing water loss from leaves. All these studies showed that *CaXTH3* protein is functional when heterologously expressed in plant cells, therefore has an important part in plant to play defence [9].

#### **1.4. PLANT CELL WALLS**

Plants are resilient to multiple stresses, which is thought to depend on the structure, mechanics and growth of the plant cell wall [17]. Given that there are many different plant

types on the planet, the physical appearance and properties of a plant are mainly determined by the structure and composition of their plant cell walls.

The structure of the plant cell wall is responsible for many of the physical traits that make plants unique, from their robustness to a variety of stresses, to their ability to grow to enormous sizes. Without this structure, plant cells would only consist of protoplasm (cytoplasm and nucleus), away from physical protection and the component that gives the cell its shape. In the early stage of plant cells, the plant cell wall, which is composed of various polysaccharides and structural proteins, is a thin flexible layer that can be visualized under light microscopy. In this meristematic stage, the plant cell wall is an active compartment since cell division is rapid and organogenesis starts. In spite of being a thin layer, the wall generates a powerful network, taking roles as a supporter and protecting the protoplast inside [18].

Plant cells adhere together via their cell walls, therefore in plant growth migration of cells is not likely. Instead, plant cells grow by a process called creep, which microfibrils and polysaccharides are newly located inside the wall resulting an irreversible extension and increase of the surface area. With this process cells can enlarge themselves 30,000 fold from their initial stage, for example young cotton seeds hair cells can elongate 1000 fold before full maturity [18].

### **1.5. TYPES OF PLANT CELL WALL**

In order to understand the mechanism and structure of plant cells and tissues, physical and mathematical modeling has been performed for decades, revealing models vary from very crude to very detailed. In simple models, tissue is considered as a homogenous layer composed of elastic material. However, when the case is fine models, heterogeneity of the cell material, geometry of individual cells, or the level of individual molecules is taken into consideration [19].

Plant cell walls comprise three types of layers including the middle lamella, the primary cell wall and the secondary cell wall. During mitosis a border is generated between two young nuclei, following this step the middle lamella starts to accumulate and once it is completed the plant cell wall is created and continues accumulation, providing cell

enlargement and growth. In this process while new material is associated, existing material is decomposed and extended allowing the formation of 0.1–10  $\mu\text{m}$  thick primary cell wall [20].

Once the cell growth is completed, secondary cell wall is accumulated inside the primary cell wall, prior to cell differentiation. Not all cell types have secondary cell wall, and the ones that have, show variability in composition depending on the cell function. Xylem cells usually have secondary cell walls consisting of lignin which improves wall strength [20].

## **1.6. PLANT CELL WALL STRUCTURE**

The accumulation and alteration of the plant cell wall has an important role in both plant growth and improvement as it controls the environmental responses, interactions between symbionts and defence against plant pathogens. In plant development, cell migration does not take a part, the process is mostly carried out via cell division and development of the cell wall which then determines the shape, size, and function of the cell. Cell wall material is considered as the most generous resource for biomass and renewable energy since harvested solar energy is deposited in photosynthetically produced carbon and included into the polymers in the wall material. Also, it is a natural fibre source for industry and nutritious food source for human and animal consumption [21, 22].

Primary cell walls are generated during cell development, thus they should be mechanically stable and flexible in order to allow cell extension and avoid rupture of the cell due to turgor pressure. The main polysaccharides that are incorporated to the primary cell wall are cellulose, cellulose-binding non-cellulosic  $\beta$ -linked polysaccharides, and pectins. The last two categories are described as matrix polysaccharides, which are produced in the Golgi cisternae and delivered to the cell wall by vesicles. On the other hand, cellulose is synthesized at the plasma membrane and impregnated into a matrix composed of other polysaccharides, glycoproteins and proteins. It can be said that cell wall composition is all about cellulose and non-cellulosic  $\beta$ -linked polysaccharides linked via lignin molecules [21, 23].

Non-cellulosic  $\beta$ -linked polysaccharides can compose about 30 per cent of the plant cell wall by weight and that ratio is much less when the case is secondary walls, except the cell walls of certain seeds. They are neutral molecules that can be extracted from the cell wall with alkali [24, 25]. These polysaccharide molecules make non-covalent associations with cellulose, especially xyloglucan molecules, as they function as primary interlocking molecules in type I cell walls. The network of xyloglucan-cellulose can be given as an example. The structure of these molecules include linear (1 $\rightarrow$ 4)- $\beta$ -linked backbone. One surface of this linear backbone binds to the surface of the cellulose microfibrils. Side branches, and single residues are included this short backbone. Cellulose and xyloglucan generate up to 50 per cent of the total cell wall polysaccharides and exist in almost equal amounts in primary cell walls. Other than binding the surface of the microfibrils, xyloglucans also fill the gaps between the microfibrils which create the cellulose-xyloglucan matrix [24, 26].

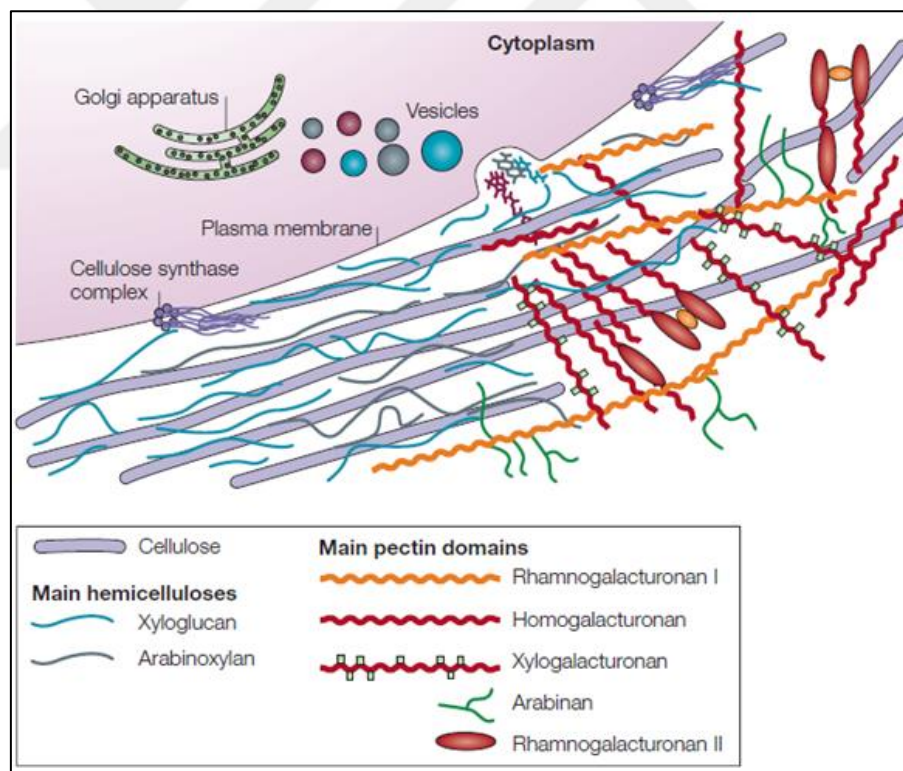


Figure 1.1. Structure of primary plant cell wall [18].

Primary cell walls mainly compose three polysaccharide domains, cellulose-xyloglucan matrix (50 per cent (w/w) of the cell wall mass), pectin (30 per cent (w/w) of the cell wall

mass) and structural proteins, for type I in dicots and smaller portion of type II in monocots, in the family Poaceae [26]. Xyloglucans compose up to 25 per cent (w/w) of the cell wall mass in type I primary cell walls of dicots this ratio however is much lower in the primary cell walls of the grasses (2 per cent -10 per cent (w/w)) [25]. Pectic polysaccharides are considered to be acidic molecules. Different structural domains are included in pectins and the level of these molecules vary according to different plants. Homogalacturonan (HG) and rhamnogalacturonan I (RGI) are considered to have a significant importance as they are quantitatively high in most of the primary cell-wall models. In these structural models a gel-like network is generated by pectin by cross linking homogalacturonan and calcium ions from their junction zones (Figure 1.1) [24].

Cellulose microfibrils are considered to be structurally important, because of their one-dimensional geometry, and high tensile strength which creates anisotropy between other mechanical properties of the plant cell wall. The anisotropy is a result of the conformation of cellulose microfibrils and other variants like the degree of cross-linking, crystallinity and the length of the microfibrils. Non-cellulosic  $\beta$ -linked polysaccharide molecules combine cellulose microfibrils together and link them into a network. This network then buried into a matrix composed of pectin and water [19]. Besides the polysaccharides, hundreds of diverse proteins are incorporated into the cell wall. While some of these proteins are described as structural proteins, the other takes part in cell modeling and turnover [21, 23].

### **1.6.1. Cellulose**

Cellulose is considered to be the most commonly found product in nature and the major compound of primary plant cell walls as it acts like a scaffold allowing other wall components to bind. It is a highly stable molecule and insoluble in water which is a result of its structure [23, 27]. In the structure of this material,  $\beta$ -linked glucose residues are composed as unbranched polymer which then line up as linear chains. Every second glucosyl residue in these chains is rotated by  $180^\circ$  about the chains longitudinal axis (Figure 1.2). Therefore, it can be said that cellulose consists of repeating units of cellobiose which is a disaccharide including two glucose molecules linked with  $\beta$ -(1 $\rightarrow$ 4) bond [28].

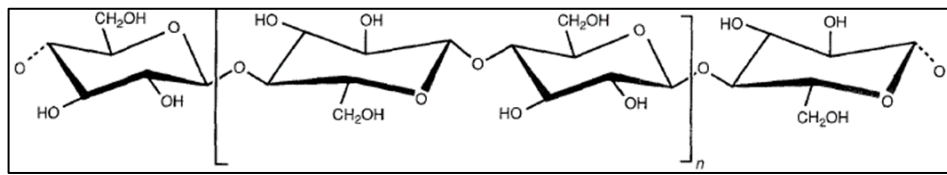


Figure 1.2. Structural formula of cellulose  $\beta$ -(1 $\rightarrow$ 4) glucan polymer chain. In brackets cellobiose is indicated [28].

Cellulose does not exist as a single chain in nature. Starting from the synthesis it is composed of many chains which together are called microfibrils. The microfibril sizes differ depending on the type of plant. The form of elementary fibril includes approximately 36 chains; this number can go up to 1200 chains in cellulosic algae. The width of these chains varies from 5 nm to 15 nm and placed approximately 20-40 nm from each other [26]. The polymeric glucosyl chains are linked together by a net of hydrogen and Van der Waals bonds. This attachment causes the crystallization of cellulose at some parts of the microfibril. The crystallized regions are strict and spaced by amorphous areas that are less crystallized. The tight crystallized alignments protect many of the glycosidic bonds from enzymatic attack and with the presence of other polysaccharides, like pectin and non-cellulosic  $\beta$ -linked polysaccharides; the cell wall structure becomes a very stable and inaccessible compound against enzymatic attacks [27].

According to the cellulose ratio in the cell, microfibrils are either highly or randomly oriented. Due to the thickness of the wall, they line up approximately parallel and generate different layers where the parallel microfibrils in different sheets exhibit varying angles (Figure 1.3). The parallel arrangement of the microfibrils is caused by two operations: the first process occurs when the early accumulation of the polymer starts at the surface of the plasma membrane and the second one is the passive rearrangement of the components transferred from the matrix material via deformation of other components [19].

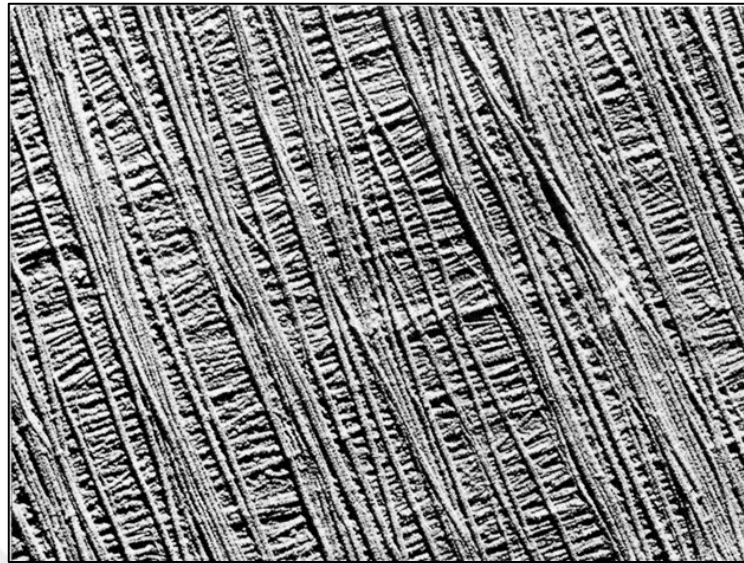


Figure 1.3. Electron micrograph of lamellae from the side wall of *Chaetomorpha melagonium* from outside the cell [29].

The complex process of cellulose biosynthesis is performed via rosette complexes at the plasma membrane. The complexes are organized as hexamers including six globular structures which enable the polymerization of glucose creating a  $\beta$ -(1 $\rightarrow$ 4) linked polysaccharide [30, 31]. The cellulose synthase (CESA) proteins are held by these globular complexes via immune-gold labeling [32]. The hexamer structures include 36 individual CESA proteins which are associated in the Golgi apparatus and transported to the plasma membrane by exocytosis (Figure 1.4). CESA proteins compose six subunits inside the structure which are assumed to synthesize six glucan chains per subunit. In order to create a functional rosette complex three distinct CESA proteins are needed. Higher plants contain multiple CESA genes, for example 10 CESA genes have been identified in the Arabidopsis genome and 18 for poplar [30]. Among the proteins coded by these genes in Arabidopsis, CesaA1, CesaA3, CesaA6, CesaA2, CesaA5, and CesaA9 are shown to be related to the generation of primary cell wall, while CesaA4, CesaA7, and CesaA8 are responsible for secondary cell wall [32].

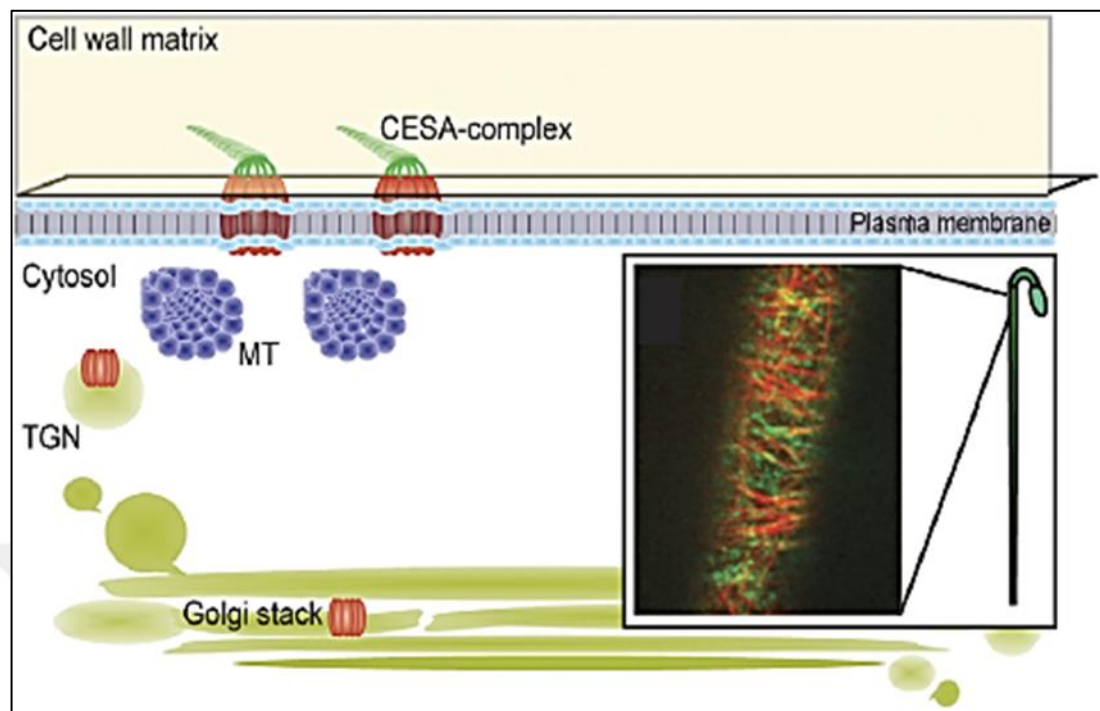


Figure 1.4. The cellulose synthase (CESA) complex in a cellular context. Trans-Golgi network (TGN), microtubules (blue; MT). In the inset a time average of a YFP-tagged CESA6 (green) and a CFP-tagged tubulin (TUA1; red) is displayed [30].

Cellulose synthase genes were first characterized in the bacterium *Acetobacter xylinum*. According to the comparison between other glycosyltransferases an amino acid sequence motif (D,D,D,QXXRW) was seen to be highly conserved in processive  $\beta$ -glycosyltransferases. After the identification of a plant cellulose synthase gene, cDNA clones were sequenced in cotton and amino acid sequence, based on two of these clones, also confirmed the presence of conserved regions. Searching databases for expressed sequence tags (ESTs) of *Arabidopsis thaliana* revealed at least 40 genes grouped into 7 families. Proteins encoded by this gene family are shown to have similarities to bacterial cellulose synthases and they are identified as CESA and cellulose synthase-like (Csl) proteins. The basic distinction between cotton cellulose synthases and Csl proteins is that the Csl proteins do not have all the additional motif sequences [33]. *Arabidopsis* comprises 29 Csl genes and the Csl gene family is categorized into into six subfamilies namely CslA, CslB, CslC, CslD, CslE and CslG. Also two subfamilies, CslF and CslH, were found in grasses (Figure 1.5) [34].

The Csl proteins have been shown to play roles in the synthesis of non-cellulosic  $\beta$ -linked polysaccharides. The highest sequence similarity between Csl family and CESAs points out that they take part in synthesizing  $\beta$ -(1 $\rightarrow$ 4)-linked glucan chains in cellulose [35]. The Csl genes are believed to be incorporated in cellulose accumulation depending on the cell type as the evidences show that they are responsible for polysaccharide synthesis in tip growth and stem development [35, 36]. In addition to the cellulose synthesis, these genes are assumed to operate as a distinct type of  $\beta$ -(1 $\rightarrow$ 4)-glucan synthase. Since there is another  $\beta$ -1 $\rightarrow$ 4- linked polysaccharide called xyloglucan in the cell wall, some of them may be involved in the synthesis of the xyloglucan backbone [36].

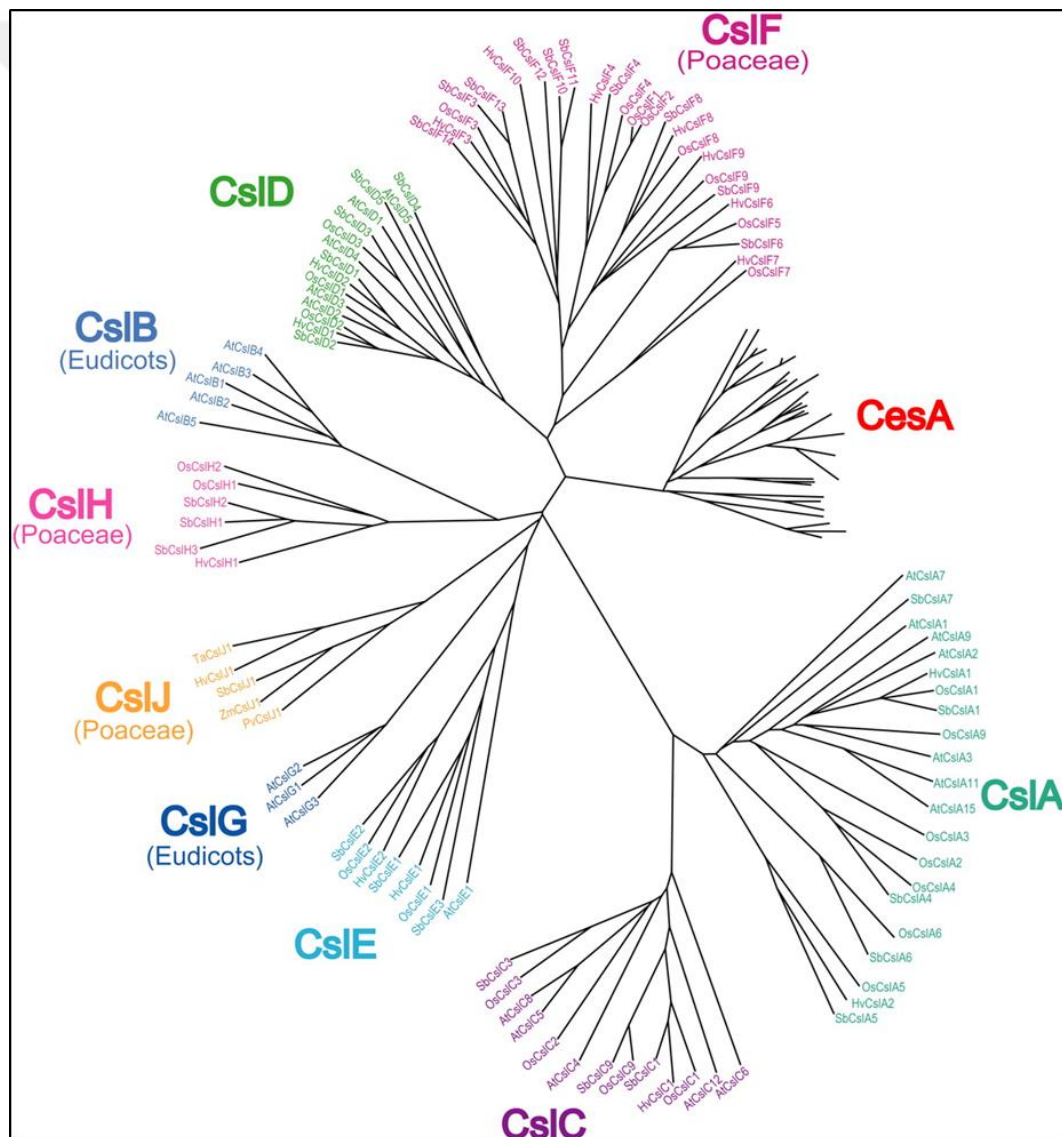


Figure 1.5. Cellulose synthase and cellulose synthase like genes in a phylogenetic tree in higher plants. Poaceae denotes grasses [37].

### 1.6.2. Pectins

Pectic substances are considered to be the most intriguing compounds between the cell wall polysaccharides in higher plants due to their complex structure and multi-tasking ability [38]. Of the primary cell wall, ~35 per cent is composed by pectins in dicots and non-graminaceous monocots [39].

This complex family of polysaccharides include (1→4)-linked  $\alpha$ -D-galactopyranosyluronic acid (GalpA) residues [40]. In cell wall, ~90 per cent of the uronic acids are assumed to be provided by the GalpA residues. Homogalacturonan (HG), xylogalacturonan (XGA), apiogalacturonan (AGA), rhamnogalacturonan II (RG-II), and rhamnogalacturonan I (RG-I) are considered to be the pectic polysaccharide classes [41].

Homogalacturonan (HG) has a linear chain structure composed of (1→4)-linked (GalpA) residues. Some of the carboxyl groups in these residues may be esterified. Depending on the type of plant, HGs can also be O-acetylated at C-3 or C-2. Rhamnogalacturonan-I on the other hand is a polymer unit of disaccharide [ $\rightarrow$ 4)-  $\alpha$ -D-GalpA-(1→2)- $\alpha$ -L-Rhap-(1→)] [40].

### 1.6.3. $\beta$ -Glucan

$\beta$ -Glucans are mostly seen in higher levels in grasses than other land plants. They are especially seen in the Poaceae and exist mostly in the cell walls of the starchy endosperm and aleurones. Cereals which are commercially important, like oats, barley, rye and wheat, are also rich in  $\beta$ -glucan (1 per cent wheat, 3-7 per cent in oats, 5-7 per cent in barley) [42, 43]. They have rich fibre content, thus have the ability to lower plasma cholesterol, improve lipid metabolism and reduce glycaemic index [37, 44].

$\beta$ -Glucans are considered to be linear homopolysaccharides composed of D-glucopyranosyl residues (GlcP). These residues are linked together via  $\beta$ -(1→3) and  $\beta$ -(1→4) linkages. The sequential (1→4) linked residues are split with (1→3) linkages [42]. Contiguous (1→4)- $\beta$ -D-oligoglucosyl compounds placed between (1→3)- $\beta$ -D-glucosyl residues are defined as cellodextrin units which comprises mostly two or three contiguous (1→4)- $\beta$ -D-glucosyl residues. In grasses, this number varies from 5 to 20. Therefore,

trimmers, dimers and longer cellodextrin units are included in the structure of polysaccharide chains with trisaccharides and tetrasaccharides comprising 90-95 per cent and longer oligosaccharides 5-10 per cent (Figure 1.6). This was also proved by (1→3, 1→4)-β-D-glucan hydrolase activity [37, 44].

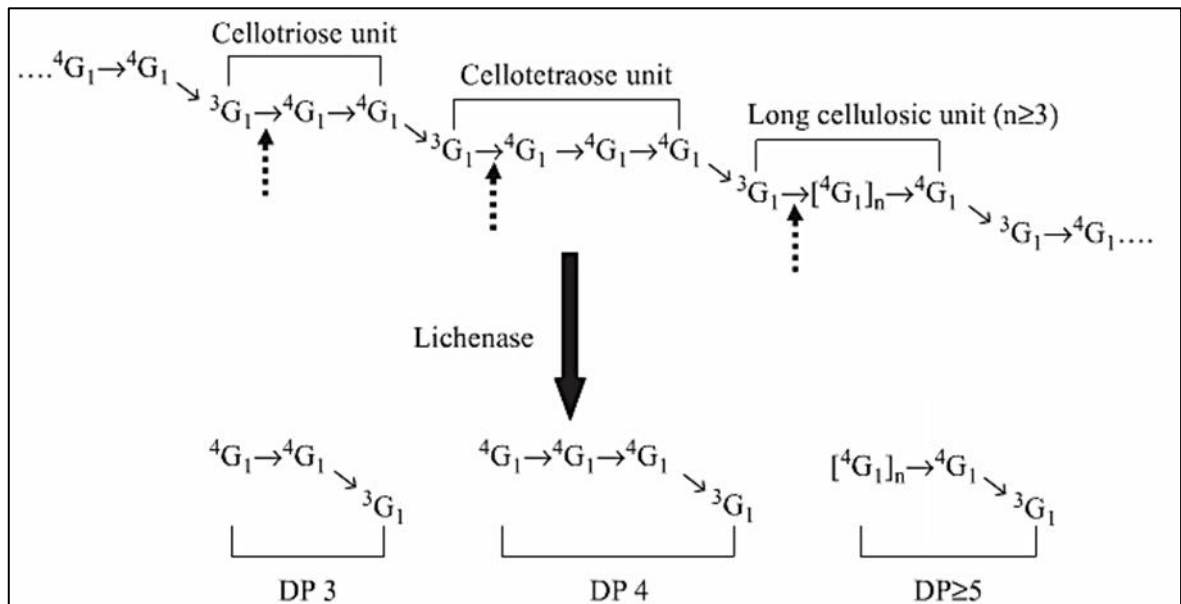


Figure 1.6. General structure of β-glucan and its debranching with lichenase. Dotted arrows show the lichenase hydrolysis sites. G: β -D-glucopyranosyl unit; DP3: 3-O- β -cellobiosyl-D-glucose; DP4: 3-O- β -cellotriosyl-D-glucose; DPX5: cellodextrin-like oligosaccharides containing more than three consecutive 4-O-linked glucose residues [42].

High performance ion exchange chromatography results showed that the cellotriosyl/cellotetraosyl ratio was higher in barley than oats. Rheological properties of β-glucans depend on the ratio of cellotriosyl/cellotetraosyl units as it affects the viscosity behaviour, food structure and nutritional characteristics. The solubility of the polymer decreases when the cellotriosyl/cellotetraosyl ratio gets high. Because when there are too many kinks in the structure the molecule get together in its self and precipitates out of the solution [43].

### 1.6.4. Arabinoxylans

Arabinoxylans compose 70 per cent of the cell wall material in wheat endosperm. The backbone of this polysaccharide includes  $\alpha$ -L-arabinofuronosyl units attached to D-xylopyronosyl residues linked by  $\beta$ -(1 $\rightarrow$ 4) linkages.  $\alpha$ -L-arabinofuronosyl side chains specifically linked to the C(O)-2 and/or C(O)-3 with O-acetyl groups (Figure 1.7). The linear chain of D-xylopyronosyl monomers forms xylan structure. The monomers in the structure can also be substituted with  $\alpha$ -D-glucopyranosyl uronic acid which also may be O-acetylated or O-methylated at C-4. Other constituents linked to the xylan backbone are D-galactose and ferulic acid residues attached to L-arabinose units [45, 46].

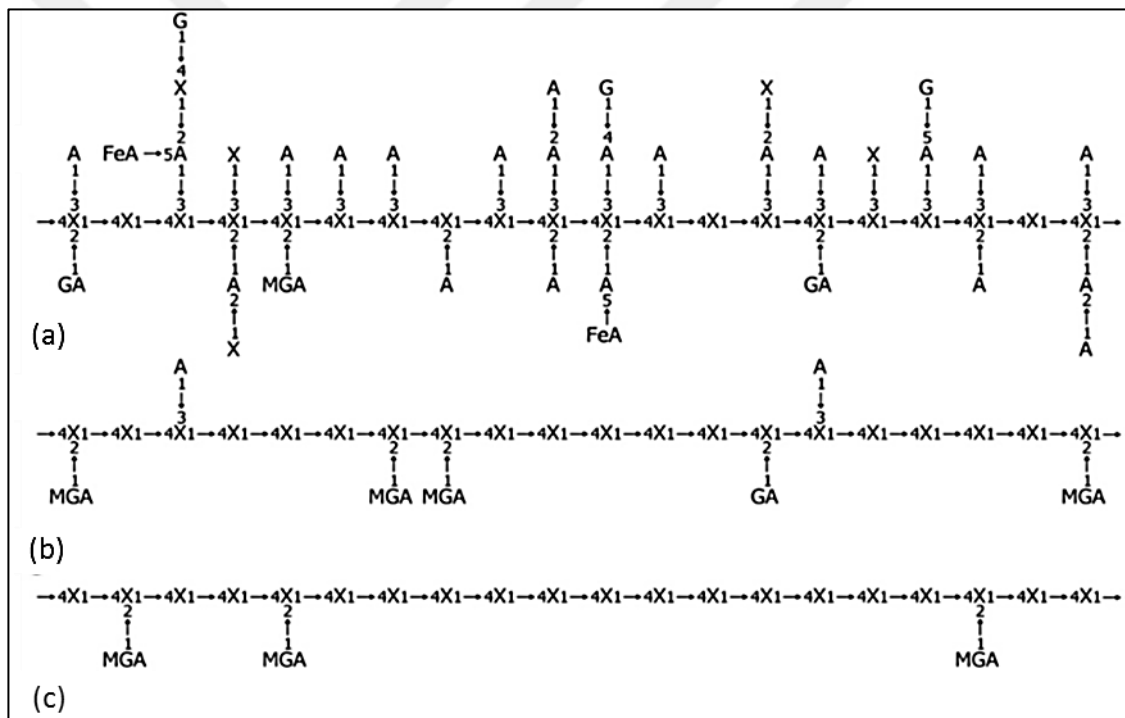


Figure 1.7. Model structures of xylans from different sources: (a) grasses and cereals, (b) softwood, and (c) hardwood, that shows major linkages and side-chains. (X - xylose, A - arabinose, G - galactose, GA - glucuronic acid, MGA - 4-O-methyl-glucuronic acid, FeA - ferulic acid) [46].

Arabinoxylan molecules form covalent and non-covalent interactions between other arabinoxylans, xylans, and also phenolic acids, proteins and  $\beta$ -glucan. Evidence has shown strong intermolecular bonds between monomeric parts of xylan chains and cellulose like  $\beta$ -

(1→4) linked substitutes of  $\beta$ -glucan. These strong interactions are the result of hydrogen bonds. Non-covalent interactions affect the structure of the molecule resulting in poor water-extractability, solubility and enzymatic indigestibility. However, these polysaccharides are also great oxygen barriers. It was seen that decreasing arabinoxylan levels increases the oxygen permeability in biodegradable film production [47, 48].

### 1.6.5. Mannans

Mannans are glycan molecules contained in the angiosperms in plant seeds and fruits. They are used as a main reserve instead of starch. There are 4 subfamilies among mannans, which are glucomannans, galactomannans, galactoglucomannans and linear mannans with less than 5 per cent of galactose. Mannans have a linear chain of D-mannosyl residues and a low degree of polymerization. In glucomannans the structure harbour both D-mannosyl and D-glucosyl residues linked via  $\beta$ -(1→4) linkage in a 3:1 ratio with also acetylation level up to 18 per cent. They contribute to the cell wall structure by interacting closely with cellulose and xylan. Mannans do not always have a linear structure. The D-mannosyl and D-glycosyl residues can be substituted with  $\alpha$ -(1→6) linked D-galactose units. When this level is above 5 per cent the polysaccharide polymers are called galactomannan and galactoglucomannan, respectively. O-acetyl groups are included in the galactoglucomannans (Figure 1.8) [49, 50].

Linear mannans give strength to the seed and protect it against mechanical damage. Depending on high insolubility in water, they keep their durability after exposure to water. In one study, it was shown that the immunochemical characteristics of *Candida dubliniensis* resulted from the cell wall mannan, which comprises antigenic factors [51]. Mannans display a similarity to cellulose by showing crystalline polymorphism in the structure. Due to the crystallinity level it is called mannan I which is highly crystalline or mannan II. Mannan I is considered to be one of the densest polysaccharides as it is an anhydrous molecule with a density of 1.63. However mannan II has a higher molecular weight and degree of polymerization. Unlike mannan, it exhibits less crystallinity and contain water molecules [50]. High level of  $\alpha$ -(1→6) linked D-galactose substitution increases water solubility by preventing close interactions between contiguous molecules

and creating a more shapeless structure with a higher water retaining capacity which is specifically important when growing plant seeds in dry areas [49].

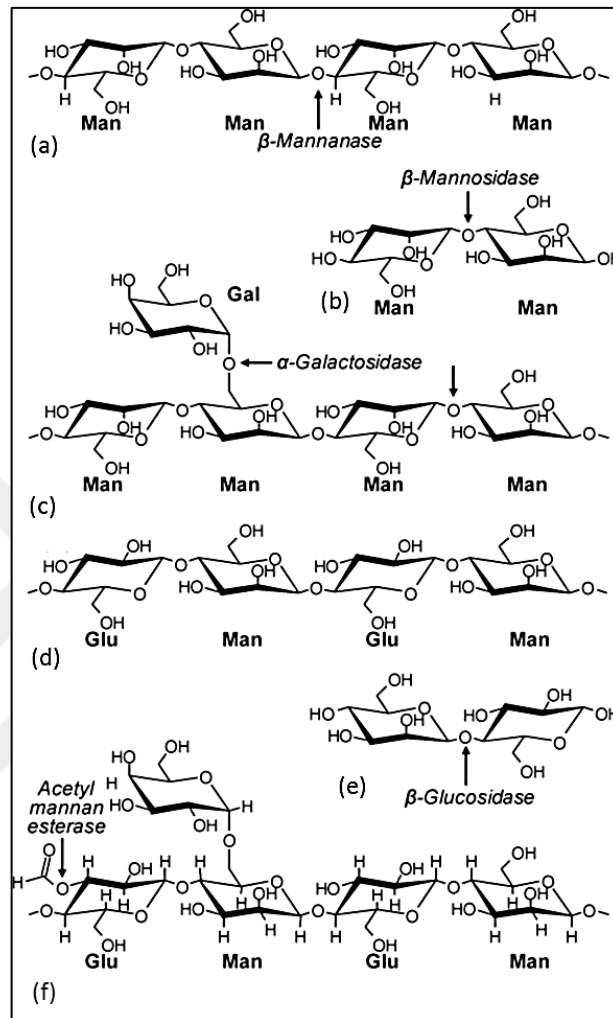


Figure 1.8. Representative structures of mannans in different forms and the enzymes required for hydrolysis. (a) linear mannan, (c) branched galactomannan, (d) linear glucomannan, (f) branched galactoglucomannan. (b)  $\beta$ -mannanase hydrolyses mannan backbone yielding mannose and glucomannose oligosaccharides. In the meantime  $\alpha$ -galactosidase and acetyl mannan esterase carry out the hydrolysis of galactose and acetyl groups, respectively. The products released by  $\beta$ -mannanase are further hydrolysed by  $\beta$ -mannosidase and  $\beta$ -glucosidase in order to yield mannose, glucose and galactose monosaccharides [49].

### 1.6.6. Xyloglucans

Xyloglucans are cell wall polysaccharides that exist in all of the land plants. Their presence and mobilization were first defined in seeds of *Impatiens balsamina*, *Tropaeolum majus* and *Cyclamen europaeum* [52]. These non-cellulosic  $\beta$ -linked polysaccharides contribute to the cell wall structure creating a network with the help of associations with cellulose. Xyloglucans can act as storage polysaccharides, especially in the seeds and cotyledons, and control cell expansion. Xyloglucan oligosaccharides also function as signal molecules. Incorporation of xyloglucans to the structure and signaling pathways make them have both regulatory and constitutional roles in the cell. Xyloglucans are used in various commercial and industrial applications as thickeners and stabilizing agents. The modification of these polysaccharides is carried out via various enzymes, glycosyl transferases for biosynthesis, transglycosylases and glycosyl hydrolases for remodeling. Xyloglucans basic structure depends on a linear chain of  $\beta$ -(1 $\rightarrow$ 4) linked glycosyl residues with different side chains. Different monosaccharides like glucose, xylose, galactose, arabinose and fucose are incorporated into the xyloglucan structure. The architecture varies according to the source of the plant and to the function. In a study, xyloglucan extracted from *Hymenaea courbaril* var. *courbaril* seeds was shown to have glucose, xylose and galactose in a molar ratio of ~4:3:2, respectively. Small amounts of arabinose was detected up to 6 per cent [53-55].

A variety of enzymes are responsible for the synthesis of the complex structure of xyloglucan. Production of this carbohydrate polymer is achieved in the Golgi apparatus. Responsible enzymes use activated nucleotide sugar molecules to add to the newly synthesized polymer chain [56, 57]. The location of the synthesis of the xyloglucan backbone is not known exactly. Some studies claim that it starts at *trans*-Golgi (142) while others indicate it happens in the *cis*-Golgi. In either case modification continues after secretion of xyloglucan from Golgi apparatus in vesicles (9, 15). The synthesis of the linear backbone of the xyloglucan, which is composed of  $\beta$ -(1 $\rightarrow$ 4) linked glycosyl residues, has been shown to be achieved by “cellulose synthase like genes”. After the discovery of *CesA1* and *CesA2* genes that are responsible for cellulose synthase in cotton, other studies were conducted using *Arabidopsis* mutants *rsw1* [58] and *irx3* [59, 60]. Both studies revealed that the two genes from these loci are highly similar to *CesA1* and *CesA2* genes

and considered to be orthologues. Database searches that were conducted based on the polypeptide sequences of Rsw1 and CesA proteins later on revealed 41 *CesA*-like genes in Arabidopsis. Among these gene families *CsID* gene family has been shown to have the most similarity to the *CesA* gene family. Studies about the intron-exon organization of the *CsID* gene family showed that there are small amount of introns in this family and they show diversity in between, which later on led the researches to think that this is the oldest in cellulose synthase superfamily and it antedates the *CesA* family [61].

Despite the fact that all of the members of *CesA* and *Csl* gene products seem to have the same amino acid motif (D,D,D,QxxRW) that is related to the catalytic site of the enzymes, the sequence similarity between these two families are small. That leads us to the conclusion of *Csl* family is responsible for the other glycosyltransferase reactions rather than cellulose synthase [62]. Contribution of the *Csl* family members to the plant cell wall has been shown with different studies. *AtCsID3* mutant Arabidopsis plants showed malformed root hairs due to the defective cell wall structure [63, 64]. In another study *AtCslA9* gene was over expressed in Arabidopsis and the plant showed increased tolerance to *Agrobacterium tumefaciens* infection which occurs in plant cell wall [65]. Database searches that were conducted by Hazen and co-workers using Arabidopsis *CesA* and *Csl* protein sequences against the rice genome also revealed 37 *Csl* genes and full length protein sequences of 23 of them was defined [34]. Although there were similarities between the *Csl* genes in the two species and they both carry *CslA*, *CslC*, *CsID* and *CslE* gene members, differences between these members were also observed, which may be associated to the different structured hemicellulose content in dicots and graminaceous monocots. The members of these gene families in rice have differences in both sequences and length, which creates a different family called *CslF* family. *CslG* family, on the other hand, does not exist in rice and other monocots but has been shown to be included in a variety of dicots [34]. Cocuron and co-workers identified a *CslC* gene from developing *Nasturtium* seeds. They conducted a cDNA library from the right developmental stage. To ensure that they used MUR3 protein homolog which is responsible for adding galactosyl residues to xyloglucan chain in Arabidopsis. Samples expressing the most MUR3 protein was chosen for further analysis. Among the cDNA clones obtained from these samples, 5 of them were identified as *CslC* homologues. All these clones seemed to come from the same gene. One of these clones (*TmCslC*) showed high sequence similarity to *AtCslC4*

gene. To ensure that these genes take a role in  $\beta$ -(1 $\rightarrow$ 4) linked glucan chain synthesis, researchers expressed them in *P. pastoris*. Different *P. pastoris* lines were created which expressed *TmCslC*, *AtCslC4* and coexpressed *AtCslC4* and *AtXT1* (gene responsible for the xylosyl addition in Arabidopsis) genes. They found that the lines carrying both *AtCslC4* and *AtXT1* genes showed the highest level of  $\beta$ -(1 $\rightarrow$ 4) linked glucan while only *AtCslC4* or *TmCslC* carrying lines showed smaller and soluble  $\beta$ -(1 $\rightarrow$ 4) linked glucans [66].

Multiple enzymes are thought to be involved in the process of xylose substitution to the glucan chain. Nucleotide sugar UDP-xylose is used as a substrate for the enzyme. First UDP-glucose is converted into UDP-glucuronic acid with the help of UDP-glucose dehydrogenase. After that decarboxylation of this molecule is achieved by UDP-glucuronic acid decarboxylase. At last the UDP-xylose is synthesized via the enzyme called UDP-xylose synthase (UXS) [67]. UDP-xylose synthesis is considered to take place in either cytosol or Golgi lumen which then a Golgi-localized UDP-glucuronic acid transporter is needed. There has not been any evidence about Golgi-localized UDP-glucuronic acid transporter existing in plants, on the other hand, a UDP-xylose transporter has been identified [68]. Faik and co-workers identified an  $\alpha$ -xylosyltransferase from *Arabidopsis*. A pea  $\alpha$ -xylosyltransferase was taken as a reference. Researchers used the fully sequenced *Arabidopsis* genome and showed that among the seven genes that revealed sequence similarity one of them had the  $\alpha$ -xylosyltransferase activity. Heterologous expression of six of these genes were conducted in *Pichia pastoris*. Enzyme assays performed with radiolabelled UDP-[<sup>14</sup>C]Xyl. Characterization of the products with high pH anion exchange chromatography (HPAEC) showed that one of the genes, *AtXT1*, was able to transfer [<sup>14</sup>C]Xyl on to cellopentaose (G5) and has the similar substrate specificity to pea enzyme [69]. In a following study, another gene among seven candidate genes of *Arabidopsis*, was investigated for xylosyl transferase activities, as it showed high sequence similarity (83 per cent identical) to *AtXT1*. *AtXT1* and At4g02500, later on it was called *AtXT2*, were expressed in both *Drosophila* S2 and *Spodoptera frugiperda* 21 cells as an alternative to *Pichia pastoris*. Cell extracts from the insect cultures were used in xylosyl transferase assays with UDP-xylose and UDP-[<sup>14</sup>C]xylose. The products were analysed via HPAEC and MALDI-TOF-MS. Both enzymes demonstrated similar characteristics. The substrate preference of the enzymes seemed to start at a degree of polymerization of 4. Therefore cellopentaose and cellohexasaccharide were used as acceptor substrates with

cellohexaose being preferred 4 times more than cellopentaose. AtXT1 and AtXT2 were proven to add multiple (mono-, di-, tri-) xyloses to cellohexaose [70]. Same study group also created *txt1*, *txt2* single mutants and *txt1-txt2* double mutant lines with T-DNA insertions. None of the single mutants showed no apparent changes in phenotype while *txt1-txt2* double mutants showed abnormal root hair growth which led to the conclusion that *AtXT1* and *AtXT2* are genetically redundant. Oligosaccharide mass profiling (OLIMP) also showed that there was no difference in xyloglucan abundance between wild type or single mutant *txt1* and *txt2* cells. However, high-performance anion-exchange chromatography-pulsed amperometric detection (HPAEC-PAD) analysis revealed that there was no detectable xyloglucan from double mutant cells [71]. In addition to *XXT1* and *XXT2*, 3 more xylosyl transferases were also proven to exist in the Arabidopsis GT34 family. Among these genes, *XXT5* was shown to be responsible of the major xyloglucan synthesis with *XXT1* and *XXT2* genes and expressed in most tissues at different stages of development while *XXT4* was expressed in more specific tissues [72].

O-acetylation is also an important process in xyloglucan synthesis and requires multiple enzymes for transferring acetyl groups into Golgi apparatus and then on to xyloglucan. The process is carried out via proteins included in Trichome Birefringence-Like (TBL) family [25]. Researchers identified a gene called *AXY4* in *Arabidopsis* and showed that the transmembrane protein coded by this gene had a TBL domain. O-acetylation of the xyloglucan structure in mutant lines lacking this gene was completely eliminated in most tissues. On the other hand, over-expressing this gene resulted in noticeable increase in o-acetylation. Also, 2D NMR studies showed that the reduction in o-acetylation in mutant lines was only observed in xyloglucan molecules, which led to the conclusion that this protein was xyloglucan specific [73]. Urbanowicz and co-workers created a recombinant ESKIMO1/Trichome Birefringence 29 (ESK1/TBL29) protein complex and performed *in vitro* assays to demonstrate its ability of O-acetyltransferase. MALDI-TOF analysis showed that the protein complex was able to transfer acetyl from acetyl-coenzyme A to 2-aminobenzamide  $\beta$ -(1 $\rightarrow$ 4)-xylohexaose [74]. Galactosylation is one of the most common ways of further substitution of xyloglucan molecules. The enzymes that are responsible for galactosylation is included in CAZy family GT47. Heterologously produced MUR3 protein was proven to add galactosyl units on the third xylosyl molecule in xyloglucan structure including (XXXG)<sub>n</sub> [75].

Carbohydrates in pyranose or furanose forms may exist in the nature in different configurations called  $\alpha$  anomer and  $\beta$  anomer. When the -OH group in C1 position is trans to the -CH<sub>2</sub>OH group at the anomeric center it is called  $\alpha$  anomer, when the -OH group in C1 position is cis to the -CH<sub>2</sub>OH group at the anomeric center it is called  $\beta$  anomer. Xyloglucans comprises  $\beta$ -(1 $\rightarrow$ 4) linked glycosyl units. The glucose, which is incorporated into the structure, is a D stereoisomer in the form of a pyranose ring ( $\beta$ -D-Glcp) (Figure 1.9).

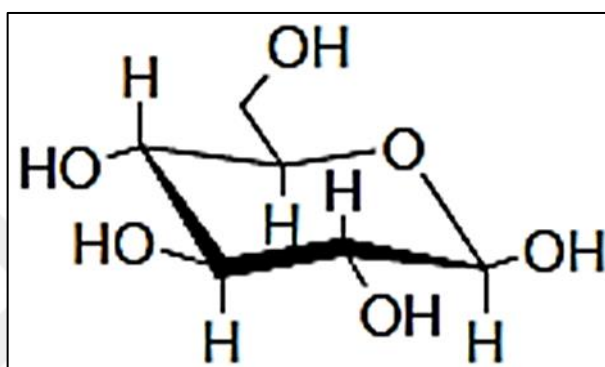


Figure 1.9. Glucopyranose ring, D stereoisomer in the chair like formation.

The glycosyl residues in the backbone is substituted with xylosyl ( $\alpha$ -D-Xylp) residues via  $\alpha$ -(1 $\rightarrow$ 6) linkages. Sometimes these  $\alpha$ -D-Xylp residues are further substituted up to four glycosyl residues in order to create extended side chains. So far, nineteen side chain structures have been defined and different structures are represented using a single-letter code. Unsubstituted  $\beta$ -D-Glcp residues are represented as G, when these residues are attached with  $\alpha$ -D-Xylp units via  $\alpha$ -(1 $\rightarrow$ 6) linkages, the side chain is defined as X. The  $\alpha$ -D-Xylp residues may be further substituted with galactosyl ( $\beta$ -D-Galp) residues at O-2 creating an L side chain or fucosyl ( $\alpha$ -L-Fucp) residues attached to  $\beta$ -D-Galp with  $\alpha$ -(1 $\rightarrow$ 2) linkages creating an F side chain. O-acetylation mostly happen for  $\beta$ -D-Galp residues at C-2 position but it was shown that, in *Nicotiana plumbaginifolia*, O-acetylation can also occur at C-6 of the fourth glucosyl residue. Arabinosyl ( $\alpha$ -L-Araf) and additional xylosyl residues ( $\beta$ -D-Xylp), attached to the xylosyl residues, may also be incorporated into the side chain structure, and form an S side chain and U side chain, respectively. The overall structure of xyloglucans and side chain variations change depending on whether it is a reserve xyloglucan or structural xyloglucan. Various xyloglucan side chains with different monosaccharide compositions may display the same stereochemical characteristics. The J

side chain, composed of  $\alpha$ -L-Galp-(1 $\rightarrow$ 2)- $\beta$ -D-Galp-(1 $\rightarrow$ 2)- $\alpha$ -D-Xylp, in seed xyloglucan from jojoba and the F side chain from mutant *Arabidopsis thaliana* are stereochemically identical seeing that L-Fuc is 6-deoxy-L-Gal (Figure 1.10) [52, 55, 76].

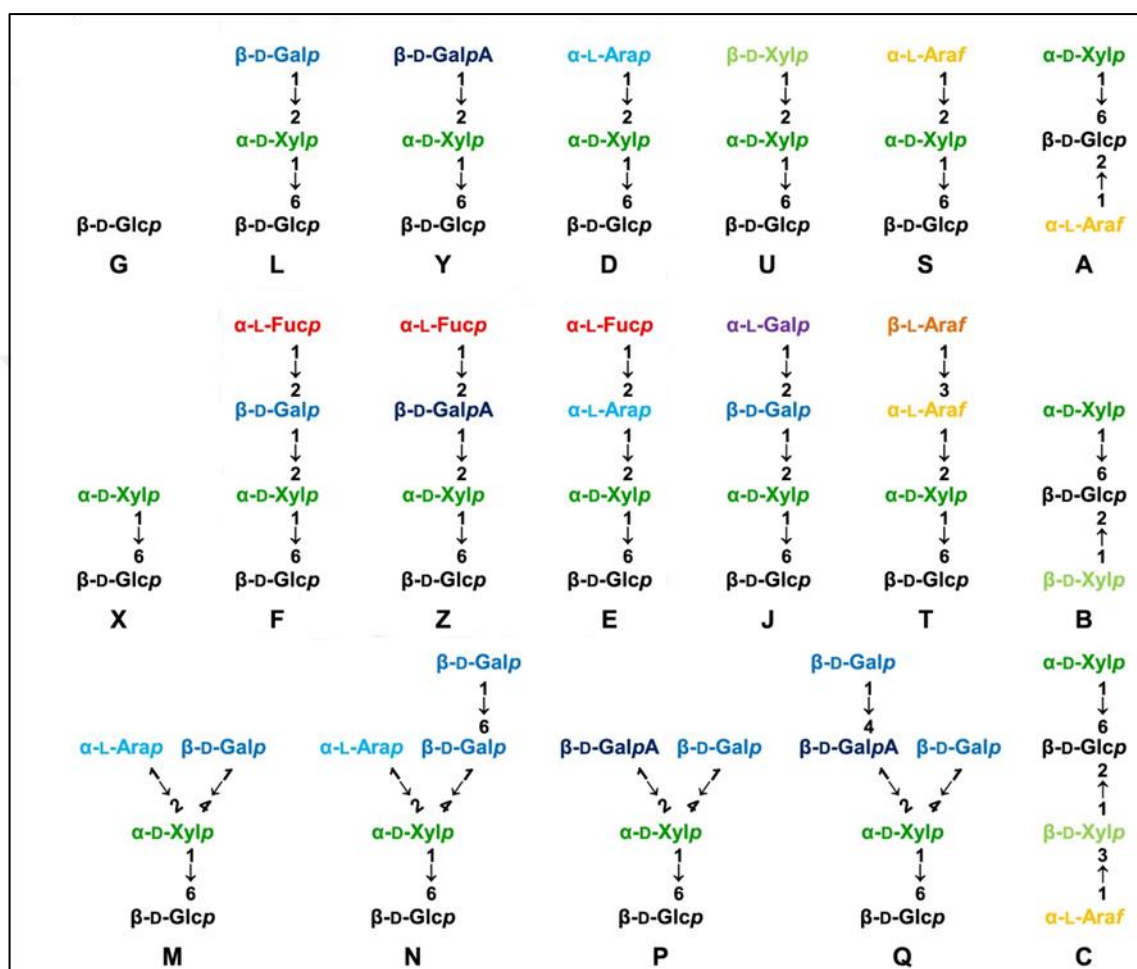


Figure 1.10. Xyloglucan side chain structures and nomenclature defined so far [55].

In a study xyloglucan from tamarind seeds was shown to have three different repeating units: heptasaccharide ( $\text{Glc}^4\text{Xyl}^3$ ), octasaccharide ( $\text{Glc}^4\text{Xyl}^3\text{Gal}$ ), and nonasaccharide ( $\text{Glc}^4\text{Xyl}^3\text{Gal}^2$ ) [77]. A comparative analysis with highly purified *Trichoderma* cellulase was performed for xyloglucan from the seeds of *Tropaeolum majus*, *Tamarindus indica* and *Copaifera langsdorffii*. The study revealed four basic structural units XXXG, XLXG, XXLG and XLLG. The ratio between these subunits would help enlighten different xyloglucan structures from distinct species [78]. Xyloglucan mobilization and degradation are carried out by the increase and decrease in the levels of four hydrolase enzymes:  $\beta$ -galactosidase, endo- $\beta$ -(1 $\rightarrow$ 4)-glucanase, xyloglucan endotransglycosylase/hydrolase

(XTH),  $\alpha$ -xylosidase and  $\beta$ -glucosidase which work together. XTH and  $\beta$ -galactosidase were shown to be the only enzymes which have the ability to attack the polymer in nasturtium. Therefore, when the xyloglucan oligosaccharide concentration is low, XTHs mostly control the hydrolytic activity producing oligosaccharides.  $\alpha$ -Xylosidase and  $\beta$ -glucosidase subsequently attack these oligosaccharides and reveal monosaccharide constituents [52].

### **1.7. XYLOGLUCAN ENDOTRANSGLYCOSYLASE/HYDROLASE ENZYMES**

The plant cell wall is an active compartment of the cell as it is incorporated into a variety of dynamic processes such as adjustment of the cell size, shape and cell to cell adhesion. It also provides the interaction of the cell with the outer environment taking part in the response to some abiotic stresses and also pathogens [79]. Cell wall modification includes basic steps in wall synthesis, deposition and rearrangement of new cell wall polysaccharides, and defining the overall morphology of a plant. Alteration in the cell wall extensibility leads to turgor-dependent cell expansion and addition of new materials ensures continuity of wall thickness and microfibril distance. All these processes require proteins which have the ability to alter wall material and are achieved by the action of synthesizing and modifying enzymes. Among these enzymes the ones that affect the xyloglucan molecules by hydrolysis or cleavage upon addition new xyloglucan chains are called xyloglucan endotransglycosylase/hydrolases (XTHs) [80, 81]. In the cell wall of dicotyledons, xyloglucans are probably the most important polysaccharide which can create crosslinks with cellulose via hydrogen bonds and with other polysaccharides contributing to the skeleton structure of the wall. These interactions between cell wall polysaccharides may generate a molecular tether between contiguous microfibrils and prevent cell expansion resulting in increased turgor pressure. Hydrolytic enzymes can allow the cell expansion by rupture of the bonds. However, this type of action can also weaken the wall. Transglycosylase activity, on the other hand, provides cell expansion without creating any damage on the wall structure as the cleaved and separated xyloglucans will be joined together with other xyloglucans protecting the stability [80].

### 1.7.1. XTH Phylogeny

A group of enzymes can act on a variety of oligosaccharide and polysaccharide substrates cleaving and forming glycosidic bonds in between. This group of enzyme has been defined as 'carbohydrate-active enzymes' (CAZymes) and divided into different families according to their amino acid sequence similarities [82]. Over 200 families of enzymes were described including polysaccharide lyases, glycosidases, glycosyltransferases and carbohydrate esterases. Glycoside hydrolases or glycosyltransferases make up to 1-3 per cent of the genes in most of the organisms [83]. XTH gene families have been defined in higher plants. The XTH families may have 20 to 60 genes which are likely to be expressed in a tissue and time dependent manner. Other stimulants like plant hormones (gibberellic acid, auxin and brassinolide) were also shown to affect the expression profile of these genes [84]. XTHs were also shown to have other roles besides cell wall modification. In nasturtium seeds, xyloglucan is deposited in high levels as it acts like a storage polysaccharide and is utilized during growth of the seedling. Development process requires hydrolysis of this polysaccharide, therefore, nasturtium seed XTHs have both abilities of transglycosylation and hydrolysis. The protein products of XTH genes can potentially perform two different activities; xyloglucan endotransglycosylase activity which results in cleavage of a xyloglucan molecule and reattachment to another, and xyloglucan hydrolase activity which causes irreversible cleavage of the chain. XTHs were first discovered in the early 1990s and since then they have been proposed to take part in different wall processes; wall loosening in fruit ripening, wall strengthening, and addition of newly synthesized xyloglucan into the cell wall during cell growth and expansion [80].

The *XTH* genes are included in a subfamily of CAZy GH16 (glycoside hydrolases) in which the enzymes have similar structural and mechanical characteristics. Substrate specificity differs in the members of GH16 family. The enzymes cleave  $\beta$ -(1 $\rightarrow$ 3) and  $\beta$ -(1 $\rightarrow$ 4) bonds in glucan and galactan chains. *XTH* gene products are more closely related to  $\beta$ -(1 $\rightarrow$ 3);(1 $\rightarrow$ 4) glucan hydrolases. Phylogenetic analyses of the XTH gene families of several species revealed that three main groups (I, II, and III) are included, with Group III being further divided into Group IIIA and Group IIIB (Figure 1.11) [81]. A fourth group comprising a small number of *XTH* genes was added to the classification, and labelled as

the Ancestral Group [85]. More recently, another group was defined (EG16) and found to have at least one gene that expressed a broad-specificity endo-glucanase [86].

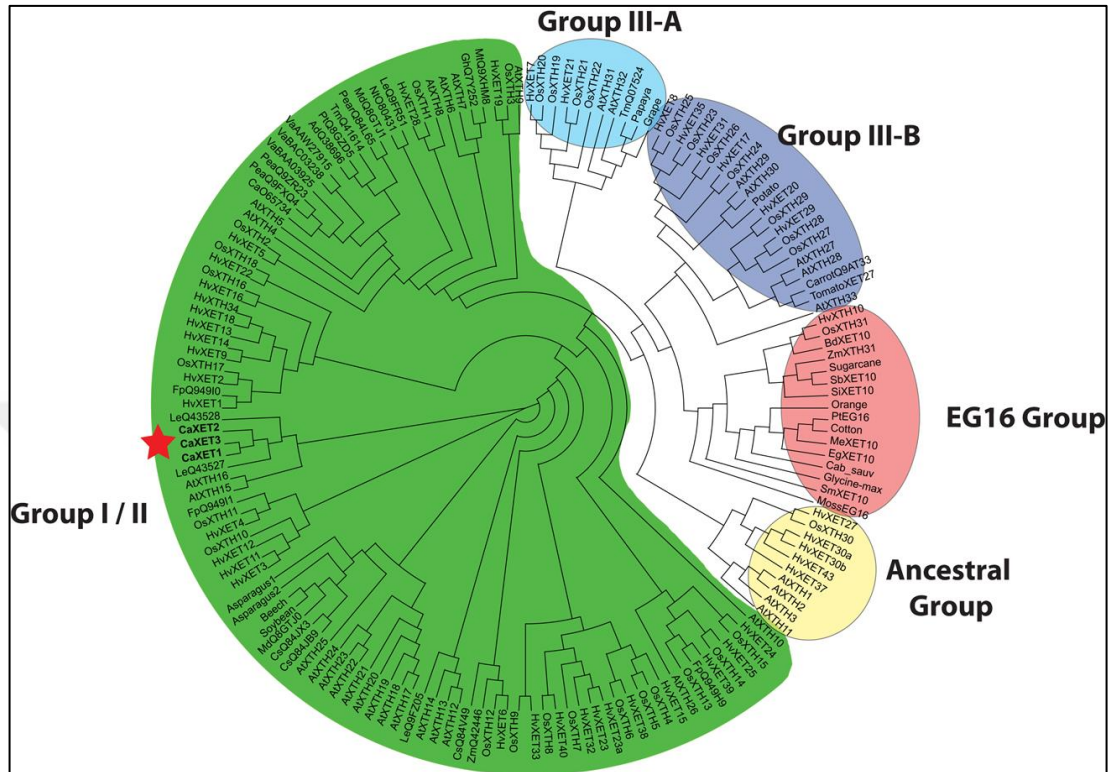


Figure 1.11. Phylogenetic tree of various GH16 plant enzymes showing the standard Groups I/II, IIIA and IIIB that contain XET-acting enzymes. The enzymes included in abiotic stress studies are marked on the tree with red star.

Comparison of rice (*Oryza sativa*; monocot) and Arabidopsis (*Arabidopsis thaliana*; dicot) genomes revealed that groups I and II are indistinguishable. *XTH* genes expressed from both groups all displayed specifically XET activity with no clear information about substrate specificities. TmNXG1 from nasturtium (*Tropaeolum majus*) and VaXGH from azuki bean (*Vigna angularis*) from Group III-A members are considered to be typical XEHs with their hydrolytic activity [87]. On the other hand, *AtXTH27* and *HvXTH8* genes from group III-B was expressed heterologously and shown to exhibit XET activities [88, 89]. Early vascular plants (lycophytes) *Selaginella kraussiana*, *Selaginella moellendorffi*; and *Physcomitrella patens* are the oldest plants to harbour *XTH* genes. The *XTH* gene similarities between these plants suggest that group I is the original *XTH* gene subfamily and that group II and III-B have risen from group I and separated afterwards. The XEH

activity showing group III-A is not present in early plants which supports the fact that XEH activity rose from XET activity. That is because before transglycosylation, the substrate molecule should be cleaved [85, 90]. Monocot and dicot plants all harbour group I genes which leads to the conclusion of ancestral gene being a precursor gene for both plants. Despite the fact that the xyloglucan level is lower in monocots, conserved sequences indicate similar roles in different species. Even the amino acid sequences are not similar, almost all XTHs exhibit hydrophobic behaviour and were shown to encode signal peptides. Signal peptides are important in the targeting of the nascent polypeptide chain to the endoplasmic reticulum leading to transportation of the newly made enzymes to the cell wall. According to a study with *Arabidopsis* genes, unlike signal peptide sequences, mature protein sequences are more conserved [80]. *Arabidopsis* was reported to have 33 open reading frames (ORFs) encoding *XTHs*. Among them *AtXTH17*, *AtXTH18*, *AtXTH19* and *AtXTH20* are the closest ones depending on their phylogeny and they play important roles in root specific elongation processes. There are more than 31 rice (*Oryza sativa*) ORFs that are also described as *XTHs* and the size of the gene family is close to that of *Arabidopsis thaliana*. *OsXTH18* and *OsXTH19* are particularly produced in elongating tissues and in addition to that, *OsXTH8* expression levels are controlled by gibberellic acid. These all lead to the idea that XTHs functions differ according to diverse cell types [91, 92]. On the other hand, not all the XTH enzymes in the phylogenetic groups have activity; some of the enzymes have been reported not to be active on any substrates [81]. Cho and colleagues identified three different *XTH* genes (*CaXTH1*, *CaXTH2* and *CaXTH3*) in pepper (*Capsicum annuum*) whose expression level was shown to be increased in response to abiotic stress conditions like water loss, salinity, draught and temperature [16].

## **1.7.2. Activity**

### ***1.7.2.1. Xyloglucan Endotransglycosylase Activity***

The enzyme uses two substrates molecules when performing XET activity: donor and acceptor. The enzyme cleaves the donor from a site preferably close to the reducing end, and then transfers the acceptor molecule which has low *Mr* (relative molecular mass). The activity can be proven with assays determining size-change and usage of <sup>3</sup>H or fluorescein



### 1.7.2.2. Xyloglucan Endohydrolase Activity

Sometimes the enzyme does not transfer another xyloglucan molecule after the cleavage of the donor, but instead attaches a H<sub>2</sub>O molecule to the cleaved site and shortens the chain irreversibly (Figure 1.13).

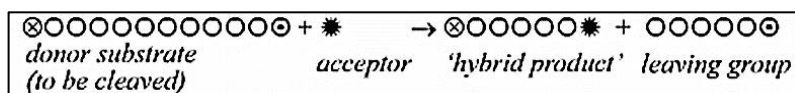


Figure 1.13. Figurative explanation of product formation from hydrolase activity.

Reducing ends are on the right [81].

Some XTHs does not show measurable hydrolase activity. Still enzymes from pea stems, nasturtium seeds, ripening tomato fruit and azuki beans were reported to display XEH activity. Most of the time, the hydrolase activity was displayed when there are no XGOs in the environment. In spite of that, an XTH from azuki bean stem showed XEH activity instead of XET activity even when there were XGOs present [87].

### 1.7.2.3. Substrate Specificity

XTH enzymes mostly prefer xyloglucans as donor substrate and very rarely Glc<sub>8</sub> based XGOs. Substrate specificity varies according to the structure of xyloglucan. Fuc residues in the structure may affect the binding of the enzyme to the substrate. XTHs from tomato prefer non-fucosylated xyloglucan, which is common in the Solanaceae family. There are XTHs which prefer to use high *Mr* xyloglucan. AtXTH22 was reported to show higher specificity to high *Mr* xyloglucan other than XLLG oligosaccharide [99]. Generally, the preferred donor substrate for most XTHs is high *Mr* donors and for some, lower *Mr* donors, although this is more like a tolerance rather than a preference. In some cases the non-reducing end of the donor may be considered as an acceptor by the enzyme. Thereby, calculating the *K<sub>m</sub>* value for an XTH is baffling.

Glc<sub>4</sub> containing XGOs with no necessity of reducing end are considered to be the appropriate acceptors for XTH enzymes. For enzyme activity, it is important for an acceptor to be rich in Xyl/Glc content in the backbone. De-xylosylation and shortening

might affect the binding to the enzyme. However, Gal and Fuc residues are not strictly required for this function [93, 97, 100-102].

### 1.7.3. Mechanisms

XTHs are located in the apoplast, outside the plasma membrane with an optimum pH varying from 5 to 6. Highly conserved amino acid sequences of the catalytic site are suggested to be DEIDFEFLG or DEIDIEFLG. Alteration of the first acidic amino acid (first E in DEIDFEFLG) Glu to Gln prevents the enzyme's XET activity showing that this amino acid is imperative for XTH-xyloglucan interaction. A glycosyl ester bond is formed between reducing part of the donor substrate and the side chain of the glutamate during enzyme-substrate interaction. This complex was reported to be stable for a while (minute to hour) until the XGO acceptor was added. The reaction steps are summarized in Figure 1.14. Independent binding of both donor and acceptor molecules to the enzyme has been indicated using poplar XET. On the other hand, there is not enough information to prove that an acceptor substrate binds to the enzyme in the absence of a donor substrate and when the reaction is complete product is released from the active site [103-105].

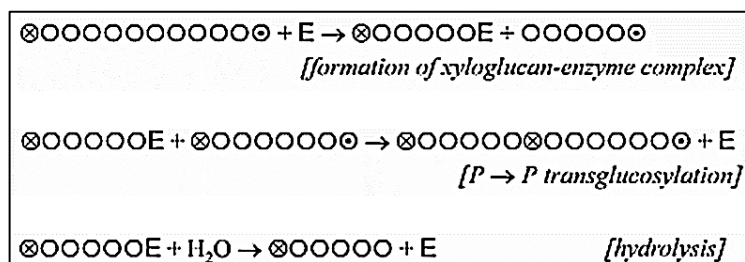


Figure 1.14. Enzyme binds to the donor substrate and cleaves it later on transglycosylation or hydrolysis activity is carried out. E stands for the enzyme [81].

An XET from the *Populus tremula* x *Populus tremuloides* hybrid (PttXET16-34) and a typical XEH from nasturtium (TmNXG1) have been structurally analysed. X-Ray crystallography results displayed a  $\beta$ -jellyroll fold for both of the enzymes similar to non-plant GH16 members. PttXET16-34 and TmNXG1 differ from GH16 enzymes depending on their specificity to highly branched substrates. The XETs and XEHs carry a major loop deletion in the active site which improves their interest against wider range of substrates

[106, 107]. The negative subsites in the molecule play an important role in binding donor substrate on the cleavage site close to the non-reducing termini. A C-terminal extension is located near the positive subsites and has been defined as a noticeable characteristic of XET enzymes. The sequence increases the substrate binding cleft with the help of an extra  $\beta$ -strand at the end of an  $\alpha$ -helix (Figure 1.15). Disulphide bonds between conserved Cys residues provide stabilization for the enzyme structure [80, 108]. N-glycan in the structure is responsible for proper protein folding and stability. Group I and II enzymes harbour one particular conserved N-glycosylation site just after the active site motif, however nearly all group III-A enzymes including TmNXG1 do not seem to have this site. Group III-B members exhibit N-glycosylation on the other site of the active cleft [85, 88, 109]. Including XET enzymes in a glycoside hydrolase family might seem irrelevant, but transglycosylation activity is a result of typical retaining catalytic mechanism displayed in all GH16 enzymes. The first step of the mechanism is the generation of covalently bonded enzyme-substrate complex. Covalent bonds in the complex are broken down either by the addition of water and leads to hydrolysis, or another xyloglucan acceptor molecule and leads to transglycosylation. In Figure 1.6, schematic expression of xyloglucan (glucosyl units of xyloglucan in blue and xylosyl units in orange) binding to the enzyme was shown. After binding, the substrate is cleaved and a covalent glycosyl-enzyme intermediate is formed (covalent bond in red). In the last step enzyme-substrate is broken down by water (XEH activity) or an acceptor molecule (XET activity) (Figure 1.16).

Glu-85 in PttXET16-34 plays an important role in the first step of the catalytic mechanism as the anomeric carbon of the Glc ring is attacked by this catalytic nucleophile. Glu-89, on the other hand, protonates the xyloglucan chain leaving the positive subsites and activates the newly arriving acceptor molecule. Asp-87 is located on the same surface of  $\beta$ -strand as Glu-85 and Glu-89 [108, 110]. The exact role of this amino acid has not been proposed, but like other GH16 enzymes it is thought to regulate the ionization state of Glu-85 [106].

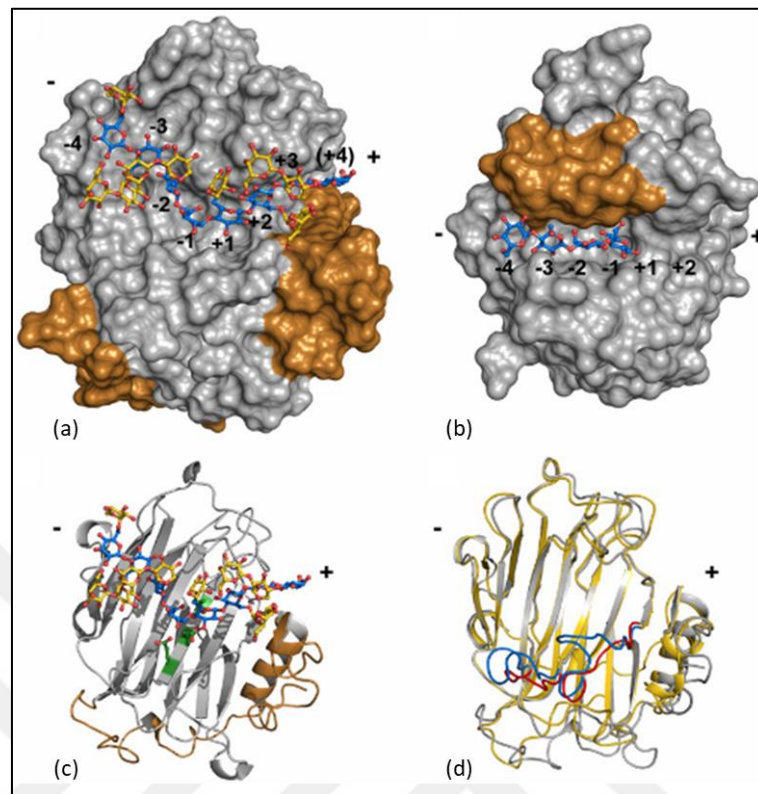


Figure 1.15. Structures of XTH enzymes and a closely related GH16  $\beta$ -(1 $\rightarrow$ 3);(1 $\rightarrow$ 4) glucanase. (a) surface representation of PttXET16-34. C-terminal extension shown in copper, in silver XLLGXLLG oligosaccharide (glucosyl backbone in blue and xylosyl and galactosyl units in gold). (b) surface representation of a  $\beta$ -(1 $\rightarrow$ 3);(1 $\rightarrow$ 4) glucanase in silver, with the loop narrowing the negative subsites in copper. (c) cartoon of PttXET16-34 showing the structure of the C-terminal extension (copper) and the catalytic amino acids (green) with a bound XLLGXLLG oligosaccharide. (d) overlay of a XET, PttXET16-34 (silver with red loops), and an XEH, TmNXG1 (gold with blue loops) [84].

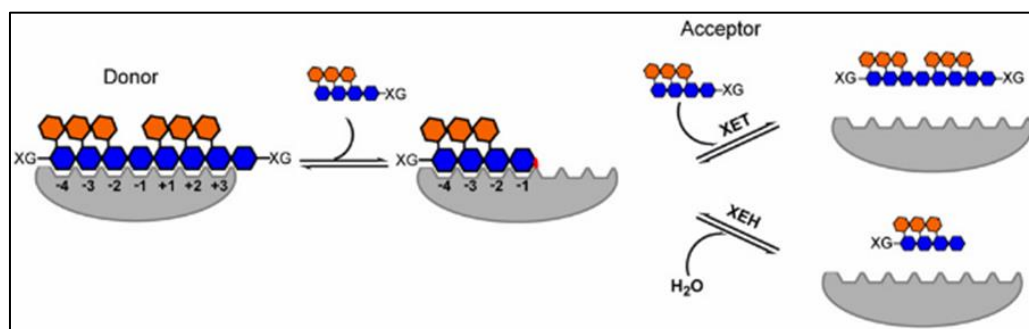


Figure 1.16. A schematic demonstration of XET and XEH mechanism [84].

## 1.8. HETEROLOGOUS PROTEIN PRODUCTION AND PICHIA PASTORIS

The methylotrophic yeast *Pichia pastoris* was first developed in the early 1970s and it became the source of interest since then due to being a preferable host for heterologous protein production. Three basic characteristics make the yeast a suitable host for heterologous expression: (1) genetic modification of this organism is easy due to the high transformation rate and gene targeting, (2) high level protein production can be obtained, and (3) most importantly post-translational modifications (creation of disulphide bonds, cleavage of newly produced protein and glycosylation) which are required in eukaryotic organisms after translation can be efficiently performed [111-113].

Heterologous production of a protein is summarized in four stages: cloning of the DNA sequence into a vector with an appropriate promoter and transcriptional termination sequences; transformation of the vector including protein coding DNA sequence to the yeast and provide stability; expression of the heterologous protein in an appropriate culture environment; and obtaining foreign protein in a pure and concentrated form [114]. *Pichia pastoris* has certain useful secretory pathways for newly synthesized foreign proteins. The proteins are guided into these pathways via signal sequences which makes it easy to purify proteins. *Pichia pastoris* does not usually secrete native proteins; therefore it is highly favoured to obtain heterologous proteins from the supernatant [111, 115].

An inducible promoter is required to control the heterologous protein production because it helps to reduce the selection of non-expressing cells throughout the cell growth, before induction. The *AOX1* (alcohol oxidase 1) promoter which is induced in the presence of methanol is considered to be an effective promoter since its highly regulated [112, 114]. When the case is expressing a foreign protein, a vector should also include a multiple cloning site (MCS) for cloning of the protein coding gene with a transcriptional termination sequence and a marker gene for selection of the transformant colonies. Vectors might also include a replication origin for reproduction in bacteria cells. However, if the plasmid or sections of it are incorporated into the genome once the plasmid is inside the cell, a replication origin is not required which is the case for yeast cells. The expression yield varies according to the amount of the transformed gene. Transformation of the foreign gene to *Pichia pastoris* can be obtained either by electroporation or lithium acetate treatment for their ease and cost efficiency, respectively [116, 117]. In spite of being such a

suitable host, there are some disadvantages in using *Pichia pastoris*. The yeast does not have the chaperone proteins that are required for proper folding of some higher eukaryotic proteins. Another problem is the secretion of the newly expressed foreign proteins into the culture medium and degradation of these proteins. Prevention of these proteins from degradation by pH and temperature rearrangement with along the optimum media conditions and using protease deficient strains can ease to overcome these problems [112, 117-120]. Certain strains of *Pichia pastoris*, such as SMD1168H, do not express the vacuolar aspartyl protease Proteinase A which is a protease in in own right and is also capable of activating other proteases. Thus, Proteinase A deficient strains show greatly reduced protease activity, a distinct advantage for a protein expression host.

#### **1.8.1. AOX1 Promoter Used in *Pichia pastoris***

One of the most important characteristics in *Pichia pastoris* is that having the alcohol oxidase 1 (*AOX1*) promoter which is incorporated in the pathway of utilizing methanol as a carbon source. The *AOX1* promoter is one of the most tightly regulated and effective promoters in eukaryotic cells allowing high expression of the heterologous protein via induction with methanol [114, 121, 122]. Up to 35 per cent of the produced proteins are attributed to the alcohol oxidase 1 in the cell. Only a small proportion of AOX2 protein was shown to be effective in methanol-grown cells, though they are both responsible for the alcohol oxidase activity and expressed up to the level of 95 per cent of the cell proteins [111, 122].

## 2. MATERIALS AND METHODS

### 2.1. TARGET/HOST SELECTION AND CODON OPTIMIZATION FOR HETEROLOGOUS PROTEIN PRODUCTION

SIXTH4 and OsXTH1 XET enzymes from agriculturally and scientifically important tomato (*Solanum lycopersicum*) and rice (*Oryza sativa*) plants were chosen for heterologous protein production in the methylotrophic yeast *Pichia pastoris*. In addition, the CaXTH1, CaXTH2 and CaXTH3 enzymes that have been shown to increase tolerance to abiotic stress in Arabidopsis and tomato [9, 16] were chosen for study from the pepper plant (*Capsicum annuum*). Gene sequence coding regions were checked and, since only the mature enzyme sequence is required, the signal peptide coding region was removed. Even though all 20 amino acids commonly exist in organisms, the preference of the codons representing different amino acids changes from organism to organism, and therefore different organisms have different amounts of the various tRNAs. For this reason, codon optimization of the plant genes according to the host organism *Pichia pastoris* was performed by the “GeneScript” company, prior to gene synthesis. The genes were cloned into the yeast expression vector pPicZ $\alpha$ -C and arrived. The cloning region of the vector included six contiguous codons for histidine amino acids which resulted in the expressed protein having a 6X-His tag at the C-terminal end which facilitated the detection and purification processes.

### 2.2. HEAT SHOCK TRANSFORMATION AND OBTAINING PLASMIDS

Lyophilized plasmids carrying the genes of interest were dissolved in ultra-pure water and transformed into *E. Coli* DH5 $\alpha$  via heat shock transformation [123]. Competent cell preparation for transformation was performed according to the instructor’s notes [124]. Transformed bacterial cells were grown in 5 ml Low Salt LB media including zeocin (EasySelect *Pichia* Expression Kit Manual, Invitrogen, CA). Plasmid isolation was performed using the “Qiagen QiaPrep Spin Miniprep” kit (Cat no: 27106, Qiagen Group)

and “Nucleospin Plasmid Isolation Kit” (Cat no:740588). Glycerol (30 per cent) stocks of the transformant cells were prepared and kept at -80°C.

### **2.3. TRANSFORMATION INTO YEAST**

pPicZ $\alpha$ -C plasmids including *OsXTH1*, *SIXTH4*, *CaXTH1*, *CaXTH2* and *CaXTH3* genes were obtained from *E. Coli* cells. Digestion of 10  $\mu$ g plasmid DNA was achieved using DraI restriction enzyme to linearize the plasmids. Linearized plasmids were then transformed into the yeast *Pichia pastoris* SMD1168H using an electroporation method [125]. “Bio-Rad Gene Pulser” with values of 1,5 kV, 25  $\mu$ F and 200  $\Omega$  was used for transformation. Streaking on YPDS + zeocin agar plates was done to determine the transformant colonies. To check the transformation efficiency, genomic DNA isolation was performed from yeast cells using lichenase enzyme. After that PCR was performed from isolated DNA using  $\alpha$ -factor 5’ and AOXI 3’ primers (Invitrogen, EasySelect Pichia Expression Kit Manual).

### **2.4. SELECTION OF THE ACTIVE ENZYME PRODUCING COLONIES**

#### **2.4.1. Selection of OsXTH1 and SIXTH4 Producing Colonies**

Selection of the transformant colonies was performed via subculturing on YPDS + zeocin agar plates according to the instructions from the “EasySelect Pichia Expression Kit, Invitrogen” (#K1740-01). Transformant colonies that grew on YPDS + zeocin plates were used to start cultures in 10 ml BMGY media. Cells were grown at 30°C and 200 rpm until OD<sub>600</sub> was between 2 to 6. After reaching the correct OD<sub>600</sub>, cells were precipitated via centrifugation and resuspended in 10 ml BMMY media to an OD<sub>600</sub> value of 1. Incubation process continued at 22°C and 135 rpm for 5 days. During that time period, induction via methanol addition (1 per cent of the media) was performed every 24 hours. At the end of the incubation process, cells were precipitated with centrifugation and the supernatant was used for further analysis.

#### **2.4.2. Selection of CaXTH1, CaXTH2 and CaXTH3 Producing Colonies**

Transformant colony selection was performed according to the instructions from the “EasySelect Pichia Expression Kit, Invitrogen” as described before. Selected colonies were used to start cultures in 10 ml BMGY media. Cells were grown at 30°C and 170 rpm until OD<sub>600</sub> values of the cultures were between 2 to 6. After reaching the correct OD<sub>600</sub>, cells were precipitated via centrifugation and resuspended in 10 ml BMMY media to an OD<sub>600</sub> value of 1. Incubation process continued at 22°C and 150 rpm for 5 days. During that time period induction via methanol addition (1 per cent of the media) was performed every 24 hours. At the end of the incubation process, cells were precipitated via centrifugation and the supernatant was used for further analysis.

#### **2.4.3. TCA-Acetone Precipitation, SDS-PAGE, Western Blotting**

TCA- acetone precipitation was applied to precipitate the proteins in the supernatant. A 900 µl aliquot of the supernatant was mixed with 100 µl TCA and incubated on ice for 1 hour. After the incubation, proteins were precipitated via centrifugation at 12000 g, at 4°C, for 10 minutes. Acetone (800 µl) was added to the tube and incubated overnight at -20°C. Undissolved proteins were then pelleted using centrifugation at 6500 g, at 4°C, for 10 minutes. The acetone wash step was repeated twice with a time interval of 30 minutes. After evaporation of all the acetone, the proteins were dissolved in ultrapure water. In order to see which culture has the protein bands of interest, SDS-PAGE gel electrophoresis was conducted using a Hoefer Minigel System attached to a Biorad Universal power source. Purified proteins were mixed with 2x Laemmli loading buffer and separated in a 12 per cent polyacrylamide gel. Visualization was achieved with either Coomassie Brilliant Blue or Silver Staining methods. Polyacrylamide gels were stained with Coomassie Brilliant Blue dye after electrophoresis and destained with ultra-pure water until the background was clear. For Silver Staining, gels were incubated in fixation solution (30 per cent EtOH, 10 per cent acetic acid) for 1 hour following electrophoresis. Then, fixation solution was changed and gels were left incubating in the fixation solution overnight. Next day, gels were washed with ultra-pure water and incubated in 50 ml 0,8 mM sodium thiosulphate for 1 min. After washing with ultra-pure water, gels were stained with 12 mM

AgNO<sub>3</sub> solution for 40 min. Following staining step, gels were washed with ultra-pure water and then incubated in developer solution (6 gr K<sub>2</sub>CO<sub>3</sub>, 50 µl formaldehyde, 25 µl 10% sodium thiosulphate in 200 ml ddH<sub>2</sub>O) until the band structures were sufficient. After that gels were incubated in stop solution (4 per cent Tris base, 2 per cent acetic acid) and washed with ultra-pure water. To confirm the protein expression results, Western blotting procedure was also performed using a Thermo Pierce Power Blotter (25 V, 30 min) and “TransBlot Turbo Transfer Pack” 0,2 µm nitrocellulose membrane. After transfer, membrane was left for incubation in blocking solution (3 per cent (w/v) non-fat milk powder/TBST) overnight. The membrane was then treated “Abcam Anti-6X His” antibody for 1 hour and images were taken using Image Lab software, right after the Amersham ECL Prime Western Blotting Detection Reagent (GE Healthcare Cat. No. Rpn232) was added.

A 2 µl aliquot of each supernatant was used for enzyme activity testing. Enzyme reactions were set up incubating 10 µl 0,4 per cent (w/v) donor substrate, 1 µl 50 µM sulforhodamine-tagged acceptor substrate and 2 µl of the culture supernatant at 30°C for 16 to 24 hours. Reactions were stopped via addition of 6 µl 90 per cent formic acid.

## 2.5. PREPARATION OF DONOR AND ACCEPTOR SUBSTRATES

All the donor and acceptor substrates used in this study were obtained as a kind gift from Megazyme (Megazyme International Ireland) company except for hydroxyethyl cellulose which was purchased from Fluka (Sigma-Aldrich). As acceptor substrates 1→4-β-mannotetraose (MT), 1→4-β-cellotetraose (CT), 1→4-β-D-xylotetraose (XT), xyloglucan oligosaccharides (XGOs), galactosyl mannotriose (GM3), 1→3;1→4-β-glucotetraose A (BA), 1→3;1→4-β-glucotetraose B (BB), 1→3;1→4-β-glucotetraose C (BC), laminaritetraose (LT), xyloglucan heptasaccharides (X7), and di-galactosyl mannopentaose (DGM) sugars were used. Oligosaccharides were tagged with the fluorescent dye sulforhodamine [126]. Prepared stocks were kept at -20°C and aliquots were diluted to 50 µM concentration and kept at +4°C until use. Hydroxyethyl cellulose (HEC), konjac glucomannan (KGM), tamarind seed xyloglucan (TXG), wheat arabinoxylan (WAX), barley β-glucan (BBG), carob galactomannan (CM), guar galactomannan (GM) and lupin galactan (LG) polysaccharides were used as donor polysaccharides. All donor substrates

were prepared at 0,8 per cent (w/v) concentration according to the manufacturers' instructions and diluted to 0,4 per cent (w/v) by mixing with 0,2 M ammonium acetate in 1:1 ratio. The pH of the ammonium acetate buffer that was used in dilution was arranged depending on the enzyme's optimum working pH.

## **2.6. HPLC ANALYSIS**

Enzyme activity analysis was performed using an "Agilent 1100 Series" high pressure liquid chromatography (HPLC) system. The chromatography system included an FLD fluorescence detector. The sulforhodamine fluorescent dye which was used in detection process is known to excite at 570 nm wavelength and emit light at 590 nm wavelength. To analyse the enzyme reactions, separation of fluorescent labelled polysaccharides and oligosaccharides was conducted using a BioSep-SEC 4000 column, 75x7,80 mm (Phenomenex, Torrance, CA) with a mobile phase comprised of 80 per cent 0,1 M pH 6,0 ammonium acetate and 20 per cent acetonitrile in 0,5 ml/min flow rate. Evaluation was performed using the ChemStation software program (Agilent Technologies, Palo Alto, CA). The 19 µl reaction volume was increased to 30 µl via the addition of 11 µl dH<sub>2</sub>O, and 15 µl of this mixture was injected by the device.

## **2.7. LARGE SCALE PROTEIN PRODUCTION AND PURIFICATION**

Active enzyme producing colonies were chosen after HPLC analysis and large scale production was achieved. Total final culture volumes were ~1 L for OsXTH1 and SIXTH4 enzymes, and ~2 L for capsicum genes, generally as 200ml cultures in 1 L flasks. Production was started with small scale (200-300 ml) BMGY culture. After reaching the correct OD<sub>600</sub> value culture, the media was changed to BMMY and the production was carried out as described previously. On the 5<sup>th</sup> day of the production, cells were pelleted via centrifugation at 3220 g for OsXTH1 and SIXTH4, 10000 g for CaXTH1, CaXTH2 and CaXTH3 for 10 minutes and supernatants were filtered using 0,2 µm RC filter (Sartorius AG, Germany) into new shot bottles. Protein precipitation was performed with an ammonium sulphate precipitation method. Culture supernatants were treated with ammonium sulphate at 4°C by adding ammonium sulphate gradually, until the

concentration reached 85-90 per cent (w/v). Afterwards, culture proteins were pelleted via centrifugation at 12000 g, +4°C for 20 minutes. The supernatant was discharged and the protein pellet was redissolved in 20 mM sodium phosphate buffer, pH 7,4. Large scale production and analysis of CaXTH2 enzyme was carried out by master's student Ezgi Türksever under my direct supervision.

Ammonium sulphate in the protein solution was removed via dialysis or by using an AKTAprime Plus (GE Healthcare) device FPLC system with a HiPrep 26/10 Desalting column (GE Healthcare). Usage of the desalting column was done according to the manufacturers' instructions. In the dialysis procedure, protein solutions were transferred into cellulose dialysis membranes and immersed into 10 L 20 mM sodium phosphate buffer, pH 7,4, at +4°C. Buffer exchange was performed twice and every 3 hours. Following dialysis, protein solution was subjected to affinity chromatography to purify 6X-His tagged heterologously produced proteins. The purification process was conducted via usage of the AKTAprime Plus (GE Healthcare) system. Protein samples were purified with a 5 ml volume HisTrap FF (GE Healthcare) column according to the manufacturers' instructions. Elution of the protein of interest was achieved using 0,5 M imidazole containing buffer via competitive binding principle. After that, buffer exchange to 0,1 M pH 6,0 ammonium acetate was performed with HiPrep 26/10 Desalting column (GE Life sciences). Obtained enzyme solutions containing OsXTH1 and SIXTH4 enzymes was concentrated using Millipore Centrifugal Units (Amicon Ultra-15 Centrifugal Filter Unit, Cat. No. UFC900324, MWCO 3000) until the volumes were ~1,5 ml. Enzyme solutions containing CaXTH1, CaXTH2 and CaXTH3 enzymes were then subjected to further purification via a polishing procedure. The enzyme solutions were passed through a Superdex 75 XK 16/100 column using the AKTAprime Plus (GE Healthcare) system. After conditioning the column with 0,1 M ammonium acetate, pH 6,0, protein samples were collected into glass tubes as the larger sized proteins would be in early fractions. Protein including fractions were combined in triplicates and concentrated via centrifuge using Millipore Centrifugal Units at 3220 g, +4°C for 40 min until the volume was 500 µl. To determine which fractions included the protein of interest, concentrated samples were loaded on to 12 per cent polyacrylamide gel and then stained with silver nitrate solution. In addition to that, proteins separated in polyacrylamide gel was transferred on to "TransBlot Turbo Transfer Pack" 0,2 µm nitrocellulose membrane using the Thermo Pierce Power

Blotter (25 V, 30 min) system and treated with “Abcam Anti-6X His” antibody. Based on the images obtained from screening, fractions revealing protein bands of interest were combined and concentrated using “Millipore Centrifugal Units” until the volume was 2 ml. Purified and concentrated enzymes were kept at +4°C until activity analysis.

Protein concentrations was assigned with Bradford analysis. A standard curve was generated using different concentrations of BSA (0,125 mg/ml BSA, 0,25 mg/ml BSA, 0,5 mg/ml BSA, 0,75 mg/ml BSA, 1 mg/ml BSA, 1,25 mg/ml BSA and 1,5 mg/ml BSA). Following that, Bradford measurements of the protein samples were taken at 595 nm wavelength and concentrations were calculated using the equation obtained from the standard curve.

## **2.8. PH OPTIMIZATION**

The optimum pH values for activity for each of the different enzymes may vary. Therefore, to determine the best working pH for each enzyme, activity tests were performed at different pH values. TXG donor stocks that were used in this process were diluted in 1:1 ratio (v/v) using McIlvaine buffer with different pH values varying from 4,04 to 8,0. Reaction volumes were completed by the addition of 1µl 50 µM XGO-SR acceptor and 2 µl of the enzyme with the required dilution factor. Incubation temperature was held at 30°C for 1 hour. Results were analysed with the HPLC system.

## **2.9. ACTIVITY ANALYSES**

Purified enzymes were used for activity analyses. Donor substrates and sulforhodamine-tagged acceptors were used to determine which donor-acceptor couple the enzyme was active on. After that, further kinetic studies were performed using these substrate couples. For each substrate couple 3 or 4 time points – including 0 hour- were determined based on the activity level of the enzyme on that specific substrate couple. Product formation was measured in fluorescence (a. u.) value for each time interval by calculating the area under the curve given in the chromatogram image from HPLC. Linear graphs of product amount (fluorescence (a. u.)) vs time were drawn. These graphics were used to calculate the enzymes’ unique activity in picokatal/mg values. In addition, picokatal/mg activity values

on different substrate couples were compared to each other by percentage type and taking activity level on expected highest activity couple, the TXG-XGO substrate couple as 100 per cent.

Enzyme kinetic studies were also performed for the produced and purified CaXTH1, CaXTH2 and CaXTH3 enzymes. For kinetic calculations, the TXG-X7 substrate couple, which showed the highest activity in substrate specificity trials, was chosen for all enzymes. Reactions prepared with TXG and X7 substrates at different concentrations were incubated at 30°C for 1 hour. Reactions were analysed using the HPLC as described before. First, the X7 concentration was kept constant at 50 µM and different concentrated TXG solutions varying from 0,05 per cent -0,8 per cent (w/v) were tested to determine the best working TXG concentration for each enzyme. Following this, the TXG concentration was kept constant at the optimum level depending on the enzyme type and enzyme reactions were set up using different concentrations of X7 solutions. Using these activity results Michaelis-Menten and Lineweaver-Burke graphics were drawn, and  $V_{max}$ ,  $K_m$ , and  $k_{cat}$  values were calculated.

## 2.10. CAPSICUM PLANT GROWTH

*Capsicum annuum* seeds were kind gifts from the “Yüksel Tohumculuk Company” and the “Menemen National Gene Bank” which included pepper seeds from 8 different varieties (Erzurum, Cila, Samuray, Aktör, Seki, Çanakkale, Kahramanmaraş, Mert). Initial germination trials were carried out in the green house to observe the germination rate of the different type of pepper seeds. Germination trials were held in soil with the temperature of 22°C and 16 hour light/8 hour dark photo-period.

Several germination methods with various environments and medias were used, depending on the further stress applications. Seeds germinations were performed on agar, MS media and perlite. To begin germination, seeds were imbibed in ultra-pure water for 24 hours to wake up the dormant seed and activate the biochemistry of the embryo. For agar germination trials, ultra-pure water including 0,5 per cent agar was used as an artificial germination environment. Before mixing it with agar, the pH of the ultra-pure water was altered to pH 5,8 using 0,1 M HCl and pepper seeds were germinated on 50 ml pH 5,8 ddH<sub>2</sub>O agar in magenta boxes [14]. Germination was achieved in Digitech DG1200 plant

growth cabinets with conditions of 22°C temperature and 50-55 per cent humidity, in the dark for 5 days. Murashige & Skoog (MS) media was also used for germination, as it has been considered to be a rich media with primary and auxiliary salts (macronutrients and micronutrients), and contains vitamins and other organic compounds in its structure. Sucrose (20 g/L) was added to the MS media as a carbon source, along with agar (0,6 per cent). The pH of the media was adjusted to pH 5,8, before sterilization by autoclave [16]. Pepper seeds were planted on to 50 ml pH 5,8 MS agar in magenta boxes and germinated in Digitech DG1200 plant growth cabinets with 22°C temperature and 50-55 per cent humidity, in the dark for 5 days. After germination, seeds were kept in a growth regime of 16 hour light/8 hour dark photo-period for 6 more days in plant growth cabinets during stress applications. At the end of this process, phenotypic results were recorded and further QPCR experiments were done.

A contamination problem was encountered during germination and growth trials on MS agar due to its rich nutrient content. To prevent this, a suitable surface sterilization method for the seed was developed after many trials, using 70 per cent EtOH and NaOCl (4 per cent Merck commercial stock) with varying concentrations for different time periods. After statistical analysis using a “Post Hoc” multiple comparison test, a method was determined and seeds were surface sterilized with incubation in 70 per cent EtOH for 1,5 min and 25 per cent NaOCl (4 per cent Merck commercial stock) for 15 min.

To obtain older pepper plants (2-4 weeks), capsicum seedlings that were germinated on MS agar media were transferred into soil-peat mix following germination in dark, and grown in the green house with a temperature varying 23°C to 28°C, 40 per cent to 50 per cent humidity and a photo-period of 16 hour light/8 hour dark. Perlite was also used as a temporary environment for seed germination. Capsicum seeds were planted in wet perlite for germination in dark for 3 weeks, in green house conditions. After 3 weeks seedlings were transferred into a soil-peat mixture or peat only. Plant growth was achieved in green house conditions as mentioned previously. When the plants were 2 to 4-week-old stress applications were performed [14].

## 2.11. SALT STRESS APPLICATIONS

Different salt stress trials were performed with ddH<sub>2</sub>O agar, MS agar and soil grown pepper plants. Following imbibition, Erzurum pepper seeds were germinated on pH 5,8 ddH<sub>2</sub>O including 0,5 per cent agar for 5 days with 22 °C temperature and 50-55 per cent humidity in dark in Digitech DG1200 plant growth cabinets and then transferred on to 0 mM (control), 50 mM and 100 mM NaCl containing pH 5,8 ddH<sub>2</sub>O agar medias and grown 6 more days with a photo-period of 16 hour light/8 hour dark. At the end of 6 days, the growth level of the roots and shoots of the seedlings were measured and statistical analysis was done using a“Post Hoc” multiple comparison test.

Based on the results of the previous trial, another trial with Erzurum variety was done with lower concentrations of NaCl in the agar media. Erzurum pepper seeds were germinated on pH 5,8 ddH<sub>2</sub>O agar medias as mentioned before and then transferred on to different concentrations of NaCl (5 mM, 10 mM, 20 mM, 30 mM, 40 mM) including pH 5,8 ddH<sub>2</sub>O agar medias and grown 6 more days in plant growth cabinets with a photo-period of 16 hour light/8 hour dark. After 6 days of growth root and shoot lengths of Erzurum seedlings were measured.

Salt stress trials on MS agar media were also held using Erzurum, Aktör, Seki, Cila and Samuray varieties. Pepper seeds were germinated on pH 5,8 MS agar in plant growth cabinets in dark as mentioned before. Seedlings were then transferred on to 0 mM, 25 mM and 50 mM NaCl containing MS agar and grown for 6 days in plant growth cabinets with a photo-period of 16 hour light/8 hour dark. After phenotypical analysis, root and leaf samples were collected, washed with ddH<sub>2</sub>O and frozen in liquid nitrogen for further experiments [9]. Experiments performed on ddH<sub>2</sub>O agar and MS agar was done duplicate and ~20 seeds were used for each variety. Salt stress experiments on agar was carried out by master's student Ezgi Türksever under my direct supervision.

Other salt stress applications were also performed with older pepper seedlings grown in soil. Upon optimizing the process different stress trials were tried, such as spraying leaves of the pepper seedlings with salt solution, or watering the soil, they were grown, with different concentrations of NaCl solutions (0 mM (control), 30mM, 50 mM, 100 mM, 200 mM and 300 mM). Phenotypic observation and further QPCR experiments were done

following the optimized salt stress experiments on soil. After optimizing the process, salt stress applications on soil were performed using Çanakkale and Kahramanmaraş pepper seedlings. Capsicum pepper seeds were germinated on perlite in green house conditions with a temperature varying from 23°C to 28°C and 40 per cent to 50 per cent humidity in dark for 3 weeks. After germination, Çanakkale and Kahramanmaraş seedlings were transferred into pots containing turf and grown in green house conditions with a photo-period of 16 hour light/8 hour dark for 3 weeks. Following growth, plants were taken out from pots and the roots were washed with water delicately to clean from remaining turf and then dunked into 200 mM NaCl solutions for different time periods (0 min (control)-10 min-30 min-120 min). After incubation in NaCl solutions phenotypic observations were done. Root and leaf samples were collected, washed with ddH<sub>2</sub>O and frozen in liquid nitrogen for storage at -80°C. Experiments were performed in duplicate and 2 seedlings were used for each time period including control for both Çanakkale and Erzurum varieties [14].

## **2.12. COLD STRESS APPLICATIONS**

To optimize the cold stress application, capsicum seedlings grown for different time periods under stress were used. Also, different sample collection methods and different cold stress conditions were used. For the initial cold stress trials, capsicum seedlings were germinated on pH 5,8 ddH<sub>2</sub>O including 0,5 per cent agar in Digitech DG1200 plant growth cabinets with 22 °C temperature and 50-55 per cent humidity in dark for 7 days. Seedlings were then transferred into pots containing a mixture of turf and soil and grown in green house conditions (23°C to 28°C temperature, 40 per cent to 50 per cent humidity and of 16 hour light/8 hour dark photo-period) for 2-4 weeks. Seedlings were then transferred into a cold-room with a temperature varying from 5°C to 7°C to create cold stress and leaf samples were collected from the seedlings at different time periods (0h-2h-4h-5h-6h-8h-12h-24h). To prevent the extra stress that would result from cutting leaves from the seedlings, experiment was repeated with Mert seedlings and different seedlings were used for each time period. Mert seeds were germinated on pH 5,8 ddH<sub>2</sub>O agar in plant growth cabinets, transferred to soil-turf mix and grown for 4 weeks in green house conditions, as described before. Mert seedlings were then transferred from green house to cold room (5°C-7°C) and leaf samples were collected at different time periods (0h-2h-4h-8h-12h-24h)

from different seedlings. However, photoperiod and humidity conditions were not possible to control in the cold room, also the temperature was not particularly stable. Therefore, to prevent inaccurate conditions and the extra stress resulted from cutting leaves from the seedlings the cold stress application was optimized, based on the previous trials.

After optimizing the process for cold stress, experiments were performed with Kahramanmaraş and Mert varieties. Pepper seeds were germinated on pH 5,8 ddH<sub>2</sub>O agar in Digitech DG1200 plant growth cabinets with 22 °C temperature and 50-55 per cent humidity in dark for 7 days. Following germination Kahramanmaraş and Mert seedlings were transferred into pots containing a soil-turf mix and grown for 3 weeks in green house conditions with a temperature varying from 23°C to 28°C temperature depending on the photoperiod, 40 per cent to 50 per cent humidity and 16 hour light/8 hour dark photoperiod. After that cold stress was applied to 3-week-old Kahramanmaraş and Mert seedlings by transferring them from green house to Aralab Fitoclima 600 plant growth cabinets. Conditions (humidity, photoperiod) of the plant growth cabinet was kept as similar with the green house, except that the temperature of the growth cabinet was arranged to 12°C in light and 6°C in dark. This arrangement of temperature was done to keep the temperature difference between the green house and the growth cabinet stable both in day time and night time [14, 16]. A control group was also included in the experiment. Control group plants were kept at the green house as the stress treatment was going on. Leaf samples were collected from stress treated and control plants simultaneously at different time points (0h-4h-8h-12h). The experiment was conducted in duplicate and one pepper seedling was assigned per one time point in order not to create leaf cutting stress on the plants. Collected leaf samples were frozen in liquid nitrogen and kept at -80°C for further experiments.

### **2.13. DROUGHT STRESS APPLICATIONS**

Mert and Cila varieties were used for drought stress applications. Pepper seeds were germinated on perlite in green house conditions with a temperature varying from 23°C to 28°C temperature and 40 per cent to 50 per cent humidity in dark and for 3 weeks. Seedlings were then transferred to pots containing turf and grown in green house conditions with a photoperiod of 16 hour light/8 hour dark for 4 weeks. Mert and Cila

seedlings were objected to drought stress after growth. Plants were taken out from pots and the roots were cleaned as delicately as possible with washing in water. After that step seedlings were left incubating on Whatman paper in plant growth cabinets with 24°C temperature and per cent 60 humidity under dim light. Water stress level was defined by reduction in fresh weight of the seedlings. For both varieties time periods to reach 5 per cent -10 per cent -20 per cent weight loss were almost the same. Therefore, leaf samples were collected at 0 min, ~6 min, ~11 min and ~40 min time periods. [16]. Collected leaf samples were frozen in liquid nitrogen and kept at -80°C for further experiments. Optimized conditions for salt, cold and salt stress applications which were followed by QPCR studies were given in a table in Appendix A.

#### 2.14. PRIMER DESIGN FOR QPCR STUDIES

Gene specific primers for *CaXTH1*, *CaXTH2* and *CaXTH3* were designed and ordered from Centromer DNA Company (Table 2.1). To prevent cross-reactivity, the primers were designed from the 3'-untranslated region since this is where it is likely to find the most sequence variation between the *XTH* genes. Primer design and validation were performed using Primer 3 program and NetPrimer, respectively. Since these genes were homologous to each other Blast studies were performed and the primer couples were checked not to comprise matching sequences. Reference genes were chosen as control genes for further QPCR studies as they should be expressed in all cells and their expression levels should not change under different circumstances. Optimization studies were held using *CaACTIN*, *CaUBIQUITIN*, *CaGAPDH*, *CaEIF5A2*,  $\alpha$ -*TUBULIN* house-keeping genes, and based on the results *CaACTIN*, *CaEIF5A2* and *Ca* $\alpha$ -*TUBULIN* were chosen for further QPCR experiments.

Table 2.1. Forward and reverse primer sequences for *CaXTH1*, *CaXTH2* and *CaXTH3* genes for QPCR studies [16].

	<b>İleri Primer Dizisi</b>	<b>Geri Primer Dizisi</b>
<b>CaXTH3</b>	GGTCTCCCAAGGCTTTCT	CCATTCATTGTTATTTTCTATTTCAAG
<b>CaXTH2</b>	ATGCAAGCGTTCAAGGTTCT	AAAACAATTCATTCTATTTCAAGATTAC
<b>CaXTH1</b>	ATGCAAGCGTTCAAGGTTCT	TTGGCAGGGGAAATGATT

## 2.15. RNA ISOLATION, CDNA SYNTHESIS, NEXT GENERATION SEQUENCING (NGS) AND QPCR

RNA isolation was conducted from leaf and root samples of stress treated and non-stress treated pepper plants using either the TRIzol method or an “iNtRON Biotechnology easy-spin (DNA free) Total RNA Extraction Kit”. A 5 µg aliquot of the isolated RNA samples was treated with DNase enzyme, and cDNA synthesis was performed using the “SuperScript® IV First-Strand Synthesis System”. The rest of the RNAs were kept at -80°C after RNA and cDNA quality was checked via agarose gel (1,5 per cent w/v) electrophoresis. Synthesized cDNAs were kept at -20°C.

Gradient PCR studies were performed to optimize the T<sub>m</sub> values of the Reference genes’ (*CaACTIN*, *CaUBIQUITIN-3*, *CaGAPDH*, *CaEIF5A2*, *Caα-Tubulin* and *Caβ-Tubulin*) primers as they were chosen control genes for further QPCR studies due to their expression stability under different conditions. PCR reactions were set up using the “Maximo Taq DNA Polymerase (Geneon)” enzyme. Products were checked via agarose gel electrophoresis. Based on the results, three reference genes (*CaACTIN*, *CaEIF5A2* and *Caα-Tubulin*) that revealed clear and sharp bands at the correct sizes were chosen for further QPCR studies and optimum T<sub>m</sub> values of the primers of these genes were determined. The same optimization studies were performed for the *CaXTH1*, *CaXTH2* and *CaXTH3* genes and the best working T<sub>m</sub> values were determined based on the agarose gel electrophoresis results.

Once the optimum T<sub>m</sub> values were chosen traditional PCR reactions were performed to bulk up the products of these genes to create calibration curves including copy numbers of the genes from 10<sup>9</sup> copies/µl to 10<sup>2</sup> copies/µl and responding cq values. After checking the product presence via agarose gel electrophoresis, reactions comprising same gene products were combined into one experiment tube as a bulk-up procedure. These reactions later on were run on the “Agilent 1260 Infinite” HPLC device using a “PLRP-S 1000A 5 µM” reverse phase column to remove impurities (primer dimers, non-specific products, buffer salts etc.) and quantify the pure gene products. Collection of the pure products was done according to the peak structures given by HPLC and the area under the curves of different products was calculated manually in arbitrary units [127].

In order to find out how many copies of the genes were included in the collected product, pUC19 vector was used as a reference. pUC19 vector was digested with HpaII enzyme and the reaction was run on the “Agilent 1260 Infinite” HPLC device using “PLRP-S 1000A 5  $\mu$ M” reverse phase column. Peak structures that were given in the chromatogram was matched with the expected fragment sizes and the areas under different peak structures was calculated and the exact size of the HpaII digestion fragments were then determined. Since the mole number of the pUC19 in the digestion reaction was already known, the weight of the fragments was calculated in nanograms. Fragment weights were then proportioned to the calculated area under the curve values to determine the sub-area unit amount per nanogram (ng/unit). Using this ratio and the area under the curve values of the collected *CaXTH2* and *CaXTH3* genes, the weight of the products was calculated in nanograms and mole amount of each gene product was determined based on their molecular weight. Following this, mole amount of the products was multiplied with Avogadro’s number and ds copy numbers of the genes were found. Solutions that contained gene products were evaporated to dryness using an “Eppendorf Concentrator 5301” and then resuspended in double distilled DNase-free water. A dilution series was created for all products from  $10^9$  copies/ $\mu$ l to  $10^2$  copies/ $\mu$ l. Using these standards and the gene specific primers QPCR reactions were set up and cq vs copy number graphics were drawn for *CaXTH2* and *CaXTH3*. Chromatogram traces obtained from the HPLC for *CaXTH1* revealed non-specific peak structures, therefore it was not used in further QPCR studies. These graphs were then used to calculate the gene expression levels from leaf and root tissues under control and stress conditions [127].

After obtaining the cDNAs from stress treated and non-stress treated tissues, QPCR reactions with primers specific to reference genes and capsicum genes were set up using “Biorad CFX96TM Real-Time System” device and “Biorad iTAO Universal SYBR Green Supermix” kit. QPCR results were analysed via the “Biorad CFX Manager” program. Using cq values of the reference genes and the “Genorm” program, a normalization factor (NF) was calculated for each sample. These NF values were applied to the cq values that were obtained from different samples using *CaXTH2* and *CaXTH3* primers to prevent any variations that may have occurred in RNA isolation and cDNA synthesis. Normalized cq values of the samples were then put into the equation of the calibration curve that were

generated for each gene and the copy numbers of the genes in the tissues were calculated in ds-DNA.

In preparation for NGS sequencing, RNA isolation methods and cDNA library synthesis were carried out in order to evaluate which methods would yield the best and most consistent results. Plant growth trials and stress treatments had determined that the greatest chance of success in terms of useful data obtained from NGS sequencing experiments would be with cold stress experiments using leaf tissue from “Kahramanmaraş” as the susceptible variety and “Mert” as the tolerant variety. In trials, RNA was isolated using different methods including a standard Trizol-type isolation, and column-based purifications using “iNtRON Biotechnology easy-spin (DNA free) Total RNA Extraction Kit” and “Norgen Plant/Fungi Total RNA Preparation Kit”. RNA from these experiments were used to create cDNA libraries for both standard PCR and QPCR testing using the “SuperScript® IV First-Strand Synthesis System”. Selected PCR products were sequenced via standard Sanger sequencing to ensure correct inserts and validate the PCR. It was determined from both running the RNA on an agarose gel, and PCR results from the cDNA libraries, that all methods/kits tested gave satisfactory quality RNA. Initial preparation of RNA for NGS sequencing was carried out as part of sample preparation for the cold-stress QPCR experiments. The quantity of RNA obtained per isolation was 40 µl of ~0,65 µg/µl for an average total of 26 µg of Total RNA. This is sufficient RNA for multiple cDNA synthesis reactions as well as giving enough for NGS sequencing. Library preparation for NGS sequencing requires >1,0µg of Total RNA, so for each sample two aliquots of approximately 1,5 µg of Total RNA was sent for NGS sequencing.

The samples used for NGS sequencing experiments were from control and stress treated leaf tissue of Kahramanmaraş and Mert varieties. Plants were grown in growth cabinets and samples taken at 0, 4, and 8 hour time points both from non-stressed (control) and cold treated (stressed) plants. Samples were taken from two duplicate plants at each time point and additional samples were taken for backup in case of RNA degradation.

RNA isolation from the samples was initially carried out using the “IntronBio Easy-Spin (DNA free) Total RNA Extraction Kit”. RNA samples were stored at -80°C until needed. A thick Styrofoam box, lined with ice blocks frozen to -80°C, was used to transport the Total RNA samples to Macrogen, Seoul, South Korea, for NGS sequencing. Enquiries into the cost of sending the samples on dry-ice showed this to be prohibitively expensive, so

standard ice blocks were used. Unfortunately, shipping through FedEx took 2 days for the samples to travel from Istanbul to Seoul so it is unknown as to what temperature the samples arrived at. Bioinformatic analyses were a combination of three steps: (1) quality checks before and after readings were aligned to reference genome, (2) determination of gene regions of interest and quantitative gene expression, (3) differential gene expression analysis and functional evaluation of the results.



### 3. RESULTS

#### 3.1. PROTEIN PRODUCTION AND ENZYME CHARACTERIZATION

##### 3.1.1. Target/Host Selection and Codon Optimization

Bioinformatics studies were performed with the selected genes (*OsXTH1*, *SIXTH4*, *CaXTH1*, *CaXTH2*, *CaXTH3*) to prepare them for cloning into the expression vector. After optimization, expected sequence length (bp) and protein weight was determined for the plant genes (Table 3.1). Signal peptide sequences of the genes were removed as well as the start and the stop codons. Signal peptide sequence and the start codon of pPicZ $\alpha$ -C was added to the 5' end and 6X-His tag was added to the 3' end of the genes. Codon optimized gene sequences that were ready for cloning and transformation were delivered in pPicZ $\alpha$ -C vector by GenScript (GenScript, NJ, USA) company.

Table 3.1. Selected plant genes for heterologous production.

Name of the gene	Plant origin	GeneBank accession number	Length (bp) after optimization	Molecular weight after optimization (kDa)
<i>OsXTH1</i>	<i>Oryza sativa</i>	Os07g0529700	837	31,15
<i>SIXTH4</i>	<i>Solanum lycopersicum</i>	NM_00124770.2	834	31,61
<i>CaXTH1</i>	<i>Capsicum annuum</i>	DQ439860.1	822	33,48
<i>CaXTH2</i>	<i>Capsicum annuum</i>	DQ439861.1	822	33,53
<i>CaXTH3</i>	<i>Capsicum annuum</i>	DQ439862.1	819	33,56

Transformation of the obtained genes were first performed with the *E. coli* cells to increase the plasmid amount. Following transformation to yeast using electroporation method, PCR was performed with  $\alpha$ -factor 5' and AOX1 3' primers to ensure the existence of the gene in yeast genome (Figure 3.1). The primer couple added an extra 304 bp sequence to the PCR product.

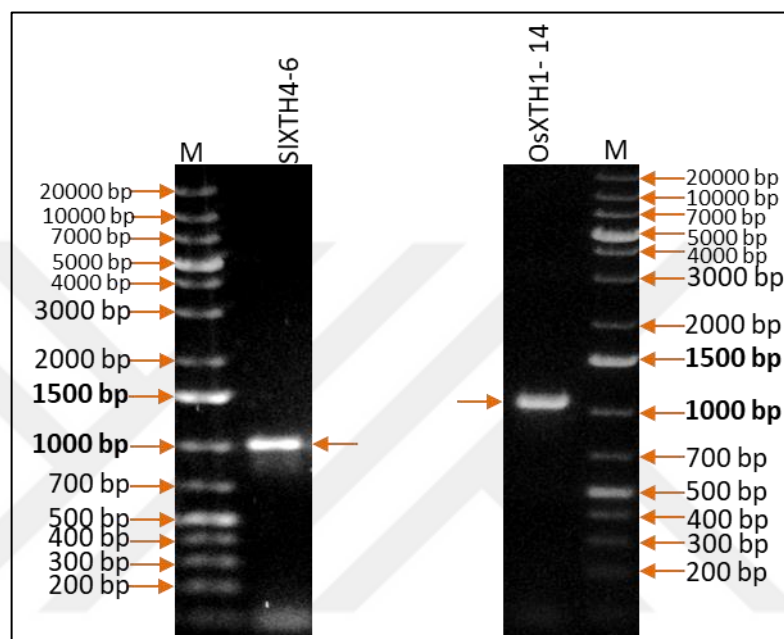


Figure 3.1. PCR results of *SIXTH4* and *OsXTH1* genes on 1 per cent agarose gel. M- Fermentas GeneRuler 1kb plus

### 3.1.2. Active Enzyme Producing Colonies

#### 3.1.2.1. *OsXTH1* and *SIXTH4* Enzymes

Several colonies were obtained for both *OsXTH1* and *SIXTH4* genes. Screening was performed with 27 colonies for each gene. For the selection of the most active enzyme producing colony, 2  $\mu$ l of the each culture supernatant was taken and incubated with 10  $\mu$ l TXG (0.4 per cent w/v) and 1  $\mu$ l of the SR-XGO (50  $\mu$ M) at 30°C for 16 hours. These enzyme reactions were then subjected to HPLC analysis. Substrates and the products in the reaction were separated with size exclusion chromatography using the BioSep-SEC 4000

Colum and fluorescent detector. Results were analysed via ChemStation software and the most active enzyme producing colonies were chosen as 14 for OsXTH1 and 6 for SIXTH4.

Protein production by colonies was proven via SDS-PAGE and Western procedures. Both procedures gave positive results for the active enzyme producing colonies. Thick band structures were observed a little higher than the expected protein size, which is most likely a result of the glycosylation process. Some of the colonies still revealed same size protein bands, even though HPLC analysis indicated that there was no activity. According to Western results, after treating the membrane with Anti-6XHis antibody, band structures that were equal to the expected protein size were observed, which ensures the protein existence in the culture for both OsXTH1 and SIXTH4 enzymes.

Production of OsXTH1 enzyme was repeated later on, in order to do further enzyme characterization. However, the enzyme seemed to lose activity quickly, and very little active enzyme remained after purification and was insufficient for further experiments.

### ***3.1.2.2. CaXTH1, CaXTH2 and CaXTH3 Enzymes***

Different numbers of transformant colonies were obtained for the *CaXTH1*, *CaXTH2* and *CaXTH3* genes. *CaXTH1* and *CaXTH2* SDS-PAGE images were quite clear for both enzymes in the screening process. No contaminating bands were observed from the gel images. For *CaXTH2* and *CaXTH1*, protein bands from the 2nd colony and the 5th colony, respectively, were the strongest looking ones (Figure 3.2). Western images of the screened colonies for both *CaXTH1* and *CaXTH2* enzymes confirmed these results (Figure 3.3). However, protein bands were visible from some other screened colonies too, but they were not as intense as the protein bands from the 2nd colony and the 5th colony which supported the fact that these other colonies did not produce as much protein as the 2nd colony and the 5th colony for *CaXTH2* and *CaXTH1*, respectively. On the other hand, western images of the protein bands from all screened colonies were not ideal. Rather than contamination smear-like structures of the protein bands were observed from the colonies that were all screened, which led to the fact that protein separation was not as efficient as it was supposed to be. The inefficiency and abnormal images of the protein bands was thought to be related to the quality of the chemicals that were used to prepare the SDS-PAGE gel and

the quality of the glass-ware. Predicted sizes of the proteins were 30,48 kDa and 30,53 kDa for CaXTH1 and CaXTH2 enzymes but band sizes were higher than 35 kDa which resulted from the glycosylation of the produced protein and additional 6X-His tag and *c-myc* epitope.

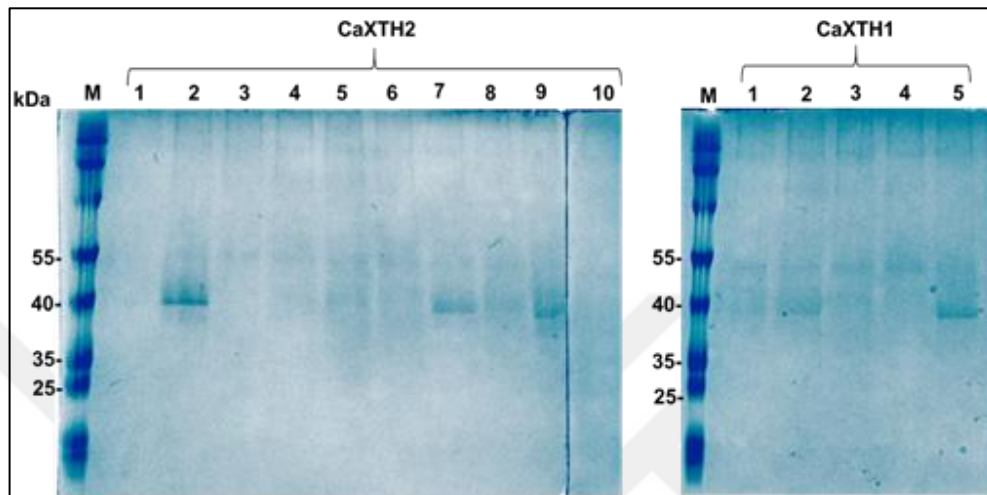


Figure 3.2. SDS-PAGE of TCA-acetone precipitated CaXTH1 and CaXTH2 proteins from small scale cultures of different colonies on 12 per cent polyacrylamide gel. M-PageRuler™ Prestained Protein Ladder.

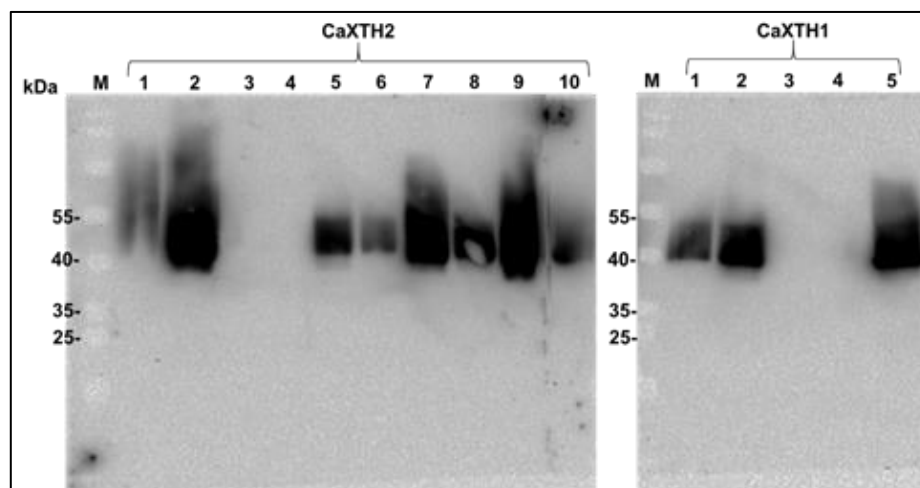


Figure 3.3. Western results of TCA-acetone precipitated CaXTH1 and CaXTH2 proteins from small scale cultures of different colonies. M-PageRuler™ Prestained Protein Ladder.

Selection of the active enzyme producing colony was performed via screening on YPDS + zeocin plates and HPLC analysis as described before. According to HPLC analysis, more than one colonies seemed to produce the active protein, which was also supported by SDS-PAGE and Western results. The most active enzyme producing colonies for CaXTH1 (Figure 3.4) and CaXTH2 (Figure 3.5) enzymes were chosen to be 5<sup>th</sup> and 2<sup>nd</sup> colon, respectively. Screening the most active protein producing colony for CaXTH3 enzyme was performed by another member of Plant Biotechnology Group and found to be 5<sup>th</sup> colony.

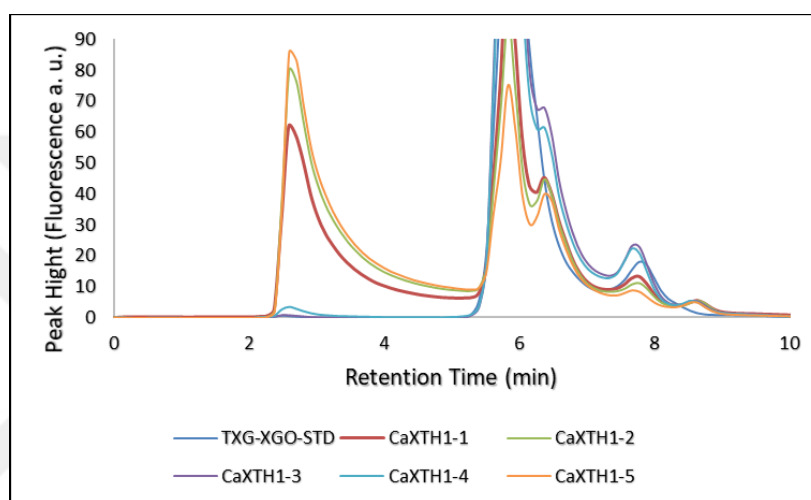


Figure 3.4. HPLC chromatogram of CaXTH1 enzyme from different colonies on TXG-XGO substrate couple.

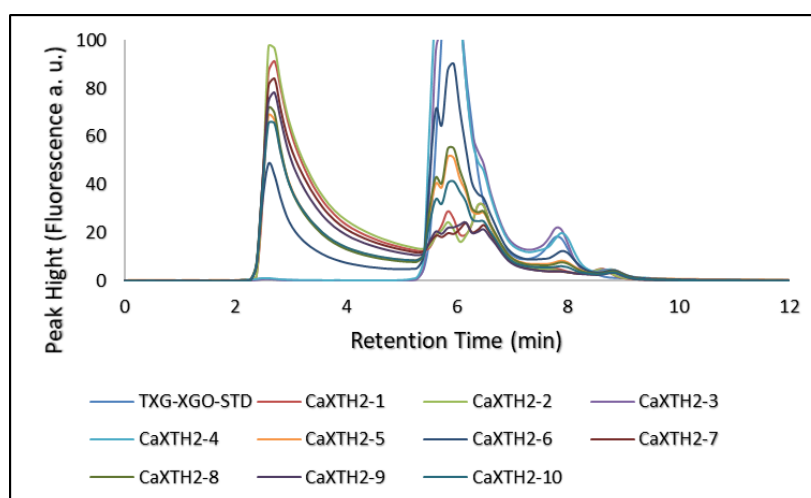


Figure 3.5. HPLC chromatogram of CaXTH2 enzyme from different colonies on TXG-XGO substrate couple.

According to the size exclusion principle the first peak, which was formed at 2,8 min, represented greater molecules, therefore it defined the product amount at the end of a reaction. Other peaks at 6 min and 7,7 min represented smaller molecules which were sulforhodamine-tagged XGO and extra sulforhodamine dye. Highest peak represented the most product amount therefore the most active enzyme.

### 3.1.3. Large Scale Production

#### 3.1.3.1. *OsXTH1* and *SIXTH4* Enzymes

After detecting the active enzyme producing colonies, large scale production was performed for the enzymes. Production was started with ~1 L culture for each enzyme. Due to some of the problems in the culturing process, like contamination or loss during filtration, culture volume in the purification process was reduced a little. After purification via affinity chromatography and buffer exchange to 0,1 M pH 6 ammonium acetate buffer, concentration of the proteins was achieved via Millipore Centrifugal Units (Figure 3.6). Protein concentrations were then measured via Bradford method and found to be 3,21 mg/ml for *OsXTH1* and 0,217 mg/ml for *SIXTH4* enzymes (Figure 3.7).

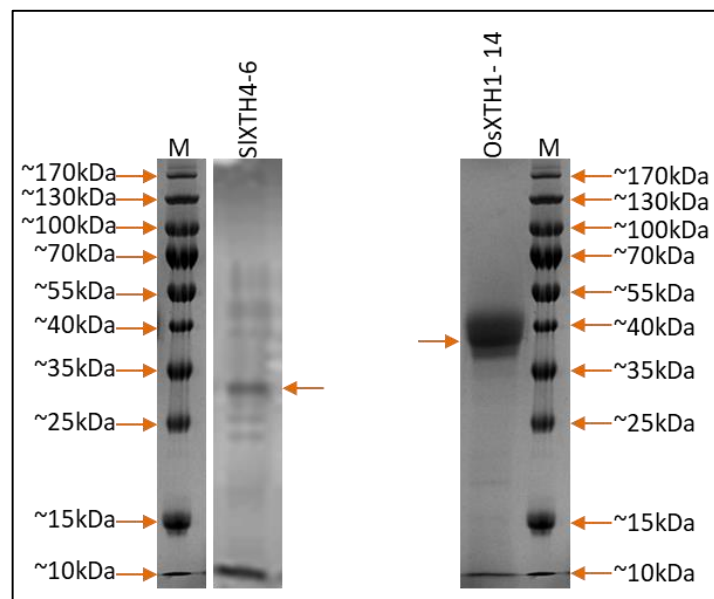


Figure 3.6. SDS-PAGE results for the active enzyme producing colonies on a Coomassie dyes 12 per cent polyacrylamide gel. M-PageRuler™ Prestained Protein Ladder.

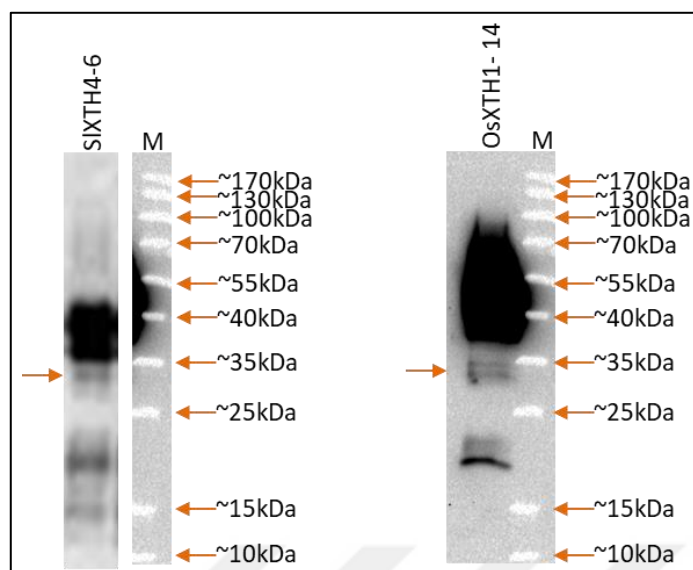


Figure 3.7. Western blotting results for the active enzyme producing colonies after treatment with Anti-6XHis antibody on a nitrocellulose membrane. M-PageRuler™ Prestained Protein Ladder.

The SDS-PAGE and Western images for purified OsXTH1 and SIXTH4 enzymes revealed fairly pure protein bands for the enzymes. Protein bands were observed above 35 kDa for both of the enzymes, which was expected. Molecular weight of OsXTH1 and SIXTH4 enzymes were 31,16 kDa and 31,62 kDa, respectively. However, 6X-His tag and *c-myc* epitope were added to the enzymes structures due to using pPicZ $\alpha$ -C vector to be able to purify and detect the proteins. It was also believed that N-glycosylation had increased the molecular weight of the proteins. Band image was stronger for OsXTH1 enzyme than it was for SIXTH4 enzyme which could be explained with higher concentration of protein as it was determined via Bradford method. However, there seemed to be some contamination for SIXTH4 enzyme in SDS-PAGE and Western images. Insignificant bad structures from 25 kDa to 70 kDa were observed for the gel image and protein bands below 25 kDa were observed for membrane image for SIXTH4 enzyme. Even though, the band structures were weak, they were still visible. SDS-PAGE image was quite pure for OsXTH1 enzyme there seemed to be no contaminating bands. On the other hand, Western image for OsXTH1 enzyme revealed contaminating bands below 25 kDa. Purification of OsXTH1 and SIXTH4 proteins was achieved via affinity chromatography and using high concentration imidazole containing elution buffer in order to induce competitive binding of imidazole to

the column to elute the proteins. Inefficiency of the purification step for SIXTH4 and OsXTH1 proteins may have been resulted from some other imidazole binding proteins. Also, non-specific band structures seen in Western images may have been degraded enzymes with their 6X-His tag intact. Polishing procedure was not applied for further purification for SIXTH4 and OsXTH1 enzymes due to the lack of equipment. Results may have been different if the polishing procedure was applied.

OsXTH1 enzyme was produced again to replicate the expression studies. The same production processes were applied for twice from the same yeast colony including *OsXTH1-4*, after the 1<sup>st</sup> production and enzyme characterization. Productions were handled as described before. The OsXTH1 enzyme obtained from both 2<sup>nd</sup> and 3<sup>rd</sup> production processes were further purified via polishing method after affinity purification. After production and purification steps were over collected fractions from the polishing procedure were combined and concentrated to 18 fractions and SDS-PAGE and western procedures were applied for fractions from both production processes. Silver staining (Figure 3.8) and Western (Figure3.9) results from the 2<sup>nd</sup> production showed that only protein revealing fractions were fraction 1, 2, 3, 4 and 5 with the first two fractions containing the most protein, but contaminated with other proteins. Since the western procedure is more sensitive, protein bands were observed for further fractions too even if they were faint. Band structures were slightly above 40 kDa.

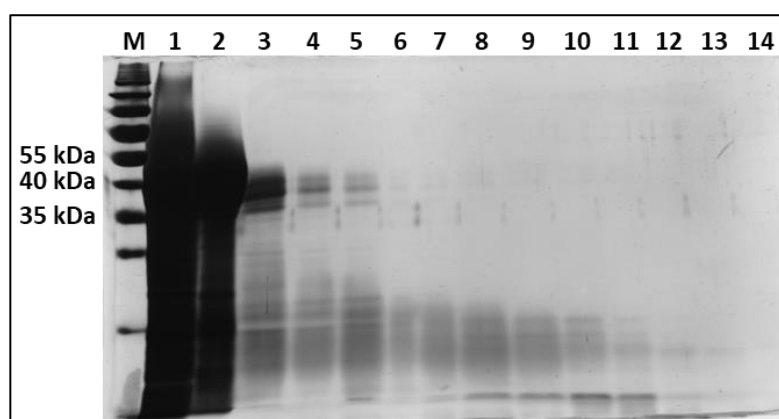


Figure 3.8. Silver staining results for OsXTH1 after Superdex 75 16/100 column chromatography, on 12,5 per cent SDS-PAGE gel. Lanes are as follows: M- PageRuler Prestained Protein Ladder, 1-14 fractions from the size-exclusion column.

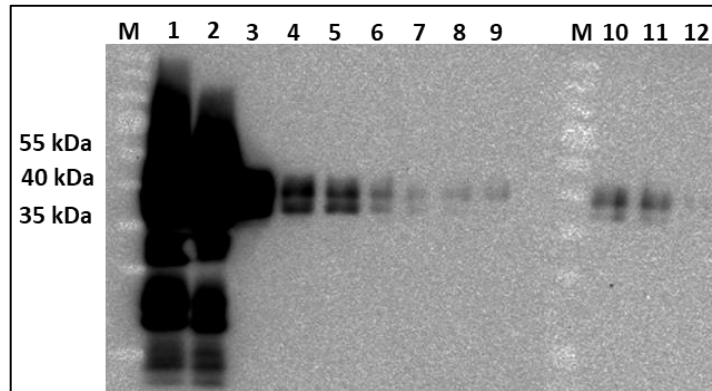


Figure 3.9. Western results for OsXTH1 after Superdex 75 16/100 column chromatography, on nitrocellulose membrane. Lanes are as follows: M- PageRuler Prestained Protein Ladder, 1-12 fractions from the size-exclusion column.

First two fractions revealed the most protein from the 2<sup>nd</sup> production process, however it was contaminated with other proteins. Therefore, these fractions were not taken and combined to other fractions. In order not to lose most of the protein of interest, these two fractions were combined together and 500  $\mu$ l of these combined fractions was used for another polishing procedure to separate more of the OsXTH1 protein. Collected fractions from the polishing procedure were combined and concentrated to 18 fractions. Later on, collected fractions from the second polishing procedure was used in SDS-PAGE to confirm the protein existence (Figure 3.10).

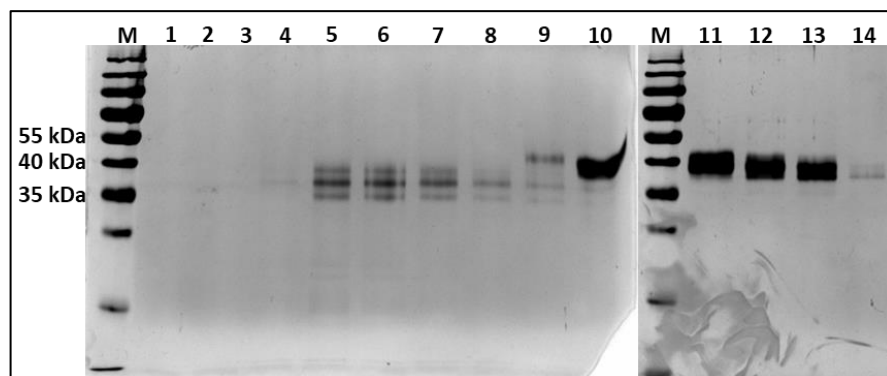


Figure 3.10. Silver staining results for the first two fractions collected from previous polishing procedure of OsXTH1 after Superdex 75 16/100 column chromatography, on 12,5 per cent SDS-PAGE gel. Lanes are as follows: M- PageRuler Prestained Protein Ladder, 1-14 fractions from the size-exclusion column.

Fractions revealed the pure protein band from the 1<sup>st</sup> and 2<sup>nd</sup> polishing procedures were combined together. However, enzyme lost its activity before starting enzyme characterization studies.

Quick loss in enzyme activity was thought to be related from 0.1 M pH6 ammonium acetate buffer, in case the buffer was not sufficient to maintain the enzyme's stability. Therefore, after the 3<sup>rd</sup> production process enzyme buffer was changed into 50 mM pH 6 MES buffer and further polishing was applied via polishing once. Silver staining and western blotting procedures were applied to the fractions obtained from polishing procedure. Fractions that revealed the pure protein bands in silver staining and Western procedures were combined together and once again the activity of the OsXTH1 protein was lost before starting the enzyme characterization.

#### ***3.1.3.2. CaXTH1, CaXTH2 and CaXTH3 Enzymes***

Large scale production was started with ~2 L of culture for CaXTH1, CaXTH2 and CaXTH3 enzymes. Large scale production and analysis of CaXTH2 enzyme was carried out by master's student Ezgi Türksever under my direct supervision. After buffer exchange to 0,1 M pH 6 ammonium acetate buffer and concentration of the proteins to ~5 ml, proteins were subjected to a further purification process called "polishing". Concentrated protein solutions were passed through "HiPrep Sephacryl S200 HR" column due to the size exclusion principle and fractionated as the bigger molecules would be in the early fractions. Further polishing step was applied to solutions including proteins, because even though the proteins of interest were purified with the help of 6X-His tag, some contamination from other proteins in culture media seemed to occur. Fractions from 9 to 118 was collected for CaXTH3 protein. These fractions later on combined and concentrated to 17 fractions using Millipore Centrifugal Units until the volume was ~1000 µl and subjected to SDS-PAGE and Western Blotting in order to determine which fractions include the purist protein of interest. According to the results that were obtained from SDS-PAGE and silver staining, 1<sup>st</sup> fraction seemed to include high amount of protein, however it was highly contaminated with other proteins in the solution (Figure 3.11). The 2<sup>nd</sup>, 3<sup>rd</sup> and 4<sup>th</sup> fractions did not seem to include pure or considerable amount of protein for CaXTH3. Protein structures became visible and started to increase in intensity from the 5<sup>th</sup>

to 9<sup>th</sup> fractions, however pure sharp band structures were not observed for these fractions. The purist protein bands were observed for the fractions 10, 11, 12, 13, 14 and 15. These results were also confirmed with Western procedure (Figure 3.12). Therefore, fractions 10, 11, 12, 13, 14 and 15 were combined and concentrated using Millipore Centrifugal Units to a volume of ~2 ml. Concentration of the CaXTH3 protein was then measured by Bradford method and found to be 0,453 mg/ml. There seemed to be two protein bands that were close to each other in size from almost all of the fractions. Those bands were identified as glycosylated and non-glycosylated forms of the enzyme. Although fractions 5, 6, 7, 8 and 9 did not include the purist form of the protein they were still considered to include good amount of CaXTH3 protein. Therefore, they were still collected and combined together separately for use in the future if needed.

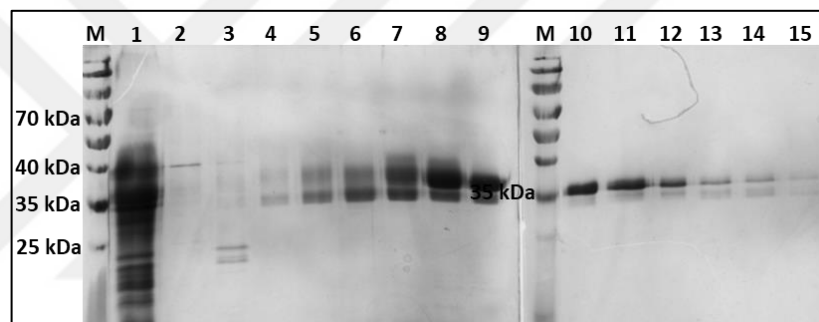


Figure 3.11. CaXTH3 fractions 1-15 that were obtained and concentrated after polishing procedure on a 12 per cent polyacrylamide gel after Silver Staining, M-PageRuler™ Prestained Protein Ladder.

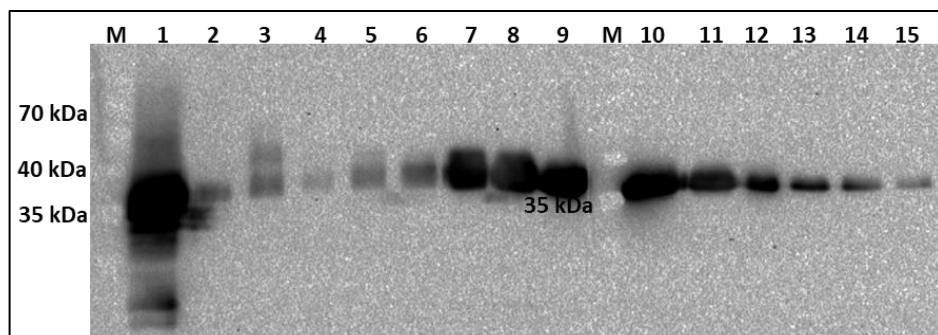


Figure 3.12. CaXTH3 fractions 1-15 that were obtained and concentrated after polishing procedure on a nitrocellulose membrane after treatment with Anti-6X His antibody, M-PageRuler™ Prestained Protein Ladder.

Although the protein's size of CaXTH3 was 30,56 kDa, band structures were observed a little higher than 35 kDa due to the glycosylation process and 6X-His tag and *c-myc* epitope addition. silver staining results showed that the purity and the concentration of the protein was decreasing in latest fractions. Weak insignificant bands that were visible in the gel structure were considered to be negligible.

Same production process was applied for CaXTH1 and CaXTH2 enzymes, as described before. Pure protein including fraction number was different for all three capsicum enzymes. The reason was that the concentrated volume of the enzymes before loading the column was not equal and the enzyme solutions did not include same amount of protein. After polishing procedure, fractions from 28 to 75 were collected for CaXTH1 protein. collected fractions were combined partially and reduced to 18 fractions by centrifugation using Millipore Centrifugal Units to a volume of ~1000  $\mu$ l. SDS-PAGE and Silver Staining were applied for the concentrated fractions. Results showed that almost all of the 18 fractions revealed the protein of interest (Figure 3.13). Fraction 17 and 18 did not indicate any specific protein bands. The purist CaXTH1 containing fractions were 5, 6, 7, 8, 9 and 10 (Figure 3.14).

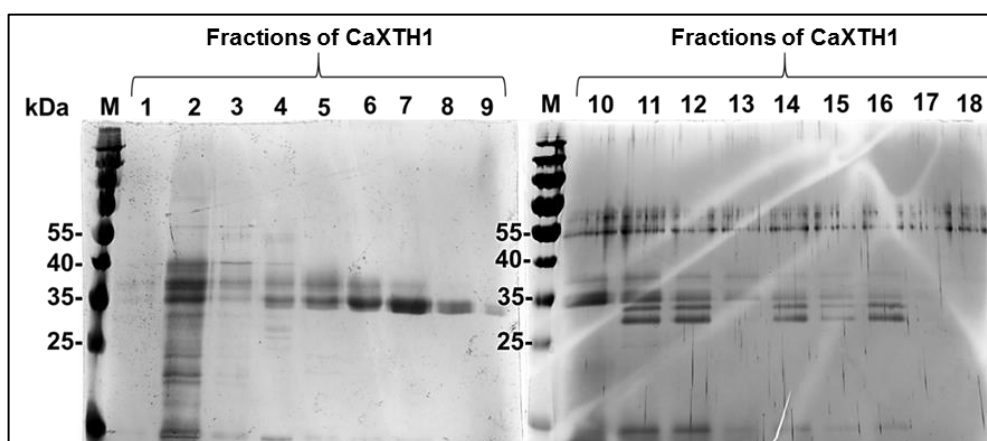


Figure 3.13. CaXTH1 fractions 1 to 18 that were obtained and concentrated after polishing procedure on 12 per cent polyacrylamide gel after Silver Staining. M-PageRuler™ Prestained Protein Ladder.

Although there seem to be the protein of interest starting from the 2<sup>nd</sup> fraction, it was contaminated with other proteins. Protein samples seem to be pure starting from 5<sup>th</sup> fraction. On the 11<sup>th</sup> fraction, contamination seemed to occur and continued for the rest of

the samples. Pollution above 55 kDa was resulted from the equipment quality and did not represent any specific case.

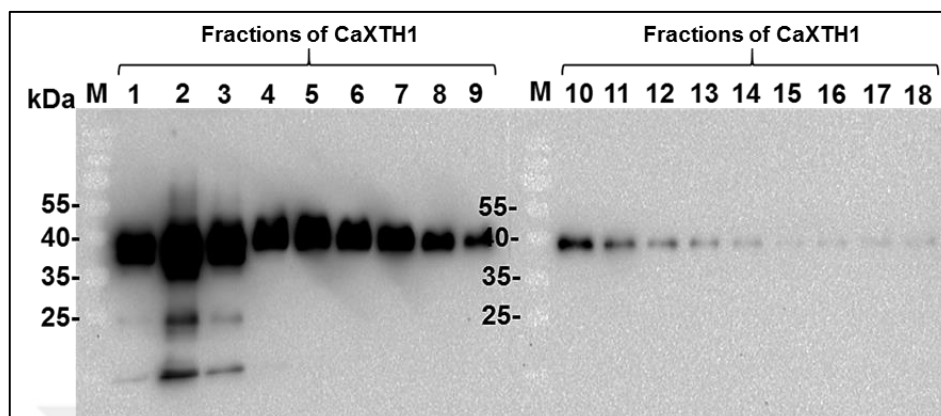


Figure 3.14. CaXTH1 fractions 1 to 18 that were obtained and concentrated after polishing procedure on nitrocellulose membrane after treatment with Anti-6X His antibody. M-PageRuler™ Prestained Protein Ladder.

All of the fractions being tested in Western Blotting were shown to have our protein. the protein amount seemed to be decreasing in last fractions. Starting from the 4<sup>th</sup> fraction protein samples seemed to be pure and the most intense band giving fraction was the 5<sup>th</sup>. Depending on the merging results of both procedures fraction 5, 6, 7, 8, 9, and 10 were combined and concentrated. Bradford method was used to measure of the concentration of CaXTH1 enzyme. Bradford measurement of the enzyme was found to be 0,224 mg/ml.

Large scale production and analysis of CaXTH2 enzyme was carried out by master's student Ezgi Türksever under my direct supervision. Fractions from 26 to 75 were collected for CaXTH2 enzyme at the end of polishing procedure. They were reduced to 17 fractions as was described for CaXTH1 and CaXTH3 enzymes. SDS-PAGE and Western Blotting results showed that only the first 9 fraction included CaXTH2. The 1<sup>st</sup> fraction did not reveal any protein bands in any procedure. CaXTH2 enzyme seemed to be getting pure starting from the 5<sup>th</sup> fraction and continued until 9<sup>th</sup> fraction even though the protein band was weak (Figure 3.15). Due to the specificity of the Western Blotting, an intense protein band was observed for the 9<sup>th</sup> fraction (Figure 3.16).

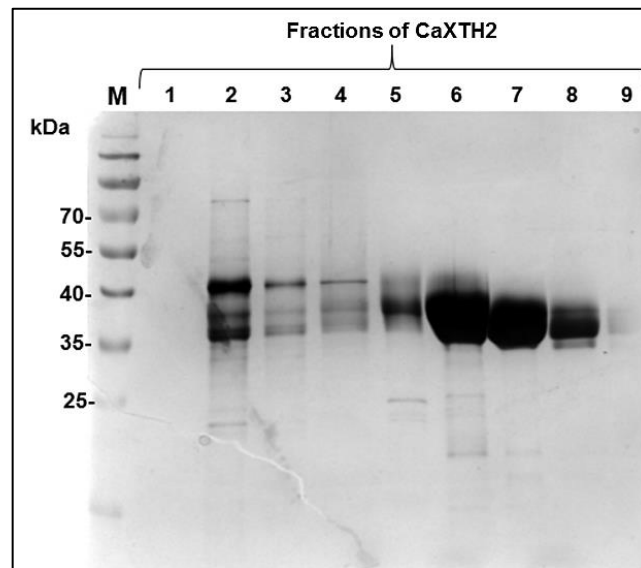


Figure 3.15. CaXTH2 fractions 1 to 9 that were obtained and concentrated after polishing procedure on 12 per cent polyacrylamide gel after Silver Staining. M-PageRuler™ Prestained Protein Ladder.

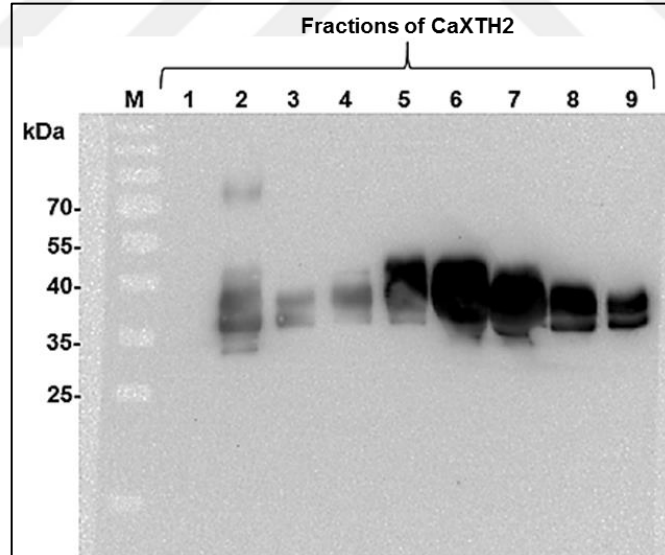


Figure 3.16. CaXTH2 fractions 1 to 9 that were obtained and concentrated after polishing procedure on nitrocellulose membrane after treatment with Anti-6X His antibody. M-PageRuler™ Prestained Protein Ladder.

The fractions 5,6,7,8 and 9 revealed the same pure looking protein bands from both procedures. Therefore, these fractions were combined and concentrated as it was described

with CaXTH1 and CaXTH3 enzymes. The concentration of the CaXTH2 enzyme was determined to be 2,723 mg/ml. Other than the equipment quality contaminating protein bands were observed from some other reactions for all the capsicum enzymes after polishing procedure. Those bands might have been immature/degraded proteins from degraded/immature proteins, protein aggregates or other imidazole binding proteins. After final purification and concentration same amount from CaXTH1, CaXTH2 and CaXTH 3 enzymes were loaded on 12 per cent and SDS-PAGE was performed (Figure 3.17). Coomassie dyed gel images supported the fact that enzyme solutions included the purist form of the proteins of interest. CaXTH2 protein had the highest concentration as it revealed the thickest, brightest protein band. CaXTH1 and CaXTH3 showed weaker bands comparing CaXTH2.

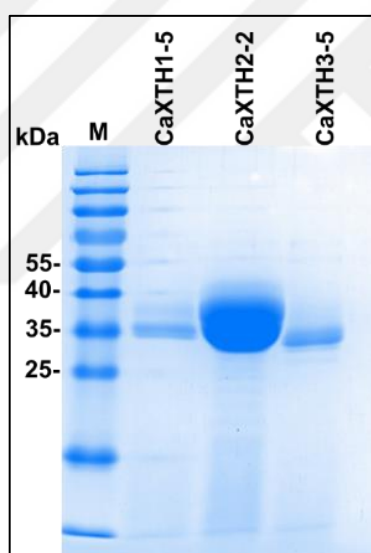


Figure 3.17. Purified and concentrated CaXTH1, CaXTH2 and CaXTH3 enzymes on 12 per cent polyacrylamide gel after coomassie blue staining. M-PageRuler™ Prestained Protein Ladder.

### 3.1.4. pH Optimization

#### 3.1.4.1. *OsXTH1 and SIXTH4 Enzymes*

The ionic force of the different XTH enzymes that were used in this study changed depending on the differences in amino acid sequences and therefore affected the optimum working pH for the enzymes. In order to determine the optimum working pH value enzymes were incubated with TXG donor dissolved in different pH valued McIlvaine buffers and XGO acceptor at 30°C for an hour. After that, HPLC analysis were used to match activity levels with pH values.

*OsXTH1* enzyme showed the most activity at pH 5,9. Activity started to drop drastically as the pH value increased. *SIXTH4* enzyme on the other hand showed activity on a broader pH range. The highest activity for *SIXTH4* was detected at pH 6,1 (Figure 3.18).

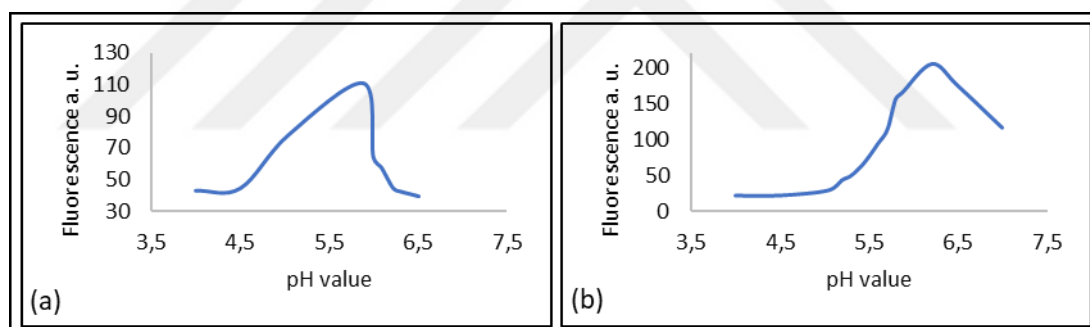


Figure 3.18. pH optimization of *OsXTH1* (a) and *SIXTH4* (b) enzyme using McIlvaine buffer between pH range 4 and 6,5.

#### 3.1.4.2. *CaXTH1, CaXTH2 and CaXTH3 Enzymes*

Enzyme reactions were set up using different pH valued McIlvaine buffer including TXG donor as described before. The pH value of the McIlvaine buffer varied from 4 to 8. All capsicum enzymes included in this study seemed to be working best between 5,5 and 6,5. For *CaXTH1* enzyme this value was pH 5,8. Activity level seemed to drop after pH 6 and continued dropping as it got close to pH 7. On the other hand, *CaXTH2* and *CaXTH3*

enzymes still had significant amount of activity after pH 7 (Figure 3.19). The highest activity for these two enzymes were shown at pH 6 and pH 5,99 respectively. pH optimization experiments of CaXTH2 enzyme was carried out by master's student Ezgi Türksever under my direct supervision.

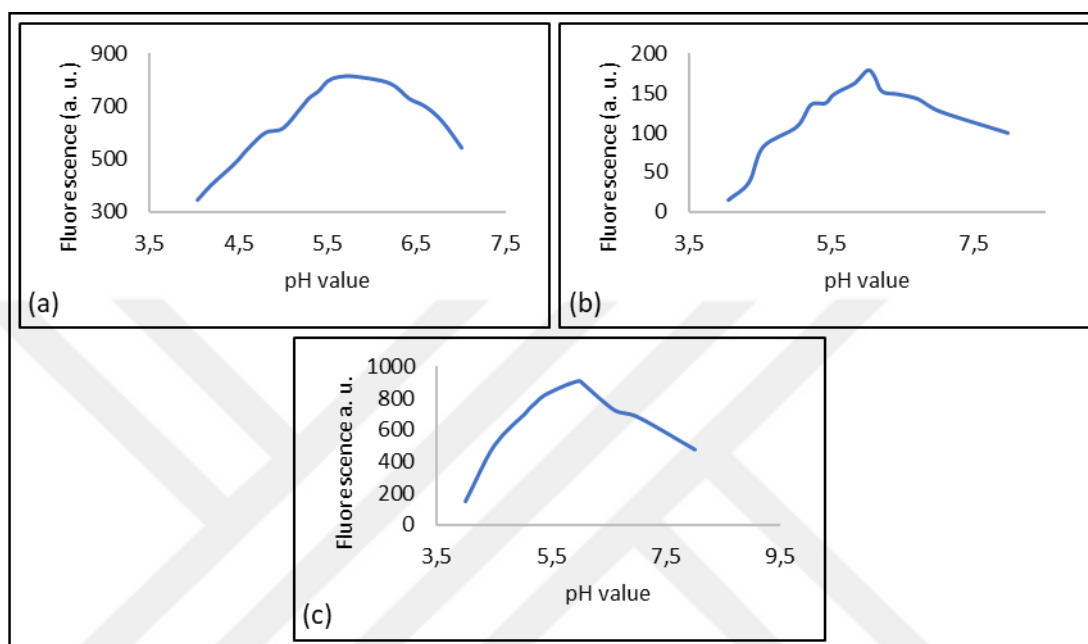


Figure 3.19. pH optimization of CaXTH1 (a) CaXTH2 (b) and CaXTH3 (c) enzyme using McIlvaine buffer between pH range 4 and 7.

### 3.1.5. Substrate Specificity

#### 3.1.5.1. *OsXTH1* Enzyme

Following pH optimization, activity status of the enzyme was tested on 88 different substrate couples. TXG, HEC, BBG, KGM, WAX, CM, GM and LG polysaccharides were used as donor substrates. XGO, X7, XT, CT, MT, BA, BB, BC, GM3, LT and DGM oligosaccharides were used as acceptor substrates. The pH of the ammonium acetate buffers including different donor substrates was arranged to 5,9. Activity status on different substrate couples was determined after HPLC analysis of 24 hour enzyme

reactions that were set up using these substrate couples. Activity showing donor and acceptor substrates were shown in table 3.2.

Table 3.2. Activity showing donor and acceptor substrates for OsXTH1 enzyme.

<b>Donors</b>	<b>Acceptors</b>									
<b>TXG</b>	XGO	X7	XT	CT	BA	BB	BC	LT	GM3	MT
<b>HEC</b>	XGO	X7	XT	CT		BB				
<b>BBG</b>	XGO	X7		CT		BB	BC			

### 3.1.5.2. *SIXTH4* Enzyme

Activity of SIXTH4 enzyme on 88 different substrate couples was detected after pH optimization. The pH of the ammonium acetate buffers including different donor substrates was arranged to 6.1. Substrate molecules, that the enzyme was active on was determined according to HPLC analysis, were given in the table 3.3.

Table 3.3. Activity showing donor and acceptor substrates for SIXTH4 enzyme.

<b>Donors</b>	<b>Acceptors</b>								
<b>TXG</b>	XGO	X7	XT	CT	BA	BB	BC	LT	GM3
<b>HEC</b>	XGO	X7							
<b>BBG</b>	XGO	X7							

### 3.1.5.3. *CaXTH1* Enzyme

Activity trials on 88 different substrate couples was performed as described before. pH value of the donor substrate buffers was arranged to the optimum working pH. Donor and substrate molecules that the enzyme was active on are given in the table 3.4.

Table 3.4. Activity showing donor and acceptor substrates for CaXTH1 enzyme.

<b>Donors</b>	<b>Acceptors</b>								
<b>TXG</b>	XGO	X7	XT	CT	BA	BB	BC	LT	GM3
<b>HEC</b>	XGO	X7	XT	CT	BA	BB	BC	LT	GM3
<b>BBG</b>	XGO	X7	XT	CT	BA	BB	BC	LT	GM3
<b>KGM</b>	XGO								

#### 3.1.5.4. *CaXTH2 Enzyme*

Enzyme reactions with 88 different substrate couples were set and analysed as described before. The pH value of the ammonium acetate buffers was arranged to the optimum working pH. Donor and substrate molecules that the enzyme was active on were given in the table 3.5.

Table 3.5. Activity showing donor and acceptor substrates for CaXTH2 enzyme.

<b>Donors</b>	<b>Acceptors</b>								
<b>TXG</b>	XGO	X7	XT	CT	BA	BB	BC	LT	GM3
<b>HEC</b>	XGO	X7	XT	CT		BB	BC	LT	
<b>BBG</b>	XGO	X7	XT	CT		BB	BC	LT	

#### 3.1.5.5. *CaXTH3 Enzyme*

Enzyme reactions with 88 different substrate couples were set and analysed as described before. The pH value of the ammonium acetate buffers was arranged to the optimum working pH. Donor and substrate molecules that the enzyme was active on were given in the table 3.6.

Table 3.6. Activity showing donor and acceptor substrates for CaXTH3enzyme.

<b>Donors</b>	<b>Acceptors</b>								
<b>TXG</b>	XGO	X7	XT	CT	BA	BB	BC	LT	GM3
<b>HEC</b>	XGO	X7	XT	CT	BA	BB	BC	LT	
<b>BBG</b>	XGO	X7	XT	CT		BB	BC	LT	GM3

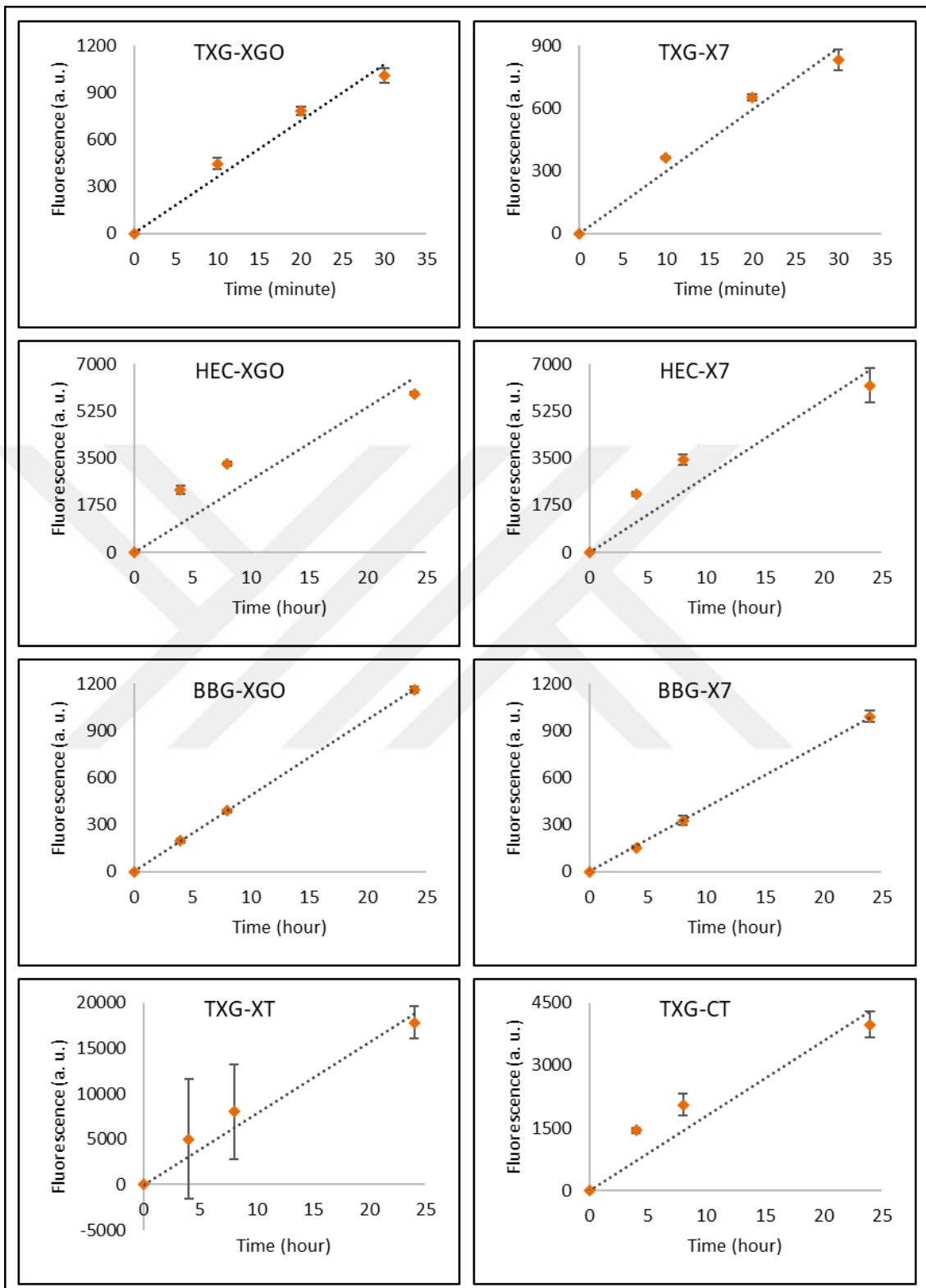
### 3.1.6. Enzyme Characterization

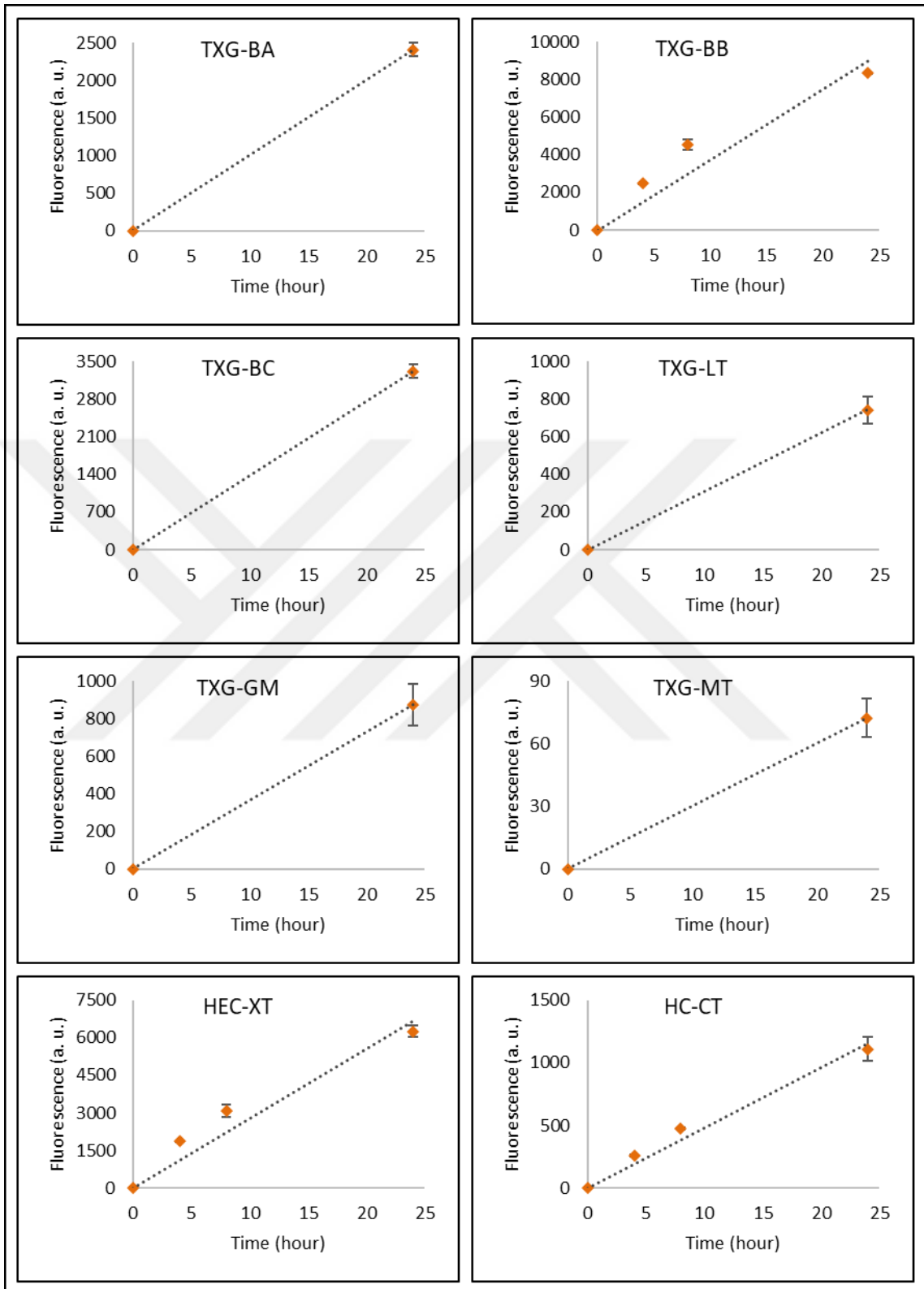
Enzyme reactions were performed using OsXTH1, SIXTH4, CaXTH1, CaXTH2 and CaXTH3 enzymes using the substrate couples that they were active on. Linear graphs of product amount (fluorescence (a. u.)) vs time, including different activity amounts in different time intervals, were drawn for each enzyme and the substrate couple that they were active on. The graphs were used to determine the optimum dilution factor of the specific amount of enzyme and the optimum time period for that enzyme to obtain an accurate time interval that the enzyme could work at its maximum performance without substrates becoming limiting to the reaction velocity. The matching fluorescence (a. u.) value which represented the maximum product amount that the specific amount of enzyme could form in this time interval was also determined. These fluorescence (a. u.) and time values later on were used to calculate the specific activity levels as in picokatal/mg values for each substrate couple. Different dilution factors and time intervals were tried for each enzyme and substrate couple and each reaction was repeated at least 3 times. Dilution factors and time intervals varied depending on the enzymes and substrate couples.

#### 3.1.6.1. *OsXTH1 Enzyme*

The substrate couples that the OsXTH1 enzyme worked on were given previously in Table 3.2. Using these substrate couples enzyme reactions were set up to test different dilution factors and time intervals to obtain an accurate time interval and the matching activity amount (fluorescence (a. u.)) for each substrate couple and create time vs activity graphs as linear as possible (Figure 3.20). Based on the calculations which were done using the accurate time interval and activity amount (fluorescence (a. u.)), a table that represents the activity levels on individual substrate couples in picokatal/mg value was drawn (Table

3.7). The enzyme showed different activity levels on different substrate couples. As the activity level of the enzyme per substrate couple increased, higher dilution factors and shorter time intervals were required in order to create linear graphs. Depending on the substrate couple, time intervals varied from 10 minutes to 24 hours. Adjustment of the accurate dilution factor and time interval got harder as the activity level increased. Among donor substrates (TXG, HEC, BBG) the enzyme seemed to work best with TXG regardless of the acceptor substrates, followed by HEC and BBG, respectively. X7 and XGO showed the highest activity level among acceptor substrates, except for the BBG-XGO substrate couple, which showed a higher activity level than the BBG-X7 substrate couple. The highest activity level was detected as 126,2 picokatal/mg with TXG as the donor substrate and X7 as the acceptor substrate. The next highest activity level was 119,98 picokatal/mg with TXG as the donor substrate and XGO as the acceptor substrate. The enzyme's activity level on the TXG-XT substrate couple was determined to be the third highest with a value of 6,227 picokatal/mg. In between BA, BB and BC acceptor substrates, BB showed the highest activity level regardless of the donor substrates. BA and BC revealed activity with only a TXG donor, with the TXG-BC activity level being higher than the TXG-BA activity level. A slight amount of activity was observed with GM3, LT and MT acceptor substrates with TXG as the donor substrate. The TXG-MT substrate couple showed the lowest activity level among all substrate couples. These three acceptor substrates did not show activity with HEC and BBG donor substrates. HEC-XGO (1,335 picokatal/mg), HEC-X7 (1,465 picokatal/mg) and HEC-XT (1,225 picokatal/mg) substrate couples demonstrated similar activity levels, with the HEC-X7 substrate couple being the highest. The lowest activity level among acceptor substrates, which were paired with HEC as the donor substrate, was displayed by the CT acceptor substrate. Activity levels of the BBG donor substrate were generally low compared to TXG and HEC donor substrates. In between substrate couples that included BBG as the donor substrate, the most activity was observed with XGO (0,1046 picokatal/mg) and X7 (0,997 picokatal/mg) acceptor substrates while the least amount of activity was shown by the BBG-BC substrate couple.





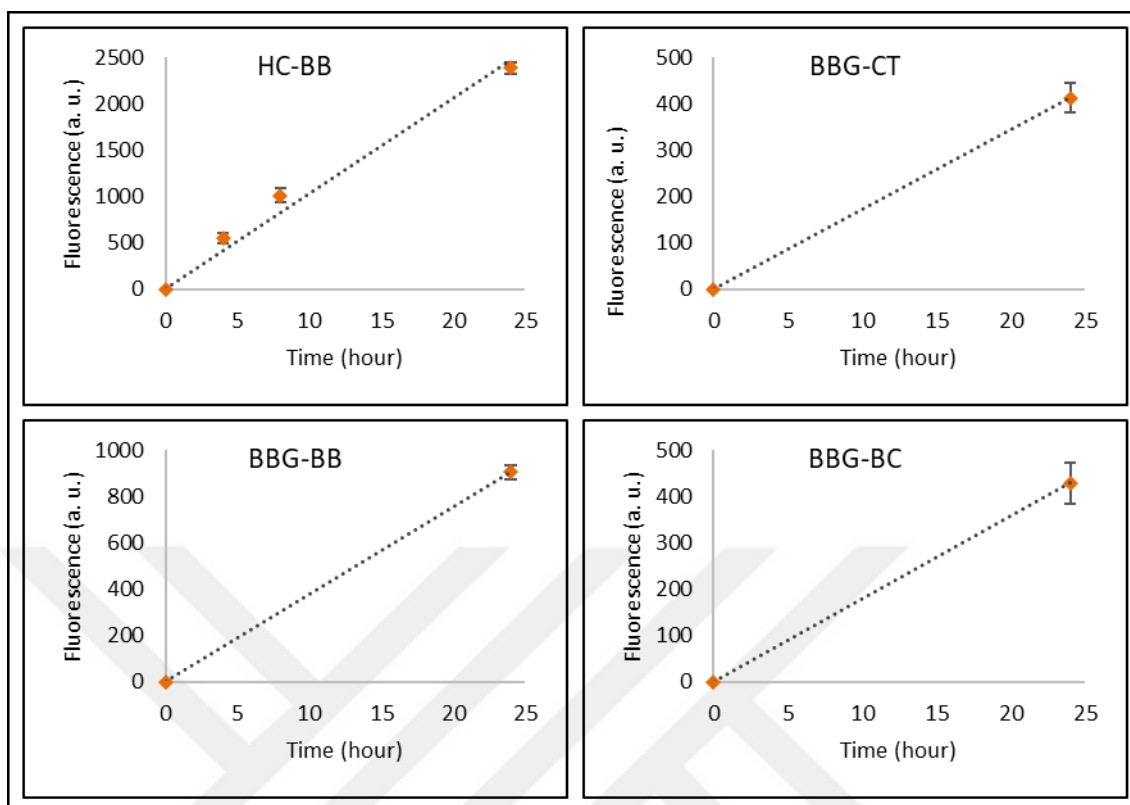


Figure 3.20. OsXTH1 enzyme activity in relation to time of incubation based on HPLC analysis, with each graph showing a different substrate couple. Activity amount is shown as in fluorescence (a. u.) value and represented by product amount.

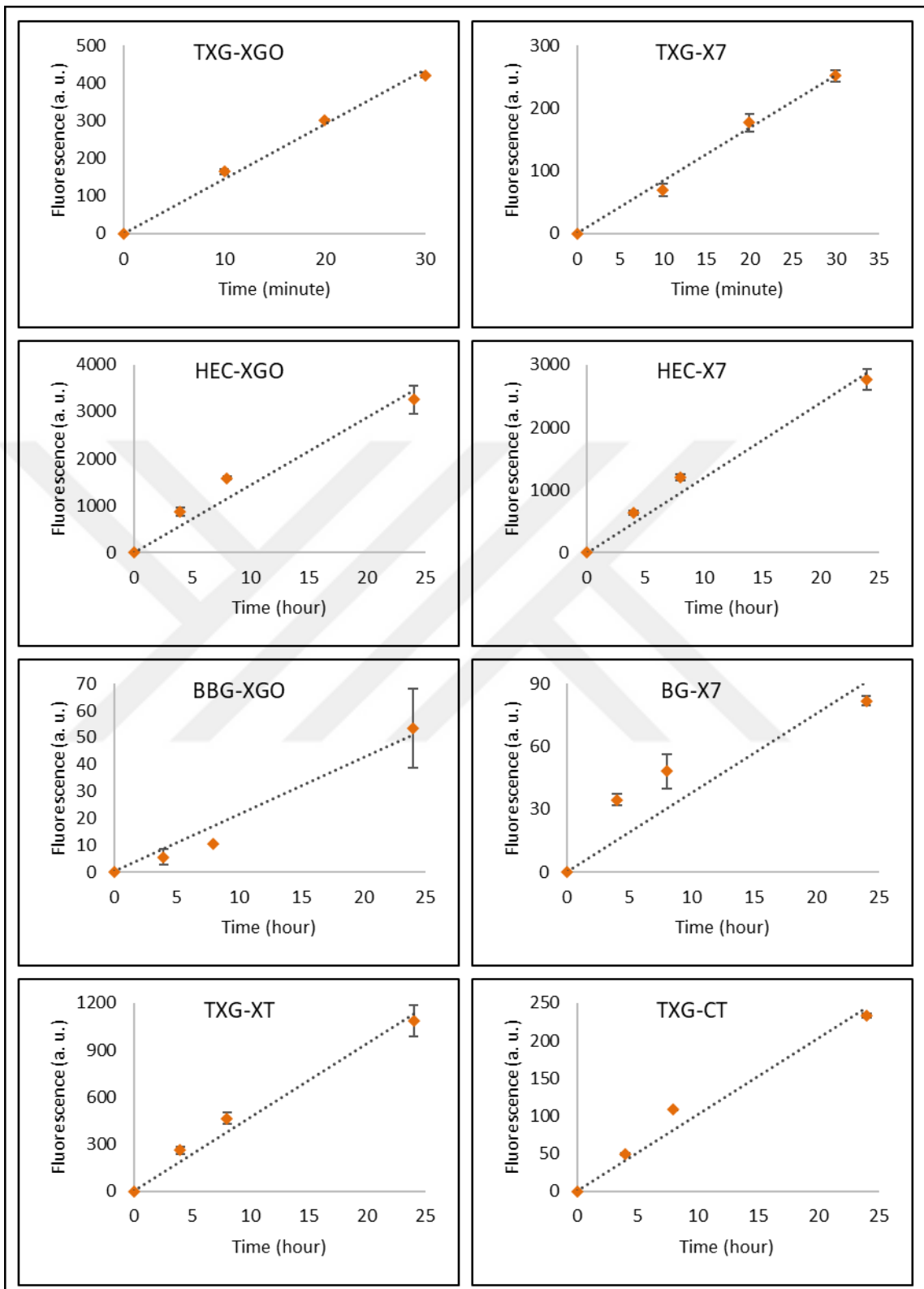
Table 3.7. The activity levels of the OsXTH1 enzyme on different substrate couples in picokatal/mg value and as percentages in relation to TXG-XGO substrate couple which was set to 100 per cent.

<b>Substrate couples</b>	<b>Activity level (picokatal/mg)</b>	<b>Activity level % relative to TXG-XGO</b>
TXG-XGO	119,98	100
TXG-X7	126,2	105,18
TXG-XT	6,227	5,19
TXG-CT	1,16	0,9664
TXG-BA	0,0216	0,018
TXG-BB	1,965	1,638
TXG-BC	0,0307	0,0255

TXG-LT	0,00558	0,00465
TXG-MT	0,000753	0,000627
TXG-GM3	0,00599	0,00499
HEC-XGO	1,335	1,112
HEC-X7	1,465	1,221
HEC-XT	1,225	1,021
HEC-CT	0,1934	0,1612
HEC-BB	0,2937	0,2448
BBG-XGO	0,1046	0,0872
BBG-X7	0,0997	0,0831
BBG-CT	0,00514	0,00429
BBG-BB	0,008	0,00667
BBG-BC	0,00336	0,0028

### 3.1.6.2. *SIXTH4* Enzyme

Reaction trials using different dilution factors and time intervals were performed for the *SIXTH4* enzyme in order to create linear time vs activity amount (fluorescence (a. u.)) graphs (Figure 3.21) as before. Specific enzyme activity levels were determined for the substrate couples that were tested and had been proven to show activity before. Activity levels varied depending on each substrate couple. Higher dilution factors and time intervals were preferred for the substrate couples for which the enzyme activity was high. After determining the accurate time interval and dilution factor, the activity level was calculated for each substrate couple (Table 3.8). The enzyme showed activity on a smaller variety of substrate couples compared to the *OsXTH1* enzyme. TXG and HEC were used as donor substrates with TXG being the most preferable donor substrate for *SIXTH4* enzyme. The highest activity levels were calculated for the TXG-XGO substrate couple and the TXG-X7 substrate couple with the values of 60,63 picokatal/mg and 42,75 picokatal/mg, respectively. These activity levels were followed by HEC-X7 and HEC-XGO substrate couples with the values of 6,171 picokatal/mg and 5,986 picokatal/mg, respectively. Among BA, BB and BC acceptor substrates, which were paired with the TXG donor substrate, BB showed the highest activity. Except for the XGO and X7 acceptor substrates, HEC did not show activity with other acceptor substrates.



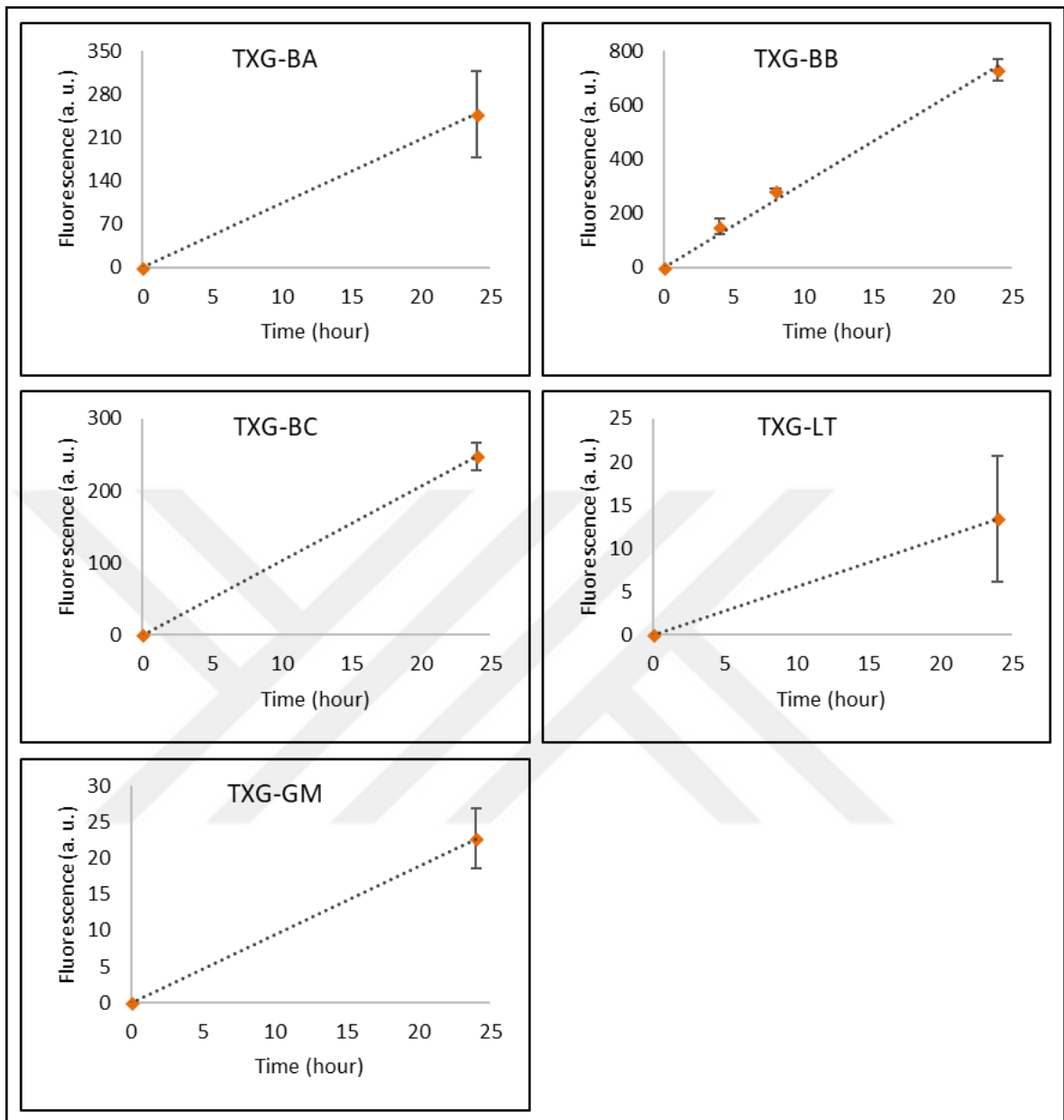


Figure 3.21. SIXTH4 enzyme activity in relation to time of incubation, with each graph showing a different substrate couple. Activity amount is shown as in fluorescence (a. u.) value and represented by product amount.

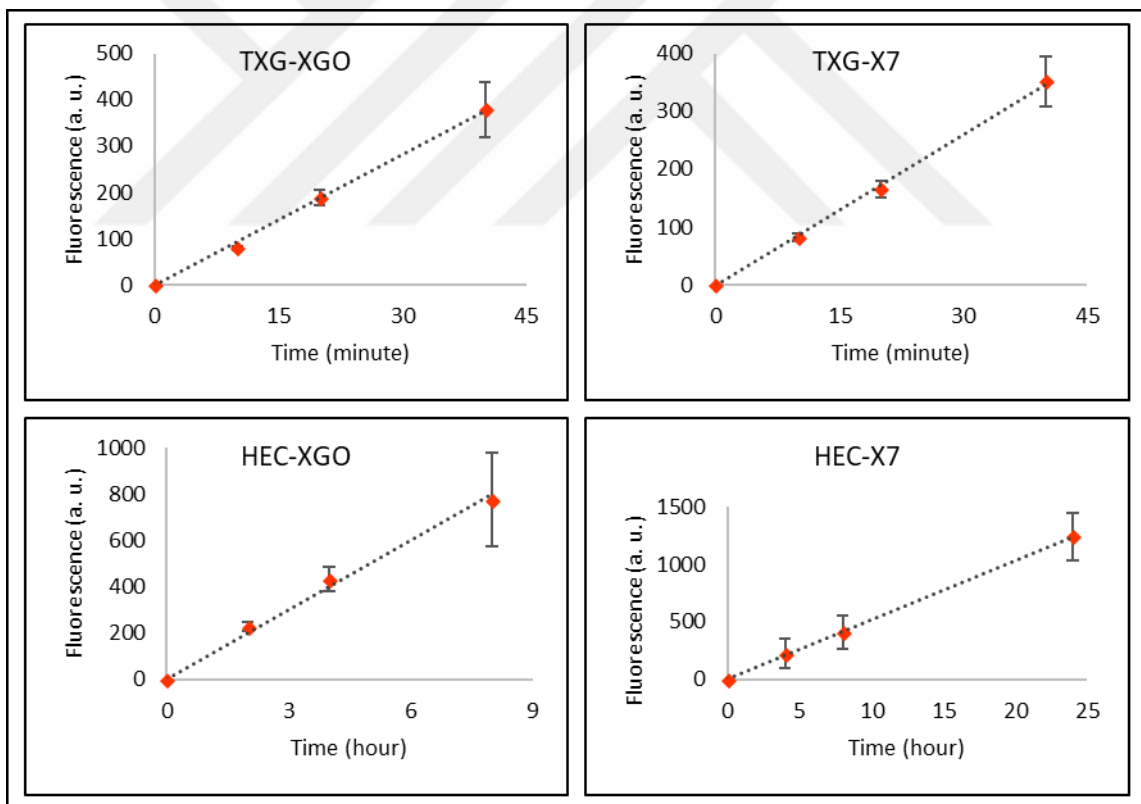
Table 3.8. The activity levels of the SIXTH4 enzyme on different substrate couples in picokatal/mg value and as percentages in relation to TXG-XGO substrate couple which was set to 100 per cent.

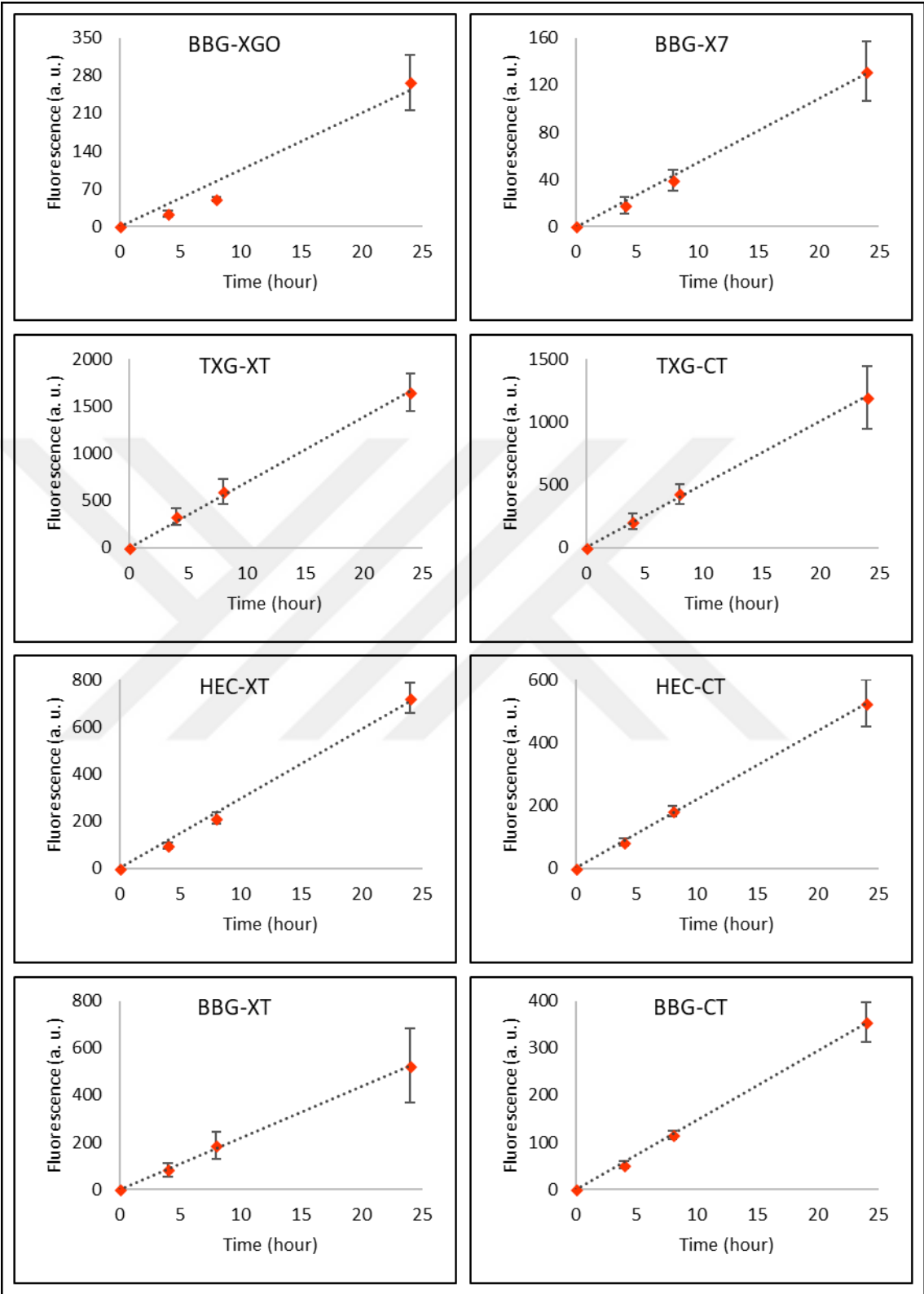
Substrate couples	Activity level (picokatal/mg)	Activity level % relative to TXG-XGO
TXG-XGO	60,63	100
TXG-X7	42,75	70,51
TXG-XT	2,378	3,922
TXG-CT	0,8859	1,461
TXG-BA	0,02701	0,04455
TXG-BB	1,5	2,474
TXG-BC	0,02854	0,04708
HEC-XGO	5,986	9,874
HEC-X7	6,171	10,18

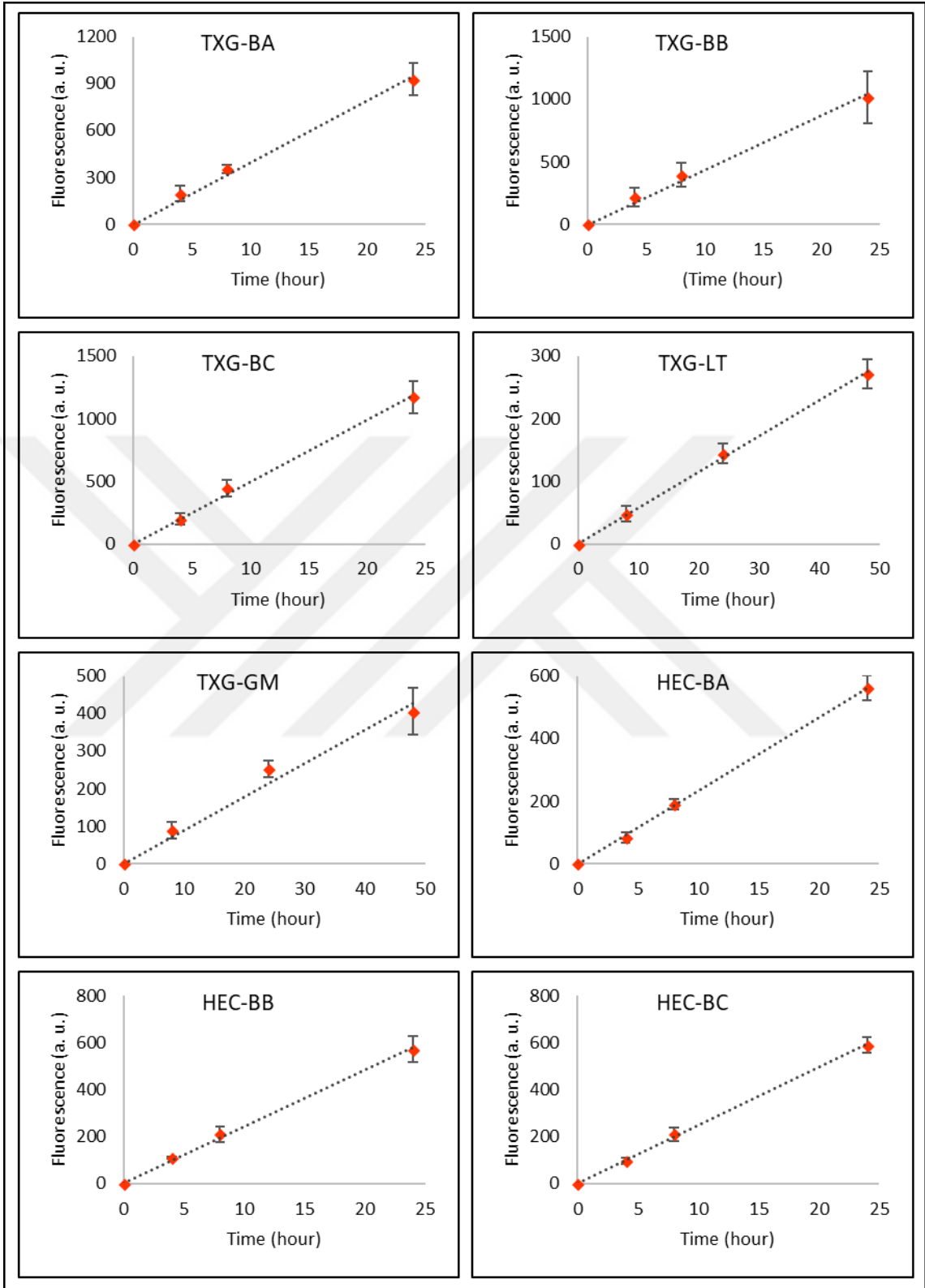
### 3.1.6.3. *CaXTH1 Enzyme*

The substrate couples that were analysed via HPLC and proven to show activity were tested to determine the accurate dilution factor and time interval to draw linear time vs activity amount (fluorescence (a. u.)) graphs (Figure 3.22). Selection of the dilution factor and time interval was performed as described before with OsXTH1 and SIXTH4 enzymes. According to the values that were given in the graphs, specific enzyme activity levels were calculated and represented in a table (Table 3.9). CaXTH1 enzyme displayed activity with TXG, HEC and BBG donor substrates. When XGO, X7, XT, CT, BA, BB and BC acceptor substrates were used the TXG donor substrate exhibited the most activity, relative to other donor substrates. The activity level of the TXG-X7 substrate couple was the highest with the value of 557,87 picokatal/mg. That was followed by the TXG-XGO substrate couple with a value of 365,23 picokatal/mg. Among the substrate couples that were paired with the TXG donor substrate, XT demonstrated the third highest activity, although with a very small value (1,095 picokatal/mg) compared to X7 and XGO acceptor substrates. HEC-XGO (3,637 picokatal/mg) and HEC-X7 (2,928 picokatal/mg) substrate couples exhibited the most activity amount among the substrate couples including HEC as the donor substrate. BA, BB and BC acceptor substrates seemed to work with all three donor

substrates. For the TXG donor substrate, activity levels of BB (0,8674 picokatal/mg) and BC (0,8195 picokatal/mg) acceptor substrates were quite close to each other and higher than the activity level of the BA (0,5649 picokatal/mg) acceptor substrate. Although the activity levels were different, a similar case was observed with HEC and BBG donor substrates when BA, BB and BC acceptor substrates were used. Regardless of the acceptor substrates, amount of activities seemed to be reduced when BBG was used as the donor substrate, instead of TXG or HEC donor substrates. The least amount of activity was observed with LT and GM3 acceptor substrates, no matter which donor substrate they were used with. A slight amount of activity (0,0077 picokatal/mg) was observed with KGM-XGO substrate couple. The KGM donor substrate was not preferable for the CaXTH1 enzyme to work on, therefore no activity was observed with any of the acceptor substrates except for the XGO acceptor substrate.







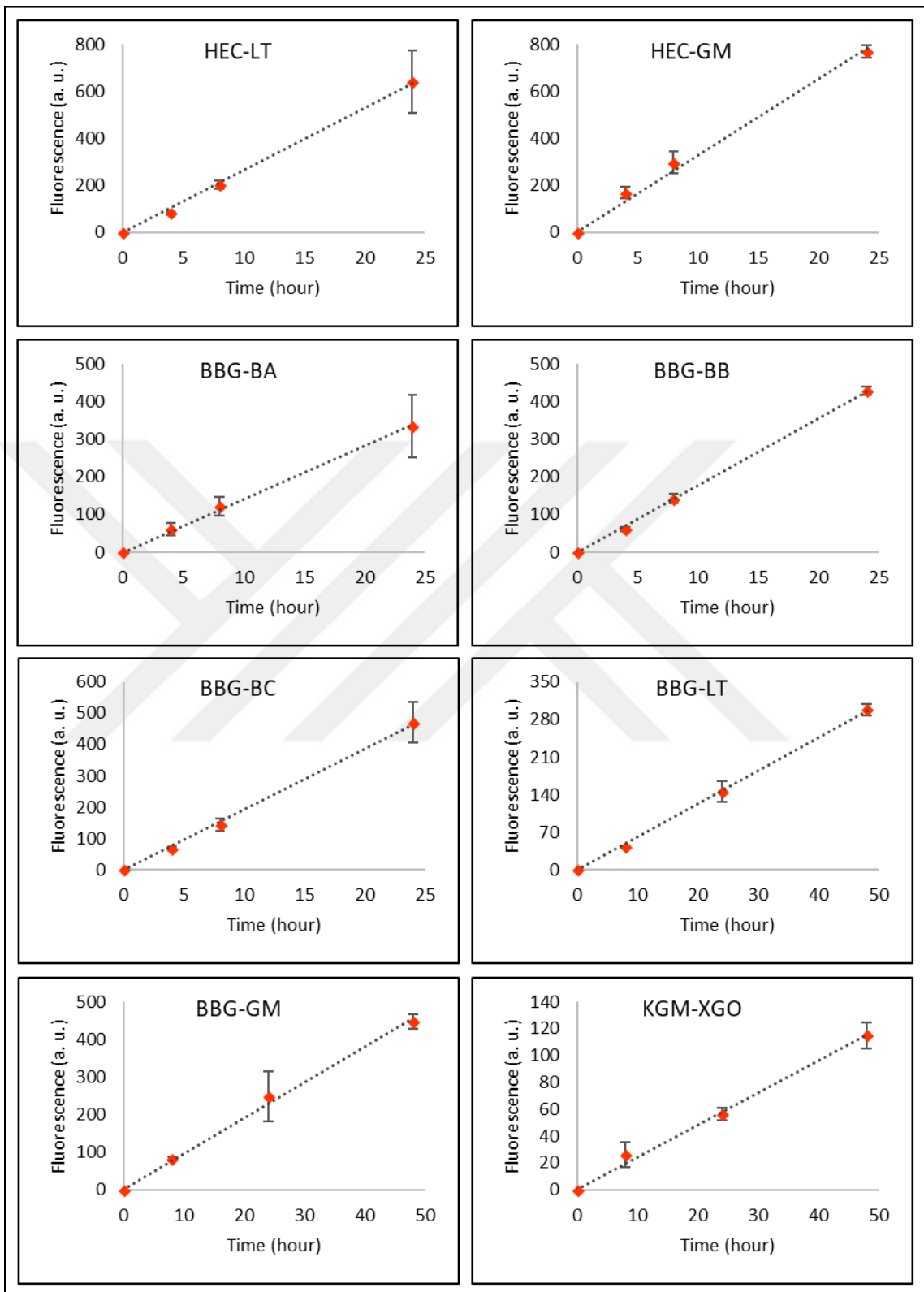


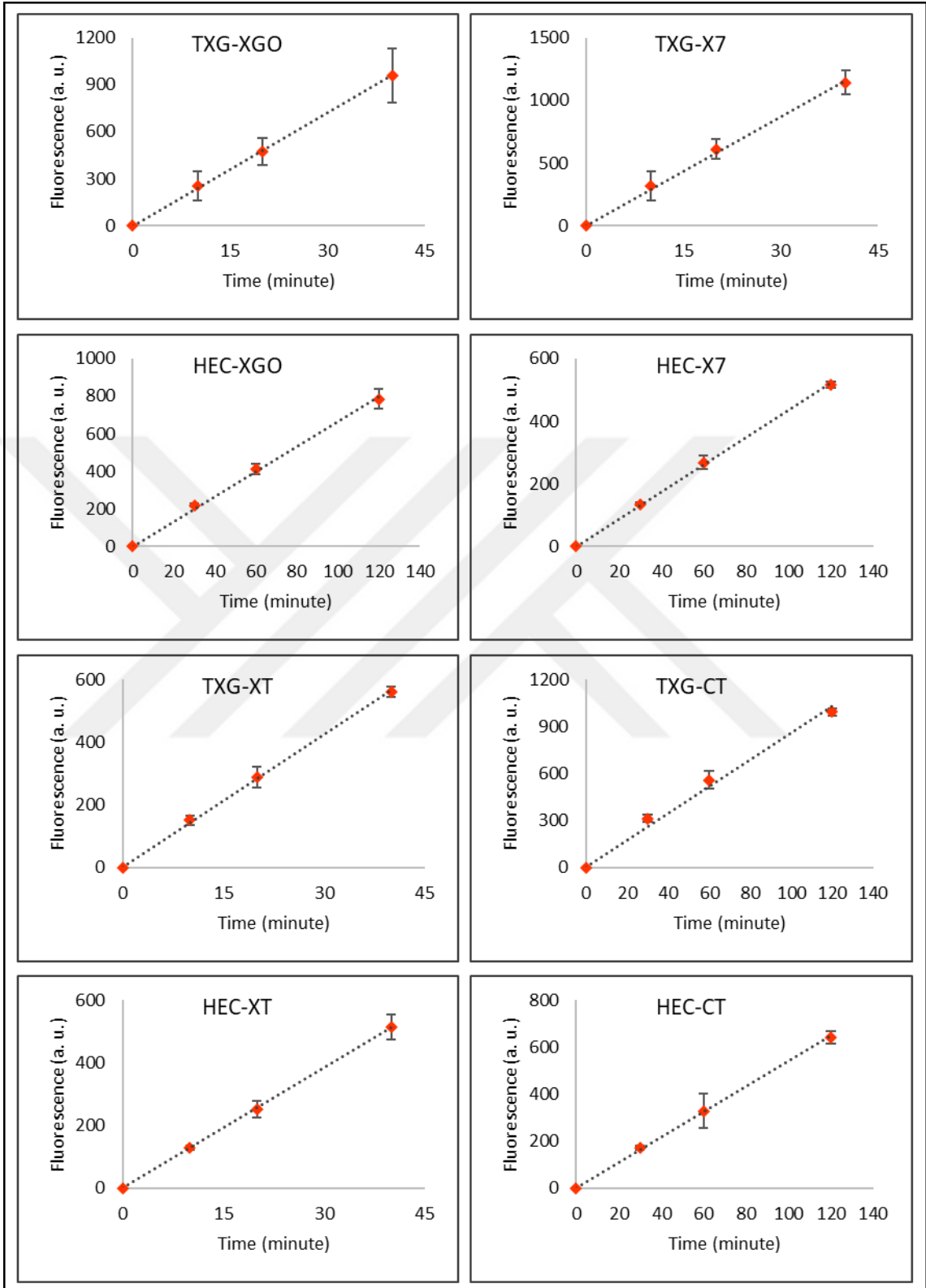
Figure 3.22. CaXTH1 enzyme activity in relation to time of incubation, with each graph showing a different substrate couple. Activity amount is shown as in fluorescence (a. u.) value and represented by product amount.

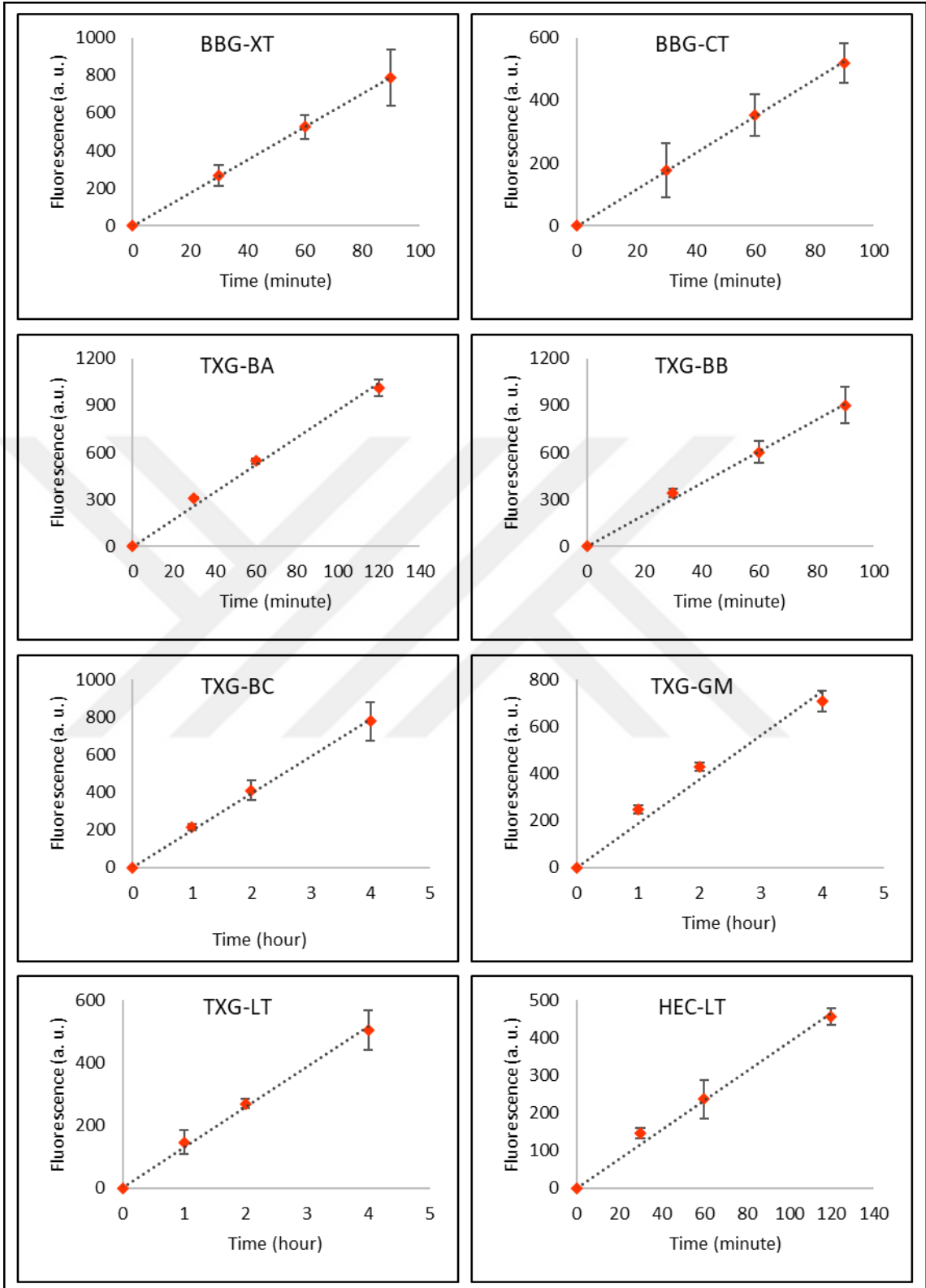
Table 3.9. The activity levels of the CaXTH1 enzyme on different substrate couples in picokatal/mg value and as percentages in relation to TXG-XGO substrate couple which was set to 100 per cent.

<b>Substrate couples</b>	<b>Activity level (picokatal/mg)</b>	<b>Activity level % relative to TXG-XGO</b>
TXG-XGO	365,23	100
TXG-X7	557,87	152,74
TXG-XT	1,095	0,2998
TXG-CT	0,5584	0,1529
TXG-BA	0,5649	0,1547
TXG-BB	0,8674	0,2375
TXG-BC	0,8195	0,2244
TXG-LT	0,05498	0,01505
TXG-GM3	0,1102	0,03017
HEC-XGO	3,637	0,9959
HEC-X7	2,928	0,8016
HEC-XT	0,7930	0,2171
HEC-CT	0,4701	0,1287
HEC-BA	0,6073	0,1663
HEC-BB	0,7643	0,2093
HEC-BC	0,7695	0,2107
HEC-LT	0,1223	0,0335
HEC-GM3	0,1471	0,04026
BBG-XGO	0,179	0,049
BBG-X7	0,1448	0,03964
BBG-XT	0,1919	0,05253
BBG-CT	0,1059	0,02901
BBG-BA	0,1292	0,03538
BBG-BB	0,1914	0,0524
BBG-BC	0,1926	0,05274
BBG-LT	0,02794	0,00765
BBG-GM3	0,03601	0,00986
KGM-XGO	0,0077	0,002108

#### 3.1.6.4. *CaXTH2 Enzyme*

Donor and acceptor substrates that were proven to show activity earlier was used to generate linear time vs activity amount (fluorescence (a. u.)) graphs (Figure 3.23). HPLC analysis was used to calculate the product amount that was later on used to create the graphs. Accurate dilution factor and time interval determination was performed as described with OsXTH1 and SIXTH4 enzymes. Time intervals varied from 10 minutes to 4 hours depending on the substrate couple. Enzyme characterization of CaXTH2 enzyme was carried out by master's student Ezgi Türksever under my direct supervision. Activity levels on different substrate couples were calculated with the information from linear time vs activity amount (fluorescence (a. u.)) graphs and presented in a table (Table 3.10). The CaXTH2 enzyme activity levels were significantly higher for TXG-X7 (4121,04 picokatal/mg) and TXG-XGO (2026,9 picokatal/mg) substrate couples relative to other substrate couples. Even though the activity level of the TXG-XGO substrate couple was half as much as the activity level of the TXG-X7 substrate couple, at 2026,9 picokatal/mg it was still between two and four orders of magnitude larger than the other substrate couples, which were all between 0,1 and 12 picokatal/mg. Among all three CaXTH enzymes which were included in this study, CaXTH2 enzyme seemed the show the most activity on each substrate couple compared to CaXTH1 and CaXTH3 enzymes. The next highest activity levels were exhibited by HEC-X7 (11,76 picokatal/mg) and HEC-XGO (11,67 picokatal/mg) substrate couples among all substrate couples. When BA, BB and BC acceptor substrates were used with the TXG donor substrate, the highest activity level was observed with the BB acceptor substrate (3,008 picokatal/mg) which was similar to the activity level of the TXG-XT substrate couple (3,254 picokatal/mg). The HEC donor substrate did not show any activity with the BA acceptor substrate, and the activity levels of HEC-BB (1,534 picokatal/mg) and HEC-BC (1,51 picokatal/mg) were pretty close to each other. A drastic drop in activity levels was observed when BBG was used as the donor substrate. LT and GM3 acceptor substrates which were the least favourable acceptor substrates for the enzyme to work on, seemed to work better with TXG as the donor substrate than HEC and BBG donor substrates. HEC and BBG donor substrates did not show any activity with the GM3 acceptor substrate.





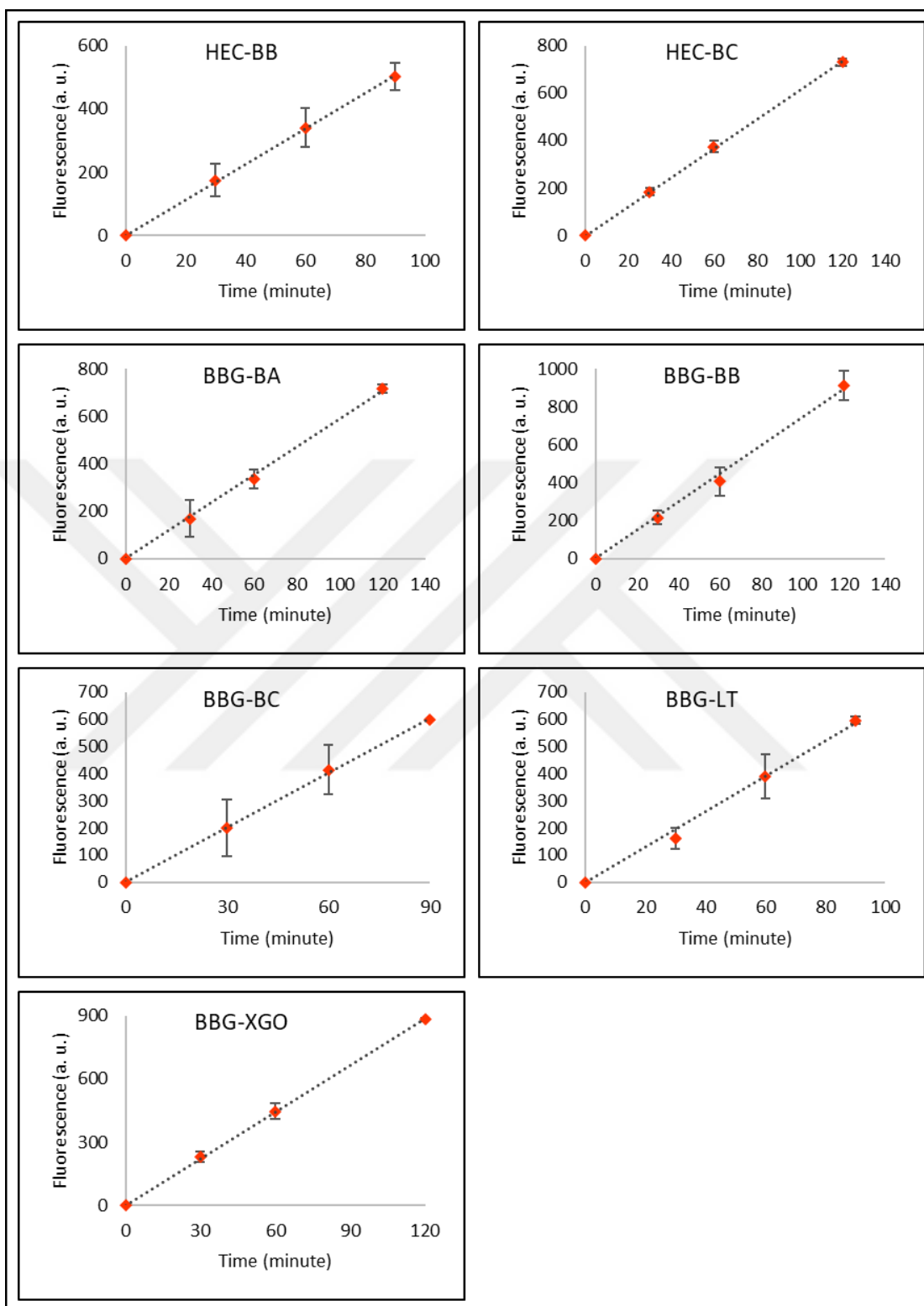


Figure 3.23. CaXTH2 enzyme activity in relation to time of incubation based on HPLC analysis, with each graph showing a different substrate couple. Activity amount is shown as in fluorescence (a. u.) value and represented by product amount.

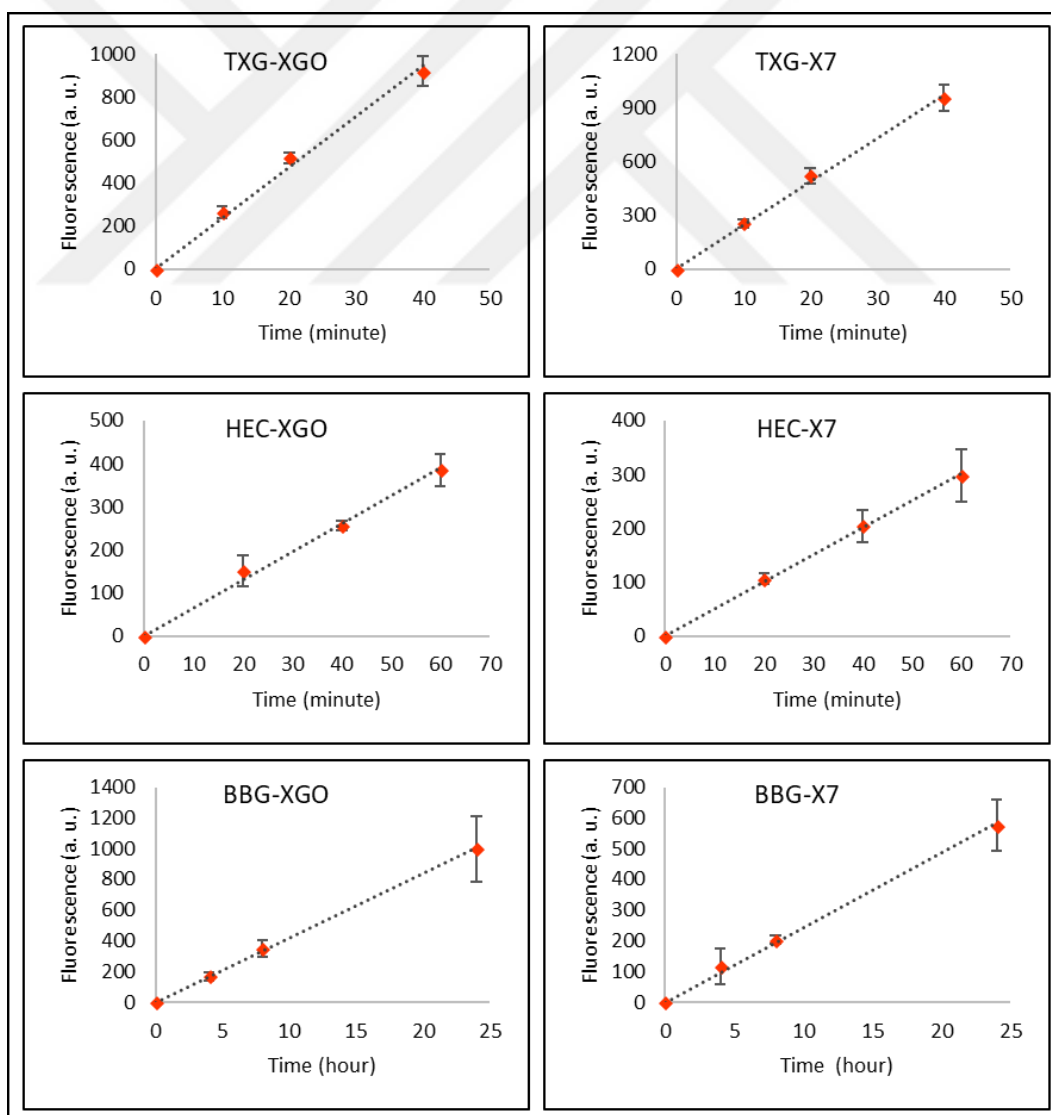
Table 3.10. The activity levels of the CaXTH2 enzyme on different substrate couples in picokatal/mg value and as percentages in relation to TXG-XGO substrate couple which was set to 100 per cent.

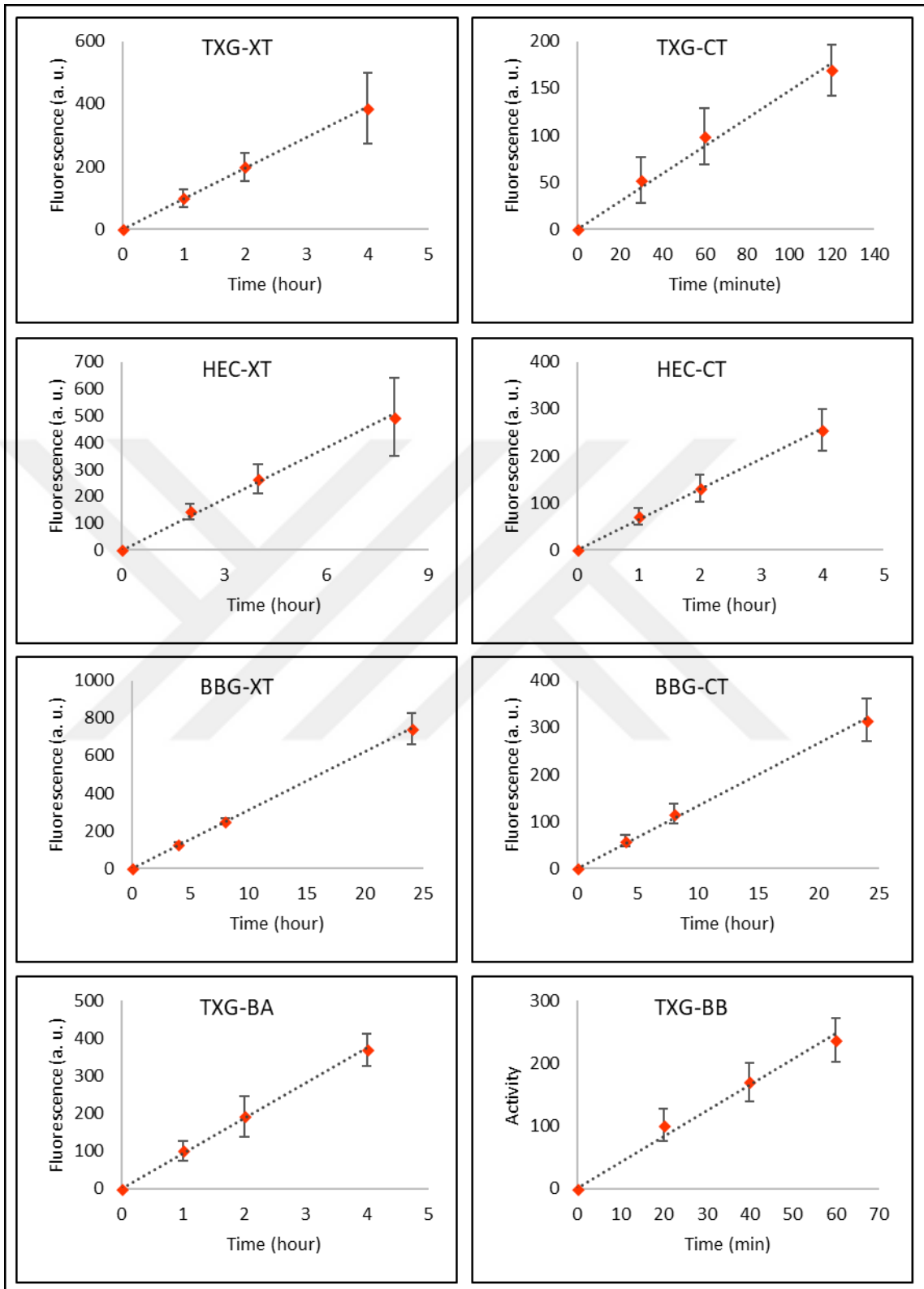
<b>Substrate couples</b>	<b>Activity level (picokatal/mg)</b>	<b>Activity level % relative to TXG-XGO</b>
TXG-XGO	2026,9	100
TXG-X7	4121,04	203,32
TXG-XT	3,254	0,1606
TXG-CT	1,842	0,09086
TXG-BA	2,164	0,1068
TXG-BB	3,008	0,1484
TXG-BC	1,654	0,08162
TXG-LT	0,2754	0,01359
TXG-GM3	0,3072	0,01515
HEC-XGO	11,67	0,5759
HEC-X7	11,76	0,5803
HEC-XT	1,364	0,06731
HEC-CT	1,0148	0,05007
HEC-BB	1,534	0,07566
HEC-BC	1,51	0,07448
HEC-LT	0,1102	0,005436
BBG-XGO	0,6053	0,02986
BBG-XT	0,3866	0,01907
BBG-CT	0,208	0,01026
BBG-BA	0,2378	0,01173
BBG-BB	0,382	0,01885
BBG-BC	0,3347	0,01651
BBG-LT	0,1206	0,005948

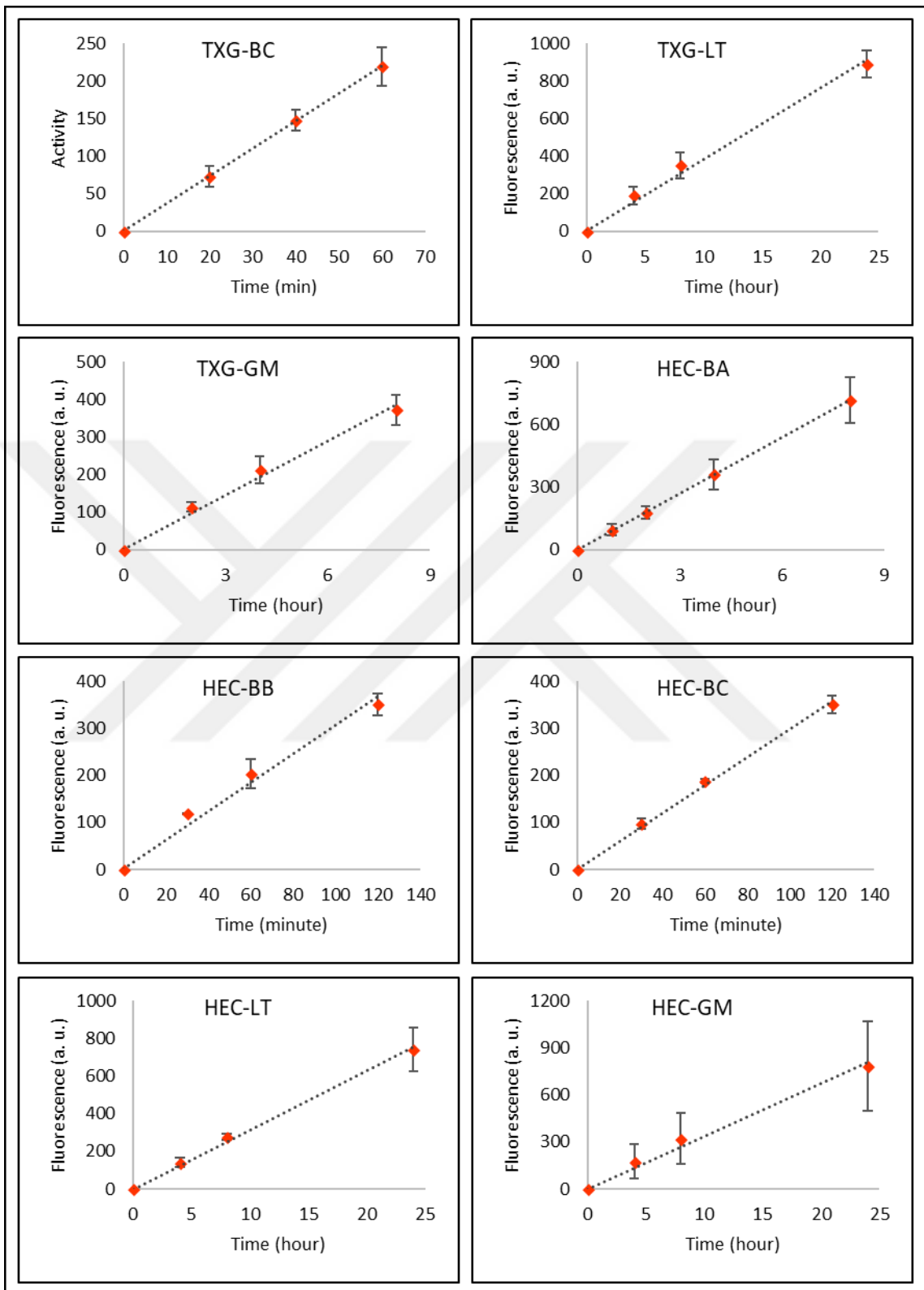
### 3.1.6.5. *CaXTH3* Enzyme

Linear time vs activity amount (fluorescence (a. u.)) graphs (Figure 3.24) and a table showing activity levels of different substrate couples (Table 3.11) were drawn as described previously. In similar fashion to previous experiments, the highest activity levels were

observed with TXG-X7 (817,22 picokatal/mg) and TXG-XGO (494,36 picokatal/mg) substrate couples, which were two to four orders of magnitude larger than other substrate couples. Activity levels of TXG-X7 and TXG-XGO substrate couples were followed by the activity levels of HEC-X7 and HEC-XGO substrate couples with values of 8,327 picokatal/mg and 7,176 picokatal/mg, respectively. Among the BA, BB and BC acceptor substrates BB demonstrated the most activity amount regardless of the donor substrate. Similar activity levels were exhibited by TXG-XT (0,651 picokatal/mg) and TXG-BA (0,6376 picokatal/mg) substrate couples. The BBG donor substrate revealed no activity with the BA acceptor substrate. Activity levels of the substrate couples seemed to decrease when BBG was used as the donor substrate. Among all the acceptors LT and GM3 showed the least activity regardless of the donor substrate.







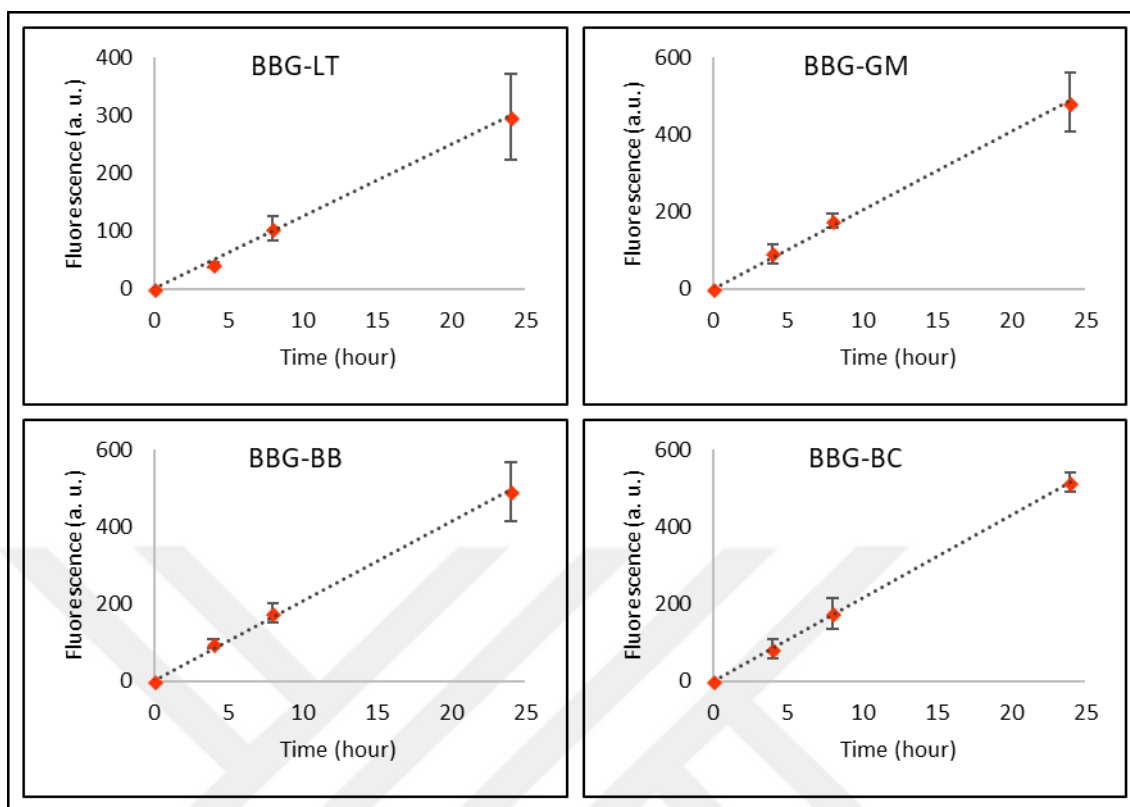


Figure 3.24. CaXTH3 enzyme activity in relation to time of incubation based on HPLC analysis, with each graph showing a different substrate couple. Activity amount is shown as in fluorescence (a. u.) value and represented by product amount.

Table 3.11. The activity levels of the CaXTH3 enzyme on different substrate couples in picokatal/mg value and as percentages in relation to TXG-XGO substrate couple which was set to 100 per cent.

Substrate couples	Activity level (picokatal/mg)	Activity level % relative to TXG-XGO
TXG-XGO	494,36	100
TXG-X7	817,22	165,31
TXG-XT	0,651	0,1317
TXG-CT	0,5276	0,1067
TXG-BA	0,6376	0,129
TXG-BB	2,426	0,4908
TXG-BC	1,61	0,3257

TXG-LT	0,1983	0,04012
TXG-GM3	0,1981	0,04007
HEC-XGO	7,176	1,452
HEC-X7	8,327	1,684
HEC-XT	0,4673	0,09452
HEC-CT	0,3833	0,07753
HEC-BA	0,6101	0,1234
HEC-BB	1,882	0,3806
HEC-BC	1,427	0,2887
HEC-LT	0,2347	0,04747
HEC-GM3	0,2079	0,04206
BBG-XGO	0,2073	0,04193
BBG-X7	0,2286	0,04623
BBG-XT	0,07005	0,01417
BBG-CT	0,0517	0,01046
BBG-BB	0,1895	0,03834
BBG-BC	0,1581	0,03198
BBG-LT	0,02958	0,005983
BBG-GM3	0,03825	0,007736

### 3.1.7. Enzyme Kinetics

Further kinetic studies were performed on CaXTH1, CaXTH2 and CaXTH3 enzymes after calculating the activity levels of different substrate couples in picokatal/mg value. All three enzymes exhibited the most activity amount with TXG-X7 substrate couple. Therefore, kinetic studies were conducted using TXG as the donor substrate and X7 as the acceptor substrate. To obtain the best working TXG concentration, different enzyme reactions were set up using TXG (10  $\mu$ l) donor substrates with different concentrations varying from 0,04 per cent (w/v) to 0,7 per cent (w/v) and the X7 (1  $\mu$ l) acceptor substrate with a constant concentration (50  $\mu$ M). Enzyme reactions were performed using predetermined dilution factors and time intervals according to enzymes and each reaction was set three times. Reaction results were analysed via HPLC and specific activity amount according to the TXG donor concentration was determined as in product amount (fluorescence (a. u.)) as described before. After defining the best working TXG donor concentration for each

enzyme, another set of enzyme reactions were performed using the TXG donor substrate with a constant concentration according to the enzyme and X7 acceptor substrates with different concentrations. Each reaction was set three times and reaction results were analysed via HPLC as described before.

### 3.1.7.1. *CaXTH1 Enzyme*

Based on the HPLC results the best working TXG donor substrate concentration for the CaXTH1 enzyme was determined as 0,6 per cent (w/v). Using TXG as the donor substrate with a constant 0,6 per cent (w/v) concentration and X7 as the acceptor substrate with different concentrations (0  $\mu\text{M}$ , 1  $\mu\text{M}$ , 5  $\mu\text{M}$ , 10  $\mu\text{M}$ , 20  $\mu\text{M}$ , 40  $\mu\text{M}$ , 100  $\mu\text{M}$ , 200  $\mu\text{M}$ , 400  $\mu\text{M}$ , 500  $\mu\text{M}$ ), 1 hour enzyme reactions were performed. Product amounts (fluorescence (a. u.)) which were formed for each different X7 concentration were calculated using HPLC analysis. A graph of product amount (fluorescence (a. u.)) vs X7 concentration ( $\mu\text{M}$ ) was drawn to find out which X7 concentration was final for the enzyme to create the maximum product amount. Molar amounts and the concentrations ( $\mu\text{M}$ ) of the products according to X7 concentration were also calculated using a standard fluorescence (a. u.) value of a sample of which mole amount was known. Final concentration of the X7 acceptor substrate in total reaction volume was defined for each reaction volume which included the X7 acceptor substrate in different concentrations. Using this information, reaction rate ( $\mu\text{M}$  product/min),  $1/\text{X7}$  final concentration ( $1/\mu\text{M}$ ) and  $1/\text{reaction rate}$  (min/ $\mu\text{M}$  product) were determined. In order to calculate the maximal velocity ( $V_{\text{max}}$ ), the turnover number ( $k_{\text{cat}}$ ) and Michaelis constant ( $K_{\text{m}}$ ) of the enzyme, Michaelis-Menten (reaction rate ( $\mu\text{M}$  product/min) vs final X7 concentration ( $\mu\text{M}$ )) (Figure 3.25) and linear Lineweaver-Burke ( $1/\text{reaction rate}$  (min/ $\mu\text{M}$  product) vs  $1/\text{X7}$  concentration ( $1/\mu\text{M}$ )) (Figure 3.26) graphs were generated. Based on the equation from the Lineweaver-Burke graph,  $V_{\text{max}}$ ,  $k_{\text{cat}}$  and  $K_{\text{m}}$  values of the enzyme were found to be 0,014  $\mu\text{M}/\text{min}$ , 2,64  $\text{min}^{-1}$  and 5,84  $\mu\text{M}$ , respectively.

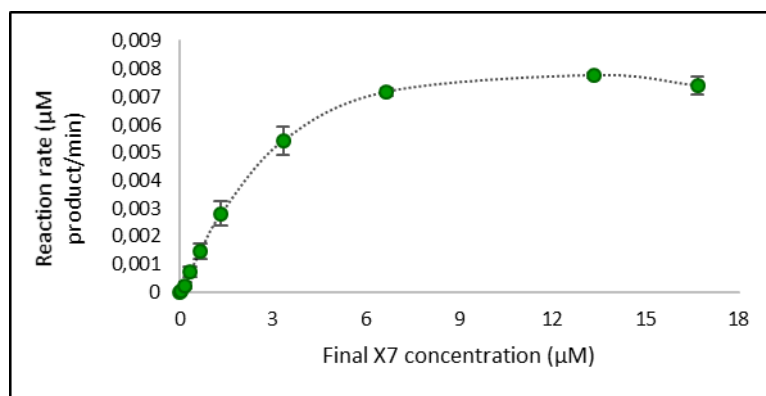


Figure 3.25. Michaelis-Menten (reaction rate (μM product/min) vs final X7 concentration (μM)) graph of CaXTH1 enzyme.

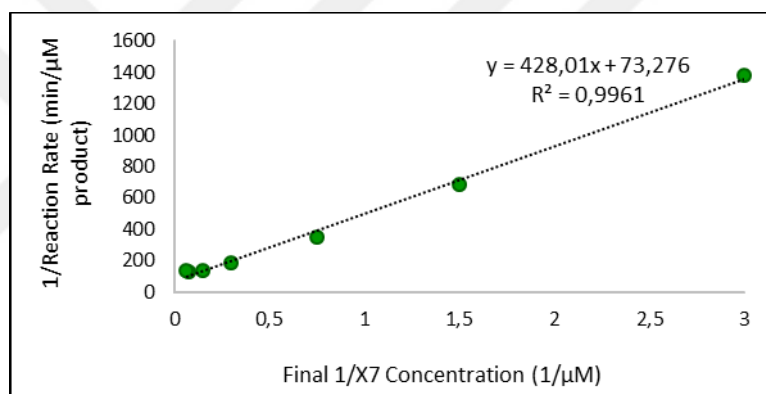


Figure 3.26. Lineweaver-Burke (1/reaction rate (min/μM product) vs 1/X7 concentration (1/μM)) graph of CaXTH1.

### 3.1.7.2. CaXTH2 Enzyme

Enzyme kinetics studies were performed with CaXTH2 enzyme based on HPLC analysis as described with CaXTH1 enzyme. Studies were conducted by master's student Ezgi Türksever under my direct supervision. The best working TXG donor substrate concentration was found to be 0,3 per cent (w/v) for the enzyme. Using 0,3 per cent (w/v) TXG as the donor substrate and X7 as the acceptor substrate with different concentrations (0 μM, 5 μM, 10 μM, 15 μM, 30 μM, 50 μM, 70 μM, 100 μM, 150 μM, 200 μM, 250 μM) enzyme reactions were performed as described before. Michaelis-Menten (Figure 3.27) and

linear Lineweaver-Burke (Figure 3.28) graphs were drawn.  $V_{max}$ ,  $k_{cat}$  and  $K_m$  values of the enzyme were calculated as 0,0063  $\mu\text{M}/\text{min}$ , 3,6  $\text{min}^{-1}$  and 0,1  $\mu\text{M}$ , respectively.

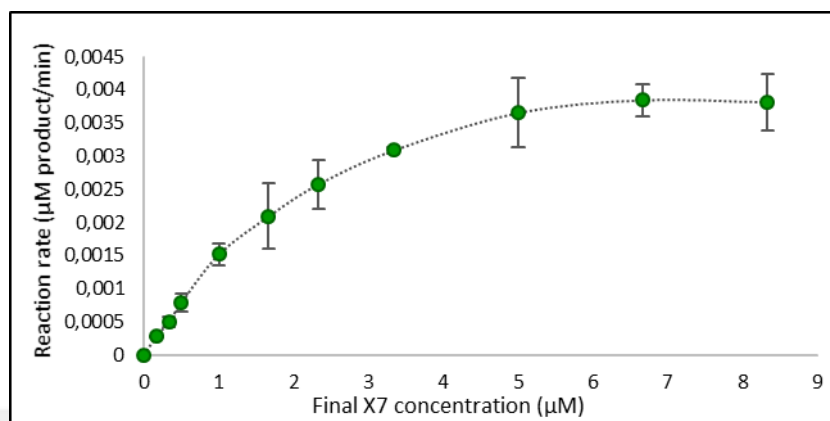


Figure 3.27. Michaelis-Menten (reaction rate ( $\mu\text{M}$  product/min) vs final X7 concentration ( $\mu\text{M}$ )) graph of CaXTH2 enzyme.

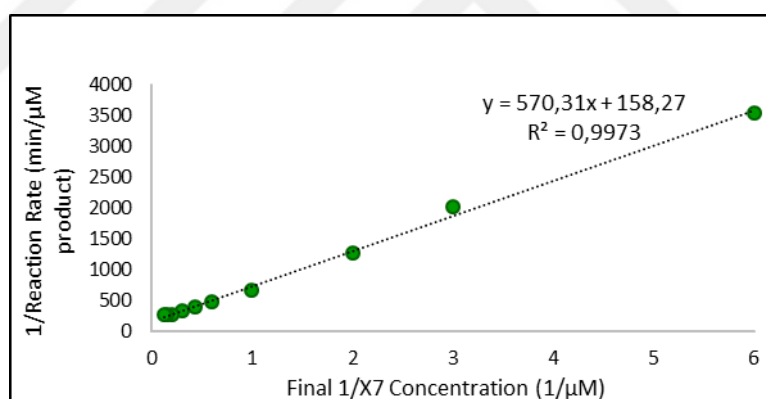


Figure 3.28. Lineweaver-Burke (1/reaction rate ( $\text{min}/\mu\text{M}$  product) vs  $1/\text{X7}$  concentration ( $1/\mu\text{M}$ )) graph of CaXTH2.

### 3.1.7.3. CaXTH3 Enzyme

Studies were conducted based on HPLC analysis of the reactions including TXG as the donor substrate and X7 acceptor substrate with different concentrations including, 0  $\mu\text{M}$ , 1  $\mu\text{M}$ , 5  $\mu\text{M}$ , 10  $\mu\text{M}$ , 20  $\mu\text{M}$ , 40  $\mu\text{M}$ , 80  $\mu\text{M}$ , 200  $\mu\text{M}$ , 400  $\mu\text{M}$ , 700  $\mu\text{M}$ . The enzyme seemed to work best with 0,6 per cent (w/v) TXG donor substrate. Michaelis-Menten

(Figure 3.29) and linear Lineweaver-Burke (Figure 3.30) graphs were drawn.  $V_{max}$ ,  $k_{cat}$  and  $K_m$  values of the enzyme were calculated as 0,046  $\mu\text{M}/\text{min}$ , 41,85  $\text{min}^{-1}$  and 2,48  $\mu\text{M}$ , respectively.

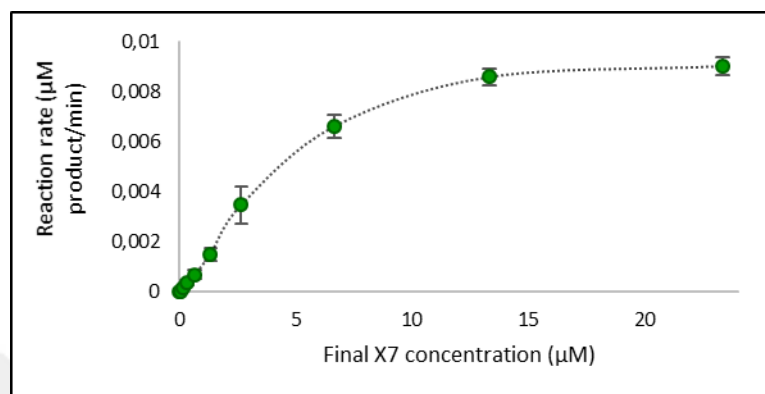


Figure 3.29. Michaelis-Menten (reaction rate ( $\mu\text{M product}/\text{min}$ ) vs final X7 concentration ( $\mu\text{M}$ )) graph of CaXTH3 enzyme.

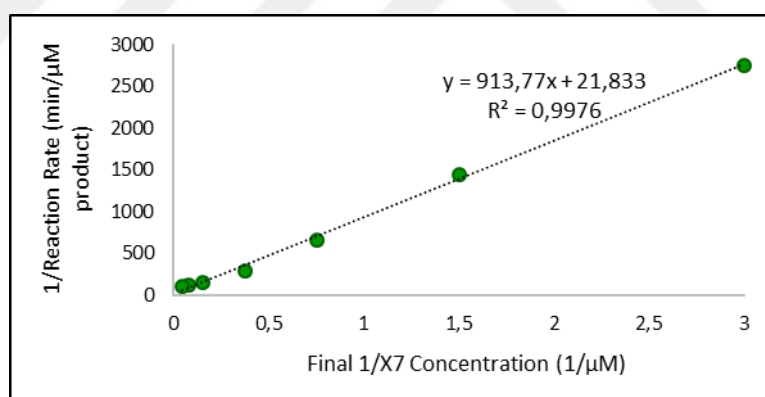


Figure 3.30. Lineweaver-Burke (1/reaction rate ( $\text{min}/\mu\text{M product}$ ) vs  $1/\text{X7}$  concentration ( $1/\mu\text{M}$ )) graph of CaXTH3.

### 3.2. CAPSICUM PLANT GROWTH TRIALS

Different trials were done with capsicum seeds from various regions of Turkey. Growth and stress studies were started with 25 varieties. However, plant seeds from different climate conditions did not germinate in standard conditions. Germination rates were not

equal and a lot of the varieties did not germinate at all. The seeds that germinated in the early trials stopped germination in the next experiments and number of the germinated seeds were lower than expected. Also, same capsicum varieties seemed to demonstrate different growth rates in equal growth times in both green house and growth cabinet conditions. Due to the inconsistency in phenotypic and relative gene expression results number of the capsicum varieties that were used in this study were reduced to 8 which were Erzurum, Aktör, Seki, Cila, Samuray, Çanakkale, Kahramanmaraş and Mert. Similar problems were encountered with these varieties too, but they were overcome with reducing the number of the seedlings that were used in each abiotic stress treatment and to use the seedlings with same growth rates.

Growth trials were performed on agar, MS-agar, perlite and soil. Contamination problems were encountered with MS media due to its rich and nutritious content. A surface sterilization method was developed. After incubating the Erzurum seeds in 70 per cent EtOH and different concentrated NaOCl solutions for different time periods, capsicum seedlings were grown on MS agar in growth cabinet conditions for 11 days. Root and shoot lengths, root numbers and germination ratios were measured (Figure 3.31). Each different trial was done with 30 plant explants and results were analysed with “Post Hoc” comparison test (Table 3.12). The results of the sterilization trials showed that the least germination rate and root-shoot lengths were observed with 10 min incubation in 15 per cent NaOCl (4 per cent Merck commercial stock) when the 70 per cent EtOH incubation was standard for all concentration trials for NaOCl. Incubation with 70 per cent EtOH for 1,5 min and 25 per cent NaOCl (4 per cent Merck commercial stock) for 10 minutes was chosen to be the best method since it provided the highest root-shoot growth and germination ratio. The results of the sterilization trials showed that least germination rate and root-shoot lengths were observed with 10 min incubation in 15 per cent NaOCl.

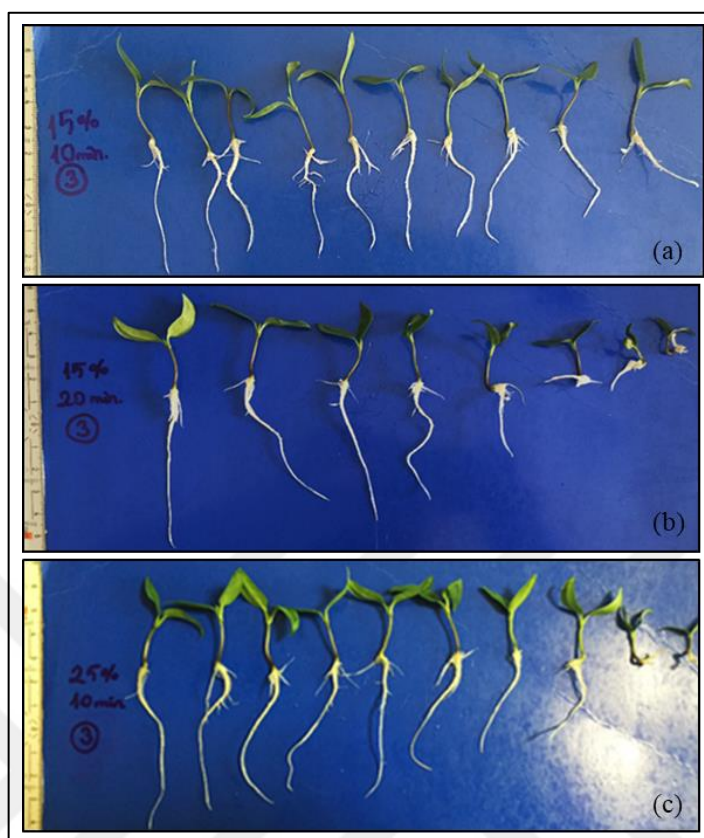


Figure 3.31. Root-shoot length comparison of the 11-day-old MS agar grown Erzurum seedlings that were incubated in 70 per cent EtOH for 1,5 min and (a) 15 per cent NaOCl for 10 min, (b) 15 per cent NaOCl for 20 min (c) 25 per cent NaOCl 10 min.

Table 3.12. Post Hoc analysis and comparison of root-shoot lengths, root numbers and germination rates of 11-day-old MS agar grown Erzurum seedlings that were treated with different concentrated NaOCl solutions for different time periods following incubation in 70 per cent EtOH for 1,5 min.

NaOCl conc.	Incubation time (min)	Primary root length Avg±SD (mm)	Shoot length Avg±SD (mm)	Root number Avg±SD	Germination percentage (%)
15%	10	48±2,5 bc	16,3±0,55 a	5,85±0,54 bc	86,6
15%	20	51±2,98 b	16,4±0,49 a	6,4±0,54 b	90
25%	10	56,2±1,91 a	16,5±0,37 a	7,58±0,46 a	93,3

### 3.3. SALT STRESS

In order to test salt stress on capsicum, Erzurum seedlings were germinated on 0,5 per cent agar including ultra-pure water (pH 5,8) and transferred on to 0,5 per cent agar including ultra-pure water (pH 5,8) including different concentrations of NaCl (0 mM, 50 mM, 100 mM). Seedlings then were grown 6 more days in plant growth cabinet conditions and phenotypic effects on root and shoot structures were examined (Figure 3.32). Germination was observed on all control, 50 mM NaCl and 100 mM NaCl medias. However, it was clear that even the 50 mM NaCl concentration was enough to inhibit the root and shoot growth. The root and shoot structures were severely affected by the salt concentration. Some of the germinated ones were able to grow their first leaves and spot of growth was observed for both root and shoot structures. When the salt concentration was increased to 100 mM growth of the seedlings were almost completely inhibited. Very little root growth was observed for some of the germinated seedlings. Salt concentrations were considered to be too high to see the effects of abiotic stress gradually. Decreased salt concentrations were used for future experiments.

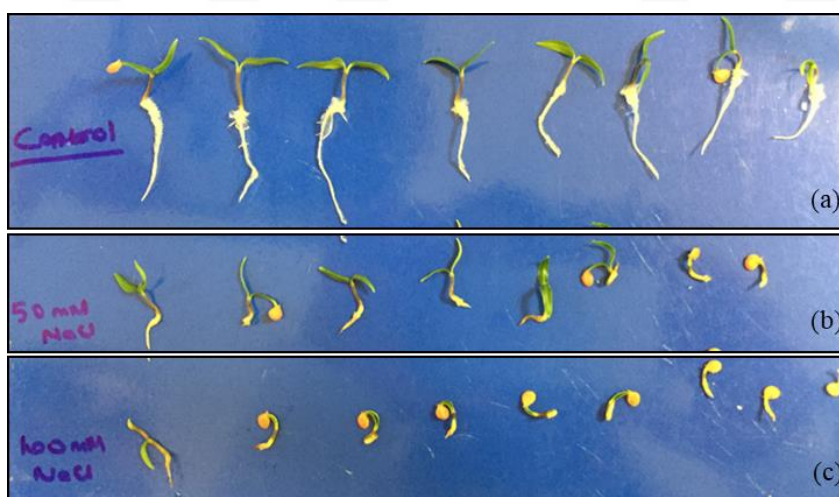


Figure 3.32. Phenotypic examination of 11-day-old Erzurum seedlings grown on (a) 0,5 per cent agar media with 0 mM NaCl, (b) 0,5 per cent agar media with 50 mM NaCl, (c) 0,5 per cent agar media with 100 mM NaCl.

Next experiment was conducted with 0,5 per cent agar medias containing less than 50 mM NaCl. Erzurum seedlings were germinated and grown on agar medias including different

concentrations of NaCl (0 mM, 5 mM, 10 mM, 20 mM, 30 mM, 40 mM) as described before. At the end of 11 days salt stress effects were studied on the seedlings (Figure 3.33). Root and shoot lengths were measured and root numbers were calculated. Results were then analysed via Post Hoc multiple comparison test (Table 3.13).

Salt concentration did not seem to affect plant growth negatively until 20 mM NaCl concentration, in fact, root lengths were shown to increase as the salt concentration was increased until 20 mM. On the other hand, when the salt concentration was 30 mM and more, root lengths were shown to decrease drastically. Based on these findings and to be able to see the inhibiting effects of the abiotic stress further experiments were performed on MS agar media with 0 mM NaCl, 25 mM NaCl and 50mM NaCl using surface sterilization method that was described before. Further salt stress trials were performed via germinating Erzurum, Cila, Aktör and Samuray pepper seedlings on MS agar media and transferring them on to MS agar media including 0 mM NaCl , 25 mM NaCl and 50mM NaCl concentrations as described before. Seedlings from different varieties were grown for 6 days after germination. At the end of this period phenotypic effects of the salt stress was studied for all varieties.

Table 3.13. Post Hoc analysis and comparison of root-shoot lengths and root numbers of 11-day-old Erzurum seedlings grown on 0,5 per cent agar medias including 0 mM NaCl, 5 mM NaCl, 10 mM NaCl, 20 mM NaCl, 30 mM NaCl and 40 mM NaCl.

<b>NaCl conc. (mM)</b>	<b>Primary root length Avg±SD (cm)</b>	<b>Shoot length Avg±SD (cm)</b>	<b>Root number Avg±SD</b>
0	2,41± 0,23 ab	0,96±0,07 a	7,00±0,88 a
5	1,85±0,24 bc	0,57±0,05 c	1,69±0,54 bc
10	2,53±0,29 ab	0,80±0,06 ab	3,16±0,85 b
20	3,09±0,66 a	0,72±0,05 b	2,35±0,64 bc
30	0,73±0,12 d	0,64±0,04 bc	1,37±0,26 c
40	0,23±0,04 d	0,40±0,05 d	1,00±0,00 c

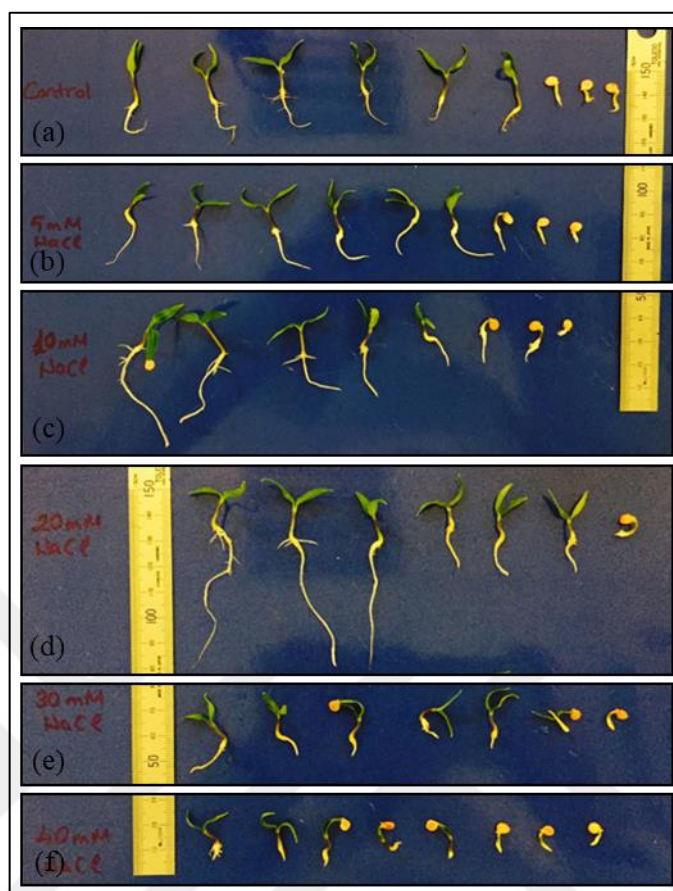


Figure 3.33. Phenotypic examination of 11-day-old Erzurum seedlings grown on (a) 0,5 per cent agar media with 0 mM NaCl, (b) 0,5 per cent agar media with 5 mM NaCl, (c) 0,5 per cent agar media with 10 mM NaCl, (d) 0,5 per cent agar media with 20 mM NaCl, (e) 0,5 per cent agar media with 30 mM NaCl, (f) 0,5 per cent agar media with 40 mM NaCl.

For Erzurum variety, primary root lengths of the control plants were quite similar to primary root lengths of the 25 mM NaCl grown plants. Slight inhibition on the growth of roots and shoots was observed for 25 mM NaCl MS agar grown Erzurum seedlings compared to control plants. When the salt concentration reached 50 mM, the effects of the salt stress were clearer. Seedlings were not as developed and root lengths were significantly shorter. A decrease in root number was also observed for these plants. To confirm that Post Hoc multiple comparison analysis was applied to compare root-shoot lengths and root numbers of the control and stress treated plants for Erzurum variety (Figure 3.34). Results confirmed the decrease in root-shoot lengths and root numbers as the salt concentration increased (Table 3.14).



Figure 3.34. Phenotypic examination of 11-day-old Erzurum seedlings grown on (a) MS agar media with 0 mM NaCl, (b) MS agar media with 25 mM NaCl, (c) MS agar media with 50 mM NaCl.

Table 3.14. Post Hoc analysis and comparison of root-shoot lengths and root numbers of 11-day-old Erzurum seedlings grown on MS agar medias including 0 mM NaCl, 25 mM NaCl, 50 mM NaCl.

NaCl conc. (mM)	Primary root length Avg $\pm$ SD (cm)	Shoot length Avg $\pm$ SD (cm)	Root number Avg $\pm$ SD
0	71,2 $\pm$ 2,53 a	23,1 $\pm$ 1,81 a	17,5 $\pm$ 1,12 a
25	70,4 $\pm$ 5,16 a	22,0 $\pm$ 1,48 a	18,8 $\pm$ 1,28 a
50	32,3 $\pm$ 3,89 b	16,2 $\pm$ 1,99 b	10,8 $\pm$ 1,81 b

No reduction in root lengths of the control and 25 mM stress treated plants was observed for varieties Cila (Figure 3.35), Aktör (Figure 3.36), Samuray (Figure 3.37) and Seki. In fact, 25 mM NaCl concentration seemed to improve the root lengths of the seedlings 7,6 per cent, 22,5 per cent, 12,3 per cent and 1,4 per cent compared to the root lengths of control seedlings from Cila (Table 3.15), Samuray (Table 3.16), Aktör (Table 3.17) and Seki (Table 3.18) varieties, respectively. For Seki variety, increase in the root lengths seemed to be less compared to Cila, Samuray and Aktör varieties when the salt concentration was 25 mM. As the NaCl concentration increased to 50 mM, 17,7 per cent reduction was observed in root lengths in comparison to control plants for Seki variety. Root lengths of the seedlings from Aktör variety kept increasing even the NaCl concentration was 50 mM and reached to 19,7 per cent more than the root lengths of control plants. Cila and Samuray varieties on the other hand, demonstrated shorter root lengths when grown on 50 mM NaCl containing MS agar compared to root lengths of 25 mM NaCl containing MS agar grown seedlings. However, root lengths for Cila and Samuray variety were still 0,5 per cent and 13 per cent more than the root lengths of control plants, respectively.

Effects of salt stress had a similar pattern on shoot lengths in a matter of increasing and decreasing according to Cila, Samuray, Aktör and Seki varieties. Shoot lengths seemed to increase 37 per cent and 20,5 per cent more than the control groups for Cila and Samuray varieties, respectively, when the salt concentration was 25 mM. Aktör variety exhibited a slight decrease (1,1 per cent), while Seki variety showed 16,8 per cent decrease in shoot lengths in comparison to control plants within the variety for 25 mM NaCl concentration. When the salt concentration was 50 mM, all varieties demonstrated a noticeable reduction in shoot lengths except for Aktör variety. Shoot lengths were 0,5 per cent less than the control plants for Aktör variety at 50 mM NaCl concentration. Eventhough the shoot lengths of Cila and Samuray seedlings were 12,4 per cent and 11 per cent less than the plants grown on 25 mM NaCl containing MS agar they were still 20,1 per cent and 7,3 per cent more than the control plants, respectively. For Seki variety, reduction in shoot lengths reacted to 26,6 per cent in comparison to control plants when the salt concentration was 50 mM.

Germination rates did not change for Cila variety depending on the NaCl concentration it was 85 per cent for all NaCl concentrations. For Samuray variety it reduced to 60 per cent

from 75 per cent for 25 mM NaCl concentration and increased to 67,22 per cent for 50 mM NaCl concentration. Germination rate increased to 100 per cent from 95 per cent for Aktör variety when the salt concentration was 25 mM but reduced to 83,33 per cent once the salt concentration reached to 50 mM. For Seki variety, the germination rate dropped to 40 per cent from 70 per cent for 25 mM NaCl concentration and to 45 per cent for 50 mM NaCl concentration. To be able to understand beyond the phenotypic effects of salt stress on these, QPCR studies were performed using root samples. Salt stress trials on agar were carried out by master's student Ezgi Türksever under my direct supervision.

Table 3.15. Average length of primary roots, shoots and germination rates of 11-day-old Cila seedlings across 3 different concentrations of NaCl.

NaCl (mM)	Primary root length Avg (cm)	Shoot length Avg (cm)	Germination rate
0	7,01	1,79	85%
25	7,96	2,59	85%
50	7,29	2,27	85%

Table 3.16. Average length of primary roots, shoots and germination rates of 11-day-old Samuray seedlings across 3 different concentrations of NaCl.

NaCl (mM)	Primary root length Avg (cm)	Shoot length Avg (cm)	Germination rate
0	6	1,51	75%
25	7,35	1,82	60%
50	6,78	1,62	67,22%

Table 3.17. Average length of primary roots, shoots and germination rates of 11-day-old Aktör seedlings across 3 different concentrations of NaCl.

NaCl (mM)	Primary root length Avg (cm)	Shoot length Avg (cm)	Germination rate
0	5,78	1,82	95%
25	6,49	1,8	100%
50	6,92	1,81	83,33%

Table 3.18. Average length of primary roots, shoots and germination rates of 11-day-old Seki seedlings across 3 different concentrations of NaCl.

NaCl (mM)	Primary root length Avg (cm)	Shoot length Avg (cm)	Germination rate
0	7,11	1,73	70%
25	7,21	1,44	40%
50	5,85	1,27	45%

Kahramanmaraş and Çanakkale pepper seeds were germinated on perlite and transferred on to soil as described before. Salt stress treatment was applied to 3-week-old seedlings. Stress treatment was achieved by soaking the roots of the plants in 200 mM NaCl solution for different time intervals (0 min-10 min-30 min-120 min). Since this method created a huge amount of stress on young pepper plants, time intervals for sample collection and phenotypic observation were kept as short as possible to observe the effects of salt stress gradually. Increasing effects of salt stress was shown to start from 10 min with a drop in the turgor pressure for both Kahramanmaraş and Çanakkale varieties. This phenotypic change was more evident with plants that were soaked in 200 mM NaCl solution for 30 min. There were no significant differences in phenotypic appearances for 30 min plants and 120 min plants for both varieties. It was detected that the general impact of stress conditions was similar for both Çanakkale (Figure 3.38) and Kahramanmaraş (Figure 3.39) pepper plants. However, Çanakkale seedlings were slightly in better shapes than Kahramanmaraş seedlings. QPCR studies were performed with root and shoot samples to have a better understanding in gene expression levels.

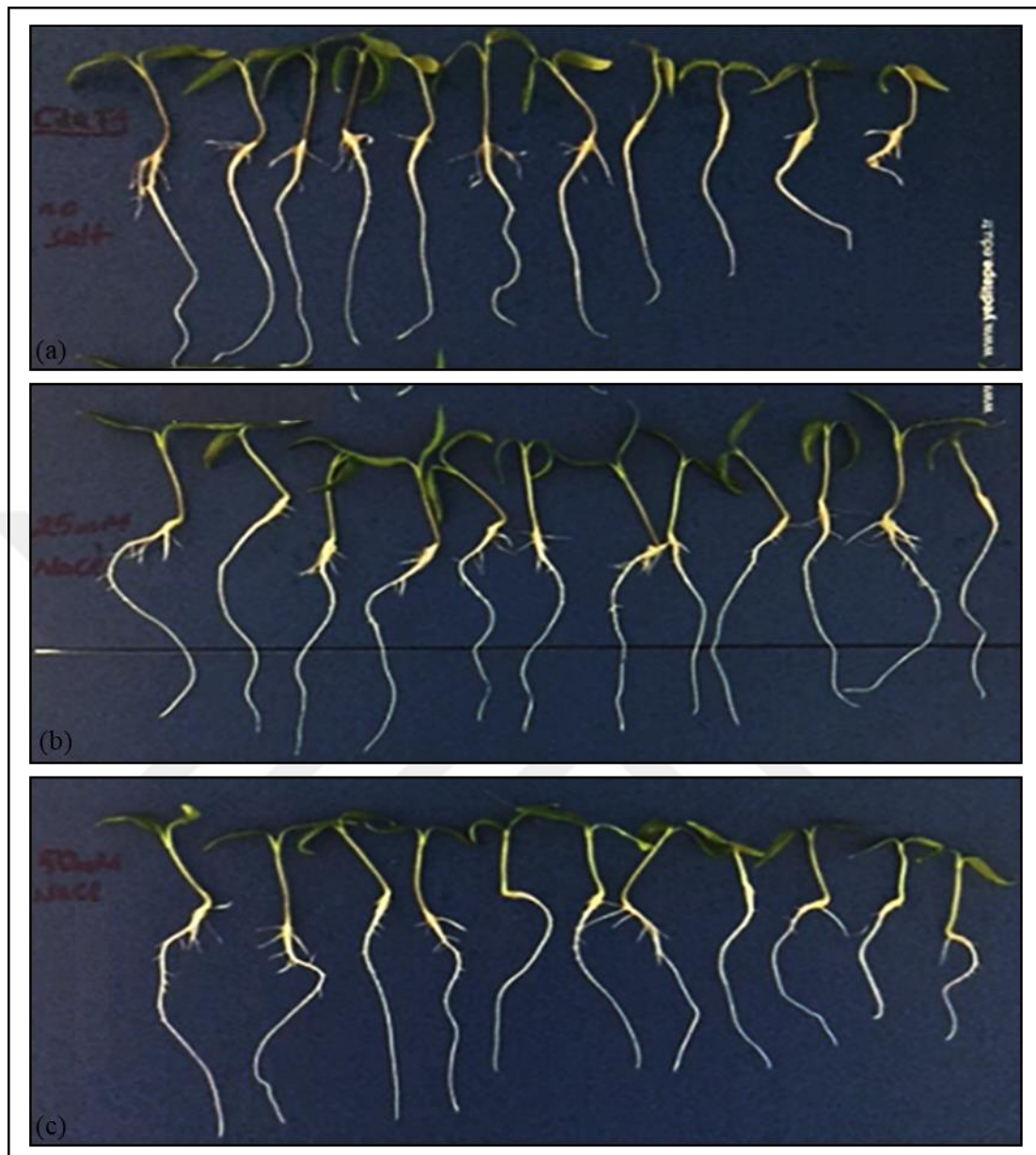


Figure 3.35. Phenotypic examination of 11-day-old *Cila* seedlings grown on (a) MS agar media with 0 mM NaCl, (b) MS agar media with 25 mM NaCl, (c) MS agar media with 50 mM NaCl.

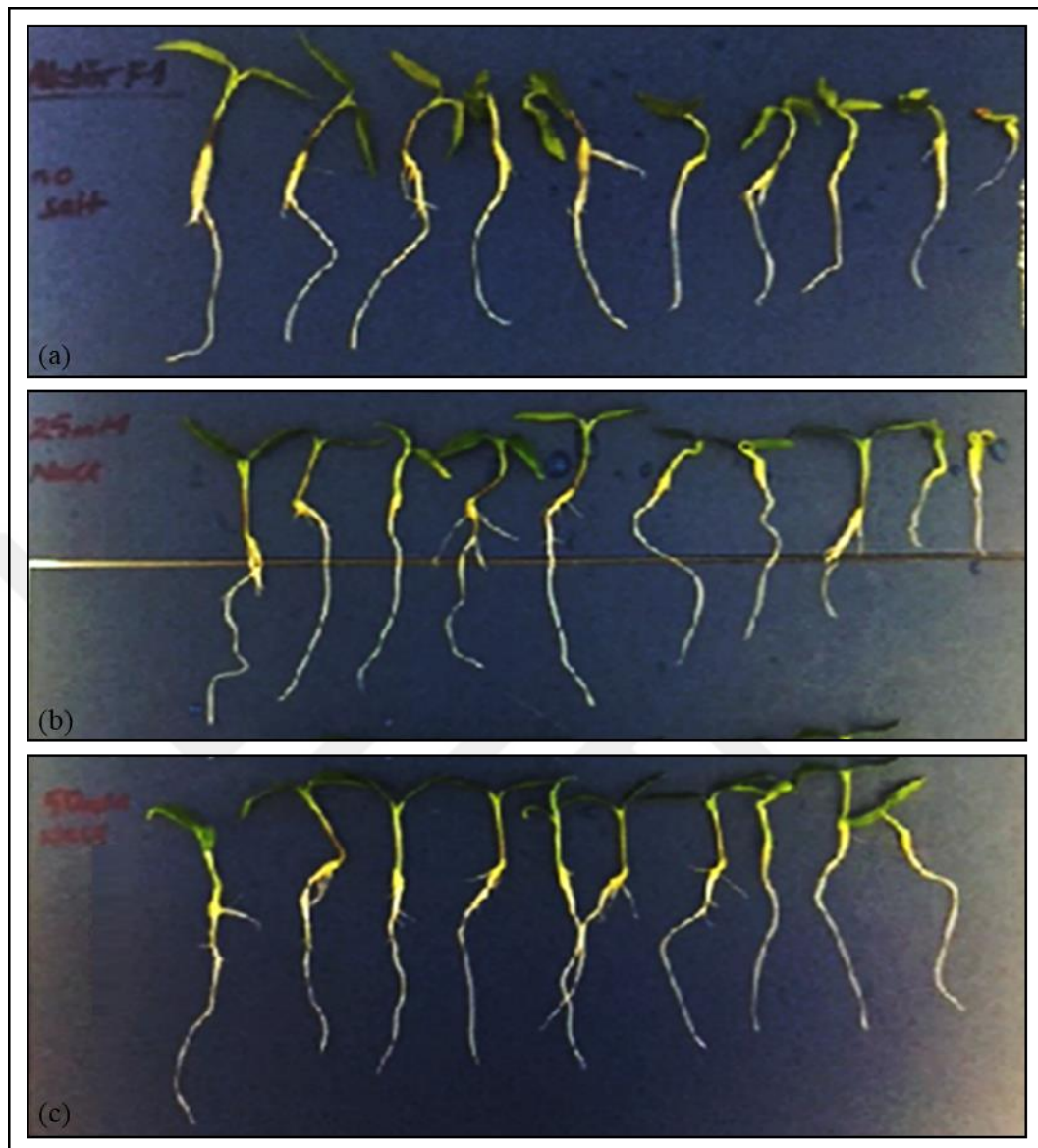


Figure 3.36. Phenotypic examination of 11-day-old Aktör seedlings grown on (a) MS agar media with 0 mM NaCl, (b) MS agar media with 25 mM NaCl, (c) MS agar media with 50 mM NaCl.

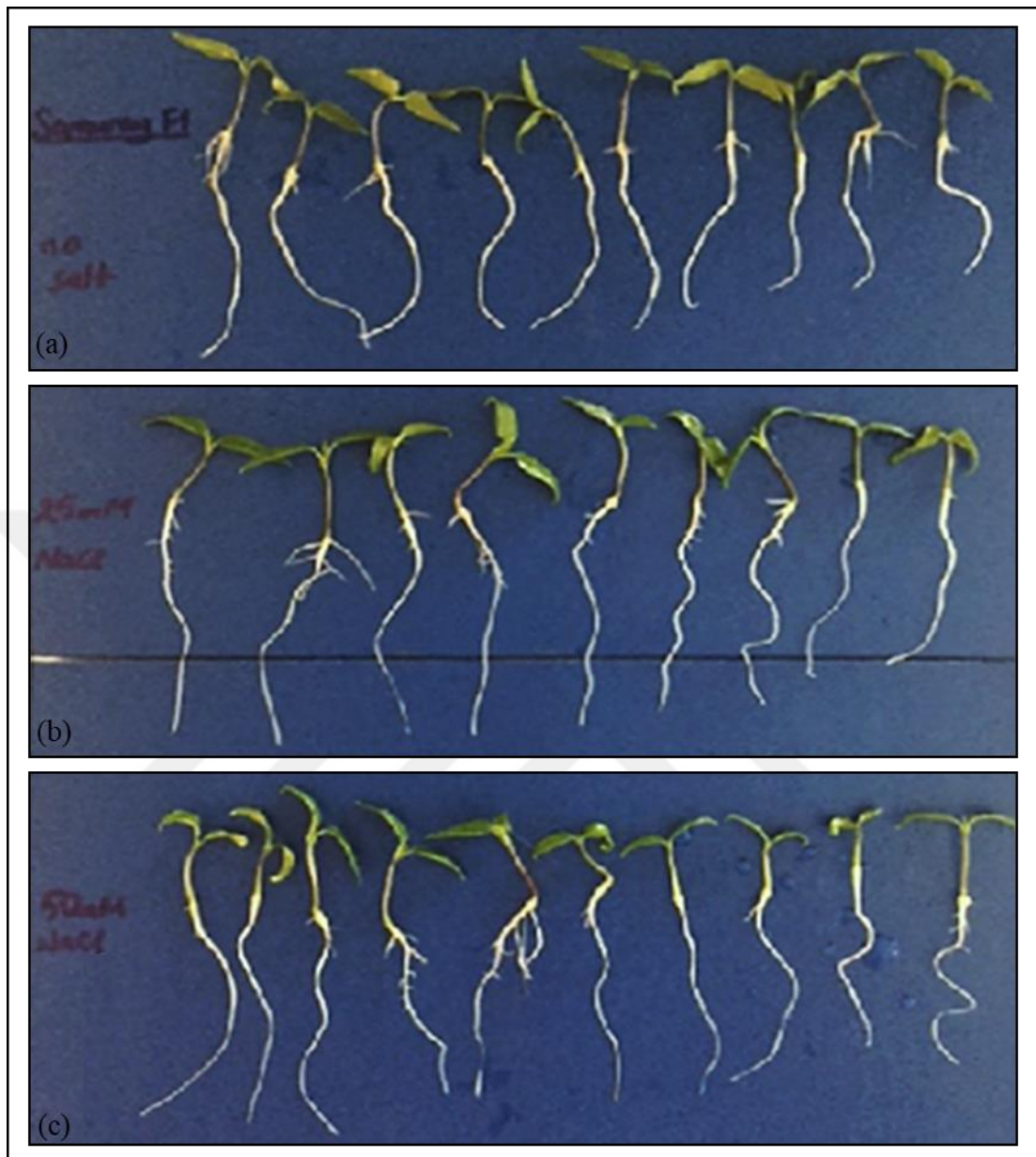


Figure 3.37. Phenotypic examination of 11-day-old Samuray seedlings grown on (a) MS agar media with 0 mM NaCl, (b) MS agar media with 25 mM NaCl, (c) MS agar media with 50 mM NaCl.

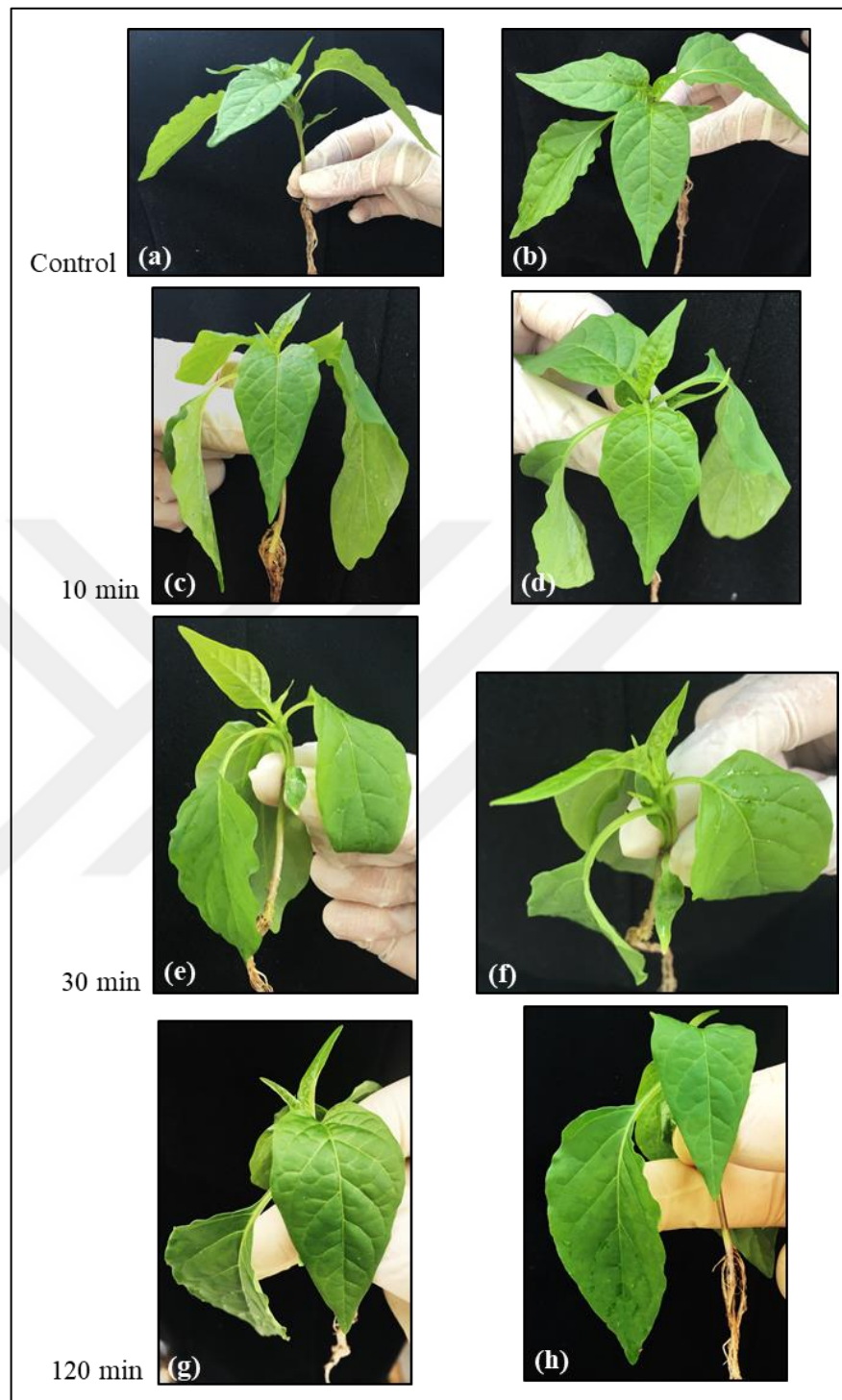


Figure 3.38. Phenotypic examination of 3-week-old Çanakkale seedlings whose roots were soaked into 200 mM NaCl solution for (a)-(b) 0 min, (c)-(d) 10 min, (e)-(f) 30 min, (g)-(h) 120 min. Side and top view of each plant were shown.

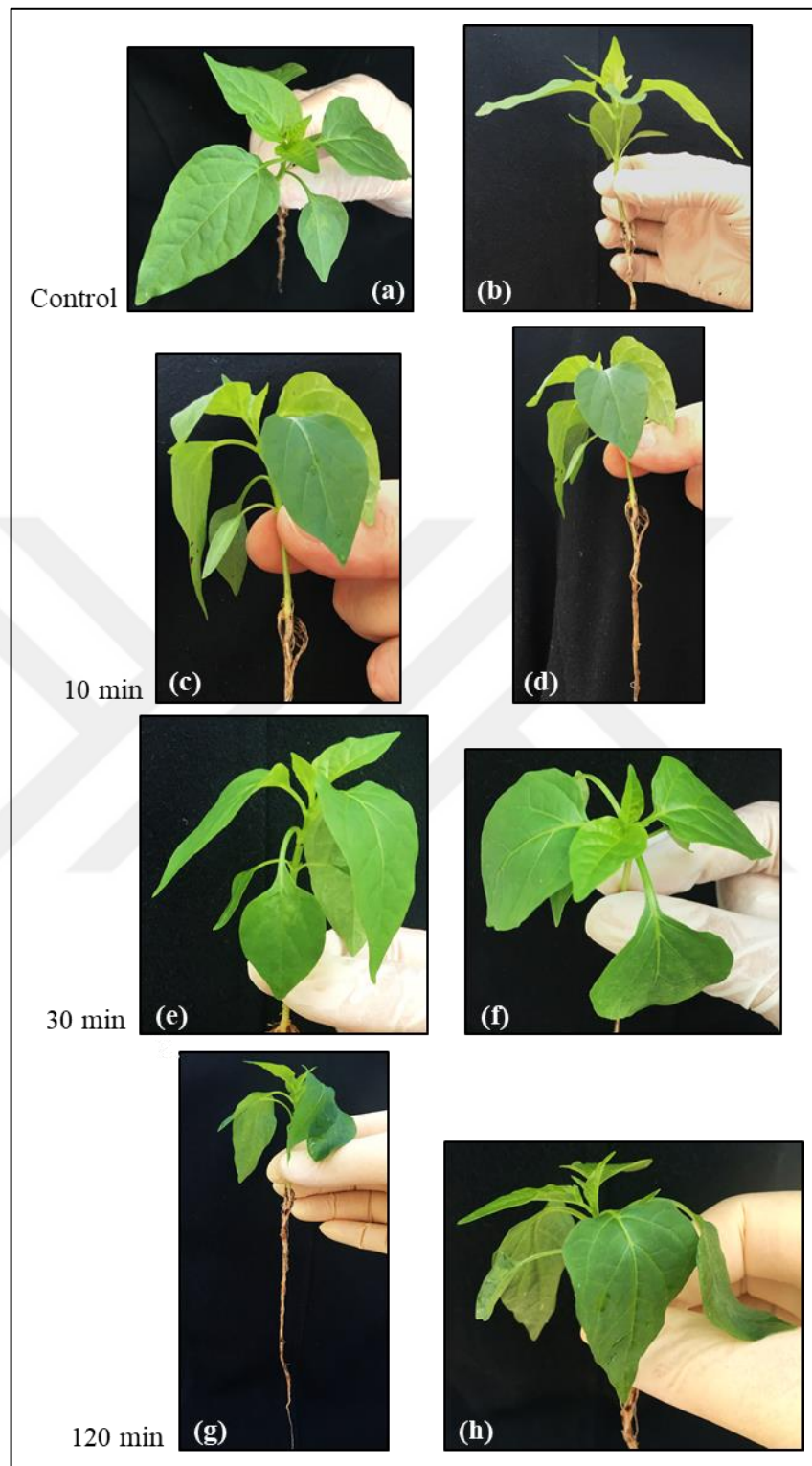


Figure 3.39. Phenotypic examination of 3-week-old Kahramanmaraş seedlings whose roots were soaked into 200 mM NaCl solution for (a)-(b) 0 min, (c)-(d) 10 min, (e)-(f) 30 min, (g)-(h) 120 min. Side and top view of each plant were shown.

### 3.4. COLD STRESS

Early cold stress trials were performed with pepper seedlings from different varieties (Artvin, Diyarbakır, Erzurum, Çanakkale, Mert and Kahramanmaraş). Seeds were germinated on perlite, transferred into soil and grown in green house conditions. Plants were exposed to cold stress via transfer from green house to cold room (5°C). However, germination rate and growth of the plants showed differences due to dissimilarities in the optimum growth conditions for different varieties. Even in the same variety seedlings demonstrated different growth levels. That case caused inaccuracy in stress response for some of the seedlings. In the same variety, some of the seedlings showed more intense phenotypic response even though they were exposed for less amount of time to stress conditions compared to other seedlings from the same variety. Also, leaf samples were collected from the plants in different time intervals (0h-2h-4h-5h-6h-8h-12h-24h) and it was observed that leaf cutting for sample collection created extra stress on the plant and affected phenotypic responses. To repeat the experiment and use a separate seedling for each time interval the number of seedlings for each variety need to ne increase. Nevertheless, there were not enough seedlings for some varieties to use for each time interval to perform a duplicate experiment due to different growth rates and low germination ratios of the varieties. Therefore, the number of varieties was reduced for the next experiments and cold stress studies were continued with Mert and Kahramanmaraş varieties.

Cold stress experiment was repeated with 4-week-old Mert seedlings. Pepper plants were transferred from green house to cold room (5°C) and exposed to stress conditions for different time periods (0h-2h-4h-8h-12h-24h) (Figure 3.40). Phenotypic effects of the cold stress were initially observed after exposure for 2 hours. Plants seemed to lose turgor pressure due to dehydration. When 2 hour and 4 hour seedlings were compared phenotypically, the response levels seemed to be similar. After 4<sup>th</sup> hour stress effects seemed to increase and became more intense by the 24<sup>th</sup> hour. However, plants still did not lose their viability even after 24 hours and recovered from the effects of cold stress after transferring to room temperature. During cold exposure, maintaining the temperature of the cold room was challenging as it was being used for other researchers. Also, plants were kept in dark during whole experiment so they were not in their usual photoperiod. Since

these factors would affect the accuracy of the gene expression results QPCR studies were not performed at the end of this experiment.

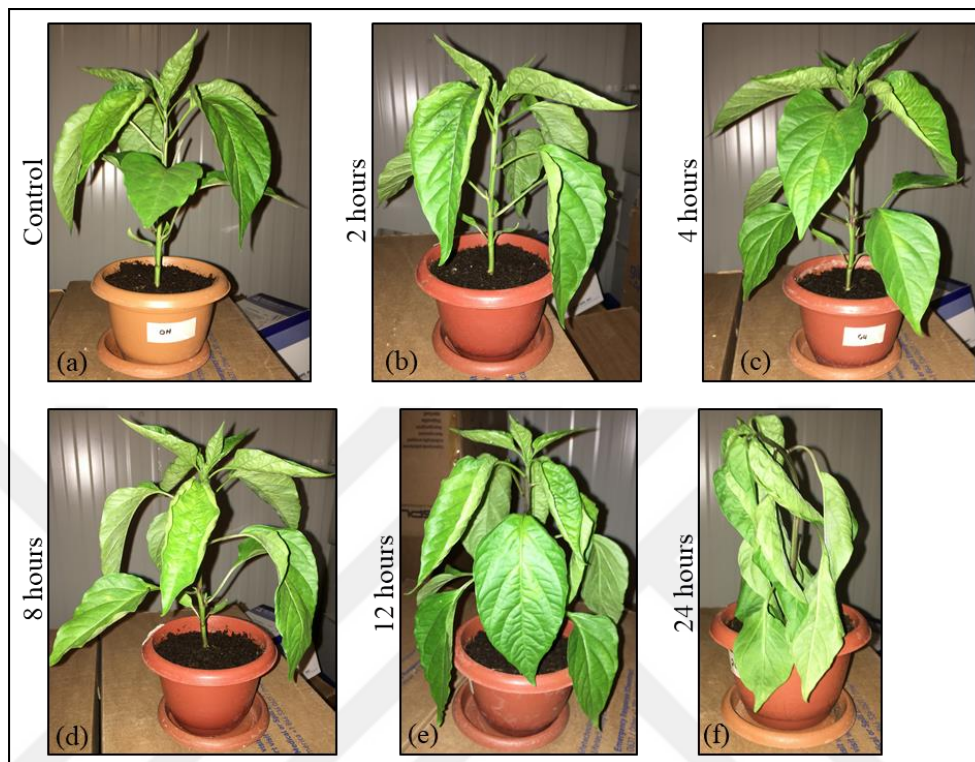


Figure 3.40. Phenotypic examination of 4-week-old Mert seedlings that were exposed to cold stress for (a) 0 hour, (b) 2 hour, (c) 4 hour, (d) 8 hour, (e) 12 hour, (f) 24 hour.

Cold stress studies were performed with Kahramanmaraş and Mert varieties again. In order to prevent the inaccuracies that were faced in previous trials more controlled conditions (temperature-photoperiod-humidity) were chosen, therefore, pepper seedlings were transferred to the plant growth cabinet to create cold stress conditions, after 3 weeks of growth in the green house. Younger seedlings were used in this experiment compared to other pepper seedlings from previous experiments. Since the stress responses would be more rapid and elevated with younger seedlings, experiment time was limited with 12 hours. For a clearer comparison of the phenotypic affects and for the accuracy of the gene expression results control plants were included for each time interval (4h-8h-12h) and kept in green house conditions. Kahramanmaraş and Mert seedlings were exposed to cold stress conditions for different time periods (4h-8h-12h). Phenotypic changes occurring in response to cold stress was observed for each time interval with comparison to control

plant of the same time interval (Figure 3.41, Figure 3.42). Leaf samples from seedlings were used for further gene expression studies.

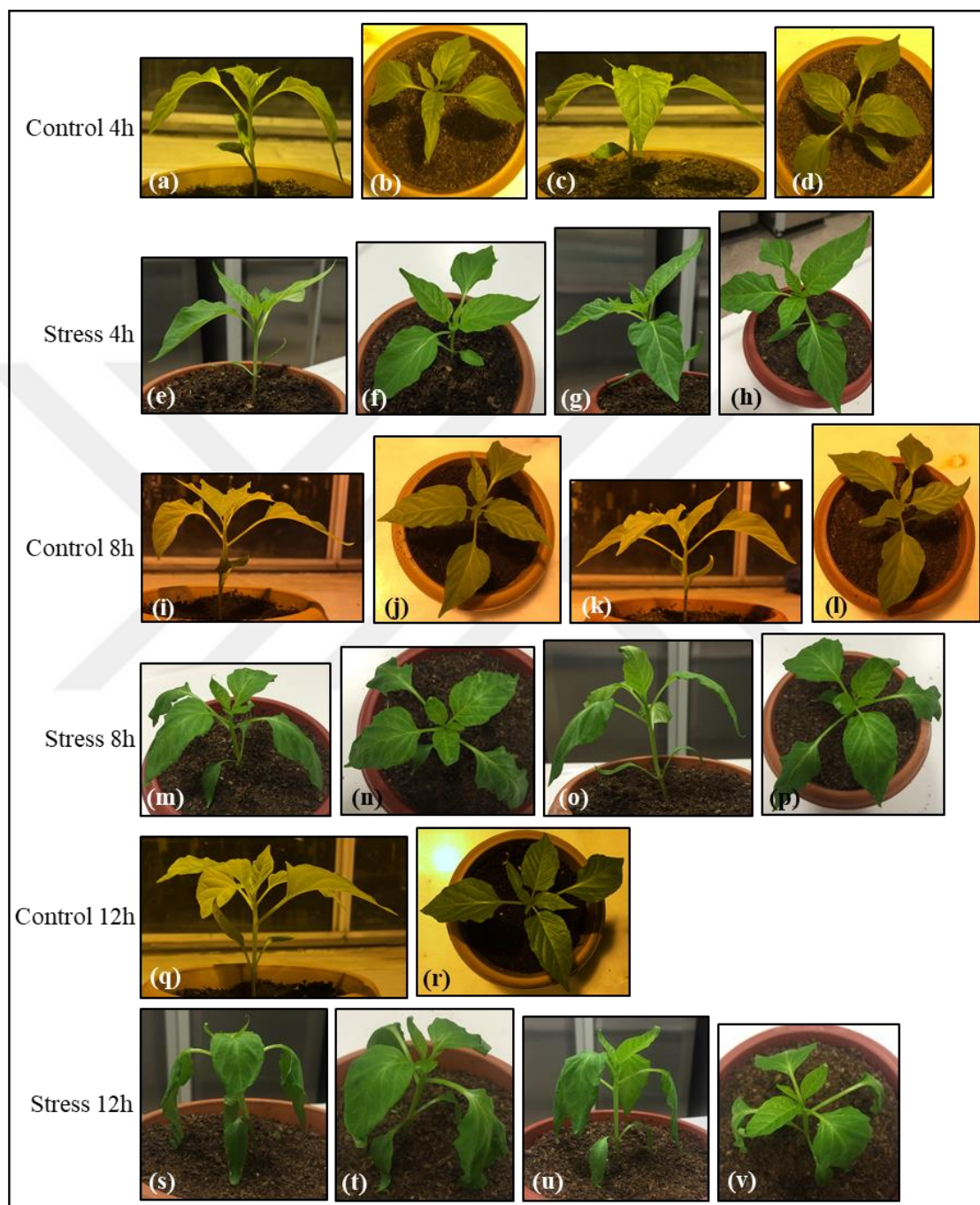


Figure 3.41. Phenotypic observation of 3-week-old Mert seedlings after 4, 8 and 12 hour cold stress treatments across the experimental and control groups. (a)-(b)-(c)-(d) 4 hour control plants, (e)-(f)-(g)-(h) 4 hour stress plants, (i)-(j)-(k)-(l) 8 hour control plants, (m)-(n)-(o)-(p) 8 hour stress plants, (q)-(r) 12 hour control plants, (s)-(t)-(u)-(v) 12 hour stress plants. Side and top view of each plant were shown.

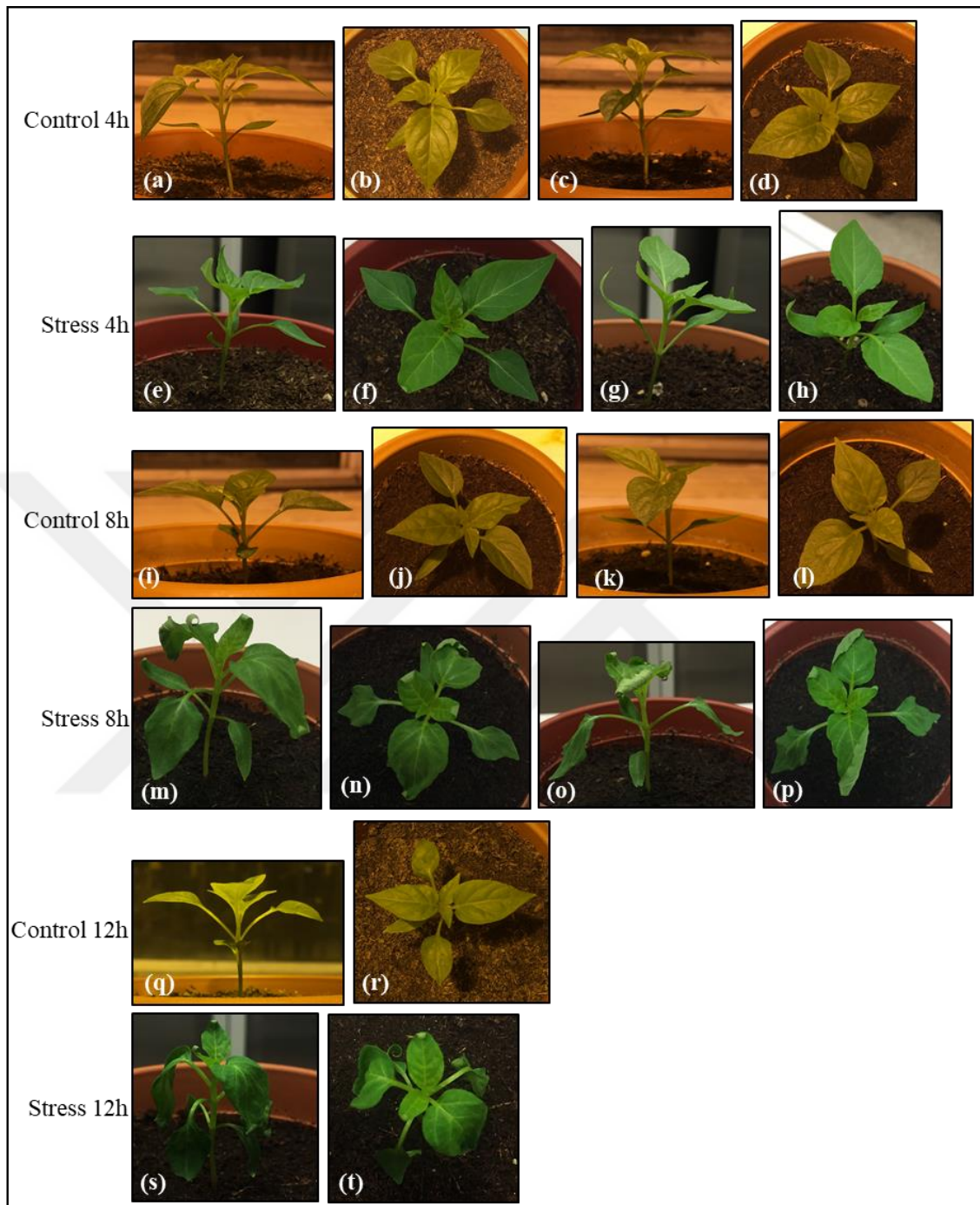


Figure 3.42. Phenotypic observation of 3-week-old Kahramanmaraş seedlings after 4, 8 and 12 hour cold stress treatments across the experimental and control groups. (a)-(b)-(c)-(d) 4 hour control plants, (e)-(f)-(g)-(h) 4 hour stress plants, (i)-(j)-(k)-(l) 8 hour control plants, (m)-(n)-(o)-(p) 8 hour stress plants, (q)-(r) 12 hour control plants, (s)-(t) 12 hour stress plants. Side and top view of each plant were shown.

Strong effects of the cold stress were seen after 8 hours for both varieties. Even though the effects of the cold stress started to show after 4 hours for Kahramanmaraş variety, they were mild, such as slight curling on the leaves. Other than that, 4 hour stress treated Kahramanmaraş seedlings were still looking pretty healthy and had a similar appearance in comparison to 4 hour control plants. There were no phenotypic effects for Mert seedlings after 4 hours of stress treatment. On the other hand, after 8 hours, the impacts of stress exposure on the seedlings from both varieties were clear. The leaves of the plants both exhibited noticeable amounts of wilting and shrivelling. It was observed that the effects of the cold stress increased gradually after 8 and 12 hours. To have a better understanding of stress response mechanism and tolerance leave samples from the seedlings of both varieties were used in QPCR studies.

### **3.5. DROUGHT STRESS**

Mert and Cila varieties were grown for 4 weeks in the green house and subjected to drought stress as described before. Stress level on the plants was determined via fresh weight loss. Plants were dehydrated on Whatman filter papers until they reach 5 per cent - 10 per cent -20 per cent loss in their fresh weight. Time required for the varieties to reach 5 per cent and 10 per cent weight loss was ~5 min and ~10 min, respectively. After 10 min 10min weight loss percentage per one minute started to decrease, and the plants reached at 20 per cent weight loss in ~40 min. The effects of osmotic stress were noticeable for Mert variety at 10 per cent weight loss level. Mert seedlings seemed to lose their turgor pressure due to dehydration at 10 per cent weight loss level, wilting and shrivelling of the leaves had initially started. The effects of drought stress became distinct for both varieties when plants reached 20 per cent weight loss. These effects were more intense for Mert variety (Figure 3.43). Cila variety did not show any significant changes until it reached 20 per cent weight loss (Figure 3.44). Leave samples from both varieties were collected for further gene expression studies.

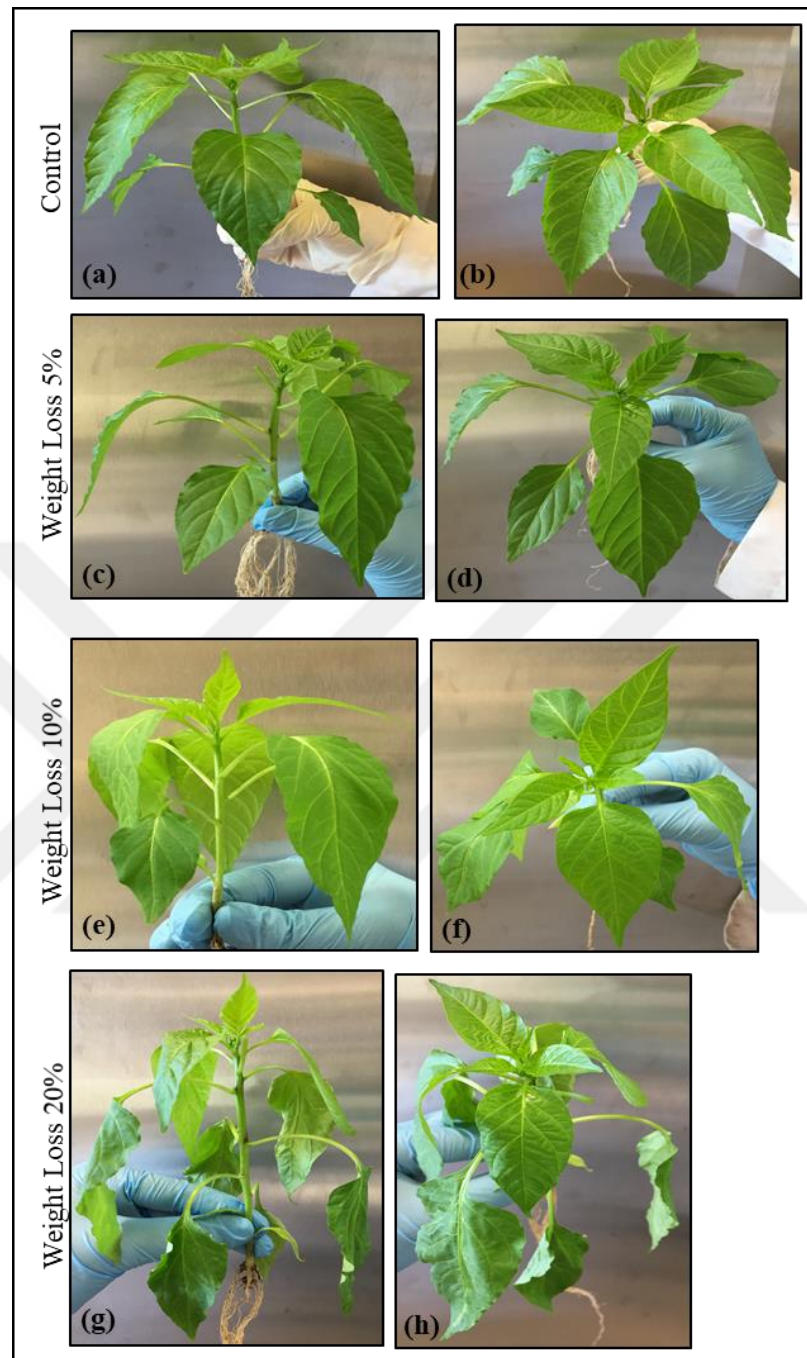


Figure 3.43. Phenotypic observation of 4-week-old Mert seedlings in response to different levels of drought stress. (a)-(b)-(c)-(d) control, (e)-(f)-(g)-(h) 5 per cent weight loss, (i)-(j)-(k)-(l) 10 per cent weight loss and (m)-(n)-(o)-(p) 20 per cent weight loss. Side and top view of each plant were shown.

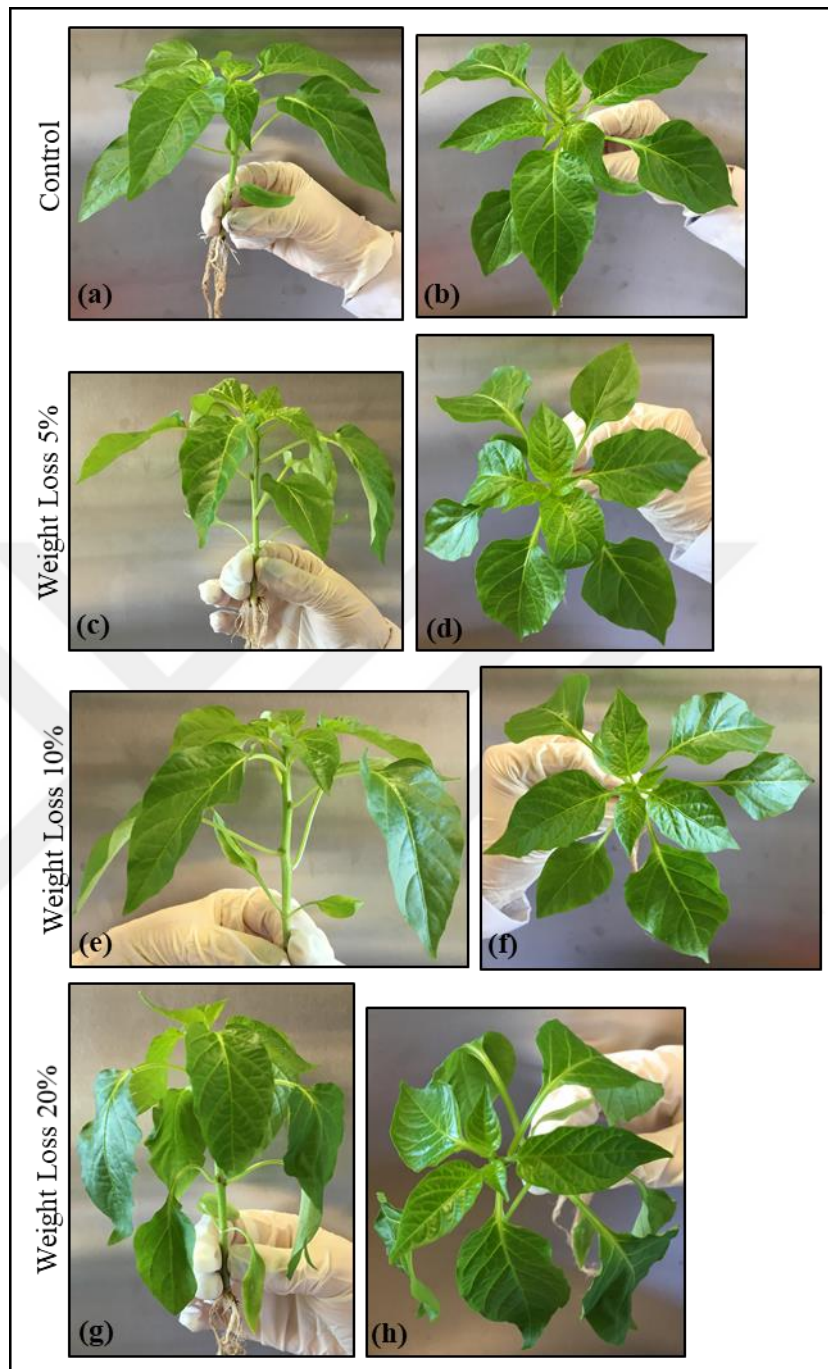


Figure 3.44. Phenotypic observation of 4-week-old Cila seedlings in response to different levels of drought stress. (a)-(b)-(c)-(d) control, (e)-(f)-(g)-(h) 5 per cent weight loss, (i)-(j)-(k)-(l) 10 per cent weight loss and (m)-(n)-(o)-(p) 20 per cent weight loss. Side and top view of each plant were shown.

### 3.6. RNA ISOLATION AND CDNA SYNTHESIS

RNAs were isolated from stress treated and non-stress treated tissues stored at  $-80^{\circ}\text{C}$  using iNtRON Biotechnology easy-spin (DNA free) Total RNA Extraction Kit or TRIzol method. OD measurements of the isolated RNA samples were taken, and cDNA synthesis was performed from these samples. Also 600 ng from each RNA sample was loaded on agarose gel for integrity check. In gel images, sharp clear RNA bands were observed which indicated that the isolated RNAs were intact (Figure 3.45, figure 3.46). OD measurements of the RNAs revealed concentration values varied from  $\sim 400$  ng/ $\mu\text{l}$  to  $\sim 1100$  ng/ $\mu\text{l}$ . The most common concentration range for the samples was between  $\sim 570$  ng/ $\mu\text{l}$  and  $\sim 800$  ng/ $\mu\text{l}$ . A280/A260 ratio was between 2,1 and 2,3. A260/A230 ratio, on the other hand, altered from 1,85 to 2,25. Low A260/A230 values might be resulted from plant carbohydrate contamination or phenol contamination. With the use of normalization factors in the calculation of QPCR results these minor errors were overcome. RNA from these experiments were used to create cDNA libraries for both standard PCR and Q-PCR testing. Also, when cDNA synthesis was performed using these RNA samples a smear like image was observed like expected. However, even though the amount of RNA taken for cDNA synthesis was approximately same for all the samples, cDNA concentrations of the different varieties were different.

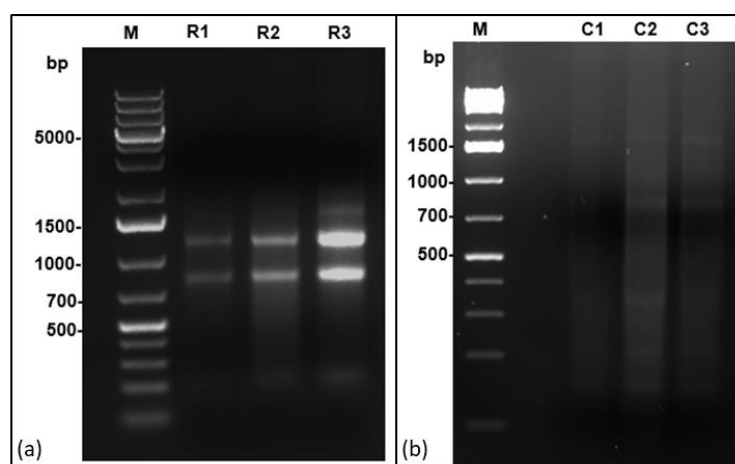


Figure 3.45. Agarose (1 per cent) gel results of the RNAs obtained from 3 different varieties of capsicum varieties. M-Thermo scientific GeneRuler 1kb Plus DNA ladder, R1-Erzurum kıl, R2-Tekirdağ kapyra, R3-Kırklareli sweet sivri. Bands represented 18S and 28S capsicum rRNA.

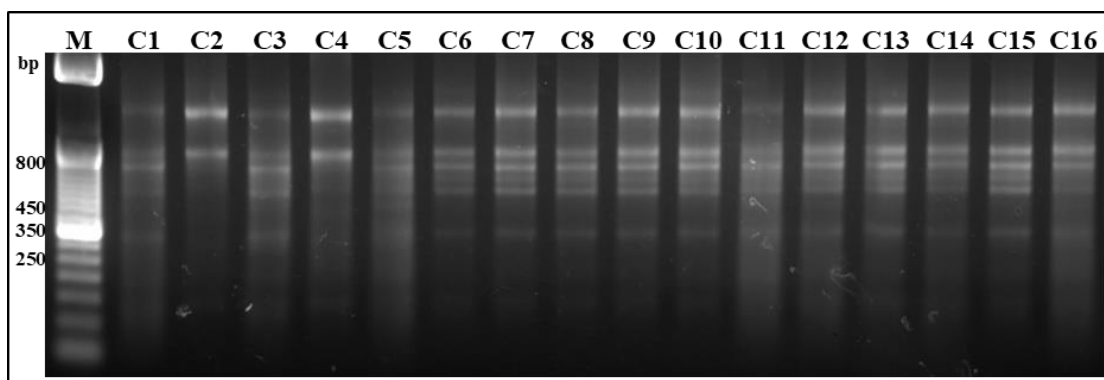


Figure 3.46. Agarose (1 per cent) gel results of the RNAs obtained from the leaf samples of drought stress treated capsicum varieties and leaf-root samples of salt stress treated capsicum varieties. M-Thermo GeneRuler 50kb DNA ladder, C1-Kahramanmaraş 2h leaf (salt), C2- Kahramanmaraş root (salt), C3-Mert 10min leaf (salt), C4-Mert 2h root (salt), C5-Mert 10min leaf (salt), C6-Cila 20 per cent weight loss (drought), C7-Cila 20 per cent weight loss (drought), C8-Aydemir 5 per cent weight loss (drought), C9-Mert cont. (drought), C10-Aydemir 20 per cent weight loss (drought), C11-Aydemir 20 per cent weight loss (drought), C12-Mert cont. (drought), C13-Aydemir 10 per cent weight loss (drought stress), C14-Aydemir 10 per cent weight loss (drought stress), C15-Cila 10 per cent weight loss (drought stress), C16-Mert 10 per cent weight loss (drought).

### 3.7. GENE EXPRESSION STUDIES

Traditional PCR studies were performed using primers specific for Reference genes. Different annealing temperatures were tried and product quality was checked via agarose gel electrophoresis. Following traditional PCR studies, *CaEIF5A2*, *Ca $\alpha$ -Tubulin* and *CaACTIN* genes were chosen as reference genes for further QPCR studies. Primers specific to Reference genes were designed and tested. Later on, Reference gene primers were used to obtain template DNAs from traditional PCR and prepare standards. In order to obtain the template DNA with traditional PCR, 5 separate PCR reactions with a volume of 20  $\mu$ l were performed for each Reference gene. Separate reactions were combined and purified with Varian PLRP-S 1000A 5  $\mu$ m 50x2.1 mm reverse phase column in HPLC. Afterwards, absorbance of the template DNAs was taken in 260 nm (Figure 3.47). Traditional PCR

studies were also performed with *CaXTH1*, *CaXTH2* and *CaXTH3* genes and their gene specific primers. Different annealing temperatures were tried for all 3 genes and optimum  $T_m$  values were determined for *CaXTH1*, *CaXTH2* and *CaXTH3* genes. Bulk-up procedure was applied to all capsicum genes by combining multiple reaction volumes to obtain higher amounts of product. These bulk-ups were later on purified in HPLC.

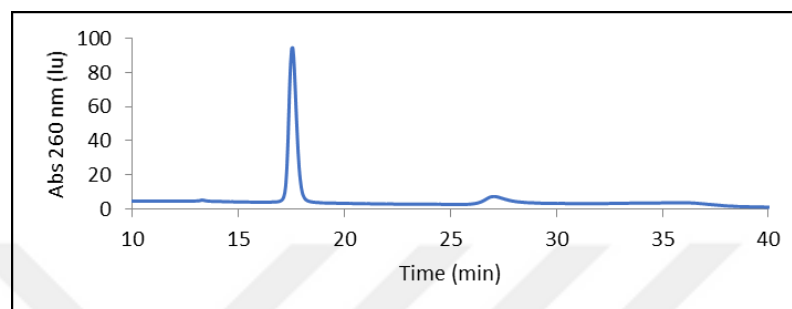


Figure 3.47. HPLC trace of the separation of Reference gene *CaActin* at 260 nm.

For quality assignment and obtaining standards for both Reference and capsicum genes, pUC19 vector was digested with HpaII (Figure 3.48). Fragments that were closest to Reference and capsicum genes in size were taken as references to calculate the copy number of genes individually. For Reference genes, serial dilutions were prepared from  $10^2$  to  $10^7$  copies/ $\mu\text{l}$  and used as template in QPCR studies in order to prepare calibration curves for the genes (Figure 3.49). Also melt curve analysis was applied to make sure that Reference primers did not generate any non-specific products and it was observed that the products obtained with Reference genes were pure (Figure 3.50).

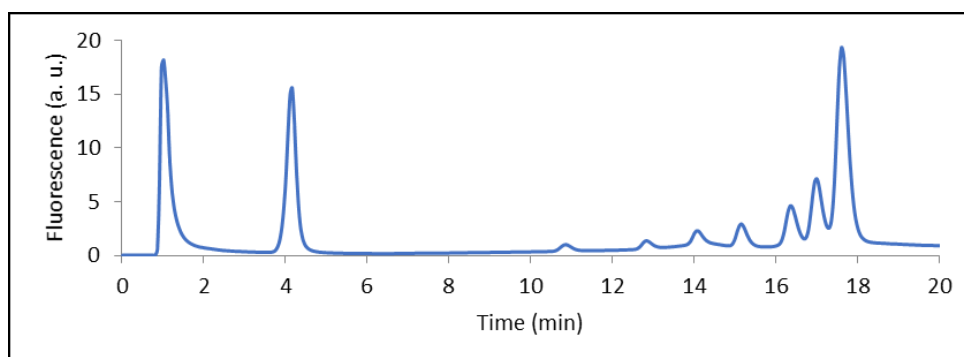


Figure 3.48. HPLC chromatogram trace of the separated fragments of pUC19 after digestion with HpaII enzyme.

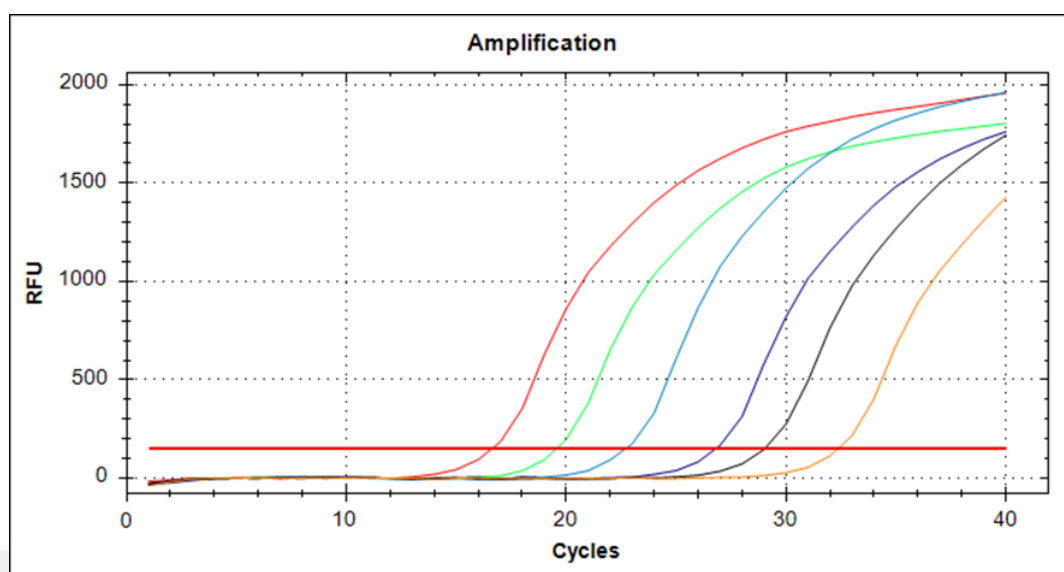


Figure 3.49. Amplification curve of *CaActin* standards from  $10^7$  to  $10^2$  copies/ $\mu$ l after performing QPCR with gene specific primers.

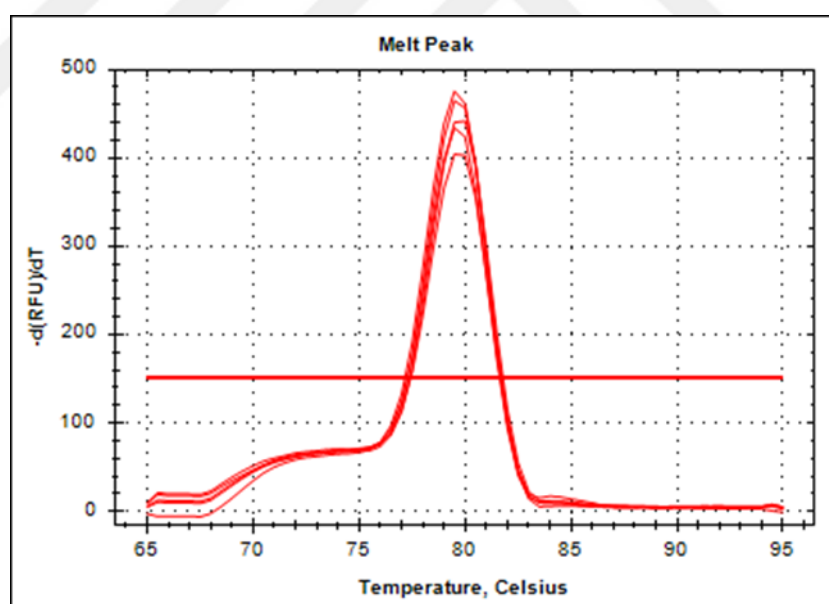


Figure 3.50. Melt curve analysis of *Caα-Tubulin* standards from  $10^7$  to  $10^2$  copies/ $\mu$ l after QPCR with gene specific primers.

Same procedures were also applied for capsicum genes. Melt curve analysis for *CaXTH2* and *CaXTH3* genes also showed that primers did not generate any non-specific products. After total copy number of the gene products were determined cq value vs copy number

graphs were generated using  $10^2$ - $10^9$  copies/ $\mu$ l standards for *CaXTH2* and *CaXTH3* genes (Figure 3.51). For *CaXTH1* gene, the process was successful until HPLC purification step. However, when chromatogram results of *CaXTH1* examined after HPLC purification it was shown that primers that were specific to *CaXTH1* gene generated more than one products. Also melt-curve analysis was applied to QPCR results of *CaXTH1* and multiple product formation was observed. The reason for this is, since *XTH* genes tend to show high levels of homology in between, it is possible that *CaXTH1* primers may go and bind non-specific regions and cause non-specific product formation. Gene expression studies were continued with *CaXTH2* and *CaXTH3* genes.

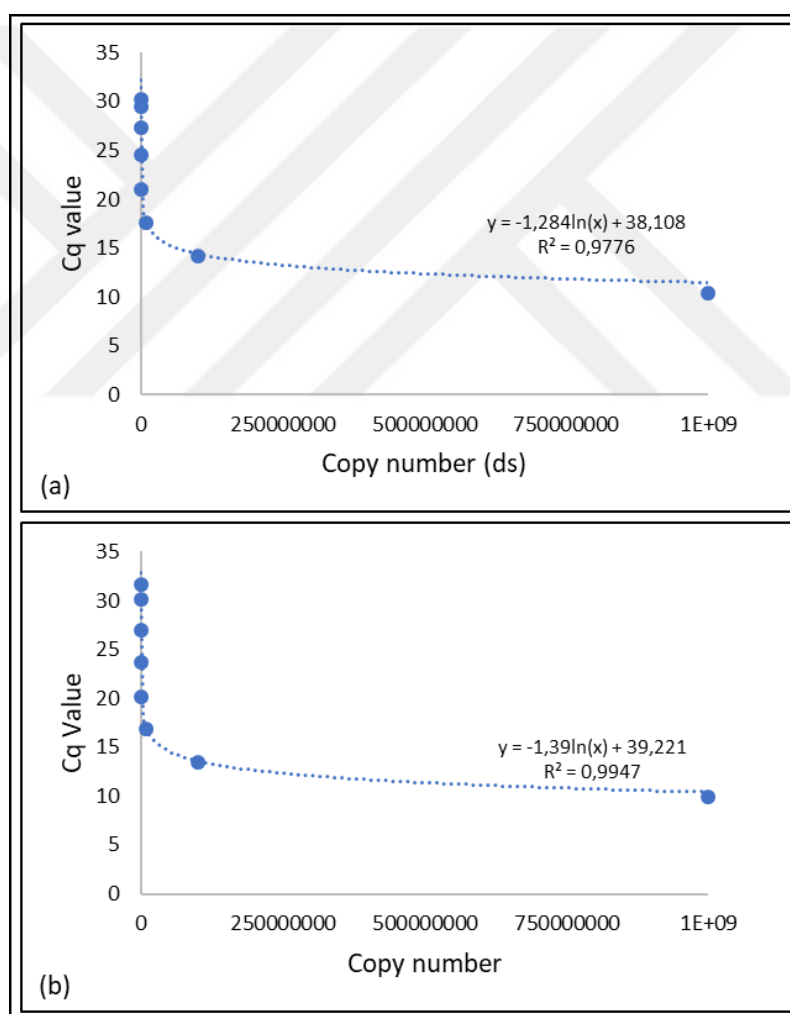


Figure 3.51. cq value vs copy number graphs of (a) *CaXTH2* and (b) *CaXTH3* that were generated following QPCR with gene specific primers and gene standards ( $10^2$ - $10^9$  copies/ $\mu$ l).

### 3.7.1. Salt Stress Expression Levels for *CaXTH2* and *CaXTH3* Genes

QPCR studies that were performed with MS agar grown and salt stress treated Aktör and Seki pepper varieties showed that NaCl concentration increase induced the expression levels of *CaXTH2* and *CaXTH3* genes in both varieties (Figure 3.52). QPCR studies with samples from root tissues showed that the increase in gene expression levels seemed to differ depending on the variety type and the gene its self. For Aktör variety, increase in expression levels of *CaXTH2* gene in root tissue were 4-fold and 5,2-fold higher than the control plants when grown on 25 mM and 50 mM NaCl containing MS agar, respectively. For *CaXTH3* gene the increase in expression levels were 1,7-fold and 2,5-fold higher in comparison to control plants when grown on 25 mM and 50 mM NaCl containing MS agar, respectively.

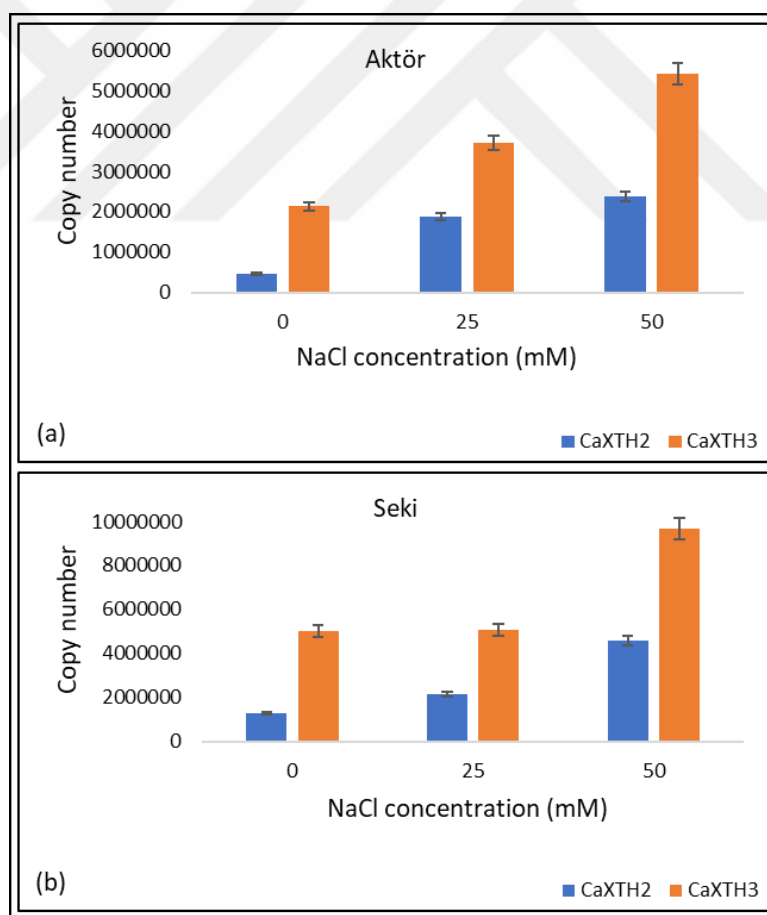


Figure 3.52. Copy numbers of *CaXTH2* and *CaXTH3* genes from root tissues of 11-day-old 0 mM, 25 mM and 50 mM NaCl containing agar grown (a) Aktör and (b) Seki varieties.

NaCl concentration increase in the media induced expression levels of both capsicum genes for Seki variety too. However, that increase was not as high as it was for the Aktör variety. Copy number of the *CaXTH2* gene increase up to 1,7-fold compared to control plants for Seki variety when grown on MS agar containing 25 mM NaCl. That increase was 3,6-fold for the *CaXTH2* gene for Seki variety when grown on 50 mM NaCl containing MS agar. Expression levels of the *CaXTH3* gene were the same for control group and 25 mM NaCl containing MS agar grown plants for Seki, but for plants that were grown on 50 mM NaCl containing MS agar *CaXTH3* gene's copy number was shown to increase up to 1,9-fold (Table 3.19).

Table 3.19. Copy numbers of *CaXTH2* and *CaXTH3* genes from root tissues of Aktör and Seki seedlings that were grown on MS agar containin 0 mM-25 mM-50 mM NaCl.

NaCl concent. (mM)	Copy number of <i>CaXTH2</i> for Aktör	Copy number of <i>CaXTH2</i> for Seki	Copy number of <i>CaXTH3</i> for Aktör	Copy number of <i>CaXTH3</i> for Seki
0	457558	1263335	2131400	5017960
25	1874675	2155880	3712606	5071757
50	2388014	4572146	5432031	9680437

Same salt stress experiments were performed for Cila and Samuray varieties. *CaXTH2* gene expression levels in root tissue increased up to 3,9-fold compared to control plants for Cila variety, when plants were grown in 25 mM NaCl containing MS agar. When the NaCl concentration reached to 50 mM, the increase in *CaXTH2* were observed to be 1,4-fold of the gene expression in control plants. *CaXTH3* gene demonstrated a higher increase compared to *CaXTH2* reaching up to 5,6-fold of the expression levels in control plants when grown on 25 mM NaCl containing agar for Cila variety. That increase dropped to 2,4-fold of the expression levels in control plants, when Cila seedlings were grown on 50 mM NaCl containing MS agar. For Cila variety, although the expression levels of both genes induced with salt stress, there had been a decrease in gene expression when the NaCl concentration was changed to 50 mM from 25 mM (Figure 3.53). Both *CaXTH2* and *CaXTH3* genes' expression levels were induced with salt stress conditions for Samuray variety too. For *CaXTH2* gene, the increase in expression levels were 1,6-fold and 1,8-fold

compared to control plants when grown in 25 mM and 50 mM NaCl containing MS agar, respectively. For *CaXTH3* gene these values were 1,04-fold and 1,44-fold for plants that were grown on 25 mM and 50 mM NaCl containing MS agar, respectively. *CaXTH3* expression levels were higher than *CaXTH2* expression levels for all varieties and in both stress and non-stress conditions. Among four varieties (Aktör, Seki, Cila and Samuray) that were used in salt stress experiments on agar, only Cila variety demonstrated a decrease in the expression levels of both genes when the salt concentration was increased (Table 3.20).

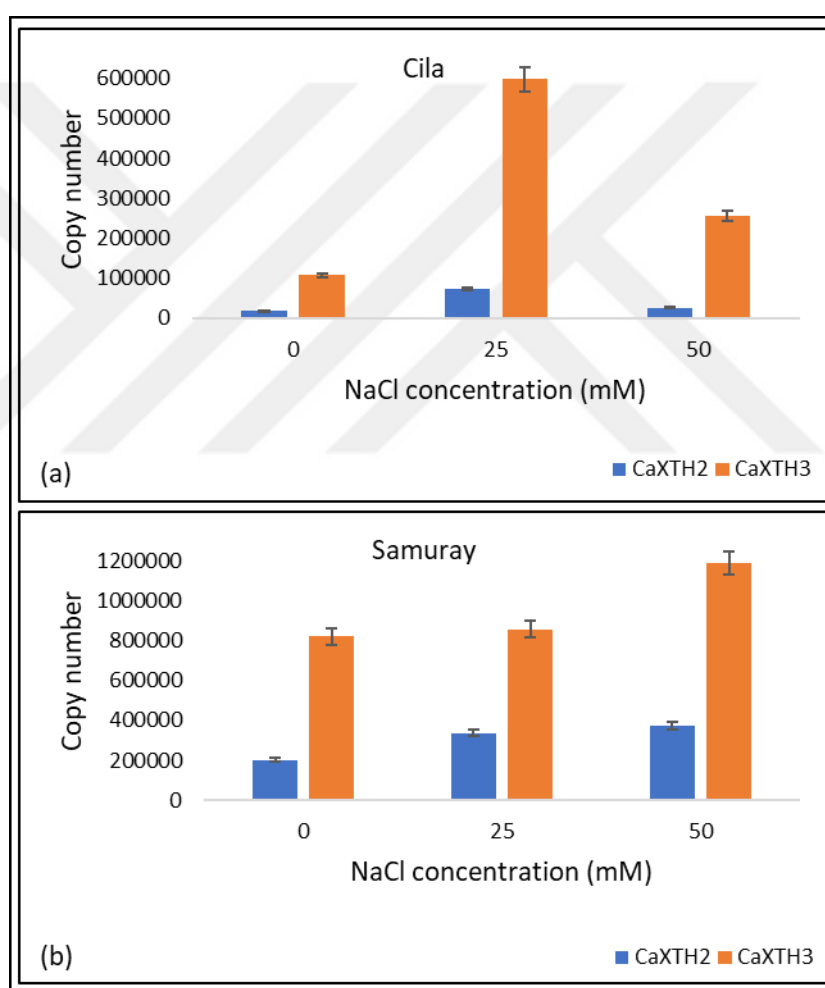


Figure 3.53. Copy numbers of *CaXTH2* and *CaXTH3* genes from root tissues of 11-day-old 0 mM, 25 mM and 50 mM NaCl containing agar grown (a) Cila and (b) Samuray varieties.

Table 3.20. Copy numbers of *CaXTH2* and *CaXTH3* genes from root tissues of Cila and Samuray seedlings that were grown on MS agar containing 0 mM-25 mM-50 mM NaCl.

NaCl concent. (mM)	Copy number of <i>CaXTH2</i> for Cila	Copy number of <i>CaXTH2</i> for Samuray	Copy number of <i>CaXTH3</i> for Cila	Copy number of <i>CaXTH3</i> for Samuray
0	18802	203182	106994	819295
25	74238	336662	598146	856865
50	26804	374879	257216	1187483

Another salt stress trial was performed with 3-week-old soil grown Çanakkale and Kahramanmaraş varieties. Seedlings roots were soaked into 200 mM NaCl solution for different time periods (0 min-10 min-30 min-120 min). QPCR was performed with leaf samples and root samples collected from control and salt stress treated plants. For Çanakkale variety, it was observed that the expression levels of *CaXTH2* and *CaXTH3* genes were induced after 10 min of stress treatment for both leaf and root tissues (Figure 3.54). *CaXTH2* increase was 1,5-fold in leaf and 2-fold in root tissue compared to control plants and *CaXTH3* increase was 3,8-fold in leaf and 1,7-fold in root tissue compared to control plants after 10 min of stress treatment. It was observed that transcription levels of *CaXTH2* gene demonstrated a drop for both leaf and root tissues when plant roots soaked in 200 mM NaCl solution for 30 min. Copy number of *CaXTH2* gene was lower in both leaf and root tissues compared to control plants for Çanakkale variety after 30 min of stress treatment and it decreased even more as the exposure time reached up to 120 min (Table 3.21). Transcription levels of *CaXTH3* gene started to decrease for both leaf and root tissues after 30 min and 120 min of stress treatment. However, copy number of *CaXTH3* gene was still 1,7-fold and 1,2-fold higher than the control group in leaf tissue after 30 min and 120 min of stress treatment, respectively. In root tissue *CaXTH3* gene demonstrated decreased expression levels compared to control group.

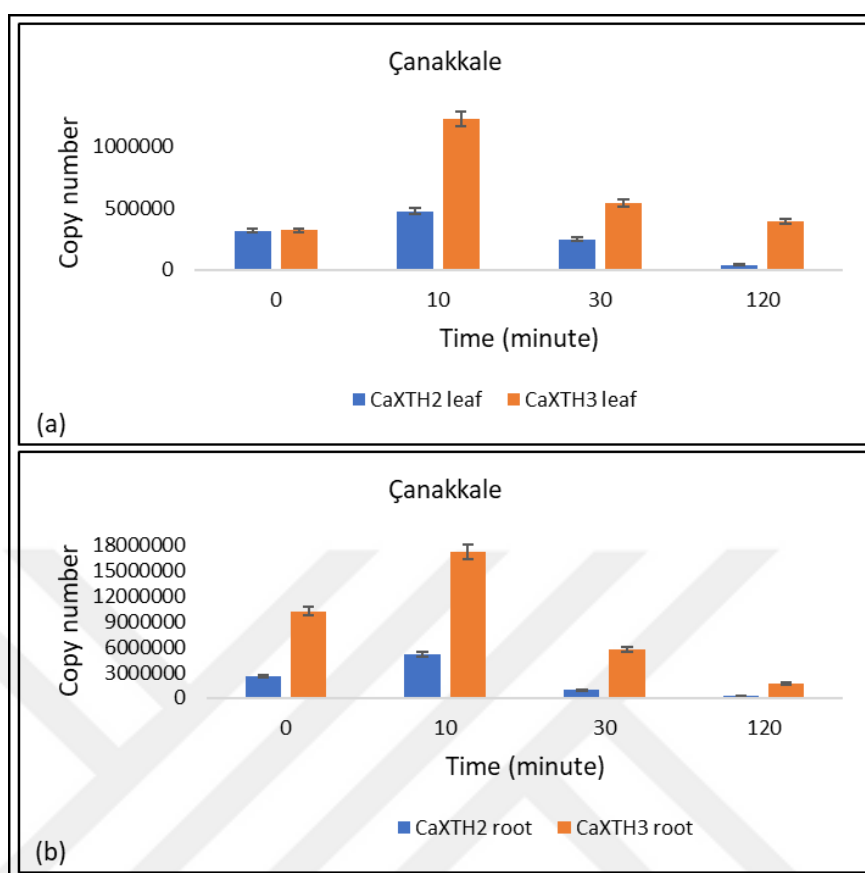


Figure 3.54. Copy numbers of *CaXTH2* and *CaXTH3* genes from (a) leaf and (b) root tissues of Çanakkale seedlings whose roots were soaked into 200 mM NaCl solution for 0 min-10 min-30 min-120 min.

Table 3.21. Copy numbers of *CaXTH2* and *CaXTH3* genes from leaf and root tissues of Çanakkale seedlings whose roots were soaked into 200 mM NaCl solution for 0 min-10 min-30 min-120 min.

Time (minute)	Copy number of <i>CaXTH2</i> for leaf tissue	Copy number of <i>CaXTH2</i> for root tissue	Copy number of <i>CaXTH3</i> for leaf tissue	Copy number of <i>CaXTH3</i> for root tissue
0	315110	2523181	321131	10235709
10	475434	5142176	1217207	17289172
30	247752	930799	541410	5746068
120	42918	309321	388131	1723558

For Kahramanmaraş variety, *CaXTH2* and *CaXTH3* genes demonstrated a drastic drop in transcription levels after 10 min of stress application, in leaf tissues. Copy numbers of *CaXTH2* and *CaXTH3* genes were 3,6-fold and 5,3-fold less than the copy numbers in control tissues from leaf samples. The rapid drop in transcription levels for Kahramanmaraş variety continued until after 30 min of stress treatment for both genes in leaf tissues (Figure 3.55). Copy numbers of the *CaXTH2* and *CaXTH3* genes became 15,2-fold and 13,7-fold less than the copy numbers in leaf control tissues when treated with 30 min of salt stress. While that drop continued for *CaXTH2* gene until the exposure time reached to 120 min, it was not as strong as it was after 10 min and 30 min stress exposure. *CaXTH3* gene demonstrated a slight increase in copy numbers after 120 min of stress treatment. The copy number of *CaXTH3* gene in 120 min stress treated leaf tissues was 1,5-fold higher than the copy number in 30 min stress treated leaf tissues, however it was still quite lower than the copy numbers in control tissues (Table 3.22). Transcription levels of *CaXTH3* gene seemed to decrease as the stress exposure time increased in root tissues for Kahramanmaraş variety. The decrease in copy number for *CaXTH3* gene was small after 10 min of stress exposure. However, copy number of *CaXTH3* gene became 3,4-fold and 20,6-fold less than the copy number in control plants from root tissues after 30 min and 120 min of stress treatment, respectively. *CaXTH2* gene exhibited a slight increase (1,4 fold) when the stress exposure time reached to 10 min in root tissues compared to control plants for Kahramanmaraş variety. However *CaXTH2* expression in root tissues was observed to decrease 6,7-fold less compared to control plants after 30 min of stress treatment and the level of decrease reached up to 20,6-fold by the stress exposure time was 120 min.

Table 3.22. Copy numbers of *CaXTH2* and *CaXTH3* genes from leaf and root tissues of Kahramanmaraş seedlings whose roots were soaked into 200 mM NaCl solution for 0 min-10 min-30 min-120 min.

Time (minute)	Copy number of <i>CaXTH2</i> for leaf tissue	Copy number of <i>CaXTH2</i> for root tissue	Copy number of <i>CaXTH3</i> for leaf tissue	Copy number of <i>CaXTH3</i> for root tissue
0	23453836	61825575	34259503	161891492
10	6588445	92172442	6503028	147109719

30	1538481	9107750	2497316	47543041
120	1479435	3210450	3668218	7834459

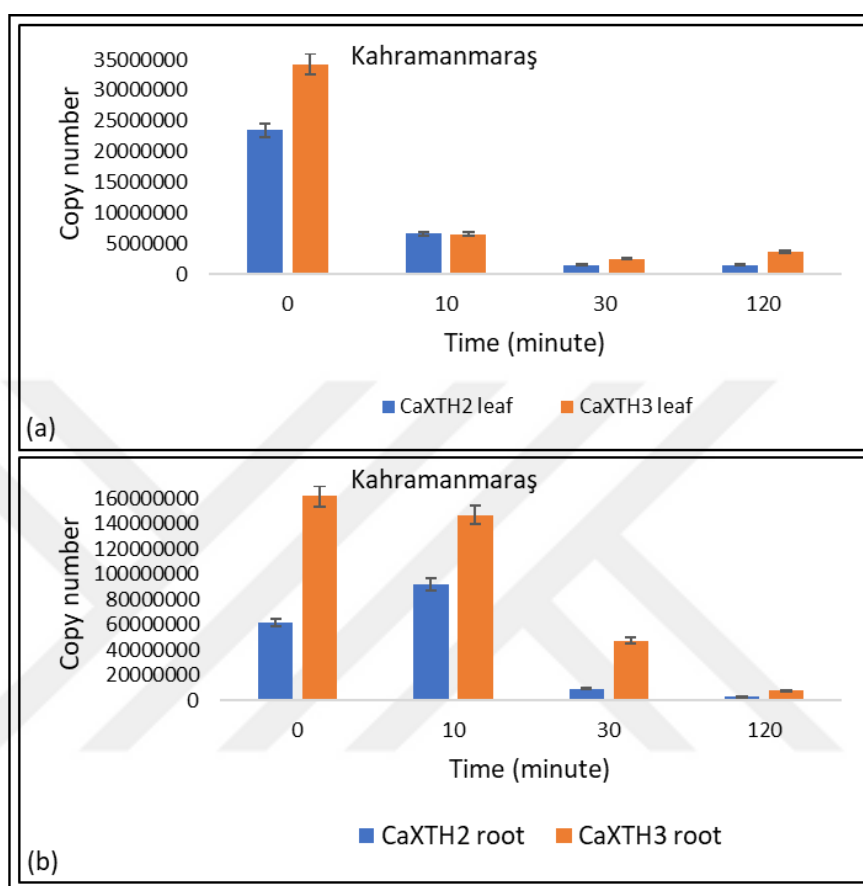


Figure 3.55. Copy numbers of *CaXTH2* and *CaXTH3* genes from (a) leaf and (b) root tissues of Kahramanmaraş seedlings whose roots were soaked into 200 mM NaCl solution for 0 min-10 min-30 min-120 min.

### 3.7.2. Cold Stress Expression Levels for *CaXTH2* and *CaXTH3*

QPCR studies were performed with leaf samples from cold stress treated Kahramanmaraş and Mert varieties. Copy numbers of both *CaXTH2* and *CaXTH3* genes were calculated from leaf samples of both control (4h-8h-12h) plants and cold stress treated (4h-8h-12h) plants. *CaXTH2* and *CaXTH3* transcription levels were observed to be induced by cold stress conditions for both Mert and Kahramanmaraş varieties, although the induction levels

were different. *CaXTH2* copy number increase in Mert variety for 4h-8h-12h cold stress treated plants were 44,2-fold, 13,2-fold and 13-fold compared to control groups at 4h, 8h, 12h, respectively. These values were 39-fold, 15,7-fold and 3,6-fold for *CaXTH3* gene for 4h-8h-12h cold stress treated plants compared to their control groups, respectively. For Kahramanmaraş, *CaXTH2* copy number increase was 13-fold, 18-fold, and 4,6-fold compared to control groups at 4h, 8h, 12h, respectively. These values were 5-fold, 17,5-fold and 3-fold for *CaXTH3* gene (Figure 3.56). Although, stress treated Kahramanmaraş samples had more copies of the both genes (Table 3.24), Mert variety seemed to show earlier and stronger increase in gene expression levels in response to cold stress conditions (Table 3.23). Copy number levels of the stress treated samples revealed a drastic drop at 12h for both genes and varieties.

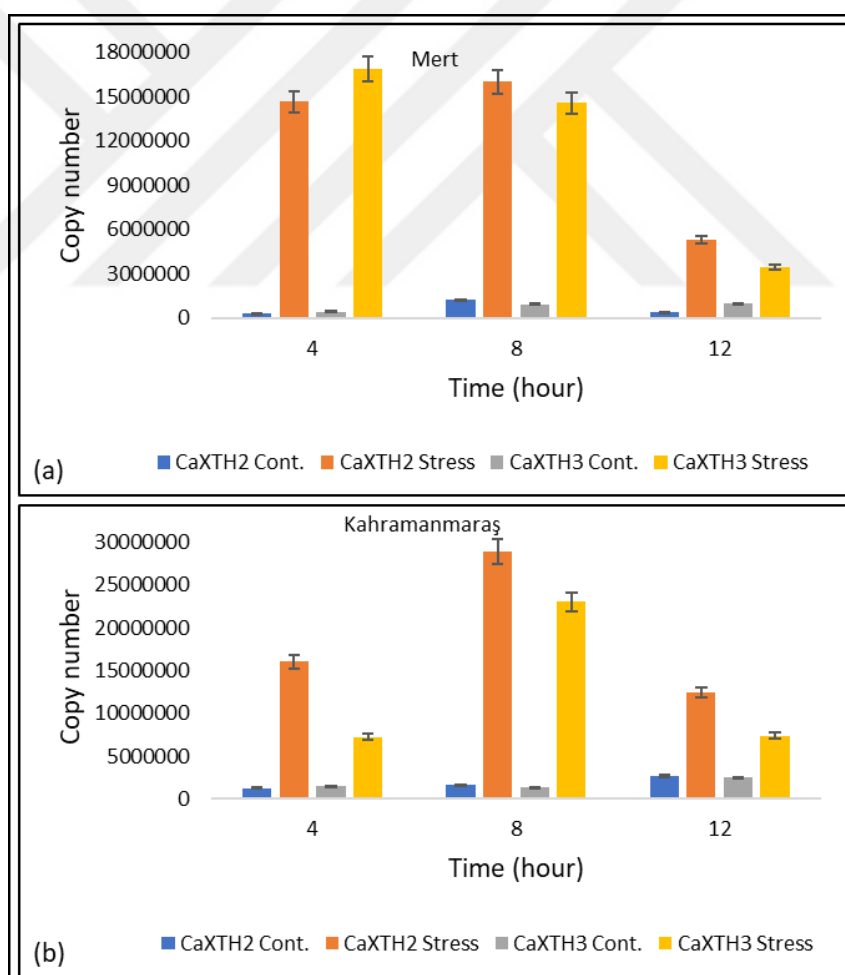


Figure 3.56. Copy numbers of *CaXTH2* and *CaXTH3* genes from leaf tissues of 3-week-old Mert (a) and Kahramanmaraş (b) seedlings after 4, 8 and 12 hour cold stress treatments across the experimental and control groups.

Table 3.23. Copy numbers of *CaXTH2* and *CaXTH3* genes from leaf tissues of 3-week-old Mert seedlings after 4, 8 and 12 hour cold stress treatments across the experimental and control groups.

Time (hour)	Copy number of <i>CaXTH2</i> for control plants	Copy number of <i>CaXTH2</i> for stress plants	Copy number of <i>CaXTH3</i> for control plants	Copy number of <i>CaXTH3</i> for stress plants
4	332018	14673972	432669	16873710
8	1214263	16032658	929788	14588191
12	407160	5291721	952270	3474999

Table 3.24. Copy numbers of *CaXTH2* and *CaXTH3* genes from leaf tissues of 3-week-old Kahramanmaraş seedlings after 4, 8 and 12 hour cold stress treatments across the experimental and control groups.

Time (hour)	Copy number of <i>CaXTH2</i> for control plants	Copy number of <i>CaXTH2</i> for stress plants	Copy number of <i>CaXTH3</i> for control plants	Copy number of <i>CaXTH3</i> for stress plants
4	1227045	16076984	1439030	7247318
8	1607911	28948743	1311372	23020593
12	2685192	12429835	2458030	7359996

### 3.7.3. Drought Stress Expression Levels for *CaXTH2* and *CaXTH3*

Drought stress trials were performed with Mert and Cila varieties. Stress levels were measured with percentage of fresh weight loss (5 per cent -10 per cent -20 per cent). QPCR was performed with leaf samples collected from stress treated and control plants. *CaXTH2* and *CaXTH3* genes were seemed to be upregulated under drought stress conditions for both varieties. Per the graph (Figure 3.57) stress response started when the plant reached 5 per cent weight loss for Mert. Copy number increases were 5,8-fold, 6,1-fold, 0,38-fold for *CaXTH2* and 4,8-fold, 3,9-fold, 0,27-fold for *CaXTH3* gene compared to control groups at 5 per cent -10 per cent -20 per cent weight loss levels, respectively. For Cila, there was no increase in transcript levels until plant reached 10 per cent weight loss (Table 3.25), and copy number increase was 0,7-fold, 1-fold, 0,05-fold for *CaXTH2* and 0,68-fold, 1,3-fold,

0,06-fold for *CaXTH3* gene compared to control groups at 5 per cent -10 per cent -20 per cent weight loss levels, respectively. Gene expression levels significantly dropped when the plants reached 20 per cent weight loss.

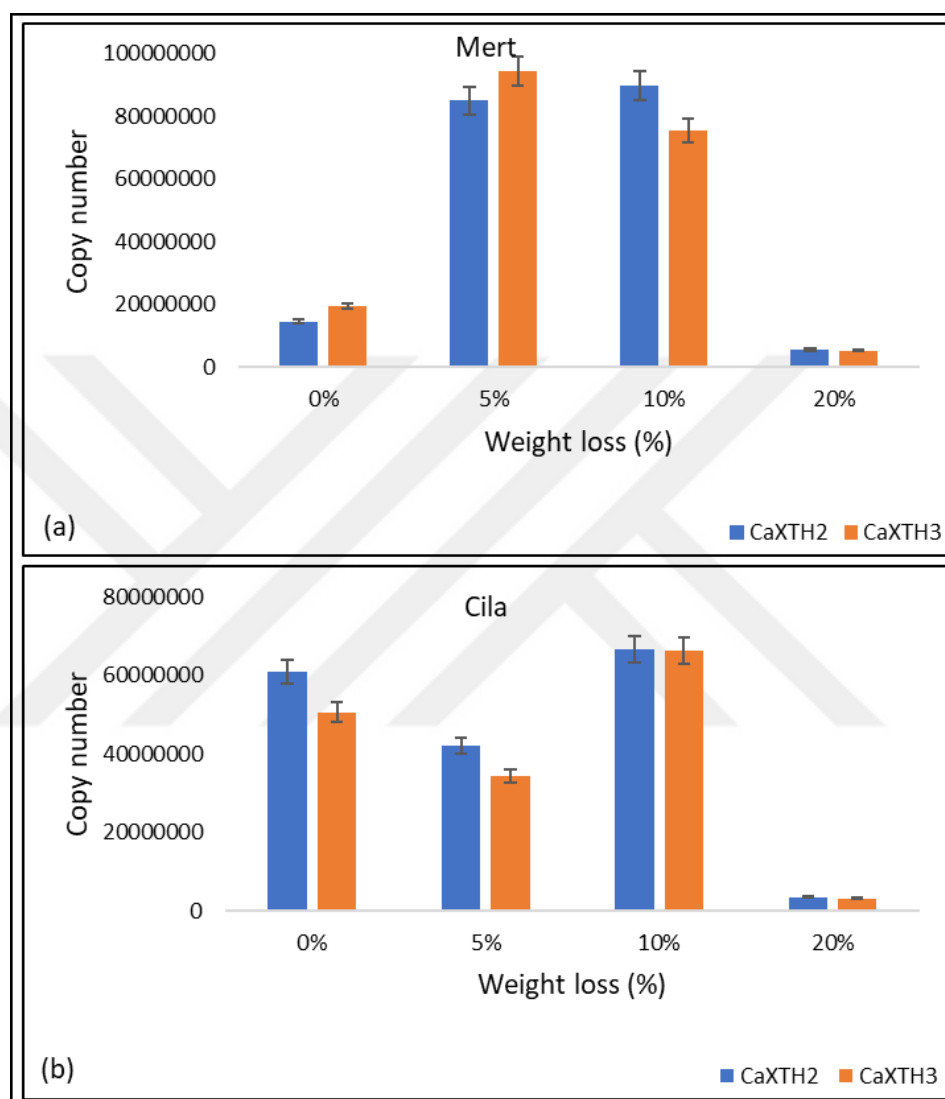


Figure 3.57. Copy numbers of *CaXTH2* and *CaXTH3* genes from leaf tissues of 4-week-old Mert (a) and Cila (b) seedlings after they reached 5 per cent -10 per cent -20 per cent loss in their fresh weight in comparison to control group plants.

Table 3.25. Copy numbers of *CaXTH2* and *CaXTH3* genes from leaf tissues of 4-week-old Mert and Cila seedlings after they reached 5 per cent -10 per cent -20 per cent loss in their fresh weight in comparison to control group plants.

Weight loss (%)	Copy number of <i>CaXTH2</i> for Mert	Copy number of <i>CaXTH2</i> for Cila	Copy number of <i>CaXTH3</i> for Mert	Copy number of <i>CaXTH3</i> for Cila
0	14653177 (100%)	60949799 (100%)	19471929 (100%)	50568030 (100%)
5	84990185 (580%)	42132216 (69%)	94348565 (485%)	34316687 (68%)
10	89754693 (613%)	66644456 (109%)	75359454 (387%)	66454680 (131%)
20	5602387 (38%)	3520193 (6%)	5303614 (27%)	3213404 (6%)

### 3.8. NEXT GENERATION SEQUENCING (NGS)

Upon arrival at MacroGen the samples were tested using an Agilent BioAnalyzer 2100 that examines RNA quality and gives a score as an RNA Integrity Number (RIN) value. RIN values should normally be >7,0 for successful NGS sequencing. Results for our capsicum samples varied from 6,4-3,9 RIN. An example RIN trace for Kahramanmaraş Stress 8 hours can be seen in Figure 3.58. MacroGen asked how we would like to proceed. Duplicate RNA samples had been sent so the duplicates of the 10 worst samples were then analyzed. The results for the duplicates were similar with values between 5,3 and 3,8. It was decided that perhaps this was due to the IntronBio RNA isolation kit that was used, therefore the duplicate leaf tissue samples kept in our -80°C freezer were used to isolate fresh Total RNA. For this second round of RNA isolation, the Norgen Plant/Fungi Total RNA Preparation Kit was used to determine if the lower RIN values are kit related. After isolation, the RNA was checked locally by Nanodrop spectrophotometer and agarose gel and confirmed to be of good quality. These replicate samples were then sent to MacroGen using the same procedure as before, on ‘wet’ ice blocks.

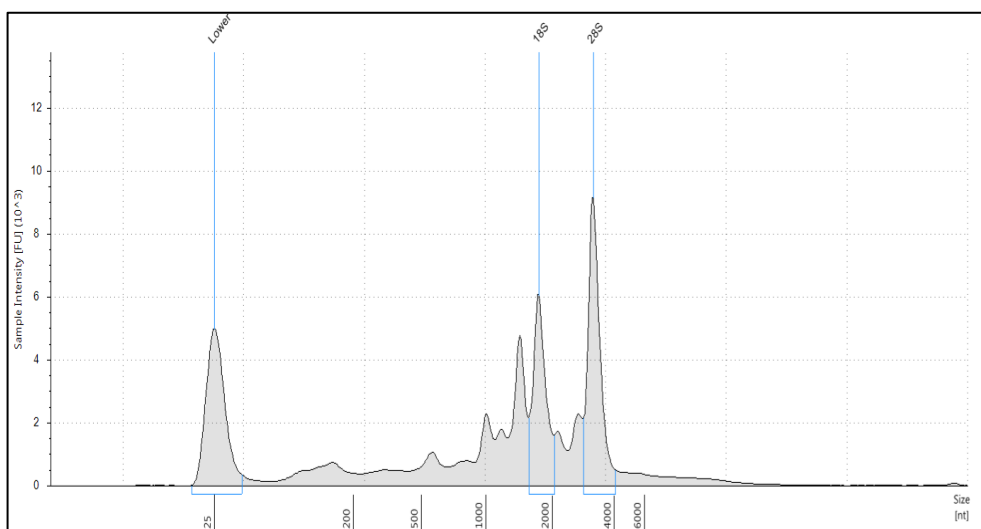


Figure 3.58. RNA Integrity analysis of Total RNA from leaf tissue of *Capsicum annum* cv. Karamanmaraş after 8 hours of cold-stress treatment. Agilent Bioanalyzer 2100 gave an RNA integrity value of 6,4 RIN. 28S and 18S peaks indicate large and small ribosomal subunit peaks, from which RIN values are calculated. The large peak that is slightly smaller than 18S is likely to be the 16S ribosomal RNA from mitochondrial and/or chloroplast ribosomes.

The samples duly arrived at Macrogen after 2 days of travel and were tested by BioAnalyzer 2100. The RIN values were in fact lower than those of the first batch, ranging from 4,7-2,3, much lower than the required RIN of >7,0. However, on further investigation, some plant samples may naturally contain inhibitors that affect the RIN measurement. In fact, leaf tissues of many plants including tobacco and tomato, which is a close relative of capsicum, routinely give RIN values well below 7. This gave confidence that although the samples may have some partial degradation, they would still be suitable for NGS library preparation and sequencing.

Samples from each time point with the best RIN values were chosen for library preparation. The library type chosen was TruSeq RNA, which involves first isolating mRNA from Total RNA by oligo-dT attached magnetic beads. The mRNA is then size-fractionated with divalent cations at high temperature to give an average fraction size of 250-300 bp. Figure 3.59 shows the Bioanalyzer trace for size-fractionated sample from Kahramanmaraş after 8 hours of cold-stress treatment. Average insert sizes were from 284-302 bp which is ideal for library preparation for paired-end sequence reads of 100 bp,

which is being performed. All samples passed library quality control and were sent for sequencing.

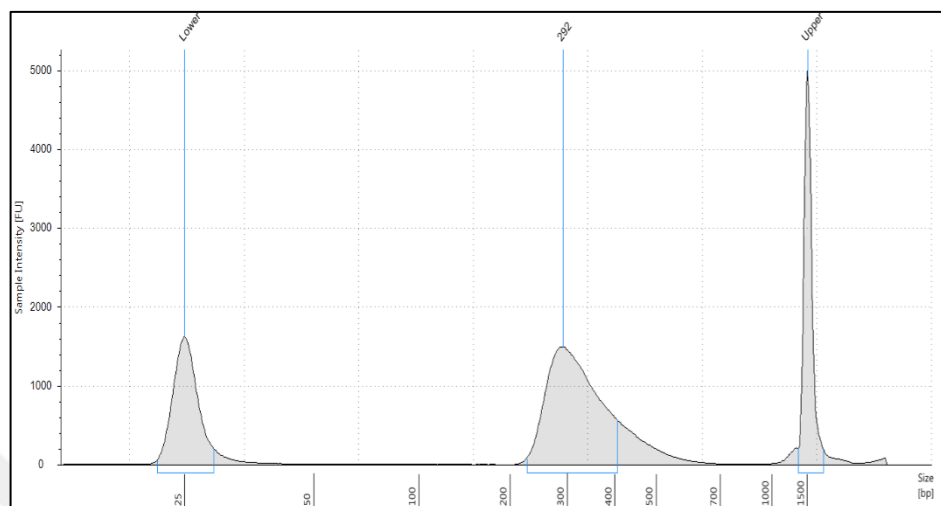


Figure 3.59. RNA size-fractionation analysis of mRNA from leaf tissue of *Capsicum annuum* cv. Karamanmaraş after 8 hours of cold-stress treatment. The fragment sizes are generally between 140-400 bp, with an average of 292 bp.

Short DNA readings (different file pair for each sample) obtained from NGS sequencing were first aligned according to the *Capsicum annuum* reference genome. Paired reading data which was combined of 100 bp and were distanced 250 bp from each other was aligned via “bowtie2” program using primarily default parameters (match bonus 2, max/min mismatch penalty 6/2, penalty for N 1, gap open penalty 5, extend penalty 3, trim length 0). *Capsicum.annuum.L\_Zunla-1\_Release\_2.0* genome was used as reference genome as the functional annotation was highest with this one.

Readings aligned to reference genome were transferred to “cufflinks” program and start and end zones of each transcript was determined. Generated gtf file was checked for the regions we were looking for in the light of previous information (partially and fractionary existing exon sequences and the results of the alignment to the reference genome). In this step, gene expression and FPKM (Fragments Per Kilobase Of Exon Per Million Fragments Mapped) were expressed as in readings in the gene region of interest in accordance with international literature (Figure 3.60, Figure 3.61, Figure 3.62, Figure 3.63).

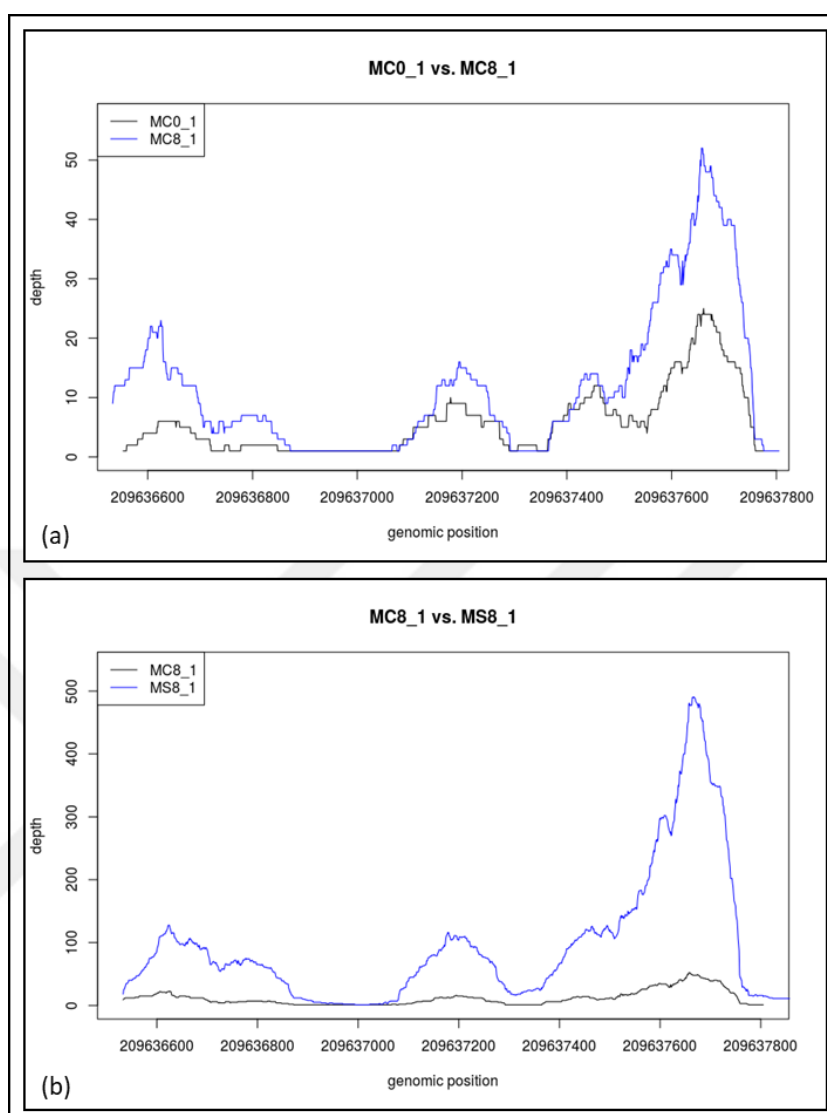


Figure 3.60. Genome position and gen expression depth graphics of *CaXTH1* gene of Mert variety obtained by NGS analyses after RNA sequencing for MC0, MC8 and MS8 samples paired with Zunla database. (a) Mert 0-hour 1<sup>st</sup> control vs Mert 8-hour 1<sup>st</sup> control. (b) Mert 8-hour 1<sup>st</sup> control vs Mert 8-hour 1<sup>st</sup> stress.

For Mert variety, 0-hour and 8-hour control samples are shown in Figure 3.60. Two times of an increment in Mert exons that are matching with Zunla genome was shown from 0-hour to 8-hour. There was a very effective and high level of increase between Mert 8-hour 1<sup>st</sup> control and Mert 8-hour 1<sup>st</sup> stress. Although it is hard to see, the control values were around 10-20 hits. Hit values in the first and second exon regions were around 100 whereas these values were 500 hits in third exon region, between control and stress samples. These changes represented differences of mRNA levels in samples.

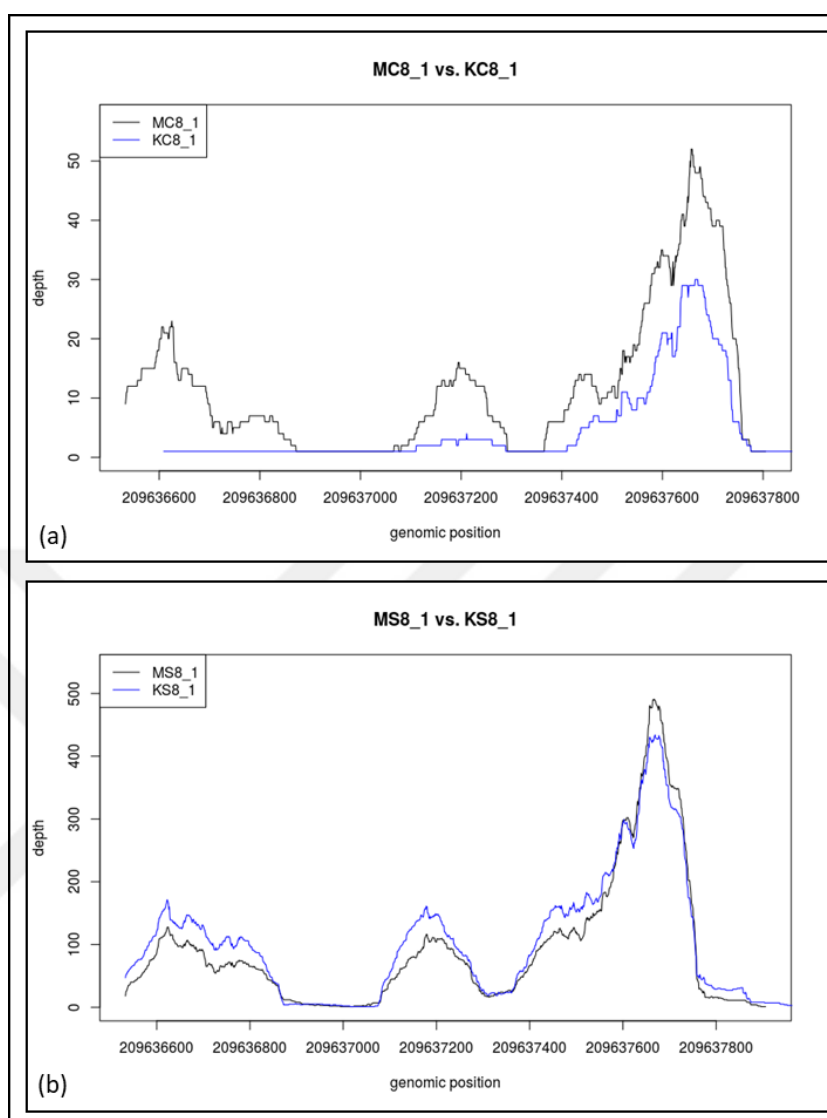


Figure 3.61. Genome position and gene expression depth graphs of *CaXTH1* gene of Capsicum varieties Mert and Kahramanmaraş, obtained by NGS analyses after RNA sequencing for MC8, KC8, KS8, an MS8, samples paired with Zunla database. (a) Mert 8-hour 1<sup>st</sup> control vs Kahramanmaraş 8-hour 1<sup>st</sup> control, (b) Mert 8-hour 1<sup>st</sup> stress vs Kahramanmaraş 8-hour 1<sup>st</sup> stress samples.

For *CaXTH1* gene, both Mert and Kahramanmaraş varieties' exons that are matching with *Capsicum annuum* cv. Zunla genome demonstrated ~150 hits in the first and second exon and 450-500 hits in the third exon. Expressions of Mert 8-hour 1<sup>st</sup> stress and, Kahramanmaraş 8-hour 1<sup>st</sup> stress samples were high and both of their levels were similar. These levels showed connection between RNA expression and stress conditions.

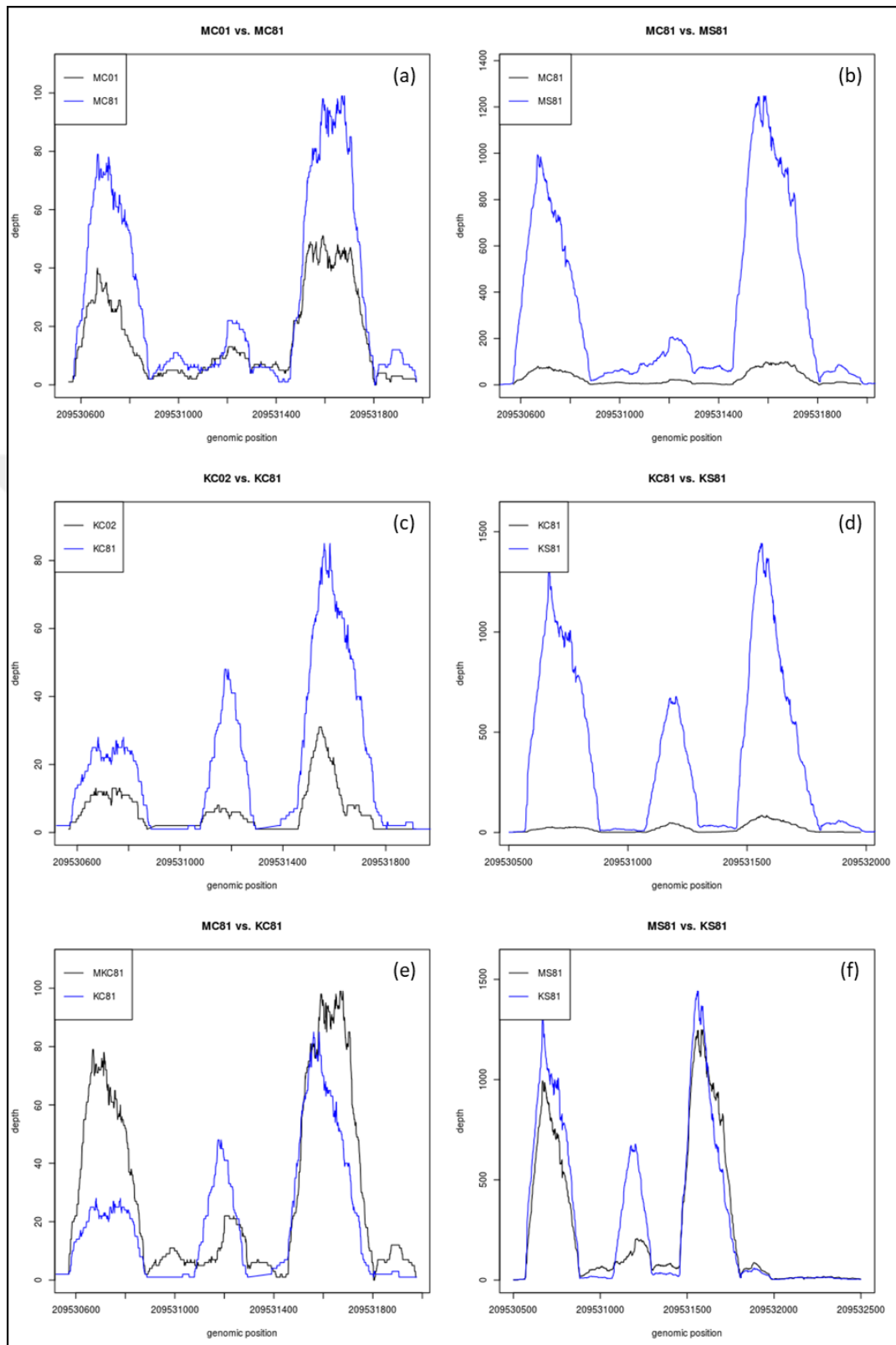


Figure 3.62. Genome position and gen expression depth graphs of *CaXTH2* gene of Capsicum varieties Mert and Kahramanmaraş, obtained by NGS analyses after RNA sequencing for MC0, KC0, MC8, KC8, KS8 an MS8 samples paired with Zunla database.

Mert 0-hour 1<sup>st</sup> control and Mert 8-hour 1<sup>st</sup> control comparisons for *CaXTH2* gene was shown in Figure 3.62a. Low expression levels of exons of Mert variety matching with Zunla genome doubled from 0-hour to 8-hour. Mert 8-hour 1<sup>st</sup> control and Mert 8-hour 1<sup>st</sup> stress samples expression difference in *CaXTH2* levels was ~120 times more in stressed samples in first and third exon regions and 20 times more in stressed samples in second exon region compared to control samples (Figure 3.62b). Increase between Kahramanmaraş 0-hour 1<sup>st</sup> control and Kahramanmaraş 8-hour 1<sup>st</sup> control samples was observed as doubling of expression from 0-hour to 8-hour (Figure 3.62c). Kahramanmaraş 8-hour 1<sup>st</sup> control and Kahramanmaraş 8-hour 1<sup>st</sup> stress samples expression for *CaXTH2* gene was 1500 hits in stressed samples in first and third exon regions and upto 500 hits in stressed samples in second exon region (Figure 3.62d). Mert 8-hour 1<sup>st</sup> control and Kahramanmaraş 8-hour 1<sup>st</sup> control samples comparison showed Mert variety was more effective and *CaXTH2* expression was in low levels (Figure 3.62e). Mert 8-hour 1<sup>st</sup> stress and Kahramanmaraş 8-hour 1<sup>st</sup> stress samples showed similar and high levels of *CaXTH2* expression (Figure 3.62f).

Mert 0-hour 1<sup>st</sup> control and Mert 8-hour 1<sup>st</sup> control comparisons for *CaXTH3* gene was shown in Figure 3.63a. Low expression levels of exons of Mert variety matching with Zunla genome doubled from 0-hour to 8-hour. Mert 8-hour 1<sup>st</sup> control and Mert 8-hour 1<sup>st</sup> stress samples expression for *CaXTH3* levels was 100 hits in control samples and 800 hits in first exon and 1000 hits in the second and third exon in stressed samples (Figure 3.63b). Small level of increase between Kahramanmaraş 0-hour 1<sup>st</sup> control and Kahramanmaraş 8-hour 1<sup>st</sup> control samples was observed. Expression in *CaXTH3* levels was 20 hits and 30 hits in stressed samples in first and second exon regions and 60 hits in stressed samples in third exon region from 0-hour to 8-hour (Figure 3.63c). Kahramanmaraş 8-hour 1<sup>st</sup> stress samples expression for *CaXTH3* gene was 800 hits in stressed samples in first exon region and upto 900 hits in stressed samples in second and third exon regions (Figure 3.63d). Mert 8-hour 1<sup>st</sup> control and Kahramanmaraş 8-hour 1<sup>st</sup> control samples comparison showed Mert variety was more effective and *CaXTH3* expression was in low levels (Figure 3.63e). Mert 8-hour 1<sup>st</sup> stress and Kahramanmaraş 8-hour 1<sup>st</sup> stress samples showed similar and high levels of *CaXTH3* expression (Figure 3.63f).

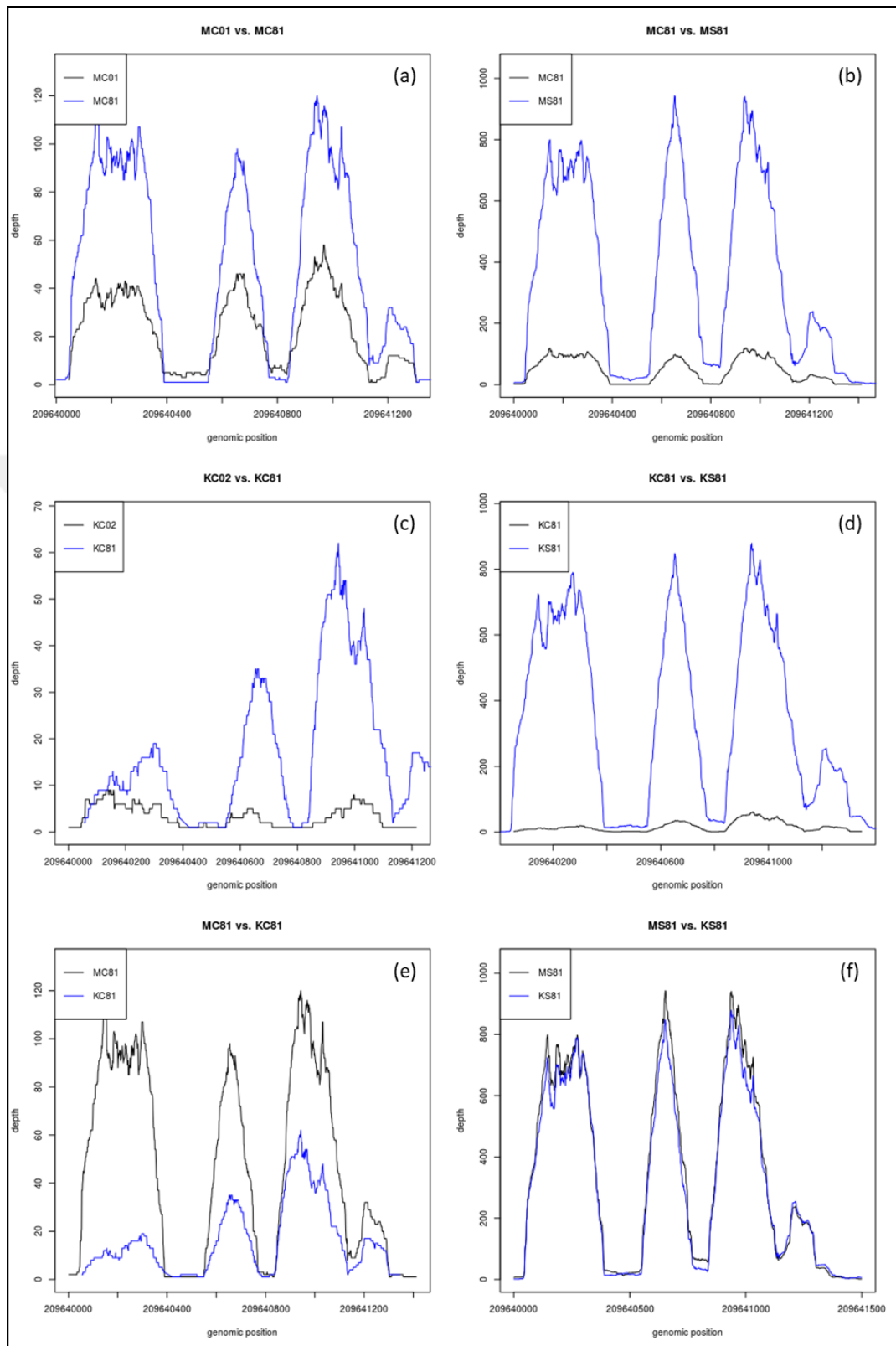


Figure 3.63. Genome position and gene expression depth graphics of *CaXTH3* gene of *Capsicum* varieties Mert and Kahramanmaraş, obtained by NGS analyses after RNA sequencing for MC0, KC0, MC8, KC8, KS8 and MS8 samples paired with Zunla database.

In a paper by Martínez-López, the researchers used Illumina MiSeq to examine fruit ripening in whole Serrano-type chili pepper fruits (*Capsicum annuum* L.; ‘Tampiqueño 74’). Transcriptome sequencing resulted in 15,550,468 Illumina MiSeq reads that were assembled de novo into 34,066 genes. Of these gene contigs, 16 were identified as having high similarity to XTH genes, and 11 of those were differentially expressed during fruit ripening [128]. Thus, Illumina sequencing has been proven to be successful for XTH genes and gene-products and was chosen to be used for our capsicum-stress studies.



## 4. DISCUSSION

Rice (*OsXTH1*), tomato (*SIXTH4*) and pepper (*CaXTH1*, *CaXTH2* and *CaXTH3*) genes within the study were obtained codon optimized, transferred and amplified in *E. coli* and heterologously expressed in the yeast *Pichia pastoris*. Production of the enzyme was achieved in BMMY media via methanol induction of the *AOXI* promoter and active enzyme producing colonies were chosen via SDS-PAGE, Western and HPLC analysis.

Based on the SDS-PAGE, Western and HPLC analysis, *OsXTH1*-14, *SIXTH4*-6, *CaXTH1*-5, *CaXTH2*-2 and *CaXTH3*-5 colonies were chosen to produce the most active producing protein. Large scale production was achieved for all the enzymes in liter scale via methanol induction of the *AOXI* promoter in order to have sufficient amount of enzyme for further studies. Protein precipitation and purification were performed using dialysis, affinity chromatography and size exclusion chromatography methods for all the enzymes. Further purification was applied for *CaXTH1*, *CaXTH2* and *CaXTH3* enzymes via polishing. After concentration of the purified enzymes Bradford measurements were found to be 3,21 mg/ml for *OsXTH1* and 0,217 mg/ml for *SIXTH4*. For *CaXTH1*, *CaXTH2* and *CaXTH3* enzymes Bradford measurements were 0,224 mg/ml, 2,723 mg/ml and 0,453 mg/ml, respectively. These enzymes are usually located in the plant apoplast which has a slightly acidic pH varying between 5 to 6 [81]. The optimum working pH for the enzymes in this study was also found to be in between 5,8 and 6,1.

The substrate specificity and the activity level among the enzymes on the same substrate couples differed. These differences likely reflected the native xyloglucan structure of the plants that the enzymes originated from. All 88 substrate couples were tried for capsicum, rice and tomato enzymes. Substrate selection was kept wide in order to see the enzymes activity on a variety of carbohydrate molecules. However, obtaining native xyloglucan structures in the substrate form was not possible. TXG, HEC, BBG, KGM, WAX, CM, GM and LG were chosen to test whether the enzymes involved in this study work on xyloglucan and representatives of other commonly found plant cell wall carbohydrate molecules. It is important to note that obtaining native xyloglucan from capsicum, rice, or tomato was not possible. Indeed, the only commercially available xyloglucan is from tamarind seeds, where it is a storage polysaccharide. TXG is composed of XXXG, XLXG, XXLG and XLLG xyloglucan subunits and has a close structural similarity to native

capsicum xyloglucan [55]. Capsicum enzymes (CaXTH1, CaXTH2 and CaXTH3) showed the highest activity level with TXG as the donor substrate, and X7 and XGO as acceptor substrates. CaXTH2 enzyme demonstrated the highest specific activity with a value of 4121,4 picokatal/mg with TXG-X7. This was the highest activity of any XTHs that have been expressed. It also seemed to be the most specific. The next highest activity observed with CaXTH2 enzyme was with the HEC-X7 substrate couple which is less than 0,3 per cent of the activity of TXG-X7 substrate couple. That might lead to the fact that the enzyme became better at catalyzing a reaction for a specific substrate and it is less able to accommodate other substrates in its active cleft. The following highest activities were 817,22 picokatal/mg and 557,87 picokatal/mg for CaXTH3 and CaXTH1 enzymes, respectively, and were also on TXG-X7. Activities of the enzymes on the TXG-XGO substrate couple level was significantly lower than the activities on the TXG-X7 substrate couples. The values for TXG-XGO activity were 365,23 picokatal/mg, 2026,9 picokatal/mg and 494,36 picokatal/mg for CaXTH1, CaXTH2 and CaXTH3 enzymes, respectively. The reason for this preference for X7 is likely due to the fact that X7 contains only XXXG oligosaccharides, while XGO includes 12 per cent XXXG (X7), 52 per cent XXLG and XLXG, and 36 per cent XLLG [129]. Capsicum cell wall xyloglucan is comprised chiefly of XXGG and XSGG subunit structures, with no substitution on the third glucosyl ring. Also, 78 per cent of the xyloglucan subunits in pepper contain an Araf(1→2)- $\alpha$ -D-Xylp side chain. However, fucosyl containing residues were not found in capsicum plants [130]. The results showed that capsicum XTH enzymes likely do not work on XLLG and XXLG due to the additional substitution on the third position. The XLXG, on the other hand, can be a substrate for the enzymes as it is more similar to the enzymes' native substrate. It is thought that the galactosyl group on the second xylose in XLXG could mimic the arabinosyl group on the XSGG.

Tamarind xyloglucan was used as the donor substrate in this study mostly because it was the only commercial product that was available. TXG was the most efficient working donor substrate for all the enzymes. That was of course related to the structure. TXG was shown to be composed of XXXG, XLXG, XXLG and XLLG subunits. Although some of them had substitution on the third position, there were still subunits (XXXG and XLXG) that were favourable for the enzymes. In addition, fucosylation which is a relatively common substitution on the galactosyl unit on the third position of many dicots, is absent

in TXG and is similarly absent in the native xyloglucan structures of tomato, pepper and rice plants. Therefore, TXG is considered to be a good model polysaccharide for cell wall studies [131]. A detailed investigation of the substrate-binding cleft using molecular modelling and docking experiments would be valuable in determining which amino acid residues are responsible for these differences in substrate specificity. Nonetheless, more interesting and accurate results would have been obtained using native substrates as the enzymes would likely have acted faster on an XXGG or XSGG backbone. Activity percentages of CaXTH1 and CaXTH3 enzymes on the TXG-X7 substrate couple were found to be 152,74 per cent and 165,31 per cent, respectively, when the activity percentage of the TXG-XGO substrate couple was set to 100 per cent. This value was 200 per cent for CaXTH2 enzyme, which led to the conclusion that the enzyme is more selective of the substrates than CaXTH1 and CaXTH3 enzymes. Thus, CaXTH1 and CaXTH3 enzymes seemed to favour XLLG and XXLG more than CaXTH2 enzyme does. Considering different cells have different substitutions on the xyloglucan backbone this may be indicative of different roles for these enzymes within the plant. Activities on other substrate couples were quite low, being less than 1 per cent of the TXG-XGO and TXG-X7 activities. The only activities that came close to 1 per cent were demonstrated by HEC-XGO, HEC-X7 substrate couples, with CaXTH2 revealing the most activity again. Capsicum plants are dicots; therefore, they have no  $\beta$ -glucan which explains the low activity on the BBG donor substrate. CaXTH1, CaXTH2 and CaXTH3 enzymes were not very active on the acceptor substrates other than XGO and X7. Activity levels on XT, CT, BA, BB and BC acceptor substrates were close and significantly lower than the activities on XGO and X7 acceptor substrates. This was considered to be related with no substitution on these acceptor substrates. Also, none of the enzymes in this study revealed any activity with the MT acceptor substrate which is probably associated with switching the position of the hydroxyl group on the C2 of the sugar ring from equatorial to axial in mannosyl residues. Once again, molecular modeling and docking studies would be valuable in elucidating this substrate preference.

The activity of SIXTH4 enzyme on TXG-XGO (60,63 picokatal/mg) and TXG-X7 (42,75 picokatal/mg) substrate couples was lower than all of the capsicum enzymes. Both tomato and pepper plants are in the *Solanaceae* family, and they share the XXGG xylosylation motif in their xyloglucan structure. Xyloglucan subunit structure in tomato leaf includes 70

per cent Araf-(1→2)- $\alpha$ -D-Xylp and 20 per cent  $\beta$ -D-Galp-(1→2)- $\alpha$ -D-Xylp substitution on the xyloglucan backbone. XXGG, XSGG, LSGG, and LLGG-type branching patterns, which are more likely to be representative of the native substrate within the plant, were also observed in a tomato leaf XET fraction [130]. Cultured tomato cells on the other hand, revealed similar but more complicated branching patterns including arabinosyl substitution on the third xylose, such as GXSG. The reason that GXSG was observed from the cultured tomato cells might have been a result from the enzyme xyloglucan-specific endoglucanase which comes from a different family than GH16. The enzyme prefers to cut on unsubstituted glucosyl units, so when the case is XSGG it may cut after either of the unsubstituted glucosyl units. Therefore, GXSG may be artificially produced, it might instead be representative of XSGG therefore our enzymes would treat it like XSGG, so the arabinose would be on the -3 or +2 positions. GXSG is not likely to be how our enzyme would recognize it or position it.

Catalá and co-workers identified an *XET* gene from tomato, *LeXTH2*. *LeXTH2* gene was found to be mostly expressed in nonelongating areas of the hypocotyl and was active on tamarind seed xyloglucan and xyloglucan from two more species. However, the activity of the heterologously produced LeXET2 was the highest with the xyloglucan obtained from suspension-cultured tomato cells [132]. Similar to capsicum enzymes, the tomato enzyme revealed no activity with BBG donor substrate as it is also a dicot plant and does not include  $\beta$ -glucan in its structure. The highest activities that were demonstrated after TXG-XGO, TXG-X7 substrate couples were HEC-XGO (5,986 picokatal/mg), HEC-X7 (6,171 picokatal/mg) substrate couples that were still 10 per cent of the activity on TXG-XGO substrate couple. HEC-XGO activity was slightly higher than the HEC-X7 activity which can be explained with activity levels of the acceptor substrates showing differences when they paired with different donor substrates. A great deal of decrease in the activity levels was also observed with XT, CT, BA, BB, and BC acceptor substrates, and activity with those acceptor substrates could only be detected when paired with the TXG donor substrate. No activity was observed when these acceptor substrates were used with the HEC donor substrate.

The rice enzyme OsXTH1, showed the most activity with the TXG-X7 (126,2 picokatal/mg) substrate couple, like all the other enzymes used in this study. The second-best activity was observed with TXG-XGO (119,98 picokatal/mg) substrate couple. The

difference in activity levels between TXG-XGO and TXG-X7 was not as significant in OsXTH1 as it was with capsicum enzymes. Rice is a commelinid monocot plant in the family of *Poaceae* (grasses and cereals) which contains glucuroarabinoxylans (GAX) in their cell walls as the major non-cellulosic polysaccharide and small amount of (1→3, 1→4)-β-glucans [133]. The amount of (1→3, 1→4)-β-glucans, was highly variable from plant to plant and even in different developmental stages of the plant [129, 134]. Small proportions of xyloglucan are also included in the primary cell walls of other commelinid order plants [135]. Compared to dicots, monocots have smaller amounts of xyloglucan in their primary cell wall. Also, the substitution in the xyloglucan subunit structure in monocots is much less than in dicots with less xylose and galactose. Substitution levels of the xyloglucan molecule was shown to change and reduce as the plant's development continued [136]. It was shown that XXGG, XXGGG, and XXGGGG were the repeating subunits in xyloglucans from the family of *Poaceae*. Smaller portions of XXG and XXGGGGG were observed. Almost no fucosylation in xyloglucans was shown for this family [129]. In one study, the carbohydrate composition of the cell walls of early barley coleoptiles included 30 mol per cent pectic polysaccharides, 25 mol per cent arabinoxylan, 25 mol per cent cellulose, 6 mol per cent xyloglucan, and 1 mol per cent (1→3,1→4)-β-glucan. However, during coleoptile growth, the pectic polysaccharide ratios seemed to reduce. Cellulose and arabinoxylan amounts stayed the same, but with a decrease in the xylose substitution in the arabinoxylan. Major subunits in xyloglucan structure were found to be XXGG and XXGGG for 3-day-old barley coleoptiles [137]. Since barley and rice come from the same *Poaceae* family, they share structural similarities in their xyloglucan composition. Repeating subunits of xyloglucan from cell walls of rice seedlings and rice hulls were shown to be XG, XXG, XGGG and XXGG in previous studies. No fucosylation was observed for the xyloglucan structures, and the xylose substitution were considerably lower in comparison to dicotyledons [138, 139]. Lower substitution levels might lead to a better binding to cellulose microfibrils [140]. On the other hand, the xyloglucan structure from the cell walls of suspension cultured rice cells revealed more complicated subunits with more substitution on the back bone (XLXG, XXXG). However, these subunits were not thought to be representative of other tissues of the plant or therefore of the native substrate of the XTH enzymes. When we look at the xyloglucan structure from rice seedling and hull cells it can be seen that there is no substitution on the third position, even with the suspension culture cells galactose substitution is on the second xylose not third, so

it is understandable that the OsXTH1 enzyme preferred X7 over XGO and XLXG substrate over XLLG or XXLG. Xylose substitution on the third position seemed to be insignificant for all the enzymes in this study, meaning that it did not affect the enzymes' action on the substrate molecules. Although, the preferences were not that much different between X7 and XGO for the OsXTH1 enzyme. It was clear that the capsicum enzymes had a distinct preference at the third position while the tomato and rice enzymes did not really differentiate. HEC and BBG activities were surprisingly low for the OsXTH1 enzyme, even though rice contains  $\beta$ -glucan in its native cell wall structure. Considering the fact that we studied only one rice XTH gene out of a family of 31 genes, it is entirely possible that OsXTH1 does not work efficiently on BBG, but others could. The results might also have been different if native rice  $\beta$ -glucan was used, since  $\beta$ -glucan structure is also known to be variable. The tomato and capsicum enzymes demonstrated similar activities with HEC-XGO and HEC-X7, which makes sense since enzymes come from the same group (Group I/II) in the phylogenetic tree. For the rice XTH, HEC-XGO (1,335 picokatal/mg) and HEC-X7 (1,465 picokatal/mg) substrate couples were not as favourable as it was for the others. Activity levels with other substrate couples were considerably lower compared to TXG-XGO and TXG-X7 substrate couples. Besides than HEC-XGO and HEC-X7 substrate couples, the only activity levels that are worth mentioning were TXG-XT (6,227 picokatal/mg), TXG-CT (1,16 picokatal/mg), TXG-BB (1,965 picokatal/mg) and HEC-XT (1,225 picokatal/mg) which were still pretty low. Activity levels for the rest of the substrates that the enzyme was active on were all below 1 picokatal/mg, therefore less than 1 per cent of the activity on TXG-XGO. Although these enzymes prefer to work on xyloglucan, that might not be the case in the wall considering they can bind to a lot of different substrates. Maybe these enzymes cut xyloglucan but then cross-link it to some other polysaccharide chains as long as they have a non-reducing end, which can be cellulose, xylan, BBG etc. With transglycosylase activity, enzymes do not have to cut the substrates and do not have to work on the donor to actually produce links in the wall.

It has been already mentioned that monocot plants contain large amounts of GAX in their primary cell wall and this might explain the activity level of the rice enzyme on TXG-XT substrate couple being higher than it was for tomato and capsicum enzymes. Still, there was no significant activity on the WAX donor substrate for OsXTH1 enzyme. These

enzymes were shown to cut the xyloglucan backbone from the unsubstituted glucose residues. Maybe if there were higher amounts of arabinose substitution on the substrate for the enzyme to cut the back bone the results might have been different. Another reason of not preferring arabinoxylan might be the substitution difference on the backbone. In an arabinoxylan molecule, a linear backbone combined of xylosyl residues are substituted with arabinose residues on the C2 and/or C3 positions which is very different from substitution on C6. Therefore, it is possible that the substitution on the C6 makes it conformationally easier for the enzyme to bind the substrate, but when it is present on the C2 or C3 the molecule does not fit well into the substrate cleft.

In terms of overall activity levels, capsicum enzymes demonstrated higher activity levels than tomato and rice enzymes did. There may be many reasons for this case. Some of the enzymes might have folded better than the others. Also, considering these are all the outcome of an experimental heterologous production, it is entirely possible that the production and the purification process was more efficient with the capsicum enzymes. Among the proteins that were obtained from the purification process, some of them might not be our protein of interest, or may be our protein but might not be active due to misfolding. Post-translational modifications of XTH enzymes also include N-glycosylation and efficiency of this process is also very important to obtain an active enzyme. An N-linked glycosylation motif (NXT) was found to be adjacent to the C-terminal side of the catalytic site motif (EIDFE) and it was conserved among most XTH enzymes [141], including all the enzymes in this study. Deglycosylation of the barley HvXET6 enzyme with PNGase F caused the total loss of the enzyme's activity within 24 hours when incubated at 20°C [142]. Deglycosylation experiments were not performed on the enzymes in this study, but would be likely to expect a similar negative effect.

Kinetic studies were performed with CaXTH1, CaXTH2 and CaXTH3 enzymes in order to have a better idea of the enzymes' working dynamics and catalytic efficiency. TXG was used as the donor substrate and XGO with different concentrations was used as the acceptor substrate.  $V_{max}$ ,  $K_m$ ,  $k_{cat}$  and  $k_{cat}/K_m$  values were calculated for all three capsicum enzymes (Table 4.1). Kinetic studies could not be performed for rice and tomato enzymes because of stability issues and amount of the enzymes remaining following substrate characterisation were insufficient.  $V_{max}$ ,  $K_m$ , and  $k_{cat}$  are the parameters in enzyme kinetics that represent the enzymes working dynamics and efficiency on a certain substrate.  $V_{max}$

represents the maximum velocity and it is calculated when the enzyme is saturated with the substrate molecules.  $K_m$  is the concentration of substrate which permits the enzyme to achieve half  $V_{max}$ . An enzyme with a high  $K_m$  has a low affinity for its substrate, and requires a greater concentration of substrate to achieve  $V_{max}$ .

Table 4.1. Kinetic parameters of CaXTH1, CaXTH2 and CaXTH3 enzymes.

Enzyme	$V_{max}$ ( $\mu\text{M}/\text{min}$ )	$K_m$ ( $\mu\text{M}$ )	$k_{cat}$ ( $\text{min}^{-1}$ )	$k_{cat}/K_m$ ( $\text{min}^{-1}\mu\text{M}^{-1}$ )
CaXTH1	0,014	5,84	2,64	0,452
CaXTH2	0,0063	0,1	3,6	36
CaXTH3	0,046	2,48	41,85	16,88

Between all capsicum enzymes CaXTH2 enzyme's activity on the TXG-X7 substrate couple was 7,4-fold higher than the activity of CaXTH1 and 5-fold higher than the activity of CaXTH3 enzyme. Also, the purified protein concentration of CaXTH2 enzyme was the highest in between enzymes that were included in this study. The protein concentration is taken into account since activity levels are stated in picokatal/mg values, thus the activity level of the protein should not be affected by the purified enzyme concentration. It was not clear whether having more of the same/similar proteins in the immediate environment affects the protein activity. In-house trials showed that the addition of BSA to other capsicum XTH enzymes did not show any effect on picokatal/mg activity levels. When we look at the  $K_m$  values of the capsicum enzymes, we can see that the CaXTH2 enzyme demonstrated the lowest  $K_m$  value, meaning that the CaXTH2 enzyme had the highest affinity for the substrate couple used. This is followed in order by CaXTH3 and CaXTH1. Although CaXTH3 showed less substrate affinity compared to the CaXTH2 enzyme, it demonstrated the highest turnover rate ( $k_{cat}$ ) which means the number of substrate molecules that were turned into products per minute was the highest for this enzyme. CaXTH1 had the highest  $K_m$  value, and therefore the lowest affinity for the substrate couple and also the lowest turnover rate. the  $V_{max}$  of this enzyme was higher than the  $V_{max}$  of the CaXTH2 enzyme. The enzymes' catalytic efficiencies were measured by  $k_{cat}/K_m$  ratio. The highest ratio was observed with the CaXTH2 enzyme, therefore, it was considered to have shown the best catalytic activity. This was followed by CaXTH3

enzyme with a  $k_{cat}/K_m$  value of  $16,88 \text{ min}^{-1}\mu\text{M}^{-1}$ , roughly half that of CaXTH2. The highest  $V_{max}$  was also shown for CaXTH3 enzyme. The lowest catalytic activity was demonstrated for CaXTH1 enzyme, as it has the lowest  $k_{cat}$  and highest  $K_m$  value. In another study, the kinetic properties of three heterologously expressed barley xyloglucan endotransglycosylases (HvXET3, HvXET4 and HvXET6) were examined on TXG and XGO as donor and acceptor substrates, respectively [143].  $K_m$  values of the HvXET3, HvXET4 and HvXET6 enzymes were found to be  $10,3 \mu\text{M}$ ,  $5 \mu\text{M}$  and  $10,6 \mu\text{M}$ , respectively while  $k_{cat}$  values were  $0,3 \text{ min}^{-1}$ ,  $0,36 \text{ min}^{-1}$  and  $3,48 \text{ min}^{-1}$ , respectively. Although the affinity was the lowest for HvXET6 enzyme, catalytic activity was shown to be highest with its high  $k_{cat}$  value ( $3,48 \text{ min}^{-1}$ ). The barley enzymes' kinetic properties were also tested on XXLG/XLXG and XLLG acceptor substrates. HvXET6 revealed increasing catalytic activity as the complexity of the acceptor molecule increased. HvXET3 on the other hand demonstrated a slightly decreasing activity trend towards increasing complexity of the acceptor substrates [143]. When we look at the kinetic results of the XTH enzymes we see great variation. The differences with substrate affinities or turnover numbers may be related to evolutionary development of the different roles of these enzymes are likely to undertake in plants. Plants have different growth times and developmental stages that may change the carbohydrate content of the cell walls, also varying growth rates in different parts of the plant. Kinetic properties of an enzyme may also change depending on the substrate structure. Xyloglucan structures vary depending on the plant type, cell type and even location around the cell, so it is possible that the enzymes that act on these xyloglucans are required to have diverse binding affinities or velocities, as well as catalytic efficiencies. An enzyme's affinity for a substrate might be affected from the side chain substitutions on the xyloglucan molecule. The interactions between side chains of the substrate molecule and the enzyme can affect the enzyme binding and even catalytic rate. It is possible that different enzymes may require different substitutions on the xyloglucan molecules for both binding and catalysis. The enzyme's own shape, amino acid positioning, side chains of the amino acids can also affect the affinity and the catalytic activity of the enzyme on a certain substrate. It was shown that some of the kinetic properties of the capsicum enzymes and barley enzymes were comparable on xyloglucan from tamarind as the donor substrate [143] The results might have been different if native barley or capsicum xyloglucans were used. It is also worth noting that the barley enzymes

were heterologously expressed in the same pPICZa/*Pichia pastoris* expression system, making comparisons between these two studies even more valid.

In a study by Fry and co-workers, it was found that XTHs can bind to glass and cellulose surfaces and are then inactivated. However, the activity was shown to recover with the help of an XTH-activating factor (XAF) present that was found in cold-water-extractable, heat-stable polymers (CHPs) from cauliflower. XTHs were re-solubilised from the surfaces they attached to and reactivated by CHPs. Also, polylysine treatment of the glassware was shown to eliminate the binding of XTHs to the surface of the material [144]. It's a known fact that hydrophobicity of these XTH proteins is high, and this is unusual for globular, soluble enzymes. Normally the enzymes within the cell wall would be hydrophilic and they would have very few hydrophobic amino acids on the surface of the protein. They can have them inside where there are hydrophobic-hydrophobic interactions, but for so many of them to be outside is surprising [145]. Our enzymes have surprisingly high hydrophobicity on their surfaces too. High hydrophobicity on their surfaces would make them prone to binding to hydrophobic surfaces. Considering that some of the cellulose microfibrillar faces are hydrophilic and some of faces are hydrophobic, our enzymes might bind to the hydrophobic faces with hydrophobic-hydrophobic interactions. It might be possible that in the plant cell, XTHs get exported to the wall and then they bind to the cellulose microfibril hydrophobic surfaces and they just sit there, inactive, until some other factor, likely a polysaccharide, comes along which resolubilizes them and reactivates them. Glass also can be hydrophobic depending on the type of the glass. In our purification process, we might be losing both enzymes and activity as they bind to glass surfaces and then inactivate.

The OsXTH1 enzyme was expressed on multiple occasions, but very little activity was observed, and even that small activity disappeared shortly after production. The activity loss might be related to some inefficiency during the post-translational modifications. The only difference between the first and second purification procedures was applying an additional polishing procedure using a Superdex 75 XK 16/100 column during the second purification. It is possible that the polishing step caused extra stress on the rice enzyme and caused the loss of activity and enzyme. Using glass-ware equipment might have also affected the activity of the enzyme. Considering all these enzymes were produced heterologously in the yeast *Pichia pastoris*, the structure of the recombinant protein might not correspond exactly to the structure of the native enzyme either. The polishing

procedure was also applied with capsicum enzymes, but decent activity was observed with all of them (Table 4.2). The protein contamination in general might have affected the picokatal/mg values for the enzymes included in this study. Also, folding in a foreign environment, such as yeast, might not be ideal for the enzymes. However, this was the best we could do since purification from the original plant tissue was not possible. The reason is that we have so many genes that are so similar, protein products would overlap with physical characteristics and therefore one isoform can not be purified from another.

Table 4.2. XTH enzymes as paired with substrates showing the highest activity.

Enzyme	The highest activity showing substrate couple	Activity level (picokatal/mg)
OsXTH1	TXG-X7	126,2
SIXTH4	TXG-XGO	60,63
CaXTH1	TXG-X7	557,87
CaXTH2	TXG-X7	4121,04
CaXTH3	TXG-X7	817,22

Optimization experiments were performed with the seeds that were obtained from the “Yüksel Tohumculuk Company” and the “Menemen National Gene Bank” in order to determine optimal germination and growth conditions on agar and soil as well as cold-drought-salt stress application methods for all of the varieties. It was observed that the germination rate and growth ratios were not the same for the different varieties and that for some of the varieties germination and plant growth could not be achieved at all. Stress trials were conducted with the varieties which demonstrated the best germination and growth ratios after optimizing application methods. QPCR studies were performed with RNA samples obtained from stress treated plants following optimized stress experiments. Capsicum varieties included in stress and QPCR studies were Erzurum, Kahramanmaraş, Mert, Çanakkale, Cila, Aktör (California wonder), Samuray and Seki.

Early stress trials on agar was performed with 0 mM, 50 mM and 100 mM NaCl concentrations and it was shown that even 50 mM NaCl concentration had highly limiting effects on the growth of pepper plants. Lower NaCl concentrations were also tested in

initial trials with Erzurum variety. No limiting effects on the plant growth or germination were observed when NaCl concentration was 20 mM. However, a drastic drop in root lengths was observed in the transition from 20 mM to 30 mM NaCl concentration. Therefore, 25 mM NaCl concentration was taken as the starting point to create and observe the first effects of salt stress on the plants. The upper limit was chosen as 50 mM NaCl to make sure to observe highly limiting effects of salt stress. Salt stress experiments that were performed later on MS agar with Erzurum variety showed that 25 mM NaCl did not create a noteworthy effect on the plant root and shoot lengths compared to control plants. A slight decrease in root and shoot lengths was still observed at 25 mM NaCl concentration which could be an indicator for the start of the initial stress conditions for Erzurum pepper plants. When the salt concentration reached to 50 mM the root and shoot lengths of the pepper seedlings were reduced 50 per cent and 30 per cent, respectively. Salt stress effects on Erzurum pepper seedlings were clearly noticeable at 50 mM NaCl concentration yet not deadly.

Salt stress experiments on MS agar were performed using Aktör, Seki, Cila and Samuray pepper seedlings. Phenotypic observation showed that Cila and Samuray varieties demonstrated improved root and shoot lengths compared to control group plants at both 25 mM and 50 mM NaCl concentrations. The Aktör variety showed a slight decrease in shoot lengths compared to control group plants but the root lengths of the pepper seedlings seemed to improve as the salt concentration increased. The Seki variety exhibited shorter shoot lengths compared to control plants as the salt concentration increased, indicating the stress was having an effect. Also, root growth was impaired at 50 mM NaCl concentration for the Seki variety. Since inhibition of shoot and root lengths is a clear sign of the effects of the stress, it is possible to say that Seki variety showed susceptibility to salt stress conditions. It can also be said that Cila and Samuray varieties were more tolerant than Aktör and Seki varieties to salt stress. Improvement of shoot and root lengths in Cila and Samuray varieties showed that plants favored the environment with increased salt concentration. The reason for that might be pepper plants lacking either sodium or chloride ions, therefore providing an improvement to their metabolism. Another theory is that the mechanism of stress tolerance is accomplished via turning stress conditions as an advantage to improve growth of the plant. Root length increase was expected before a decrease as a stress response from the plants. Abiotic stresses, like cold and salinity will

eventually lead to an osmotic stress as they would reduce the amount of water that is available for the plant's use. The increase in root lengths, in the initial stages of salt stress, was considered as a result of pepper plants growing their roots deeper to be able to reach water rich zones. That was considered to be the case for Aktör variety, as the roots of the plants kept growing when the shoots almost stayed the same. Eventhough Aktör variety was under stress too, it demonstrated an earlier and more persistent response compared to the Seki variety. Therefore Aktör variety was found to be more tolerant than Seki variety. For Cila and Samuray variety, shoot and root improvement was less at 50 mM salt concentration than it was at 25 mM salt concentration. This may indicate that the conditions were harsher at 50 mM NaCl concentration than they were at 25 mM NaCl concentrations and plants were slightly stressed, which, supports the theory of Cila and Samuray varieties' ability of growth improvement under these salt conditions. In comparison of shoot lengths between Cila and Samuray, the plants showed that shoot length improvement was more for the Cila variety than it was for the Samuray variety. Therefore, based on the phenotypic observations, Cila variety was found to be more tolerant to salt stress than the Samuray variety. Root tissues of control and stress treated plants from Aktör, Seki, Cila and Samuray varieties were used for QPCR studies in order to understand the expression patterns of *CaXTH2* and *CaXTH3* genes salt stress applications on MS agar.

In the Cila variety, expression levels of *CaXTH2* and *CaXTH3* genes demonstrated an extreme increase at 25 mM NaCl (295 per cent and 459 per cent respectively) concentration which was when the plants had the longest shoot and root lengths. Although the expression levels of these two capsicum genes were upregulated at 50 mM NaCl concentration compared to control group plants, the copy numbers of the genes were much lower than they were at 25 mM concentration. Reduction in shoot-root lengths and copy numbers of the genes seemed to be simultaneously happening in Cila variety as the salt concentration reached 50 mM (66 per cent) from 25 mM (4 per cent). Induction levels of *CaXTH2* and *CaXTH3* genes in Samuray variety were not as high as they were in Cila variety and unlike Cila copy numbers of the genes exhibited an increasing pattern as the salt concentration was increased. However, root and shoot lengths of the Samuray pepper seedlings were reduced at 50 mM NaCl concentration compared to 25 mM concentration. Simultaneous reduction of gene expression and shoot-root lengths was not the case for

Samuray variety. Aktör variety also showed extreme expression levels for *CaXTH2* gene at 25 mM (310 per cent) and 50 mM (422 per cent) salt concentrations but the increase in *CaXTH3* expression at 25 mM (74 per cent) and 50 mM (155 per cent) salt concentration was not as pronounced as the increase in *CaXTH2* expression. Copy numbers of the genes and root lengths showed an increasing pattern as the salt concentration increased for the Aktör variety for both 25 mM and 50 mM salt concentrations but no shoot improvements were observed. Expression levels of *CaXTH2* and *CaXTH3* genes increased as the salt concentration was increased in Seki variety. Although this upregulation was very little for *CaXTH3* gene at 25 mM NaCl (1 per cent) concentration, increase in copy numbers of this gene was significant at 50 mM NaCl (93 per cent) concentration for Seki plants. Shoot lengths of Seki pepper seedlings, on the other hand, had gotten shorter and shorter when the salt concentration reached up to 50 mM. Root length reduction was also observed at 50 mM salt concentration for Seki plants. Upregulation of *CaXTH2* and *CaXTH3* genes did not correlate with any improvement in shoot or root growth.

*CaXTH2* and *CaXTH3* genes demonstrated great variation in expression patterns according to variety, salt concentration and genes themselves. A noticeable amount of increase in expression levels of *CaXTH2* and *CaXTH3* genes was observed for Cila, Samuray, Aktör and Seki varieties, compared to their control groups under increased salt conditions. Root length improvement and gene upregulation was observed together for both *CaXTH2* and *CaXTH3* genes in Cila, Samuray and Aktör varieties.

This brings out the idea that these genes are upregulating under salt stress as some kind of a response to stress conditions. One might think that a rapid increase in gene expression for Cila and Aktör varieties at 25 mM salt concentration may indicate a fast and intense response to salt stress or at least them being involved in the process. However, Seki variety demonstrated shorter roots at 50 mM NaCl concentration even though the gene expression levels highly increased for both genes. The reason might be that Seki is starting to show susceptibility causing general inhibition of the metabolism and *Capsicum* genes are not enough to provide tolerance or response mechanism. A decreasing pattern was observed in the copy numbers of *Capsicum* genes from susceptible variety to tolerant variety under non-stress conditions. Cila variety had the lowest and Seki variety had the highest copy numbers of the *CaXTH2* and *CaXTH3* genes at 0 mM NaCl concentration. This similar trend in copy numbers might be related to stress tolerance level of the plants. Susceptible

plants might be storing the genes for a precaution as they do not have a rapid increase mechanism. Maybe these genes are co-expressed with other genes that take a role in stress response mechanisms therefore *CaXTH* genes only are not enough to create a response or tolerance but they are involved in a more complex mechanism. Once again, XTH enzymes are thought to be involved in cell elongation processes as well as cell wall strengthening, but it is more difficult to imagine how the same enzyme can play a role in both loosening and strengthening processes. That is of course unless the local substrate concentrations change in which case a change to cross-linking to other polysaccharides can create greater local rigidity in the wall. This in turn can help to resist forces brought about by the stress induced in the plant. Stress tolerance is a highly complex process that involves gene networks and complex mechanisms, therefore creating a linear relationship between physiological features and gene expression is difficult to determine most of the time. Since different varieties have different genetic backgrounds, they may or may not include different elements that play roles in global stress response and that might also diversify expression levels of capsicum genes.

Abiotic stress experiments were also conducted with older, soil grown pepper plants. Salt stress studies in soil were performed with 3-week-old Çanakkale and Kahramanmaraş varieties. The roots of the seedlings were soaked into 200 mM NaCl solution for various time periods (10 min-30 min -120 min) and root and leaf samples of control and stress treated pepper seedlings were collected. QPCR was performed from cDNA synthesised from each of the samples. There were no extreme phenotypic changes for either of the pepper varieties. Although phenotypic changes, such as wilting due to loss of turgor pressure, became clearer when incubation time increased, both Çanakkale and Kahramanmaraş pepper seedlings still looked alive and quite healthy. Therefore, it is possible to say that the application of the salt stress by soaking of the roots in 200 mM NaCl for 120 min was not enough to put the plants beyond recovery. Gene expression levels for *CaXTH2* and *CaXTH3* genes were upregulated at 10 min of incubation time in both leaf and root tissues for the Çanakkale variety. Upregulation levels showed variation depending on the gene and tissue type. For Kahramanmaraş variety, copy numbers of the capsicum genes seemed to drop as the incubation time in 200 mM NaCl increased. Even though *CaXTH2* gene expression was upregulated a little at 10 min in root tissue for Kahramanmaraş seedlings, copy numbers of this gene dropped as the incubation time

increased. Initial salt stress conditions caused an upregulation of the capsicum *XTH* genes for the Çanakkale variety to a certain level while Kahramanmaraş variety demonstrated decreased expression levels of the genes. If these genes are involved in a greater mechanism to cope with stress conditions it is possible to say that Çanakkale variety acts faster when stressed in comparison to Kahramanmaraş variety. A drop in gene expression levels, as the time increased, might indicate inhibition of the metabolism due to heavy stress conditions or adaptation to stress conditions by closure of the stomata to prevent further water loss, or increasing cross-linking and rigidifying the cell wall to resist the stress conditions. Based on the previous findings of another study group, Kahramanmaraş was considered to be a stress susceptible variety [146]. In this case when we look at the phenotypic results, eventhough there were no extreme changes phenotypically, Kahramanmaraş did look slightly more wilted than Çanakkale variety at 120 min time point and was late to respond in terms of gene upregulation, compared to Çanakkale variety. That might be an indication of Kahramanmaraş being more susceptible than Çanakkale variety. Also, gene copy numbers in Kahramanmaraş control plants were much higher than the copy numbers in Çanakkale control plants, which coincided the scenario from MS agar salt stress experiments that less tolerant varieties had more of the capsicum genes under non-stressed conditions compared to tolerant varieties. As seen with MS agar experiments *CaXTH2* and *CaXTH3* do not seem to be directly involved in the stress response/resistance. They more appear to be involved in some other generalized wall response.

QPCR studies were performed following cold stress studies with Mert and Kahramanmaraş varieties which had been referred to as tolerant and susceptible varieties, respectively, in a previous study [146]. Results showed that *CaXTH2* and *CaXTH3* genes were upregulated under cold stress conditions at all exposure times (4 h, 8 h, 12 h) compared to their control plants for Mert and Kahramanmaraş varieties. An increase in copy numbers of *CaXTH2* (4300 per cent more than control) and *CaXTH3* (3800 per cent more than control) genes was excessive at 4-hour cold exposure time with Mert variety compared to 4-hour control plants. Kahramanmaraş variety also demonstrated extreme levels of expression of *CaXTH2* and *CaXTH3* genes at 4-hour time period compared to 4-hour control plants. However, the increase in expression levels of *CaXTH2* and *CaXTH3* genes were 3,6-fold and 9,4-fold less, respectively, for Kahramanmaraş within the variety compared to Mert variety.

Considering Kahramanmaraş is reported to be a susceptible variety, again a rapid increase in capsicum XTH gene levels was observed at the initial stage of stress conditions for the possibly tolerant variety, Mert. Copy number increase in capsicum XTH genes continued until the 8<sup>th</sup> hour and then dropped at 12<sup>th</sup> hour for Kahramanmaraş variety. For Mert variety, copy number increase in cold stress treated plants was less after 8-hour cold exposure than it was after 4-hour cold exposure compared to their control plants, for both *CaXTH2* and *CaXTH3* genes. Based on this, it might be possible for Kahramanmaraş to be still under stress and still trying to respond by making changes in its metabolism at 8<sup>th</sup> hour while Mert might have already adapted. After 12-hour cold stress exposure expression levels of the capsicum genes dropped for both cold stress treated Mert and Kahramanmaraş plants. Our findings demonstrated that Kahramanmaraş was phenotypically less tolerant than the Mert variety. Kahramanmaraş was also slow in responding via upregulation of capsicum XTH genes and had more of the capsicum XTH genes under non-stress conditions compared to Mert variety. Cell specific expression studies could be very useful in further elucidating the role/s of these genes. In particular, stomatal guard cell expression studies could confirm or disprove the role of *CaXTH2* and 3 in stomatal closure. Throughout the drought stress experiments via fresh weight loss, Mert variety was observed to be phenotypically less tolerant than the Cila variety. However, gene expression results showed that at 5 per cent weight loss level, *CaXTH2* and *CaXTH3* expression levels were highly upregulated in Mert variety while Cila variety demonstrated lower copy numbers of the genes compared to control plants at 5 per cent weight loss level. Capsicum XTH gene expression levels increased for Cila variety compared to control group plants when the fresh weight loss reached 10 per cent while copy numbers of the capsicum genes started to decrease for Mert variety at 10 per cent weight loss level. That leads to the fact that, even though Cila looked healthier phenotypically, genetically it responded slower to stress conditions and had more copies of the capsicum gene products compared to the Mert variety. It would seem from this analysis, and in comparison to other experiments, that the Mert variety seems to be more tolerant in terms of gene expression. However, there was no phenotypic evidence to support that. When the fresh weight loss reached to 20 per cent, the expression levels of *CaXTH2* and *CaXTH3* genes were highly reduced for Mert and Cila variety compared to the unstressed control group plants, which may be an indication of increasing drought stress effects. On the other hand, the pepper plants did not lose their liveliness even when the weight loss reached 20 per cent. It took almost the same period of

time for pepper plants from both Mert and Cila varieties to reach 5 per cent -10 per cent - 20 per cent fresh weight loss.

The NGS data also confirmed upregulation in *CaXTH2* and *CaXTH3* expression levels. Analysing 4-hour samples would have given a clearer difference in upregulation levels. Especially if we consider the fact that possibly tolerant variety Mert showed extreme increase in gene expression levels at 4-hour time period. However, it was not possible to analyse 4-hour samples due to the low RIN values.



## 5. CONCLUSION

In all land plants, their *XTH* genes form a large gene family with distinct branches on a phylogenetic tree and their specific roles in plants remains enigmatic. For an enzyme that is supposed to work on a single simple substrate, all plant genomes so far surveyed contain a lot of genes (30-60). If the enzyme only works on one type of substrate xyloglucan that exists in all plants, different types of xyloglucan may require a variety of enzymes which might be a reason for the diversity of *XTH* genes. Still, one might think that such large gene family that work on a substrate that is very plain should require minimum control, yet, here's this large gene family which have different promoters and different abilities like temporal control, tissue specific regulation, stress control, hormonal control etc. *XTH* genes probably have interesting roles in plants but these roles have not yet been enlightened. Hence, we conducted a multi-omics approach with xyloglucan endotransglycosylases within various species in order to gain some insight into the function of these genes. The chosen CaXTH1-2-3, SIXTH4 and OsXTH1 enzymes chosen were heterologously produced and purified. Following purification, enzyme characterisation was performed. In addition, expression levels of *CaXTH2* and *CaXTH3* genes was examined under different stress conditions for different capsicum varieties.

Xyloglucan with xyloglucan oligosaccharides is by far and away the most preferred substrate couple of all five XTH enzymes studied here. When TXG was used as the donor substrate, the next highest activity after xyloglucan oligosaccharides was observed with the XT acceptor substrate for all XTH enzymes included in this study (0,1-5 per cent of TXG-XGO) and there was some activity with CT substrate also. Even though the activity on TXG-CT was 1 per cent of the activity of TXG-XGO for rice and tomato enzymes, which does not seem like a big number, the activity efficiency on different carbohydrate molecules in the cell wall depends on what is actually available in the wall. More interesting results in substrate preferences was obtained for OsXTH1 and SIXTH4 enzymes. TXG-XT activity was 5 per cent and 4 per cent of the TXG-XGO activity for rice and tomato enzymes, respectively. Together, the CT and XT results actually are important findings because it says that even though these enzymes highly prefer xyloglucan and xyloglucan oligosaccharides, they are capable of working with cellulose or cello oligosaccharides and other oligosaccharides such as xylans and are certainly capable of linking to non-reducing end of a xylan chain or xylan oligosaccharides. Arabinoxylan

can comprise up to 40 per cent of the plant cell walls of monocot plants such as rice, however 5 per cent activity on xylan molecules for an enzyme specified to only work on xyloglucan is still unexpected. Activity on HEC-X7 substrate couple was 10 per cent of the activity on TXG-XGO substrate couple for SIXTH4 enzyme which was quite a lot of activity for a non-xyloglucan donor molecule. This clearly shows that these enzymes are capable of heterotransglycosylation. In other publications, XTHs have been shown to perform heterotransglycosylation, however, to our knowledge they have never before been shown to work with XT as the acceptor substrate. Capsicum enzymes, on the other hand were more specific in their substrate preferences. The activity levels on TXG-XT and TXG-CT were less than 1 per cent of the activity on TXG-XGO. Even though there was still a decent amount of activity on HEC-X7 for CaXTH2 enzyme (11,8 picokatal/mg), it was still less than 1 per cent of the activity on TXG-XGO. Similar cases were observed for CaXTH1 and CaXTH3 enzymes too. Therefore, it can be said that capsicum enzymes are more specific to xyloglucan, showing much reduced activity against other substrates, less than 1 per cent but the overall activity levels of capsicum enzymes were higher than the overall activity of OsXTH1 and SIXTH4 enzymes. It must be noted that, TXG was the only available xyloglucan donor for characterization studies and that highly limited the xyloglucan substrate profile to XXXG, XLXG, XXLG and XLLG subunits. Therefore, while capsicum XTH enzymes appear to be more specific on xyloglucan only, it must be remembered that capsicum xyloglucan is going to be different from the TXG that we used here and presumably the activity of the enzyme would be even greater on its native substrate. As we have shown, these XTH enzymes are capable of cross-linking different polysaccharides in the wall and this might be linked to their roles in stress response. The expression studies showed that the actual overall expression level is higher in the susceptible plant under non-stress conditions, but these genes are upregulated faster under stress conditions in the capsicum plants that are more tolerant. Although, upregulation of capsicum genes did not provide a response for all of the pepper varieties, the case might have been different if the other polysaccharides that they work on were available in higher levels in tolerant plants. The enzymes might cross-link with other polysaccharides and provide extra strength within the wall. The mechanism for stress response/tolerance was shown to be more complicated and is not likely to have a linear relationship with single gene expression. These findings do not prove that *XTH* genes have no effect in stress response/tolerance but that they are likely to be part of a larger, more complex mechanism.

Therefore, future research should include expression studies with genes that take roles in global stress response mechanisms in plants and their relation to plant cell wall modification and *XTH* expression profiles.

Future studies should also include, expression studies from different tissues and if possible from specific cells/cell types. Perhaps, rather than isolating a whole leaf under stress, we should look at specific cells to be able to see high expression levels. Tissue specific expression might give an idea of whether expression of *XTH* genes in stomatal guard cells are involved in stress response. Laser capture microdissection might be done just to isolate guard cells that are stress responding and QPCR or NGS examination can be performed to see whether our genes are upregulated and to what extent. Molecular modelling and/or protein crystallization studies can be performed to elucidate which amino acids affect the binding/catalysis, and to have more information about enzyme structure and substrate interactions. It would also be highly instructive to know the xyloglucan type, or the xyloglucan repeat units not only in the different plants, but also in the different tissues and cells. This information can be linked with expression profiles of the *XTH* genes to predict far more about their actual roles.

## REFERENCES

1. Chillies and Peppers (Green) Harvested Area [cited 2016 9 November]. Available from: <http://chartsbin.com/view/41158>.
2. Silva LR, Azevedo J, Pereira MJ, Valentao P, Andrade PB. Chemical Assessment and Antioxidant Capacity of Pepper (*Capsicum Annuum* L.) Seeds. *Food Chem Toxicol.* 2013;53:240-248.
3. Loizzo MR, Pugliese A, Bonesi M, Menichini F, Tundis R. Evaluation of Chemical Profile and Antioxidant Activity of Twenty Cultivars from *Capsicum Annuum*, *Capsicum Baccatum*, *Capsicum Chacoense* and *Capsicum Chinense*: A Comparison between Fresh and Processed Peppers. *LWT - Food Science and Technology.* 2015;64(2):623-631.
4. Zhigila DA, AbdulRahaman AA, Kolawole OS, Oladele FA. Fruit Morphology as Taxonomic Features in Five Varieties of *Capsicum Annuum* L. Solanaceae. *Journal of Botany.* 2014;2014:6.
5. Kothari SL, Joshi A, Kachhwaha S, Ochoa-Alejo N. Chilli Peppers--a Review on Tissue Culture and Transgenesis. *Biotechnol Adv.* 2010;28(1):35-48.
6. Barceloux DG. Pepper and Capsaicin (*Capsicum* and *Piper* Species). *Dis Mon.* 2009;55(6):380-390.
7. Lahbib K, Dabbou S, Bok SEL, Pandino G, Lombardo S, Gazzah MEL. Variation of Biochemical and Antioxidant Activity with Respect to the Part of *Capsicum Annuum* Fruit from Tunisian Autochthonous Cultivars. *Industrial Crops and Products.* 2017;104:164-170.
8. Livingstone KD, Lackney VK, Blauth JR, van Wijk R, Jahn MK. Genome Mapping in *Capsicum* and the Evolution of Genome Structure in the Solanaceae. *Genetics.* 1999;152(3):1183-1202.
9. Choi JY, Seo YS, Kim SJ, Kim WT, Shin JS. Constitutive Expression of Caxth3, a Hot Pepper Xyloglucan Endotransglucosylase/Hydrolase, Enhanced Tolerance to Salt

- and Drought Stresses without Phenotypic Defects in Tomato Plants (*Solanum Lycopersicum* Cv. Dotaerang). *Plant Cell Rep.* 2011;30(5):867-877.
10. Kosova K, Vitamvas P, Prasil IT, Renaut J. Plant Proteome Changes under Abiotic Stress--Contribution of Proteomics Studies to Understanding Plant Stress Response. *J Proteomics.* 2011;74(8):1301-1322.
  11. Zhou Y, Shao HB. The Responding Relationship between Plants and Environment Is the Essential Principle for Agricultural Sustainable Development on the Globe. *C R Biol.* 2008;331(4):321-328.
  12. Roy SJ, Tucker EJ, Tester M. Genetic Analysis of Abiotic Stress Tolerance in Crops. *Curr Opin Plant Biol.* 2011;14(3):232-239.
  13. Sasidharan R, Voeselek LACJ, Pierik R. Cell Wall Modifying Proteins Mediate Plant Acclimatization to Biotic and Abiotic Stresses. *Critical Reviews in Plant Sciences.* 2011;30(6):548-562.
  14. Park JA, Cho SK, Kim JE, Chung HS, Hong JP, Hwang B, Hong CB, Kim WT. Isolation of Cdnas Differentially Expressed in Response to Drought Stress and Characterization of the Ca-Leal1 Gene Encoding a New Family of Atypical Lea-Like Protein Homologue in Hot Pepper (*Capsicum Annuum* L. Cv. Pukang). *Plant Science.* 2003;165(3):471-481.
  15. Dong J, Jiang Y, Chen R, Xu Z, Gao X. Isolation of a Novel Xyloglucan Endotransglucosylase (Oxset9) Gene from Rice and Analysis of the Response of This Gene to Abiotic Stresses. *African Journal of Biotechnology.* 2011;10(76):17424-17434.
  16. Cho SK, Kim JE, Park JA, Eom TJ, Kim WT. Constitutive Expression of Abiotic Stress-Inducible Hot Pepper Caxth3, Which Encodes a Xyloglucan Endotransglucosylase/Hydrolase Homolog, Improves Drought and Salt Tolerance in Transgenic Arabidopsis Plants. *FEBS Lett.* 2006;580(13):3136-3144.
  17. Cosgrove DJ. Expansive Growth of Plant Cell Walls. *Plant Physiol Biochem.* 2000;38(1-2):109-124.

18. Cosgrove DJ. Growth of the Plant Cell Wall. *Nature Reviews Molecular Cell Biology*. 2005;6(11):850.
19. Geitmann A. Mechanical Modeling and Structural Analysis of the Primary Plant Cell Wall. *Curr Opin Plant Biol*. 2010;13(6):693-699.
20. Popper ZA. Evolution and Diversity of Green Plant Cell Walls. *Curr Opin Plant Biol*. 2008;11(3):286-292.
21. Reiter WD. Biosynthesis and Properties of the Plant Cell Wall. *Curr Opin Plant Biol*. 2002;5(6):536-542.
22. Sarkar P, Bosneaga E, Auer M. Plant Cell Walls Throughout Evolution: Towards a Molecular Understanding of Their Design Principles. *J Exp Bot*. 2009;60(13):3615-3635.
23. Lerouxel O, Cavalier DM, Liepman AH, Keegstra K. Biosynthesis of Plant Cell Wall Polysaccharides - a Complex Process. *Curr Opin Plant Biol*. 2006;9(6):621-630.
24. Reid JG. Cementing the Wall: Cell Wall Polysaccharide Synthesising Enzymes. *Curr Opin Plant Biol*. 2000;3(6):512-516.
25. Pauly M, Keegstra K. Biosynthesis of the Plant Cell Wall Matrix Polysaccharide Xyloglucan. *Annu Rev Plant Biol*. 2016;67:235-259.
26. Carpita NC, Gibeaut DM. Structural Models of Primary Cell Walls in Flowering Plants: Consistency of Molecular Structure with the Physical Properties of the Walls During Growth. *Plant J*. 1993;3(1):1-30.
27. Levy I, Shani Z, Shoseyov O. Modification of Polysaccharides and Plant Cell Wall by Endo-1,4-Beta-Glucanase and Cellulose-Binding Domains. *Biomol Eng*. 2002;19(1):17-30.
28. Brown Jr RM, Saxena IM, Kudlicka K. Cellulose Biosynthesis in Higher Plants. *Trends in Plant Science*. 1996;1(5):149-156.
29. Frei E. Cell Wall Organization and Wall Growth in the Filamentous Green Algae *Cladophora* and *Chaetomorpha* Ii. Spiral Structure and Spiral Growth. *Proc R Soc Lond B*. 1961;155(958):55-77.

30. Mutwil M, Debolt S, Persson S. Cellulose Synthesis: A Complex Complex. *Curr Opin Plant Biol.* 2008;11(3):252-257.
31. Slabaugh E, Davis JK, Haigler CH, Yingling YG, Zimmer J. Cellulose Synthases: New Insights from Crystallography and Modeling. *Trends Plant Sci.* 2014;19(2):99-106.
32. Endler A, Persson S. Cellulose Synthases and Synthesis in Arabidopsis. *Mol Plant.* 2011;4(2):199-211.
33. Saxena IM, Brown RM, Jr. Cellulose Synthases and Related Enzymes. *Curr Opin Plant Biol.* 2000;3(6):523-531.
34. Hazen SP, Scott-Craig JS, Walton JD. Cellulose Synthase-Like Genes of Rice. *Plant Physiol.* 2002;128(2):336-340.
35. Qi G, Hu R, Yu L, Chai G, Cao Y, Zuo R, Kong Y, Zhou G. Two Poplar Cellulose Synthase-Like D Genes, PdcslD5 and PdcslD6, Are Functionally Conserved with Arabidopsis CslD3. *J Plant Physiol.* 2013;170(14):1267-1276.
36. Cutler S, Somerville C. Cloning in Silico. *Curr Biol.* 1997;7(2):R108-111.
37. Fincher GB. Exploring the Evolution of (1,3;1,4)-Beta-D-Glucans in Plant Cell Walls: Comparative Genomics Can Help! *Curr Opin Plant Biol.* 2009;12(2):140-147.
38. Yapo BM. Pectic Substances: From Simple Pectic Polysaccharides to Complex Pectins—a New Hypothetical Model. *Carbohydrate Polymers.* 2011;86(2):373-385.
39. Mohnen D. Pectin Structure and Biosynthesis. *Curr Opin Plant Biol.* 2008;11(3):266-277.
40. Ridley BL, O'Neill MA, Mohnen D. Pectins: Structure, Biosynthesis, and Oligogalacturonide-Related Signaling. *Phytochemistry.* 2001;57(6):929-967.
41. Caffall KH, Mohnen D. The Structure, Function, and Biosynthesis of Plant Cell Wall Pectic Polysaccharides. *Carbohydr Res.* 2009;344(14):1879-1900.

42. Lazaridou A, Biliaderis C. Molecular Aspects of Cereal B-Glucan Functionality: Physical Properties, Technological Applications and Physiological Effects. *Journal of Cereal Science*. 2007;46(2):101-118.
43. Brennan CS, Cleary LJ. The Potential Use of Cereal (1→3, 1→4)-B-D-Glucans as Functional Food Ingredients. *Journal of Cereal Science*. 2005;42(1):1-13.
44. Izydorczyk M, Dexter J. Barley B-Glucans and Arabinoxylans: Molecular Structure, Physicochemical Properties, and Uses in Food Products—a Review. *Food Research International*. 2008;41(9):850-868.
45. Sørensen HR, Pedersen S, Meyer AS. Characterization of Solubilized Arabinoxyloligosaccharides by Maldi-Tof Ms Analysis to Unravel and Direct Enzyme Catalyzed Hydrolysis of Insoluble Wheat Arabinoxylan. *Enzyme and Microbial Technology*. 2007;41(1-2):103-110.
46. Deutschmann R, Dekker RF. From Plant Biomass to Bio-Based Chemicals: Latest Developments in Xylan Research. *Biotechnology Advances*. 2012;30(6):1627-1640.
47. Roubroeks J, Andersson R, Åman P. Structural Features of (1→3),(1→4)-B-D-Glucan and Arabinoxylan Fractions Isolated from Rye Bran. *Carbohydrate Polymers*. 2000;42(1):3-11.
48. Sárossy Z, Tenkanen M, Pitkänen L, Bjerre A-B, Plackett D. Extraction and Chemical Characterization of Rye Arabinoxylan and the Effect of B-Glucan on the Mechanical and Barrier Properties of Cast Arabinoxylan Films. *Food Hydrocolloids*. 2013;30(1):206-216.
49. Van Zyl WH, Rose SH, Trollope K, Görgens JF. Fungal B-Mannanases: Mannan Hydrolysis, Heterologous Production and Biotechnological Applications. *Process Biochemistry*. 2010;45(8):1203-1213.
50. Petkowicz CdO, Reicher F, Chanzy H, Taravel F, Vuong R. Linear Mannan in the Endosperm of *Schizolobium Amazonicum*. *Carbohydrate Polymers*. 2001;44(2):107-112.

51. Ližičárová I, Matulová M, Capek P, Machová E. Human Pathogen *Candida Dubliniensis*: A Cell Wall Mannan with a High Content of B-1, 2-Linked Mannose Residues. *Carbohydrate Polymers*. 2007;70(1):89-100.
52. Buckeridge MS, dos Santos HP, Tiné MAS. Mobilisation of Storage Cell Wall Polysaccharides in Seeds. *Plant Physiology and Biochemistry*. 2000;38(1-2):141-156.
53. Mahajan HS, Tyagi VK, Patil RR, Dusunge SB. Thiolated Xyloglucan: Synthesis, Characterization and Evaluation as Mucoadhesive in Situ Gelling Agent. *Carbohydrate Polymers*. 2013;91(2):618-625.
54. Arruda IR, Albuquerque PB, Santos GR, Silva AG, Mourao PA, Correia MT, Vicente AA, Carneiro-da-Cunha MG. Structure and Rheological Properties of a Xyloglucan Extracted from *Hymenaea Courbaril* Var. *Courbaril* Seeds. *Int J Biol Macromol*. 2015;73:31-38.
55. Tuomivaara ST, Yaoi K, O'Neill MA, York WS. Generation and Structural Validation of a Library of Diverse Xyloglucan-Derived Oligosaccharides, Including an Update on Xyloglucan Nomenclature. *Carbohydr Res*. 2015;402:56-66.
56. Barber C, Rösti J, Rawat A, Findlay K, Roberts K, Seifert GJ. Distinct Properties of the Five Udp-D-Glucose/Udp-D-Galactose 4-Epimerase Isoforms of *Arabidopsis Thaliana*. *Journal of Biological Chemistry*. 2006;281(25):17276-17285.
57. Seifert GJ. Nucleotide Sugar Interconversions and Cell Wall Biosynthesis: How to Bring the inside to the Outside. *Current Opinion in Plant Biology*. 2004;7(3):277-284.
58. Arioli T, Peng L, Betzner AS, Burn J, Wittke W, Herth W, Camilleri C, Hofte H, Plazinski J. Molecular Analysis of Cellulose Biosynthesis in *Arabidopsis*. *Science*. 1998;279(5351):717-720.
59. Turner SR, Somerville CR. Collapsed Xylem Phenotype of *Arabidopsis* Identifies Mutants Deficient in Cellulose Deposition in the Secondary Cell Wall. *The Plant Cell*. 1997;9(5):689-701.
60. Taylor NG, Scheible WR, Cutler S, Somerville CR, Turner SR. The Irregular Xylem3 Locus of *Arabidopsis* Encodes a Cellulose Synthase Required for Secondary Cell Wall Synthesis. *Plant Cell*. 1999;11(5):769-780.

61. Richmond TA, Somerville CR. The Cellulose Synthase Superfamily. *Plant Physiol.* 2000;124(2):495-498.
62. Richmond TA, Somerville CR. Integrative Approaches to Determining Csl Function. *Plant Cell Walls*: Springer; 2001:131-143.
63. Favery B, Ryan E, Foreman J, Linstead P, Boudonck K, Steer M, Shaw P, Dolan L. Kojak Encodes a Cellulose Synthase-Like Protein Required for Root Hair Cell Morphogenesis in Arabidopsis. *Genes Dev.* 2001;15(1):79-89.
64. Wang X, Cnops G, Vanderhaeghen R, De Block S, Van Montagu M, Van Lijsebettens M. Atcsld3, a Cellulose Synthase-Like Gene Important for Root Hair Growth in Arabidopsis. *Plant Physiol.* 2001;126(2):575-586.
65. Nam J, Mysore K, Zheng C, Knue M, Matthysse A, Gelvin S. Identification of T-DNA Tagged Arabidopsis Mutants That Are Resistant to Transformation by Agrobacterium. *Molecular and General Genetics MGG.* 1999;261(3):429-438.
66. Cocuron JC, Lerouxel O, Drakakaki G, Alonso AP, Liepman AH, Keegstra K, Raikhel N, Wilkerson CG. A Gene from the Cellulose Synthase-Like C Family Encodes a Beta-1,4 Glucan Synthase. *Proc Natl Acad Sci U S A.* 2007;104(20):8550-8555.
67. Pattathil S, Harper AD, Bar-Peled M. Biosynthesis of Udp-Xylose: Characterization of Membrane-Bound Atuxs2. *Planta.* 2005;221(4):538-548.
68. Ebert B, Rautengarten C, Guo X, Xiong G, Stonebloom S, Smith-Moritz AM, Herter T, Chan LJ, Adams P. Identification and Characterization of a Golgi-Localized Udp-Xylose Transporter Family from Arabidopsis. *Plant Cell.* 2015;27(4):1218-1227.
69. Faik A, Price NJ, Raikhel NV, Keegstra K. An Arabidopsis Gene Encoding an Alpha-Xylosyltransferase Involved in Xyloglucan Biosynthesis. *Proc Natl Acad Sci U S A.* 2002;99(11):7797-7802.
70. Cavalier DM, Keegstra K. Two Xyloglucan Xylosyltransferases Catalyze the Addition of Multiple Xylosyl Residues to Cellohexaose. *J Biol Chem.* 2006;281(45):34197-34207.

71. Cavalier DM, Lerouxel O, Neumetzler L, Yamauchi K, Reinecke A, Freshour G, Zabolina OA, Hahn MG, Burgert Iand. Disrupting Two Arabidopsis Thaliana Xylosyltransferase Genes Results in Plants Deficient in Xyloglucan, a Major Primary Cell Wall Component. *Plant Cell*. 2008;20(6):1519-1537.
72. Vuttipongchaikij S, Brocklehurst D, Steele-King C, Ashford DA, Gomez LD, McQueen-Mason SJ. Arabidopsis Gt34 Family Contains Five Xyloglucan Alpha-1,6-Xylosyltransferases. *New Phytol*. 2012;195(3):585-595.
73. Gille S, de Souza A, Xiong G, Benz M, Cheng K, Schultink A, Reca IB, Pauly M. O-Acetylation of Arabidopsis Hemicellulose Xyloglucan Requires Axy4 or Axy4l, Proteins with a Tbl and Duf231 Domain. *Plant Cell*. 2011;23(11):4041-4053.
74. Urbanowicz BR, Pena MJ, Moniz HA, Moremen KW, York WS. Two Arabidopsis Proteins Synthesize Acetylated Xylan in Vitro. *Plant J*. 2014;80(2):197-206.
75. Madson M, Dunand C, Li X, Verma R, Vanzin GF, Caplan J, Shoue DA, Carpita NC, Reiter W-D. The Mur3 Gene of Arabidopsis Encodes a Xyloglucan Galactosyltransferase That Is Evolutionarily Related to Animal Exostosins. *The Plant Cell*. 2003;15(7):1662-1670.
76. Pena MJ, Darvill AG, Eberhard S, York WS, O'Neill MA. Moss and Liverwort Xyloglucans Contain Galacturonic Acid and Are Structurally Distinct from the Xyloglucans Synthesized by Hornworts and Vascular Plants. *Glycobiology*. 2008;18(11):891-904.
77. Simi CK, Abraham TE. Physico Chemical Properties of Aminated Tamarind Xyloglucan. *Colloids Surf B Biointerfaces*. 2010;81(2):513-520.
78. de Alcântara PH, Dietrich SM, Buckeridge MS. Xyloglucan Mobilisation and Purification of a (Xllg/Xlwg) Specific B-Galactosidase from Cotyledons of Copaifera Langsdorffii. *Plant Physiology and Biochemistry*. 1999;37(9):653-663.
79. Liu YB, Lu SM, Zhang JF, Liu S, Lu YT. A Xyloglucan Endotransglucosylase/Hydrolase Involves in Growth of Primary Root and Alters the Deposition of Cellulose in Arabidopsis. *Planta*. 2007;226(6):1547-1560.

80. Campbell P, Braam J. Xyloglucan Endotransglycosylases: Diversity of Genes, Enzymes and Potential Wall-Modifying Functions. *Trends in Plant Science*. 1999;4(9):361-366.
81. Rose JK, Braam J, Fry SC, Nishitani K. The Xth Family of Enzymes Involved in Xyloglucan Endotransglucosylation and Endohydrolysis: Current Perspectives and a New Unifying Nomenclature. *Plant Cell Physiol*. 2002;43(12):1421-1435.
82. Cantarel BL, Coutinho PM, Rancurel C, Bernard T, Lombard V, Henrissat B. The Carbohydrate-Active Enzymes Database (Cazy): An Expert Resource for Glycogenomics. *Nucleic Acids Research*. 2008;37(suppl\_1):D233-D238.
83. Davies GJ, Gloster TM, Henrissat B. Recent Structural Insights into the Expanding World of Carbohydrate-Active Enzymes. *Current Opinion in Structural Biology*. 2005;15(6):637-645.
84. Eklof JM, Brumer H. The Xth Gene Family: An Update on Enzyme Structure, Function, and Phylogeny in Xyloglucan Remodeling. *Plant Physiol*. 2010;153(2):456-466.
85. Baumann MJ, Eklof JM, Michel G, Kallas AM, Teeri TT, Czjzek M, Brumer H, 3rd. Structural Evidence for the Evolution of Xyloglucanase Activity from Xyloglucan Endo-Transglycosylases: Biological Implications for Cell Wall Metabolism. *Plant Cell*. 2007;19(6):1947-1963.
86. Eklof JM, Shojanian S, Okon M, McIntosh LP, Brumer H. Structure-Function Analysis of a Broad Specificity Populus Trichocarpa Endo-Beta-Glucanase Reveals an Evolutionary Link between Bacterial Licheninases and Plant Xth Gene Products. *J Biol Chem*. 2013;288(22):15786-15799.
87. Tabuchi A, Mori H, Kamisaka S, Hoson T. A New Type of Endo-Xyloglucan Transferase Devoted to Xyloglucan Hydrolysis in the Cell Wall of Azuki Bean Epicotyls. *Plant Cell Physiol*. 2001;42(2):154-161.
88. Campbell P, Braam J. In Vitro Activities of Four Xyloglucan Endotransglycosylases from Arabidopsis. *Plant J*. 1999;18(4):371-382.

89. Kaewthai N, Harvey AJ, Hrmova M, Brumer H, Ezcurra I, Teeri TT, Fincher GB. Heterologous Expression of Diverse Barley Xth Genes in the Yeast *Pichia Pastoris*. *Plant Biotechnology*. 2010;27(3):251-258.
90. Van Sandt VS, Guisez Y, Verbelen J-P, Vissenberg K. Analysis of a Xyloglucan Endotransglycosylase/Hydrolase (Xth) from the Lycopodiophyte *Selaginella Kraussiana* Suggests That Xth Sequence Characteristics and Function Are Highly Conserved During the Evolution of Vascular Plants. *Journal of Experimental Botany*. 2006;57(12):2909-2922.
91. Yokoyama R, Rose JK, Nishitani K. A Surprising Diversity and Abundance of Xyloglucan Endotransglucosylase/Hydrolases in Rice. Classification and Expression Analysis. *Plant Physiology*. 2004;134(3):1088-1099.
92. Jan A, Yang G, Nakamura H, Ichikawa H, Kitano H, Matsuoka M, Matsumoto H, Komatsu S. Characterization of a Xyloglucan Endotransglucosylase Gene That Is up-Regulated by Gibberellin in Rice. *Plant Physiology*. 2004;136(3):3670-3681.
93. Fry S, Smith RC, Renwick KF, Martin DJ, Hodge S, Matthews KJ. Xyloglucan Endotransglycosylase, a New Wall-Loosening Enzyme Activity from Plants. *Biochemical Journal*. 1992;282(Pt 3):821.
94. Ito H, Nishitani K. Visualization of Exgt-Mediated Molecular Grafting Activity by Means of a Fluorescent-Labeled Xyloglucan Oligomer. *Plant and Cell Physiology*. 1999;40(11):1172-1176.
95. Smith RC, Fry S. Endotransglycosylation of Xyloglucans in Plant Cell Suspension Cultures. *Biochemical Journal*. 1991;279(Pt 2):529.
96. Nishitani K, Tominaga R. Endo-Xyloglucan Transferase, a Novel Class of Glycosyltransferase That Catalyzes Transfer of a Segment of Xyloglucan Molecule to Another Xyloglucan Molecule. *Journal of Biological Chemistry*. 1992;267(29):21058-21064.
97. Farkas V, Sulova Z, Stratilova E, Hanna R, Maclachlan G. Cleavage of Xyloglucan by *Nasturtium* Seed Xyloglucanase and Transglycosylation to Xyloglucan Subunit Oligosaccharides. *Archives of Biochemistry and Biophysics*. 1992;298(2):365-370.

98. McDougall GJ, Fry SC. Xyloglucan Oligosaccharides Promote Growth and Activate Cellulase: Evidence for a Role of Cellulase in Cell Expansion. *Plant Physiology*. 1990;93(3):1042-1048.
99. Yokoyama R, Nishitani K. A Comprehensive Expression Analysis of All Members of a Gene Family Encoding Cell-Wall Enzymes Allowed Us to Predict Cis-Regulatory Regions Involved in Cell-Wall Construction in Specific Organs of Arabidopsis. *Plant and Cell Physiology*. 2001;42(10):1025-1033.
100. Lorences EP, Fry SC. Xyloglucan Oligosaccharides with at Least Two A-D-Xylose Residues Act as Acceptor Substrates for Xyloglucan Endotransglycosylase and Promote the Depolymerisation of Xyloglucan. *Physiologia Plantarum*. 1993;88(1):105-112.
101. Fanutti C, Gidley MJ, Reid JG. Substrate Subsite Recognition of the Xyloglucan Endo-Transglycosylase or Xyloglucan-Specific Endo-(1→4)-B-D-Glucanase from the Cotyledons of Germinated Nasturtium (*Tropaeolum Majus* L.) Seeds. *Planta*. 1996;200(2):221-228.
102. Steele NM, Fry SC. Differences in Catalytic Properties between Native Isoenzymes of Xyloglucan Endotransglycosylase (Xet). *Phytochemistry*. 2000;54(7):667-680.
103. Okazawa K, Sato Y, Nakagawa T, Asada K, Kato I, Tomita E, Nishitani K. Molecular Cloning and Cdna Sequencing of Endoxyloglucan Transferase, a Novel Class of Glycosyltransferase That Mediates Molecular Grafting between Matrix Polysaccharides in Plant Cell Walls. *Journal of Biological Chemistry*. 1993;268(34):25364-25368.
104. Campbell P, Braam J. Co-and/or Post-Translational Modifications Are Critical for Tch4 Xet Activity. *The Plant Journal*. 1998;15(4):553-561.
105. Sulová Z, Takacova M, Steele N, Fry S, Farkas V. Xyloglucan Endotransglycosylase: Evidence for the Existence of a Relatively Stable Glycosyl-Enzyme Intermediate. *Biochemical Journal*. 1998;330(Pt 3):1475.
106. Planas A. Bacterial 1,3-1,4-Beta-Glucanases: Structure, Function and Protein Engineering. *Biochim Biophys Acta*. 2000;1543(2):361-382.

107. Davies GJ, Wilson KS, Henrissat B. Nomenclature for Sugar-Binding Subsites in Glycosyl Hydrolases. *Biochem J.* 1997;321( Pt 2):557-559.
108. Johansson P, Brumer H, 3rd, Baumann MJ, Kallas AM, Henriksson H, Denman SE, Teeri TT, Jones TA. Crystal Structures of a Poplar Xyloglucan Endotransglycosylase Reveal Details of Transglycosylation Acceptor Binding. *Plant Cell.* 2004;16(4):874-886.
109. Kallas AM, Piens K, Denman SE, Henriksson H, Faldt J, Johansson P, Brumer H, Teeri TT. Enzymatic Properties of Native and Deglycosylated Hybrid Aspen (*Populus Tremulaxtremuloides*) Xyloglucan Endotransglycosylase 16a Expressed in *Pichia Pastoris*. *Biochem J.* 2005;390(Pt 1):105-113.
110. Mark P, Baumann MJ, Eklof JM, Gullfot F, Michel G, Kallas AM, Teeri TT, Brumer H, Czjzek M. Analysis of Nasturtium Tmnxg1 Complexes by Crystallography and Molecular Dynamics Provides Detailed Insight into Substrate Recognition by Family Gh16 Xyloglucan Endo-Transglycosylases and Endo-Hydrolases. *Proteins.* 2009;75(4):820-836.
111. Potvin G, Ahmad A, Zhang Z. Bioprocess Engineering Aspects of Heterologous Protein Production in *Pichia Pastoris*: A Review. *Biochemical Engineering Journal.* 2012;64:91-105.
112. Wang Y, Wang Z, Xu Q, Du G, Hua Z, Liu L, Li J, Chen J. Lowering Induction Temperature for Enhanced Production of Polygalacturonate Lyase in Recombinant *Pichia Pastoris*. *Process Biochemistry.* 2009;44(9):949-954.
113. Cereghino GP, Cereghino JL, Ilgen C, Cregg JM. Production of Recombinant Proteins in Fermenter Cultures of the Yeast *Pichia Pastoris*. *Curr Opin Biotechnol.* 2002;13(4):329-332.
114. Cereghino GP, Cregg JM. Applications of Yeast in Biotechnology: Protein Production and Genetic Analysis. *Curr Opin Biotechnol.* 1999;10(5):422-427.
115. Abdelmoula-Souissi S, Rekik L, Gargouri A, Mokdad-Gargouri R. High-Level Expression of Human Tumour Suppressor P53 in the Methylophilic Yeast: *Pichia Pastoris*. *Protein Expression and Purification.* 2007;54(2):283-288.

116. Çelik E, Çalık P, Oliver SG. A Structured Kinetic Model for Recombinant Protein Production by Mut<sup>+</sup> Strain of *Pichia Pastoris*. *Chemical Engineering Science*. 2009;64(23):5028-5035.
117. Romanos M. Advances in the Use of *Pichia Pastoris* for High-Level Gene Expression. *Current Opinion in Biotechnology*. 1995;6(5):527-533.
118. Demain AL, Vaishnav P. Production of Recombinant Proteins by Microbes and Higher Organisms. *Biotechnol Adv*. 2009;27(3):297-306.
119. Kobayashi K, Kuwae S, Ohya T, Ohda T, Ohyama M, Ohi H, Tomomitsu K, Ohmura T. High-Level Expression of Recombinant Human Serum Albumin from the Methylophilic Yeast *Pichia Pastoris* with Minimal Protease Production and Activation. *J Biosci Bioeng*. 2000;89(1):55-61.
120. Soyaslan EŞ, Çalık P. Enhanced Recombinant Human Erythropoietin Production by *Pichia Pastoris* in Methanol Fed-Batch/Sorbitol Batch Fermentation through Ph Optimization. *Biochemical Engineering Journal*. 2011;55(1):59-65.
121. Celik E, Calik P. Production of Recombinant Proteins by Yeast Cells. *Biotechnol Adv*. 2012;30(5):1108-1118.
122. Chiruvolu V, Cregg JM, Meagher MM. Recombinant Protein Production in an Alcohol Oxidase-Defective Strain of *Pichia Pastoris* in Fedbatch Fermentations. *Enzyme and Microbial Technology*. 1997;21(4):277-283.
123. Fregel R, Rodriguez V, Cabrera VM. Microwave Improved *Escherichia Coli* Transformation. *Lett Appl Microbiol*. 2008;46(4):498-499.
124. Li X, Sui X, Zhang Y, Sun Y, Zhao Y, Zhai Y, Wang Q. An Improved Calcium Chloride Method Preparation and Transformation of Competent Cells. *African Journal of Biotechnology*. 2010;9(50):8549-8554.
125. Lin-Cereghino J, Wong WW, Xiong S, Giang W, Luong LT, Vu J, Johnson SD, Lin-Cereghino GP. Condensed Protocol for Competent Cell Preparation and Transformation of the Methylophilic Yeast *Pichia Pastoris*. *Biotechniques*. 2005;38(1):44, 46, 48.

126. Kosik O, Farkas V. One-Pot Fluorescent Labeling of Xyloglucan Oligosaccharides with Sulforhodamine. *Anal Biochem.* 2008;375(2):232-236.
127. Burton RA, Shirley NJ, King BJ, Harvey AJ, Fincher GB. The Cesa Gene Family of Barley. Quantitative Analysis of Transcripts Reveals Two Groups of Co-Expressed Genes. *Plant Physiol.* 2004;134(1):224-236.
128. Martínez-López LA, Ochoa-Alejo N, Martínez O. Dynamics of the Chili Pepper Transcriptome During Fruit Development. *BMC Genomics.* 2014;15(1):143.
129. Hsieh YS, Harris PJ. Xyloglucans of Monocotyledons Have Diverse Structures. *Molecular Plant.* 2009;2(5):943-965.
130. Hoffman M, Jia Z, Peña MJ, Cash M, Harper A, Blackburn AR, Darvill A, York WS. Structural Analysis of Xyloglucans in the Primary Cell Walls of Plants in the Subclass Asteridae. *Carbohydrate Research.* 2005;340(11):1826-1840.
131. Marry M, Cavalier DM, Schnurr JK, Netland J, Yang Z, Pezeshk V, York WS, Pauly M, White AR. Structural Characterization of Chemically and Enzymatically Derived Standard Oligosaccharides Isolated from Partially Purified Tamarind Xyloglucan. *Carbohydrate Polymers.* 2003;51(3):347-356.
132. Catalá C, Rose JK, York WS, Albersheim P, Darvill AG, Bennett AB. Characterization of a Tomato Xyloglucan Endotransglycosylase Gene That Is Down-Regulated by Auxin in Etiolated Hypocotyls. *Plant Physiology.* 2001;127(3):1180-1192.
133. Harris PJ. Primary and Secondary Plant Cell Walls: A Comparative Overview. *New Zealand Journal of Forestry Science.* 2006;36(1):36.
134. Smith BG, Harris PJ. The Polysaccharide Composition of Poales Cell Walls: Poaceae Cell Walls Are Not Unique. *Biochemical Systematics and Ecology.* 1999;27(1):33-53.
135. Brennan M, Harris PJ. Distribution of Fucosylated Xyloglucans among the Walls of Different Cell Types in Monocotyledons Determined by Immunofluorescence Microscopy. *Molecular Plant.* 2011;4(1):144-156.

136. Hayashi T. Xyloglucans in the Primary Cell Wall. *Annual Review of Plant Biology*. 1989;40(1):139-168.
137. Gibeaut DM, Pauly M, Bacic A, Fincher GB. Changes in Cell Wall Polysaccharides in Developing Barley (*Hordeum Vulgare*) Coleoptiles. *Planta*. 2005;221(5):729-738.
138. Kato Y, Ito S, Iki K, Matsuda K. Xyloglucan and R $\beta$ -D-Glucan in Cell Walls of Rice Seedlings. *Plant and Cell Physiology*. 1982;23(3):351-364.
139. Watanabe T, Shida M, Murayama T, Furuyama Y, Nakajima T, Matsuda K, Kainuma K. Xyloglucan in Cell Walls of Rice Hull. *Carbohydrate Research*. 1984;129:229-242.
140. Chambat G, Karmous M, Costes M, Picard M, Joseleau J-P. Variation of Xyloglucan Substitution Pattern Affects the Sorption on Celluloses with Different Degrees of Crystallinity. *Cellulose*. 2005;12(2):117-125.
141. Henriksson H, Denman SE, Campuzano ID, Ademark P, Master ER, Teeri TT, Brumer H, 3rd. N-Linked Glycosylation of Native and Recombinant Cauliflower Xyloglucan Endotransglycosylase 16a. *Biochem J*. 2003;375(Pt 1):61-73.
142. Vaaje-Kolstad G, Farkas V, Hrmova M, Fincher GB. Xyloglucan Xyloglucosyl Transferases from Barley (*Hordeum Vulgare* L.) Bind Oligomeric and Polymeric Xyloglucan Molecules in Their Acceptor Binding Sites. *Biochim Biophys Acta*. 2010;1800(7):674-684.
143. Vaaje-Kolstad G, Farkas V, Fincher GB, Hrmova M. Barley Xyloglucan Xyloglucosyl Transferases Bind Xyloglucan-Derived Oligosaccharides in Their Acceptor-Binding Regions in Multiple Conformational States. *Arch Biochem Biophys*. 2010;496(1):61-68.
144. Sharples SC, Nguyen-Phan TC, Fry SC. Xyloglucan Endotransglucosylase/Hydrolases (Xths) Are Inactivated by Binding to Glass and Cellulosic Surfaces, and Released in Active Form by a Heat-Stable Polymer from Cauliflower Florets. *Journal of Plant Physiology*. 2017;218:135-143.

145. Campbell P, Braam J. Xyloglucan Endotransglycosylases: Diversity of Genes, Enzymes and Potential Wall-Modifying Functions. *Trends Plant Sci.* 1999;4(9):361-366.
146. Esra K, İşlek C, Üstün AS. Effect of Cold on Protein, Proline, Phenolic Compounds and Chlorophyll Content of Two Pepper (*Capsicum Annuum* L.) Varieties. *Gazi University Journal of Science.* 2010;23(1):1-6.



## APPENDIX A: OPTIMIZED STRESS CONDITIONS

Table A.1. Optimized stress conditions for different abiotic stresses included in this study.

Type of Abiotic Stress	Pepper Variety	Germination Conditions	Growth Conditions	Stress conditions	Sampling Time	Sampling Tissue
Cold stress	Mert K.Maraş	<ul style="list-style-type: none"> <li>pH 5,8 ddH<sub>2</sub>O agar, growth cabinet</li> <li>22 °C, 50-55 % humidity</li> <li>dark, 7 days</li> </ul>	<ul style="list-style-type: none"> <li>soil, green house</li> <li>23°C-28°C, 40-50% humidity</li> <li>16 hour light/8 hour dark, 3 weeks</li> </ul>	<ul style="list-style-type: none"> <li>Plant growth cabinet</li> <li>12°C in light and 6°C in dark</li> <li>40-50% humidity</li> <li>16 hour light/8 hour dark</li> </ul>	<ul style="list-style-type: none"> <li>4-hour</li> <li>8-hour</li> <li>12-hour</li> </ul>	Leaf
Drought stress	Mert Cila	<ul style="list-style-type: none"> <li>perlite, green house</li> <li>23°C-28°C, 40-50% humidity</li> <li>dark, 3 weeks</li> </ul>	<ul style="list-style-type: none"> <li>turf, green house</li> <li>23°C-28°C, 40-50% humidity</li> <li>16 hour light/8 hour dark, 4 weeks</li> </ul>	<ul style="list-style-type: none"> <li>Placement of pepper seedlings on Whatman paper after roots cleaned from soil</li> <li>Incubation in plant growth cabinet</li> <li>24°C, 60% humidity</li> <li>Dim light</li> </ul>	<ul style="list-style-type: none"> <li>~0 min (0% weight loss)</li> <li>~6 min (5% weight loss)</li> <li>~11 min (10% weight loss)</li> <li>~40 min (20% weight loss)</li> </ul>	Leaf
Salt stress (MS agar)	Cila Samuray Aktör Seki	<ul style="list-style-type: none"> <li>pH 5,8 MS agar, growth cabinet</li> <li>22 °C, 50-55 % humidity</li> <li>dark, 5 days</li> </ul>	<ul style="list-style-type: none"> <li>pH 5,8 MS agar, growth cabinet</li> <li>22 °C, 50-55 % humidity</li> <li>16 hour light/8 hour dark, 6 days</li> </ul>	<ul style="list-style-type: none"> <li>MS agar 25 mM NaCl</li> <li>MS agar 50 mM NaCl</li> </ul>	6 <sup>th</sup> day	Leaf
Salt stress (soil)	Çanakkale K.Maraş	<ul style="list-style-type: none"> <li>perlite, green house</li> <li>23°C-28°C, 40-50% humidity</li> <li>dark, 3 weeks</li> </ul>	<ul style="list-style-type: none"> <li>turf, green house</li> <li>23°C-28°C, 40-50% humidity</li> <li>16 hour light/8 hour dark, 3 weeks</li> </ul>	<ul style="list-style-type: none"> <li>Soaking roots in 200 mM NaCl</li> </ul>	<ul style="list-style-type: none"> <li>0 min</li> <li>10 min</li> <li>30 min</li> <li>120 min</li> </ul>	Leaf Root